

INFORMATION TO USERS

This manuscript has been reproduced from the microfilm master. UMI films the text directly from the original or copy submitted. Thus, some thesis and dissertation copies are in typewriter face, while others may be from any type of computer printer.

The quality of this reproduction is dependent upon the quality of the copy submitted. Broken or indistinct print, colored or poor quality illustrations and photographs, print bleedthrough, substandard margins, and improper alignment can adversely affect reproduction.

In the unlikely event that the author did not send UMI a complete manuscript and there are missing pages, these will be noted. Also, if unauthorized copyright material had to be removed, a note will indicate the deletion.

Oversize materials (e.g., maps, drawings, charts) are reproduced by sectioning the original, beginning at the upper left-hand corner and continuing from left to right in equal sections with small overlaps.

ProQuest Information and Learning
300 North Zeeb Road, Ann Arbor, MI 48106-1346 USA
800-521-0600



UNIVERSITY OF CALIFORNIA

Santa Barbara

The Mesozoic and Cenozoic Depositional, Structural, and Tectonic Evolution of the
Ross Sea, Antarctica

A Dissertation submitted in partial satisfaction of the requirements
for the degree of

Doctor of Philosophy

in

Geological Sciences

by

Robert Charles Decesari

Committee in charge:

Professor Bruce Luyendyk, Chairman

Doctor Douglas Wilson

Professor James Kennett

Professor Kenneth Macdonald

March 2006

UMI Number: 3208727

Copyright 2006 by
Decesari, Robert Charles

All rights reserved.



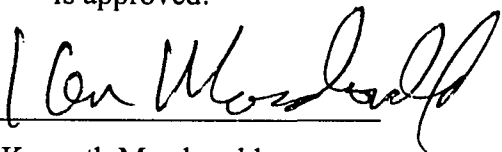
UMI Microform 3208727

Copyright 2006 by ProQuest Information and Learning Company.
All rights reserved. This microform edition is protected against
unauthorized copying under Title 17, United States Code.

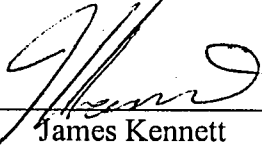
ProQuest Information and Learning Company
300 North Zeeb Road
P.O. Box 1346
Ann Arbor, MI 48106-1346

The dissertation of Robert Charles Decesari

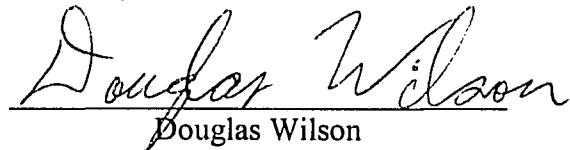
is approved:



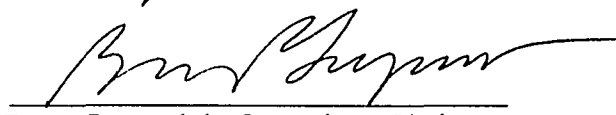
Kenneth Macdonald



James Kennett



Douglas Wilson



Bruce Luyendyk: Committee Chairman

March, 2006

ACKNOWLEDGMENTS

First and foremost I would like to thank my academic advisor, Bruce Luyendyk, for his guidance, support, and interest throughout my graduate studies. I am extremely grateful for his frequent help, advice with my project, and for always urging me on to the next level. I have learned much from him regarding research, writing, and good science. Bruce's enthusiasm and professionalism have made being a graduate student at UCSB a pleasure. I would also like to thank Doug Wilson for his guidance with my project. Doug knows a lot about everything and has played an integral part in my research. I am grateful for being able to discuss ideas with him and asking question about how things work. Thanks are due to Jim Kennett and Ken Macdonald for their help with guiding my graduate career and for their outside view of my research. I am very grateful for the time and effort my committee has invested in me.

Without Chris Sorlien, I would still be trying to figure out how to get the seismic processing software working! Chris has come to my rescue numerous times when everything was going wrong. He has gone from being a teacher to a colleague and friend. We have an inside joke that he is the world's best seismic interpreter. But always remember Chris, I'm faster and will come up with the same interpretation! Between the two of us, we make a great team.

I would like to thank the captain, crew, and science personnel of the RVIB *Nathaniel B. Palmer* for two excellent and exciting cruises across the Ross Sea.

Without them and their expertise, the data I worked with would not be nearly as good. John Diebold can be credited with the excellent quality of our seismic data. I learned a lot from him about how to acquire first class seismic data. Thanks are due to Matt Ralston and Dan Herold, from Parallel Geoscience, for taking time to come to Antarctica and assist with top-notch ship board data processing. Much was learned from them. Special thanks to Matt Ralston for his expertise and help in solving processing problems back at UCSB. Also, thanks to Seismic Micro Technology for use of their Kingdom Suite seismic interpretation software.

Thank you to UCSB students Tom Carpenter, Emily Crawford, Tonya Del Sontro, Michael Faulkner, Sarah Hopkins, Jared Marske, Robin Matoza, Adam Morely, Gabriel Rotberg, Catherine Schindler, Michelle Thibault, Michael Tritchler, and Karen Vasko, for participating in the Ross Sea cruises. These students helped to make sure the cruises were successful. Michael Faulkner, Sarah Hopkins, Robin Matoza, and Adam Morely participated in research projects that included processing and interpreting Ross Sea data. Their work has been incorporated into this dissertation. Special thanks to Michael Faulkner for setting up the Matlab subsidence code. Thank you to Dr. Lou Bartek his students Laura Callihan, Dan Pignatiello, Heather Ramsey, Kathryn Sowder, Jeffery Warren, Brandon Wood, and Pres Viator from the University of North Carolina for also participating in the Ross Sea cruises. This research has primarily been funded by the National Science Foundation, Office of Polar Programs and fellowships from the UCSB Affiliates and the Department of Earth Science, University of California, Santa Barbara.

For most of my time at UCSB, Susie Leska was the person in charge of making sure all of the grads had our paper work together and took our exams on time. I would like to thank Susie for her help and dedication to her job. I would also like to thank her for being a great friend and always listening to me complain about the inevitable obstacles that come with research. The graduate students at UCSB made the daily grind fun and exciting. Special thanks to Chris Ehrhardt for the daily ping pong games. Our little rivalry was always a nice break from interpreting data. I will miss our one o'clock game time!

The support of my family has been exceptional throughout my pursuit for a Ph.D. My grandparents, my uncle, and my parents have given me nothing but encouragement throughout this degree. I thank you all very much. Special thanks to my parents, Robert J. and Susan Decesari, for standing by me along this journey. They have instilled in me the ability to work hard and never give up. And finally, my fiancé, Sarah Hopkins, and daughter, Chloe, have been a constant source of inspiration and support. Sarah has helped me formulate ideas and make my work better. She has taken time out of her hectic schedule to listen to my thoughts and read my work. In many ways she has been my partner in the research I have done. Quite literally, this dissertation brought us together. Chloe has contributed too by helping me interpret seismic data even at 4 years of age. She told me once that she was looking at mountains in the seismic sections one day....she was quite right! But more importantly, Chloe always puts a smile on my face. I dedicate this volume to my Mom, Dad, Sarah, and Chloe. Thank you for all of your love and support.

VITA

Robert C. Decesari

EDUCATION

Bachelor of Science in Earth Science, Minor in History, University of California,
San Diego, 2001

Doctor of Philosophy in Geological Sciences, University of California, Santa
Barbara, March 2006 (expected)

POSITIONS

Graduate Student Research Assistant, Dept. of Earth Science, University of
California, Santa Barbara, 2001-2006

Teaching Assistant, Dept. of Earth Science, University of California, Santa Barbara,
2002-2003

Undergraduate Research Assistant, Scripps Institution of Oceanography, University
of California, San Diego, 2000-2001

AWARDS

UCSB Affiliates Doctoral Dissertation Fellowship, 2005

Geological Sciences Doctoral Fellowship, UCSB, 2001

Preston Cloud Fellowship, Department of Geological Sciences, UCSB, 2001

Eagle Scout, Boy Scouts of America, 1996

PUBLICATIONS

Decesari R.C., Wilson D. S., Faulkner, M., Luyendyk B. P., Sorlien C. C., A model for Cretaceous and Tertiary extension of the Ross Sea, Antarctica, AGU, Vol. 85, Fall Meeting Suppl., Abstract, T53E-08, 2005.

Decesari R.C., Luyendyk B. P., Bartek L. R., Sorlien C. C., Wilson D. S., Diebold J. D. Hopkins S. E., Ice Shelf Drill Sites Proposed to Study Pre-Late Oligocene Climate and Tectonic History, Coulman High, Southwestern Ross Sea, Antarctica, AGU, Vol. 85, Fall Meeting Suppl., Abstract, F5320, 2004.

Decesari R.C., Sorlien C.C., Luyendyk B.P., Bartek L.R. Diebold, J.B. and Wilson, D.S., Tectonic Evolution of the Coulman High and Central Trough along the Ross Ice Shelf, Southwestern Ross Sea, Antarctica, AGU, Vol. 84, Fall Meeting Suppl., Abstract, F1343, 2003.

Decesari, R. C., Luyendyk, B.P., Bartek, L.R., Diebold, J.B., Sorlien, C.C., Wilson, D.S., Tectonic Evolution of the East Flank of the Victoria Land Basin Along the Ross Ice Shelf, Southwestern Ross Sea, Antarctica, ISAES Abstract, 2003

Luyendyk, B.P., Wilson, D. S., Decesari, R.C., New Maps of Gravity and Bedrock-Bathymetry of the Ross Sea Sector of Antarctica, AGU, Vol.83, Fall Meeting Suppl., Abstract, 2002.

Sclater, J.G. and Decesari, R.C., A Compilation of Marine Heat Flow Data within the Gulf of California and the California Borderland, Scripps Institution of Oceanography Reference Series, No. 01-04, 2001.

FIELDS OF STUDY

Major Field: Development of Continental Rift Systems, Tectonics, and Exploration Geophysics.

Studies in Tectonics: Professor Bruce Luyendyk and Professor Ken Macdonald.

Studies in Basin Evolution: Dr. Douglas Wilson and Professor Bruce Luyendyk.

Studies in Seismic Stratigraphy: Dr. Christopher Sorlien, Professor Bruce Luyendyk, and Professor James Kennett.

ABSTRACT

The Mesozoic and Cenozoic Depositional, Structural, and Tectonic Evolution of the Ross Sea, Antarctica

by
Robert Charles Decesari

Many first order questions have not been answered regarding the timing and magnitude of tectonic events in the Ross Sea. New geophysical data collected across the Ross Sea were used to investigate the structural framework and tectonic history of the region. Outstanding questions include: 1. What is the timing and magnitude of tectonic events in the Ross Sea?, 2. What is the subsidence history of the Ross Sea, 3. What does the sedimentary infill tell about the tectonic history of the Ross Sea?

New multichannel seismic reflection data, collected in front of the Ross Ice Shelf, shows that Oligocene sediments can be correlated between the Ross Sea basins. Below the Oligocene sediment are two synrift packages that are interpreted across the Ross Sea. The synrift sediments suggest two phases of Ross Sea extension and have not been sampled. Extension most likely occurred in the Cretaceous, resulting in crustal thinning of the region. A second extension phase probably occurred in the Tertiary and was associated with seafloor spreading of the Adare Trough north of the Ross Sea. Potential drill sites designed to target pre-Oligocene synrift strata have been selected along the Ross Ice Shelf front and plan on using the ice shelf as the drilling platform.

Subsidence modeling indicates that Cretaceous extension, followed by Tertiary extension can explain the observed Ross Sea subsidence. Crustal models constrained by subsidence results indicate the Ross Sea was a region of thickened, elevated crust, significantly above sea level prior to Cretaceous rifting. Cretaceous extension thinned the crust to the present-day thickness of the Ross Sea basement highs. Further extension in the Tertiary thinned localized regions of the Ross Sea resulting in the formation of the present-day basins. All extension was completed by 30 Ma as constrained by the stratigraphic record. Thermal subsidence resulted in accommodation space for the deposition of Oligocene and younger sediments. The Transantarctic Mountains may be a high remnant piece of the pre-extension Ross Sea lithosphere that was not extended by either the Cretaceous or Tertiary rifting events.

TABLE OF CONTENTS

ACKNOWLEDGEMENTS	iv
VITA	vii
ABSTRACT	ix
<hr/>	
Preface	1
<hr/>	
Chapter 1: Tectonic and Geological History of the East Gondwana Margin: Similarities between the New Zealand, Tasmanian Region, and the Ross Sea Sector of Antarctica	3
1) Introduction	3
2) Gondwana Breakup	4
3) Tectonic and Geological Description of the Ross Sea, Antarctica	9
4) Tectonics and Geology of Marie Byrd Land, West Antarctica	15
5) Tectonic and Geological Description of the New Zealand Region	25
6) Tectonic and Geological Description of the Tasmanian Region	34
7) Integrated History of the Circumpacific Region	38
8) Outstanding Problems	47
<hr/>	
Chapter 2: Regional Seismic Correlations of the Ross Sea: Implications for the Tectonic History of the West Antarctic Rift System	57
Abstract	57
1) Introduction	58
2) Seismic Reflection Data and Methods	64
3) Correlation Results	68
4) Discussion: Implications for the Tectonic History of the Ross Sea	84
5) Summary and Conclusions	92
<hr/>	

Chapter 3: A Model for Two Stage Extension of the Ross Sea	99
Abstract	99
1) Introduction	100
2) Geohistory and Backstripping Methods	103
3) Observations and Results	114
4) Discussion	122
5) Conclusions	137
<hr/>	
Chapter 4: The Tectonic Framework of the Coulman High and Central Trough; Implications for Ice Shelf Drill Sites Proposed to Study Ross Sea Climate and Tectonic History	146
Abstract	146
1) Introduction	147
2) Geophysical Data	148
3) Interpretations and Observations	151
4) Discussion	163
5) Summary and Conclusions	178
<hr/>	
Chapter 5: A Model for the Tectonic Evolution of the Ross Sea	185
<hr/>	
Appendix A: NBP-0301 and NBP-0306 Cruise Details	194
Appendix B: Seismic Processing	204
Appendix C: Seismic Processing Lists	213
Appendix D: Interpretation and Archiving	217
Appendix E: DSDP Site 270, 271, and 271 Core Data	219
Appendix F: Backstripping Technique and Code	222

LIST OF FIGURES

Chapter 1

Figure 1-1	8
Figure 1-2	10
Figure 1-3	14
Figure 1-4	27
Figure 1-5	36
Figure 1-6	45

Chapter 2

Figure 2-1a	60
Figure 2-1b	61
Figure 2-1c	62
Figure 2-2	67
Figure 2-3a	70
Figure 2-3b	71
Figure 2-4	74
Figure 2-5	75
Figure 2-6	76
Figure 2-7	79
Figure 2-8	82

Chapter 3

Figure 3-1	102
Figure 3-2	105
Figure 3-3	109
Figure 3-4a	115
Figure 3-4b	116
Figure 3-5	118

Figure 3-6	119
Figure 3-7	120
Figure 3-8	125
Figure 3-9a-c	127
Figure 3-9d-f	128
Figure 3-10	135

Chapter 4

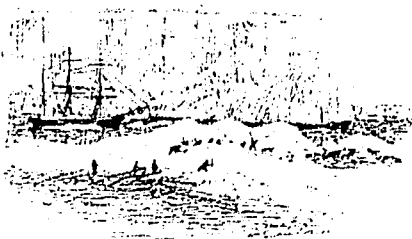
Figure 4-1	149
Figure 4-2	150
Figure 4-3	153
Figure 4-4	154
Figure 4-5	158
Figure 4-6a & b	159
Figure 4-6c	160
Figure 4-7	170
Figure 4-8	173
Figure 4-9	176

Appendix A

Figure 1	203
----------	-----

Appendix B

Figure 1	207
Figure 2	211
Figure 3	212



Preface

The Ross Sea is an unique area to study the formation and evolution of continental rift systems due to its remoteness, harsh environment, and difficulty obtaining data. Because of these reasons, many first order questions regarding the tectonic history and formation of the Ross Sea have remained unanswered. Some of these questions include: What is the relationship between stratigraphy of the eastern Ross Sea to the stratigraphy of the western Ross Sea? What can the stratigraphic record tell about the tectonic and climatic history of this sector of Antarctica? What is the timing and magnitude of extension in the Ross Sea? Was there Cenozoic motion between East and West Antarctica? What was the pre-rift Ross Sea crustal structure?

This dissertation uses newly acquired geophysical data from across the Ross Sea to investigate these questions and to test the hypothesis that the Ross Sea was a region of thick continental crust, with significant elevation above sea level, prior to the onset of Cretaceous extension. Parallel geology from conjugate rift margins, once attached to the Ross Sea region, are used to determine similarities with the geology of the Ross Sea. Only a handful of widely spaced core holes constrain the stratigraphy of the Ross Sea. Furthermore, a complete stratigraphic section has not yet been sampled

anywhere in the Ross Sea. Therefore, comparison of geology from conjugate rift margins is needed to infer stratigraphic and tectonic history of the Ross Sea. Geologic parallels are also drawn from the Transantarctic Mountains and western Marie Byrd Land to better understand the tectonic evolution of the West Antarctic Rift System (WARS) and the Ross Sea.

The WARS has significant implications for the evolution of the present day plate boundaries of the Southern Ocean and the tectonic and structural development between East and West Antarctica. Tectonic events in the Southern Ocean have been shown to result in major global climatic and environmental changes. Therefore, the sedimentary fill of the Ross Sea likely records the onset of global cooling and the formation of the east and west Antarctic ice sheets. The Ross Sea also has important implications for understanding the development of other continental rift systems such as the West African Rift, the Basin and Range of western North America and the continued opening of the Gulf of California.



Chapter 1

Tectonic and Geological History of the East Gondwana Margin: Similarities Between the New Zealand, Tasmanian Region, and the Ross Sea Sector of Antarctica

1-1. Introduction

The complex tectonic setting of the South Pacific region can be traced to the Mesozoic breakup of the Gondwana super-continent. Prior to the breakup, Gondwana included the present-day continents of South America, Africa, Australia, Antarctica, and the New Zealand subcontinents. Tectonic forces began to rift Gondwana apart during the middle Cretaceous resulting in the development of the present-day plate boundaries of the southern ocean. This chapter will focus on the middle to Late Cretaceous rifting of the New Zealand and Tasmanian region from the Ross Sea sector of Antarctica. More specifically, the tectonic histories of the Ross Sea-Marie Byrd Land sectors of Antarctica and the Campbell Plateau-Chatham Rise-New Zealand-Tasman Rise regions are examined by comparing the geologic records interpreted on each side of the Pacific-Antarctic spreading center.

1-2. Gondwana Breakup

During the early to mid-Mesozoic, East Gondwana included what are now the New Zealand subcontinents, the Tasman Rise and the Ross Sea/Marie Byrd Land sectors of Antarctica. The New Zealand subcontinents are composed of the North and South Islands, Lord Howe Rise, Chatham Rise and the Campbell Plateau (Fig.1-1a). They were situated adjacent to the Ross Sea margin of West Antarctica (WANT) before rifting initiated the breakup of the supercontinent.

Prior to the breakup, collisional tectonics occurred between the now defunct Phoenix Plate and Gondwana. Throughout the Mesozoic, the Phoenix Plate was subducting under East Gondwana. According to Bradshaw [1989], the tectonic regime change at 105 Ma, from collisional to extensional tectonics throughout the region, is supported by the onset of extension between Australia and East Gondwana at 125 Ma (Fig. 1-1a). Rifting may have continued eastward between New Zealand and Antarctica [Laird, 1993; Lawver and Gahagan, 1994]. The onset of seafloor spreading between Australia and East Antarctica (EANT) began by 95 Ma, while seafloor spreading between the New Zealand continental fragments and Antarctica did not begin until after 83 Ma [Stock and Cande, 2002].

Although spreading rates were fast in the Pacific during the Cretaceous, the rate of subduction between the Phoenix Plate and Gondwana was greater than the rate of spreading. As a result, the Pacific-Phoenix spreading ridge slowly migrated toward the subduction zone. Eventually spreading ceased outboard of the subduction zone along the Pacific margin of Australia, New Zealand and WANT [Bradshaw, 1989;

Lawver and Gahagan, 1994; Luyendyk, 1995; Larter, 2003]. By 105 Ma, spreading ceased along the northern margin of New Zealand, resulting in the end of subduction and reorganization of plate boundaries that transferred New Zealand continental crust to the Pacific Plate [Bradshaw, 1989; Lawver and Gahagan, 1994; Luyendyk, 1995]. Continued cessation of the Pacific-Phoenix spreading center continued along the WANT continental margin [Bradshaw, 1989; Lawver and Gahagan, 1994; Luyendyk, 1995].

Initiation of extension at 105 Ma denotes the initial break up of this sector of Gondwana. One possible mechanism for the shift to extension is through the slab capture theory proposed by Luyendyk [1995]. As the Pacific-Phoenix ridge ceased spreading near the trench, the subducting Phoenix slab was transferred to the Pacific Plate. The down going Phoenix slab acquired the motion of the Pacific Plate, which was moving north with respect to Gondwana. The subducted slab was pulled north, and due to friction, the overlying continental crust extended in the direction of Pacific Plate motion. The immediate response to the Pacific-Phoenix ridge demise was extension in the New Zealand region and the initiation of Tasman Sea spreading [Bradshaw, 1989; Luyendyk, et al., 2001].

Mid Cretaceous extension of the New Zealand region occurred primarily between western New Zealand and the Campbell Plateau, resulting in the formation of the Great South Basin (GSB) rift system (Fig. 1-1a) [Lawver and Gahagan, 1994; Cook, et al., 1999]. The rift system is thought to have connected to the remaining Pacific-Phoenix ridge to the west and east of New Zealand [Lawver and Gahagan,

1994; *Cook, et al.*, 1999]. Beggs [1993] suggests rifting of the GSB may overlap in time with the last stages of subduction on the northeast margin of New Zealand. Grabens interpreted in the GSB may be an example of foreland extension related to plate convergence [Beggs, 1993]. Graben systems within the GSB are mostly part parallel to the trend of the Late Cretaceous spreading axes that formed during the rifting of New Zealand from Antarctica [Adams, 1986; Laird, 1993]. Rift systems of similar age to the GSB are known to exist onshore the South Island of New Zealand [Beggs, 1993].

As the Pacific-Phoenix ridge died west of New Zealand, the active segments of the ridge to the east of New Zealand most likely resulted in deformation between the Campbell Plateau and Chatham Rise, propagating into the Bounty Trough (Fig. 1-1a) [Lawver and Gahagan, 1994]. Rifting started at approximately 100 Ma in this sector with the main phase of rifting forming horst and grabens on the Chatham Rise, accompanied by widespread volcanism [Wood and Herzer, 1993]. By 90 Ma the Chatham Rise rifted off and the opening of the Bounty Trough commenced [Larter, et al., 2002]. The Bounty Trough may represent an extension of the Lord Howe Rise Rift System that was active in the Tasman Sea during this period [Laird, 1993]. As cessation of the Pacific-Phoenix spreading center continued east, crustal extension shifted to between East and West Antarctica in the Ross Sea region during the mid-Cretaceous (~95 Ma) (Fig 1-1a). Extension at this time is thought to have formed the rifted continental crust of the Ross Sea. The Ross Sea is a series of rift basins bounded by the Marie Byrd Land (MBL) continental block of WANT to the east and

the Transantarctic Mountains (TAM) to the west. This extension may have resulted in crustal thinning of the Ross Sea and the formation of the four major depositional basins [Davey and Brancolini, 1995].

By 85 Ma major plate reorganizations occurred as the western most branch of the Pacific-Phoenix spreading ridge east of New Zealand ceased spreading. At this time a new Pacific-Antarctic spreading center propagated from the Pacific-Antarctic-Farallon triple junction in the east, to between the Campbell Plateau and MBL sector of Antarctica at 83 to 79.1 Ma (Fig. 1-1b) [Adams, 1986; Lawver and Gahagan, 1994; Larter, et al., 2002]. Generation of oceanic lithosphere between New Zealand and WANT commenced with the rifting of the Campbell Plateau from MBL and eastern Ross Sea at approximately 79.1 Ma (Fig. 1-1b) [Davey and Brancolini, 1995; Larter, et al., 2002; Stock and Cande, 2002]. The oldest identified magnetic anomaly offshore and south of the Campbell Plateau is Chron 33y (~73.6 Ma). The old edge of Chron 33 (79.1 Ma) is not continuously observed on the ocean floor off the Campbell Plateau. As a result, rifting between the Campbell Plateau and MBL, as well as the production of oceanic lithosphere, was still in its early stages at 79 Ma [Adams, 1986; Larter, et al., 2002; Stock and Cande, 2002]. However, seafloor adjacent to the Chatham Rise contains the old edge of Chron 33, indicating that oceanic lithosphere was being created between the Chatham Rise and WANT before rifting of the Campbell Plateau and the Ross Sea region progressed to full seafloor spreading [Adams, 1986; Larter, et al., 2002; Stock and Cande, 2002].

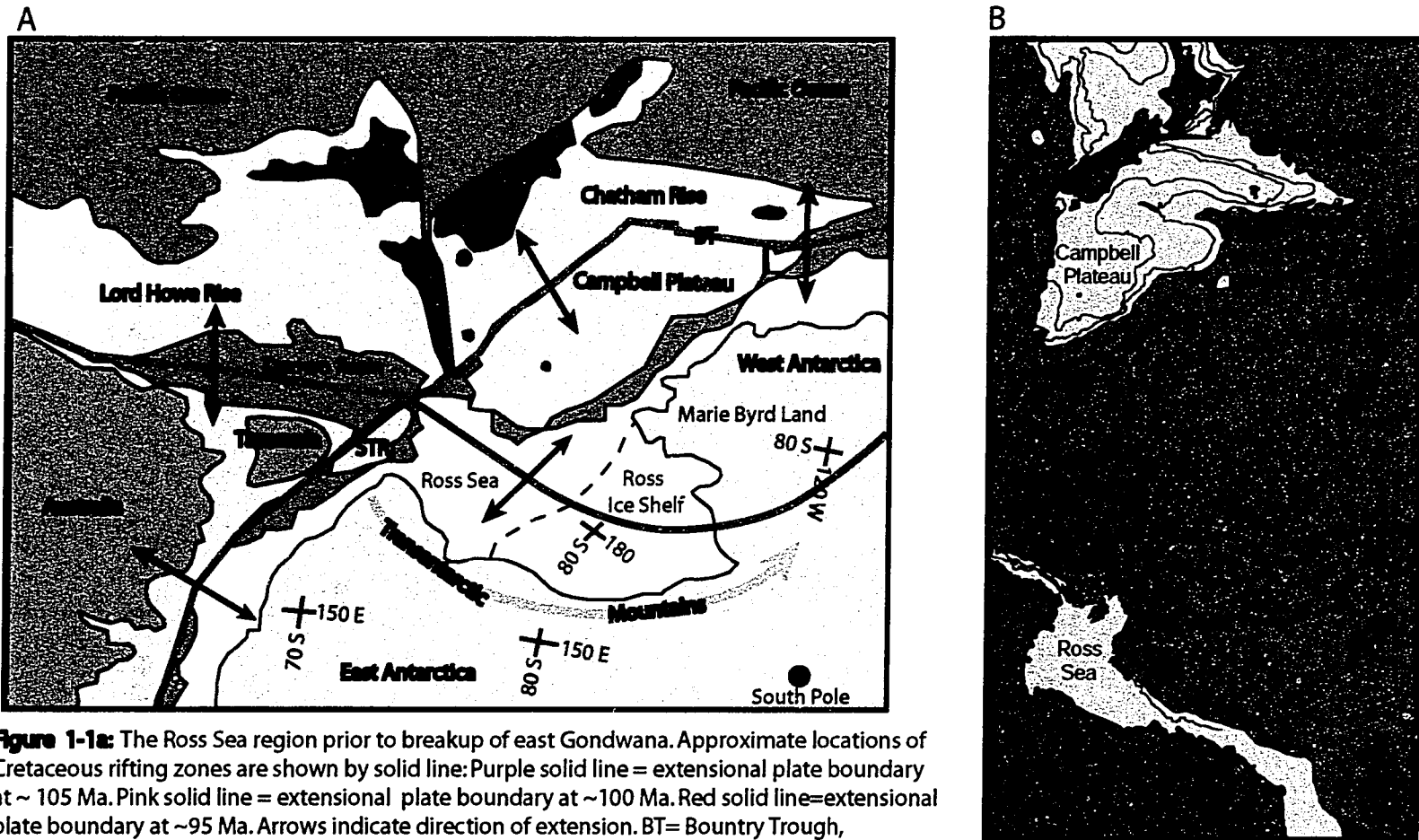


Figure 1-1a: The Ross Sea region prior to breakup of east Gondwana. Approximate locations of Cretaceous rifting zones are shown by solid line: Purple solid line = extensional plate boundary at ~ 105 Ma. Pink solid line = extensional plate boundary at ~100 Ma. Red solid line=extensional plate boundary at ~95 Ma. Arrows indicate direction of extension. BT= Bounty Trough, STR = South Tasman Rise. Figure modified from Grindley & Davey [1982]; Luyendyk et.al. [1992]. Plate boundaries from Lawver and Gahagan [1994]. **1-1b:** Present-day plate configuration of the Southwest Pacific region. Seafloor spreading initiated between WANT and the Campbell Plateau at 79 Ma. Adare Trough spreading initiated in the Eocene. After Luyendyk et.al. [2001]; Isochrons from Cande et.al. [2000] & Stock and Cande [2002].

1-3. Tectonic and Geological Description of the Ross Sea, Antarctica

The structural framework of the Ross Sea is four, north-south trending depocenters across the continental shelf. The four main basins are: the Victoria Land Basin (VLB), Northern Basin (NB), Central Trough (CT) and Eastern Basin (EB) (Fig 1-2) [Davey and Brancolini, 1995]. The basins form asymmetrical grabens up to 175 km wide and are filled with up to 8 km of layered strata [Cooper, et al., 1991]. Strata in the EB comprise the Ross Sea Sequences (RSS) and are numbered from RSS-1 (oldest) through RSS-8 (youngest) [Cooper, et al., 1995; Davey and Brancolini, 1995; Luyendyk, et al., 2001]. The sequences are separated by unconformities numbered RSU1 (youngest) through RSU7 (oldest) (Fig. 1-3). The Ross Sea is bounded to the west by the TAM and to the east by the mountain ranges of western Marie Byrd Land. It is widely believed that two main rifting episodes occurred in the Ross Sea region, forming the West Antarctic Rift System (WARS). The first being an early non-magmatic rifting event throughout the Ross Sea that formed the main depocenters and the second was a late rifting event associated with alkali basalt volcanics localized in the western sector of the Ross Sea [Davey and Brancolini, 1995].

The WARS is a region of extended lithosphere between cratonic East Antarctic and the microplates of Pacific West Antarctica [Dalziel and Elliot, 1982; LeMasurier and Rex, 1990; Luyendyk, et al., 2003] and comprises one of the largest extensional regions on Earth, comparable to the Basin and Range province of western

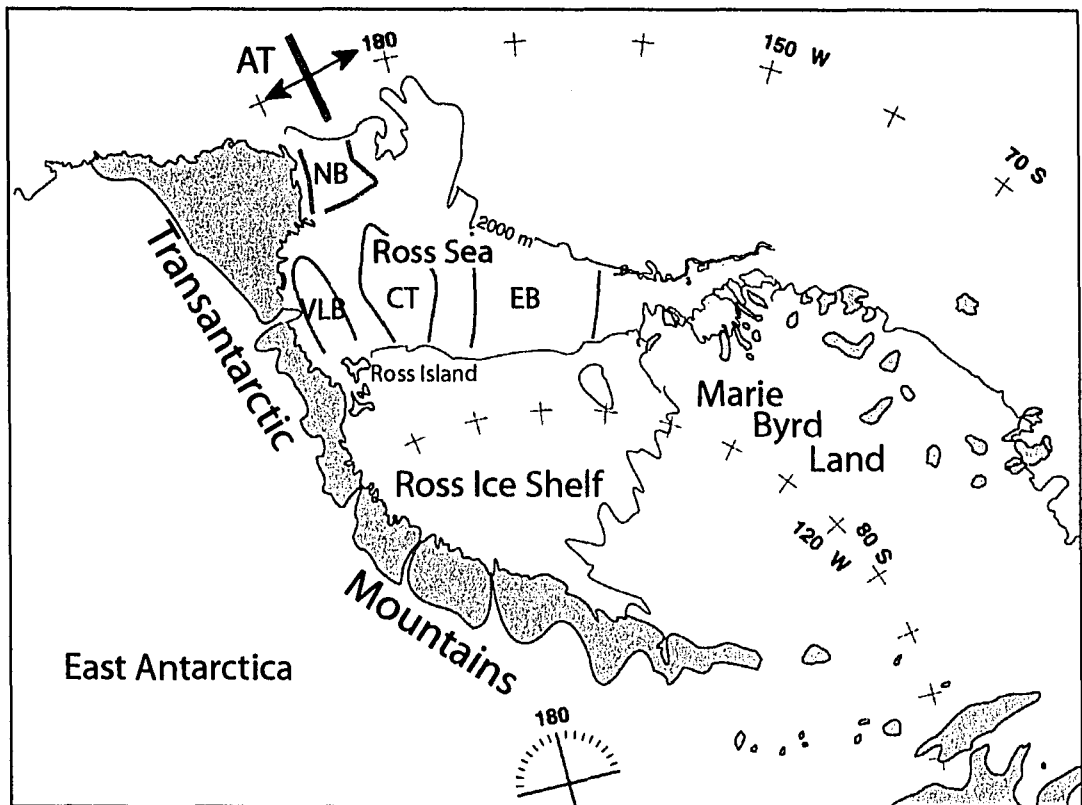


Figure 1-2: Ross Sea region map showing locations of the major sedimentary basins and the Transantarctic Mountains. AT, Adare Trough (arrows indicate former spreading direction [Cande et.al. 2000]); NB, Northern Basin; VLB, Victoria Land Basin; CT, Central Trough; EB, Eastern Basin.

North America. For the most part, the WARS is overlain by the West Antarctic Ice Sheet (WAIS) and the Ross Ice Shelf, making it difficult to determine the tectonic history of the region. Although the full extent of current activity of the West Antarctic Rift System is not completely understood, many researchers consider the western rift shoulder to be active because of Cenozoic volcanism that is currently occurring there. The most prominent topographic feature of the WARS east of the TAM is wMBL. The tectonic history of the eastern side of the rift and its relation the western side of the rift has remained largely unknown due to the lack of data.

1-3.1. Ross Sea Basement

Cores obtained from Deep Sea Drilling Program DSDP Site 270, in the eastern Ross Sea, indicate the basement in this location is dense, non-magnetic Cretaceous mylonite [Hayes, et al., 1975]. Dredging off Cape Colbeck has also recovered well linedated Cretaceous mylonitic-granitic gneiss, as well as both Cretaceous Swanson Formation metasediments and Byrd Coast granites [Luyendyk, et al., 2001; Siddoway, et al., 2004]. The mylonites exhibit fabrics indicative of a brittle-ductile shear zone [Luyendyk, et al., 2001]. Other constraints on Ross Sea basement can be drawn from parallels with the Greater New Zealand region. The basement rocks of the Campbell Plateau are Paleozoic metasediments faulted into grabens and half-grabens [Beggs, 1993]. These rocks correlate to the quartz meta-turbidites of the Greenland Group on South Island, New Zealand, the Lachlan Group in Australia, the Robertson Bay Group in northern Victoria Land, and to the Swanson

Formation in western Marie Byrd Land (wMBL) [Coney, et al., 1990; Cooper and Tulloch, 1992; Bradshaw, et al., 1997]. Also, the basement of the Campbell Plateau is intruded by mid-Cretaceous granites and may be correlated to the Byrd Coast granites in wMBL [Luyendyk, et al., 2001]. Luyendyk, et al. [2001] proposed basement rocks identified on the Colbeck Shelf in the eastern Ross Sea are Swanson Formation and Byrd Coast granites of wMBL.

Major tectonic features of the western Ross Sea include the VLB and the TAM. The major exhumation of the TAM has been linked to E-W extension in the Eocene [Fitzgerald, 1992; Davey and Brancolini, 1995; Hamilton, et al., 2001]. Evidence for mid-Cretaceous exhumation of the western TAM has been shown by Fitzgerald, et al. [2000]. Apatite fission track ages indicate that significant exhumation of the TAM in southern Victoria Land began at ~55 Ma [Fitzgerald, 1992, 1994, 1999]. Magnetic anomaly data across the Adare Trough, north of the western Ross Sea, indicates up to ~180 km of E-W seafloor spreading in the Eocene [Cande, et al., 2000]. This event may have influenced extension in the western Ross Sea and can account for Eocene extension of the VLB (Fig.1-2) [Cande, et al., 2000; Hamilton, et al., 2001; Stock and Cande, 2002]. Normal faults interpreted in the VLB, parallel to the TAM front, are interpreted as controlling the major subsidence of the VLB, indicating the VLB basin fill may be of Eocene age and younger strata [Hamilton, et al., 2001].

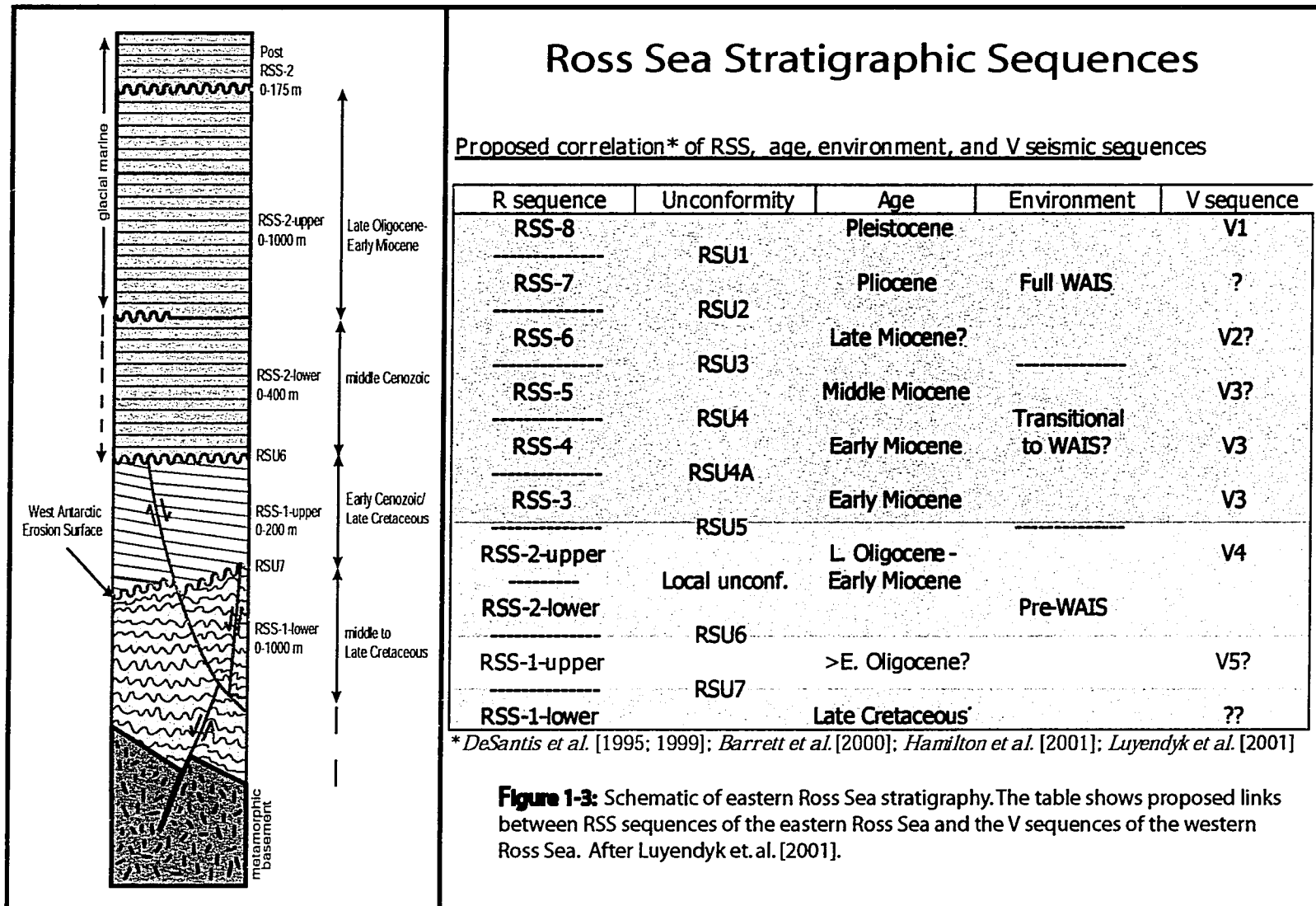
Within the TAM are the widespread Jurassic Kirkpatrick Basalts and the Ferrar Dolerites [Kyle, et al., 1981; Elliot, 1992]. Also widespread throughout the

TAM is the Paleozoic Beacon Sandstone, interpreted in the Cape Roberts Project core holes in McMurdo Sound [*Cape-Roberts-Science-Team*, 2000]. These rocks found in the TAM may be present in the VLB or elsewhere in the Ross Sea.

1-3.2. Stratigraphy of the Ross Sea

Deep Sea Drilling Project (DSDP) Site 270 sampled a synrift sedimentary breccia in a basement half-graben. The seismic character of the sedimentary breccia at DSDP Site 270 is characterized by “disrupted stratal reflectors”, distinctive of a synrift unit [Busetti and Zayat, 1994]. Drilling results indicate the unit was locally derived in a subaerial environment [Hayes and Frakes, 1975]. Luyendyk et al. [2001] named the synrift unit RSS-1-lower and renamed the early Oligocene (?) or older RSS-1 unit of Hinz and Block [1984], RSS-1-upper. RSS-1-lower is separated from RSS-1-upper by angular unconformity RSU7 (Fig. 1-3) [Luyendyk, et al., 2001]. RSS-1-lower is assumed to have been deposited and deformed in the early Late Cretaceous, consistent with ages obtained for basement rocks [Luyendyk, et al., 2001]. Unconformity RSU7 and overlying RSS-1-upper are deformed by normal faults. RSS-1-upper is characteristic of a synrift unit.

Separating the RSS-1-upper from overlying RSS-2 is angular unconformity RSU6 (Fig. 1-3). Both RSS-1-upper and unconformity RSU6 were not sampled by the DSDP. Unconformity RSU6 is interpreted as the boundary between glacially derived strata above and terrigenous rift related strata below. Units above RSU6 are un-deformed except for a slight westward tilt [Luyendyk, et al., 2001]. The RSS-2



sequence is interpreted as late-Oligocene-early Miocene in age [Hayes and Frakes, 1975; Hayes, et al., 1975] and is broken into the RSS-2-upper and RSS-2-lower units [Luyendyk, et al., 2001]. RSS-2-upper has been constrained to the Late Oligocene, indicating that RSS-2-lower is older [Hayes, et al., 1975; Luyendyk, et al., 2001]. Above the RSS-2 unit are unconformities RSU5 through RSU1, separating post RSS-2 glacially derived sequences RSS-3 through RSS-7.

1-4. Tectonics and Geology of Marie Byrd Land, West Antarctica

The geologic histories of the Campbell Plateau and Chatham Rise should be similar to their Antarctic counterparts up to ~79 Ma, at which point the production of oceanic lithosphere between the New Zealand region and Antarctica began. Although there are many similarities in the Mesozoic geology of MBL and New Zealand, several contrasts can be made. During the Mesozoic, deformed accretionary complex rocks dominated New Zealand. With the advent of extension throughout the region, basins formed along the New Zealand margin conjugate to an uplifted MBL [Weaver, et al., 1994].

1-4.1. Marie Byrd Land

Marie Byrd Land is usually regarded as a single continental block. However, paleomagnetic studies suggest that during Cretaceous times MBL consisted of a system of microplates and accreted terranes [DiVenere, et al., 1994; Luyendyk, et al., 1996; Pankhurst, et al., 1998]. Even though thick ice sheets cover most of wMBL,

exposed outcrops reveal a Cambrian-Ordovician meta-greywacke basement of Swanson Formation intruded by Mississippian-Devonian Ford granodiorite [Luyendyk, et al., 1992] and Cretaceous Byrd Coast Granite [Davey and Brancolini, 1995; Pankhurst, et al., 1998]. The basement is overlain by younger, Cenozoic basaltic volcanics with a Late Cretaceous to early Cenozoic (~80 to 28 Ma) erosion surface observed separating the two units [LeMasurier and Landis, 1996]. Mafic dykes are also observed parallel to the wMBL coast and are dated as middle to Late Cretaceous in age (108-104 Ma) [Storey, et al., 1999]. These dykes are interpreted to record the onset of breakup between MBL and New Zealand. Their emplacement into the MBL crust represent upwelling and decompression melting of subcontinental lithospheric mantle in response to extension [Weaver, et al., 1994].

Pre-Mesozoic basement rocks are thought to comprise two major belts in MBL, that can be correlated to Paleozoic superterrane identified on the New Zealand subcontinents [Bradshaw, 1989; Pankhurst, et al., 1998]. The superterrane are subdivided into the Western and Eastern Provinces. The Western Province is composed of mainly early Paleozoic rocks, intruded by late Paleozoic and late Mesozoic granitoids [Bradshaw, 1989]. The Eastern Province is composed of younger Permian to Cretaceous convergent margin structures. This includes volcanic arc complexes, forearc basins and accretionary rocks [Bradshaw, 1989].

The greywacke-argillite metaturbidites of the Swanson Formation, found in the Edward VII Peninsula and the northern Ford Ranges, are interpreted as metamorphosed in the Late Ordovician and are considered to be the oldest rocks in

MBL [Pankhurst, et al., 1998]. East of Edward VII Peninsula, in the Ford Ranges, outcrops of the late Paleozoic Ford Granodiorite are observed intruding into the Swanson Formation [Weaver, et al., 1994]. Geochemical analysis of the granodiorite suggests that parental magmas were generated by active subduction along the Gondwana margin and emplaced throughout the Late Devonian to Early Carboniferous [Pankhurst, et al., 1998].

The Fosdick metamorphic complex of the Ford Ranges is interpreted as forming in the Cretaceous, coinciding with igneous intrusions suspect of being rift related [Luyendyk and Smith, 1994; Siddoway, et al., 2004]. The proposed heat source for the generation of the metamorphic complex is a high geothermal gradient formed from the close proximity of the Pacific-Phoenix spreading center to the continental margin [Luyendyk and Smith, 1994; Siddoway, et al., 2004]. Metamorphism of crustal rocks occurred by 104 Ma and by 100 Ma, granites were intruded into the metamorphic complexes [Richard, et al., 1994]. This was followed by rapid exhumation, accompanied by N-NNE extension, consistent with dextral rifting [Luyendyk, et al., 1992]. Between 94 Ma and 80 Ma, the cooling rate in the Ford Ranges slowed significantly. Between 80 Ma and 70 Ma, a period of rapid cooling of crustal rocks began nearly coeval to the initiation of seafloor spreading between WANT and New Zealand [Richard, et al., 1994]. This can be related to further exhumation of the Fosdick metamorphic complex and possible N-S extension and faulting. Since 70 Ma, slow cooling and exhumation of the region occurred with possible minor faulting. As a result, a Late Cretaceous to early Tertiary erosion

surface developed over most of West Antarctica defining an uplifted region called the Marie Byrd Land Dome [LeMasurier and Landis, 1996]. A possible mechanism for uplift of the MBL Dome is the inception of Tertiary plume activity in Marie Byrd Land [LeMasurier and Landis, 1996].

Work by Luyendyk, et al. [2003] has shown three dominant fault and fracture patterns exist in the Ford Ranges. These populations include an ESE-WNW orientation, a NNW-SSE orientation, and a NE-SW trend [Luyendyk, et al., 2003]. Thermochronology and paleomagnetic data from these ranges suggest a first stage of NNE extension occurred 105-103 Ma [Luyendyk, et al., 1996; Luyendyk, et al., 2003]. Faulting and fracture patterns observed in the Ford Ranges indicate the eastern Ross Sea Rift, including wMBL, developed through NNE-SSW and NE-SW regional extension, deforming Cretaceous and older rocks [Luyendyk, et al., 2003].

Luyendyk, et al. [2003] proposes that the coastal wMBL, including the Ford Ranges, provides regional exposures of the basement geology and tectonic structure of the eastern WARS. They also propose that wMBL is a region of extended continental crust, with the boundary of this zone located just to the east of the Ford Ranges. A sub-ice volcanic field has been identified from magnetic anomalies and is situated along or near the eastern boundary of extended continental crust [Luyendyk, et al., 2003]. The width of the Ross Sea rift can be measured to be ~1200 km from this boundary to the TAM [Luyendyk, et al., 2003].

1-4.2. The West Antarctic Erosion Surface

The West Antarctic Erosion Surface (WAES) is a low relief, preserved surface that has been discovered along a 2,500 km coastal belt in the MBL sector of WANT. The surface consists of flat mountain summits, beveled granites, volcanic rocks, and metasedimentary rocks Cretaceous in age and older [LeMasurier and Landis, 1996]. The erosion surface is separated from late Cenozoic volcanic rocks above by low relief unconformities. Relief of the surface is less than 100 m throughout WANT and less than 50 m in most MBL localities [LeMasurier and Rex, 1989]. No evidence for multiple erosion surfaces has been found and dissection of the surface is not extensive. Also, no sedimentary rocks have been discovered anywhere on the surface [LeMasurier and Landis, 1996]. Although the surface is represented by multiple exposures in wMBL, the full extent of the WAES is poorly known.

Rocks cut by the WAES are composed of Paleozoic and Mesozoic granitic, volcanic, and metaclastic rocks dominated by granitoids. Rb-Sr and K-Ar dating revealed the granitoids range in age from 90 to 371 Ma, but 90-110 Ma are most common and are the youngest rocks beveled by the erosion surface [Adams, 1987; Pankhurst and Rowley, 1991; Weaver, et al., 1991; Mukasa, et al., 1994; Weaver, et al., 1994; LeMasurier and Landis, 1996]. The oldest rocks identified on the WAES are breccias with K-Ar ages of ~22.2 to 25.3 Ma [LeMasurier and Rex, 1989]. These data suggest the formation of the WAES occurred mainly in the Late Cretaceous to early Paleocene [LeMasurier and Landis, 1996].

Across the rift in New Zealand, is another well-preserved, low-relief erosion surface called the Waipounamu Erosion Surface. It occurs as a flat surface, approximately 100,000 km², which truncates upper Paleozoic-Mesozoic schist and greywacke [LeMasurier and Landis, 1996]. The surface is veneered in many areas by fluvial gravel and thin sequences of shallow-marine sediments [LeMasurier and Landis, 1996]. Offshore seismic profiles and scattered drill holes reveal a low-relief erosion surface beneath the Chatham Rise [Wood, et al., 1989], Challenger Plateau [Nathan, et al., 1986], Campbell Plateau [Houtz, et al., 1976], Otago continental shelf [Carter, 1988] and Canterbury Basin [Field and Browne, 1989] and is Late Cretaceous in age [LeMasurier and Landis, 1996]. These data indicate that the original surface may have been as extensive as 106 km² and was formed by fluvial erosion, followed by marine transgression and wave planation [LeMasurier and Landis, 1996].

The Chatham Islands contain exposures of the Waipounamu Erosion Surface closest to West Antarctica. The geological history recorded here is very similar to interpretations from the erosion surface on the South Island of New Zealand. The youngest surface exposures at this location are mid-Cretaceous graben-fill clastic rocks [Grindley, et al., 1977], resting unconformably on basement rocks composed of Jurassic schist [Adams and Robinson, 1977; Campbell and others, 1993; LeMasurier and Landis, 1996]. The basin fill contains igneous and metamorphic clasts, suggesting they were possibly derived from MBL prior to the breakup of the region [Grindley, et al., 1977; Dean, 1993; LeMasurier and Landis, 1996].

1-4.2.1: Formation of the WAES: The West Antarctic Erosion Surface and the Waipounamu Erosion Surface may have formed at approximately the same time before rifting initiated between the two regions. However, there are two different hypotheses for the formation of the WAES. Both interpretations will be explored in this section.

Hypothesis #1: The first interpretation comes from LeMasurier and Landis [1996]. After the breakup of the New Zealand region from WANT in the Late Cretaceous, tectonic activity throughout most of New Zealand was insignificant except for thermal subsidence [Carter, 1988; Beggs, 1993; LeMasurier and Landis, 1996]. The thermal subsidence during the Late Cretaceous (75-65 Ma) was accompanied by marine transgression and aggradation, which is recorded in the New Zealand sedimentary record. LeMasurier and Landis [1996] interpret this to mean the final leveling of the Waipounamu Erosion Surface occurred during this marine transgression and resulted from wave planation over large areas of the South Island of New Zealand.

Due to the low relief and the regional extent of the WAES, it is plausible that it could have formed under prolonged fluvial erosion, marine planation or a combination of the two [LeMasurier and Landis, 1996]. However, LeMasurier and Landis [1996] propose the possibility leveling took place by fluvial erosion graded to upland interior basins cut off from the sea does not seem likely. Therefore, if leveling began early in the breakup and continued after separation, the Late Cretaceous histories of the WAES and Waipounamu Erosion Surface are closely related, or are

the same, resulting from formation at sea level [LeMasurier and Landis, 1996]. LeMasurier and Landis [1996] argue that uplift and subsequent denudation of the WAES occurred during the formation of the Marie Byrd Land Dome in the Tertiary resulting from the initiation of a volcanic plume in MBL.

Hypothesis #2: The second interpretation comes from Luyendyk, et al. [2001]. Unlike LeMasurier and Landis [1996], who argue that the WAES formed at sea level, Luyendyk, et al. [2001] argues that the WAES remained largely above sea level during formation. The eastern Ross Sea may share a common tectonic history with MBL throughout much of the Cretaceous, with plutonism, extensional denudation, and the formation of the WAES [Luyendyk, et al., 2001]. This conclusion is based on the seismic evidence indicating the shelf of the eastern Ross Sea does not contain significant sediment thickness of early Tertiary age [Luyendyk, et al., 2001]. Reflection data collected in the eastern Ross Sea lack the thickness of marine sediments expected for a subsiding Cretaceous margin. Findings from DSDP Site 270 require a 54 my delay from the end of extension to the onset of marine sedimentation [Hayes, et al., 1975]. Luyendyk, et al. [2001] concludes that the shelf, and thus the WAES, remained high above sea level for much of this time period.

There are three possible explanations for the long absence of marine sedimentation according to Luyendyk, et al. [2001]: 1) the WAES may have formed significantly above sea level and slowly subsided to sea level in the eastern Ross Sea, 2) the WAES may have formed near sea level and then was submerged, yet sediment

starved, 3) formation could have been at sea level followed by a large delay between extension and subsidence.

The preferred interpretation for the origin of the WAES stated in Luyendyk, et al. [2001] is of a highly elevated WAES because the shelf of the eastern Ross Sea does not contain significant sediment thickness of early Tertiary age. Approximately 105 to 94 Ma the Ross Sea-Marie Byrd Land region was involved in an extensive orogeny, which involved significant magmatic input and an elevated thermal profile, followed by extreme denudation and faulting [Richard, et al., 1994; Smith, 1995; Luyendyk, et al., 2001]. Regionally distributed deformation, resulting from the formation of an extensional province, gave way to the rifting of the Campbell Plateau from Antarctica [Luyendyk, 1995]. Vertical tectonics between the Campbell Plateau and MBL do not agree with each other and have been explained by Luyendyk, et al. [1992] by using a continental rift detachment-fault model. High surface elevation is possible and thermal subsidence is likely due to the decay of the thermal anomaly [Luyendyk, et al., 2001]. Luyendyk, et al. [2001] interpret post-extensional vertical motion of the Ross Sea/wMBL region as being dominated by thermal subsidence of an elevated region. The WAES is explain by Luyendyk, et al. [2001] to have formed at its present elevation in MBL compared to LeMasurier and Landis [1996], who argue the WAES was uplifted from sea level to its present elevation by a Tertiary plume. Luyendyk, et al. [2001] also argues it is easier to accept the WAES forming well above sea level than for it to form at sea level and then be uplifted as much as 3km in Marie Byrd Land.

1-4.3. Mantle Plume Tectonics and West Antarctic Breakup?

Both Weaver, et al., [1994] and Storey, et al. [1999], propose that a mantle plume existed under West Antarctica during Cretaceous-Cenozoic times and played an important role in the Cretaceous rifting of New Zealand from MBL. They suggest that a plume was responsible for the large volume of magmatism in MBL during the mid-Cretaceous and for the uplift of MBL during that time. The Tertiary plume proposed by LeMasurier and Landis [1996] may be the remnants of a Cretaceous mantle plume and can explain the high elevation of the Marie Byrd Land Dome. Furthermore, the volcanic centers interpreted by Luyendyk, et al. [2003] in MBL may be surface expressions of the plume.

The conjugate block to MBL contains the 97 Ma Mandamus Complex of southern New Zealand and the 80 Ma alkaline volcanic rocks of the Chatham Islands. Both rock types are geochemically similar to mantle plume magmas. This indicates a mantle plume may have been present beneath the region and was tapped at the time of rifting of New Zealand from Marie Byrd Land [Weaver, et al., 1994]. Storey, et al. [1999] also propose that the Hikurangi Plateau, a large basaltic province north of the Chatham Rise, was erupted from this plume as the Pacific-Phoenix spreading center was ceasing and converging with the trench off the New Zealand crustal block. If these interpretations are correct, the Hikurangi Plateau, mid-Cretaceous volcanic rocks of southern New Zealand and Chatham Island, and the mid-Cretaceous dykes of MBL may have all been generated by a mantle plume, which aided in the rifting of the Campbell Plateau-Chatham Rise from West Antarctica [Storey, et al., 1999].

However, it is important to note the role of plume tectonics during Cretaceous time is not certain. The extensional regime that developed throughout the region was most likely related to the cessation of the Pacific-Phoenix spreading ridge and associated subduction zone under east Gondwana resulting in plate reorganization. However, Storey, et al. [1999] proposes the eventual locus of seafloor spreading between the Campbell Plateau-Chatham Rise and Marie Byrd Land was controlled by the position of a mantle plume during the mid to Late Cretaceous. Furthermore, a Cretaceous plume may account for contrast between a thermally buoyant and uplifted Marie Byrd Land crustal block and its conjugate New Zealand margin, which subsided and continued to extend as it moved away from the effects of the plume [Weaver, et al., 1994].

1-5. Tectonic and Geologic Description of the New Zealand Region

From the Late Paleozoic to Early Cretaceous most of the rocks in the New Zealand region were formed under the influence of subduction and collisional tectonics. These rocks include remnants of magmatic arcs, forearc basins and accretionary complexes [Laird, 1993]. Basement rocks throughout the region are broken into two major terranes termed the Western and Eastern Province. The Western Terrane comprises Early Paleozoic and Late Mesozoic granitoids, while the Eastern Terrane is made up of volcanic arcs, forearc basins and accretionary rocks [Bradshaw, 1989]. Much of New Zealand basement was affected by the Mesozoic Rangitata Orogeny, which is separated from younger, less deformed strata above, by

a major unconformity found throughout the region [Laird, 1993]. The unconformity documents the shift from collisional to extensional tectonics at 105 Ma [Bradshaw, 1989]. Extensional tectonics of the New Zealand region is best shown by post-unconformity development of mid-Cretaceous half-grabens both onshore and offshore the New Zealand crustal block [Laird, 1993].

Graben development throughout New Zealand, both onshore the South Island and offshore on the Campbell Plateau and Chatham Rise, is thought to have occurred in two phases: one in the mid-Cretaceous (~105 Ma), resulting in widespread half-graben formation, and a second phase in Late Cretaceous (80-84 Ma), resulting in more restricted graben formation associated with widespread subsidence and transgression [Laird, 1993]. Also, a mid-Cretaceous magmatic event is locally recognized throughout the Campbell Plateau and Chatham Rise. The South Island exhibits two distinct mid-Cretaceous patterns of faulting. A WNW-oriented fault system has been identified along the west coast of the South Island and is parallel to the trend of Cretaceous spreading axes in the Tasman Sea (Fig. 1-4) [Laird, 1993]. The WNW trend of these faults is probably related to early rifting associated with the separation of New Zealand from Australia. These faults may also represent a failed attempt of the Lord Howe Rise Rift System to propagate through the New Zealand region [Laird, 1993]. The second fault trend includes NNE-NE trending faults of the Great South and southern Canterbury Basins in the south east of the South Island (Fig. 1-4). The NNE-NE fault trends dominating the southeast sector of the South

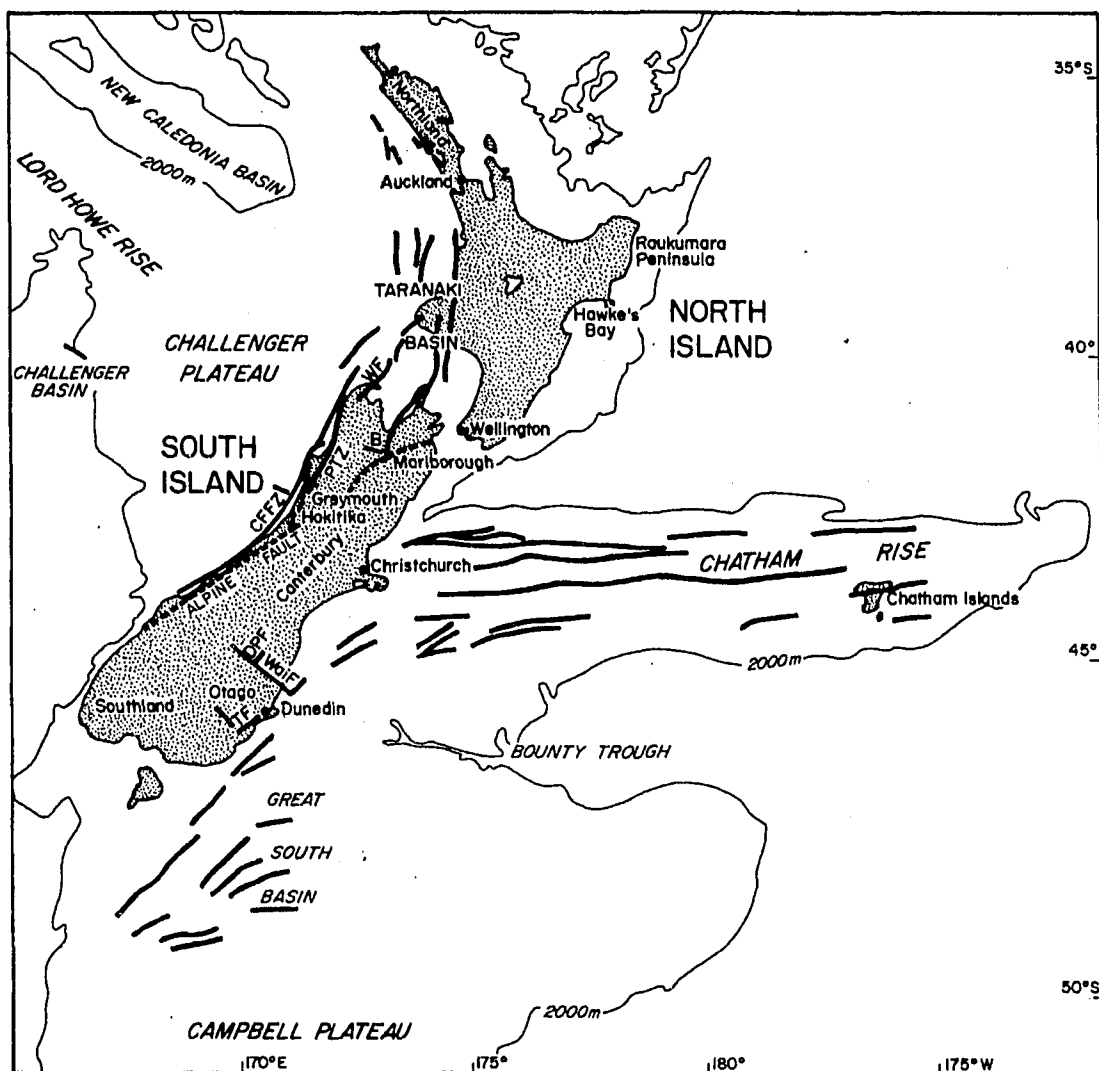


Figure 1-4: Map of the New Zealand region showing the major Cretaceous fault trends both onshore the New Zealand Islands and offshore on the Campbell Plateau and Chatham Rise. From Laird [1993].

Island are sub-parallel to the trend of spreading axes formed during the rifting of New Zealand from Antarctica and are thought to be related [Laird, 1993].

1-5.1. The Chatham Rise and Bounty Trough Rift System

The Chatham Rise is a linear feature, extending for over 1,000 km, due east from central South Island, New Zealand. The Chatham rise forms the northern margin of the Bounty Trough. Knowledge of the region comes from seismic reflection profiles, boreholes, sparse onshore outcrops and dredge samples. Several prominent seismic reflectors have been correlated across the region and mapped with sedimentary sequences to illustrate the geological history of the Chatham Rise. The seismic reflectors include: top of acoustic basement; Late Cretaceous breakup unconformity; top of Cretaceous; near top of Paleocene; mid-Cenozoic unconformity [Wood and Herzer, 1993].

The basement of the Chatham Rise is a broad east-west trending high, broken by rift basins of Cretaceous age filled with Cretaceous-Cenozoic sediment [Wood and Herzer, 1993; Sutherland, 1999]. Half-grabens are plentiful on the rise crest and the flank facing the Bounty Trough. Basement rocks are interpreted as Upper Paleozoic and Mesozoic schist and greywacke, comprising Seismic Sequence I. Outcrops of this sequence are found on the Chatham Islands, in the Canterbury region of the South Island and were dredged from the rise crest [Wood and Herzer, 1993]. The rift sequence and basement units are covered by Late Cretaceous and Cenozoic sediment.

Mid-Cretaceous E-W trending faults and half-grabens of the Chatham Rise and Bounty Trough are oblique to the dominant WNW-NW mid-Cretaceous fault trend on the South Island (Fig. 1-4). However, the orientation of New Zealand continental fragments changed during the fragmentation of Gondwana [Laird, 1993]. Therefore, the orientation of graben, fault, and basin trends have also changed. Based on the reconstruction of Kamp [1986], the Bounty Rift and Chatham Rise fault and graben trends were originally oriented parallel to the Lord Howe Rift System and the Tasman spreading center during the mid-Cretaceous [Laird, 1993]. The Bounty Trough may represent an extension of the Lord Howe Rift System, an extension of the Pacific-Phoenix spreading center west of the Pacific-Phoenix-Antarctic triple junction, through the New Zealand region [Laird, 1993; Lawver and Gahagan, 1994].

The Bounty Trough rift system appears to have controlled Chatham Rise sedimentation. The oldest preserved sedimentary sequence, Seismic Sequence IIA, is interpreted as Early Cretaceous in age. The sequence was folded and faulted prior to the main phase of rifting and is interpreted between basement blocks as well as separated from the overlying strata by a large angular unconformity [Wood and Herzer, 1993]. Although sequence IIA's origins are not known, possible sources are: 1) a remnant of a pre- or synrift forearc; 2) remnant of a pre-rift continental shelf; 3) sedimentary infill of an inactive continental borderland; or 4) a marine or lacustrine infill of a very early rift basin [Wood and Herzer, 1993].

Approximately 100 Ma to 80 Ma, the main phase of Chatham Rise and the Bounty Trough rifting took place and was accompanied by widespread volcanism

[Adams and Oliver, 1979; Barley, et al., 1988; Wood and Herzer, 1993]. Rift basins opened over wide areas of the crest and the southern flank of the Chatham Rise forming E-W striking half-grabens [Wood and Herzer, 1993]. Seismic Sequence IIB is interpreted as mid to Late Cretaceous in age and fills basement grabens. Volcanic features are observed in graben structures, adjacent to faults and on basement highs. Stratigraphic relationships with Seismic Sequence IIB indicate the volcanics were erupted in the mid to Late Cretaceous [Wood and Herzer, 1993]. At approximately 80 Ma, Bounty Trough rifting ended and regional subsidence initiated. The top of the rift sequence is marked by an unconformity, which cuts basement blocks and graben fill. The onset of regional subsidence resulted in the deposition of a blanket of transgressive sands, silts, and mud on the flank of the Chatham Rise, and in bathymetric lows on the rise crest [Wood and Herzer, 1993]. This sediment layer is labeled Seismic Sequence IIC. By Cenozoic time, the rise submerged completely and subsidence ended by the mid-Oligocene. Sedimentation shifted from clastic to carbonate in nature resulting in Seismic Sequences IIIA-C and IV.

1-5.2. The Campbell Plateau and Great South Basin Rift System

The Campbell Plateau is composed of two classes of basement rocks: silicic to intermediate plutonic rocks and quartzose metasedimentary rocks [Beggs, et al., 1990]. The plutonic basement comprises Cretaceous granites emplaced into early Paleozoic quartz-rich metasedimentary rocks. The metasedimentary portions of the basement have the following characteristics: 1) The rocks are highly quartzose; 2)

Feldspar is virtually absent from the rocks; 3) Muscovite Mica is abundant and crystals are strongly aligned producing a schist or phyllite; 4) Calcium is extremely low [Beggs, et al., 1990]. Correlatives of the Campbell Plateau metasediments, from East Antarctica (Robertson Bay Group), Marie Byrd Land (Swanson Formation), South Tasman Rise and West Coast South Island of New Zealand (Greenland Group) [Bradshaw, et al., 1983; Nathan, et al., 1986] show similar features but generally contain feldspar and sedimentary rock fragments [Beggs, et al., 1990].

Within the Campbell Plateau is the Great South Basin (GSB). The GSB occupies an area of approximately 85,000 km² along the northwestern margin of the Campbell Plateau and contains a complex series of northeast trending system of grabens and half-grabens that formed within relatively thin continental crust during the mid-Cretaceous (Fig. 1-4) [Anderton, et al., 1982; Beggs, 1993]. This rifting event is widespread throughout New Zealand region and follows a period of terrain accretion and subduction along this section of the Gondwana margin [Laird, 1993]. Beggs [1993] suggests the onset of rifting in the GSB may have overlapped in time with the last stages of subduction, thus resulting in foreland extension related to plate convergence and the formation of the graben system in the GSB. Rifting ceased by 80 Ma [Sherwood, et al., 1999] and was succeeded by a passive margin phase in the Late Cretaceous, when seafloor spreading initiated between the Campbell Plateau and West Antarctica and in the Tasman Sea between New Zealand and Australia [Beggs, 1993; Balance, 1993]. At this time, subsidence of the Campbell Plateau occurred

resulting in the flooding of the GSB and the initiation of marine deposition environment.

The basement of the Great South Basin is equivalent to the surrounding Campbell Plateau basement. However, the northern part of the GSB cuts across late Paleozoic and Mesozoic terrains accreted onto the Gondwana margin during the late Mesozoic [Beggs, 1993]. Above the basement is the mid to Late Cretaceous Hoiho Sequence that filled active grabens and half-grabens during the initial rifting sequence of the GSB [Beggs, 1993; Cook, et al., 1999; Sutherland, et al., 2001]. This sequence has low dips, displaced by moderate to steeply dipping normal faults, and is inferred to have been deposited between 105 and 85 Ma [Sherwood, et al., 1999]. Core data indicates the unit is terrestrial in origin, composed primarily of sandy coal measures in a relatively fine-grained terrestrial facies [Beggs, 1993]. Separating the Hoiho Sequence from the overlying Late Cretaceous to Paleocene Pakaha Sequence is a regional transgressive unconformity [Beggs, 1993; Cook, et al., 1999; Sutherland, et al., 2001]. The Pakaha sequence is composed of shallow marine sandstones over most of the GSB [Beggs, 1993]. The sequence also contains coal measures in the western portion of the unit, mudstones in the eastern facies and organic rich shale at the top [Beggs, 1993]. The top of the Pakaha Sequence is a prominent seismic reflector and is dated as Late Paleocene in age. The sequence was deposited following the initiation of seafloor spreading around southern New Zealand. Rapid subsidence from the east to the west of the Campbell Plateau occurred at this time due to a change in the thermal regime associated with the transition from intracontinental rifting to seafloor

spreading, thus allowing for deposition of the marine-derived Pakaha Sequence at ~ 85 Ma [Beggs, 1993; Sherwood, et al., 1999].

The late Paleocene-early Oligocene Rakiura Sequence is marked by the development of dark shale over much of the GSB [Beggs, 1993; Cook, et al., 1999; Sutherland, et al., 2001]. The sequence is composed of sandy near shore facies, which transitions into a fine grained and increasingly calcareous facies, showing westward stepping of clastic shoreline related facies, and is identical with the Waipawa Black Shale found on the eastern North Island of New Zealand [Carter, 1988; Moore, 1989; Beggs, 1993]. As with the underlying Pakaha Sequence, the deposition of the Rakiura Sequence occurred in a passive margin setting. Overlying the Rakiura Sequence is a thin veneer of mid-Oligocene and younger carbonate sediments. This unit is termed the Penrod Sequence and is dominated by pelagic carbonates. [Beggs, 1993; Sherwood, et al., 1999].

Seismic profiles across the GSB show small volcanic bodies intruding into the sedimentary sequences. The volcanic intrusions are interpreted as Miocene to Pleistocene in age and are analogous to alkali volcanics found on Auckland, Campbell, and Antipoded Islands, located on the Campbell Plateau and the Urry Knolls on the western Chatham Rise [Adams and Oliver, 1979; Herzer, et al., 1989; Beggs, 1993]. Of all the sedimentary basins in the New Zealand region, the Great South Basin follows most closely to a simple model of rift origin followed by passive margin thermal subsidence [Beggs, 1993].

1-6. Tectonic and Geological Description of the Tasmanian Region

Large submerged continental plateaus adjoin the island of Tasmania. To the south is the South Tasman Rise (STR) and to the east is the East Tasman Plateau (ETP) (Fig. 5). Within the submerged continental crust are large sedimentary basins filled with Cretaceous through Cenozoic sediments [Hill and Exxon, 2004]. During the Late Jurassic, Tasmania was part of the eastern Gondwana supercontinent and was positioned adjacent to the Northern Victoria Land sector of Antarctica to the southwest, and the Lord Howe Rise/Challenger Plateau to the east [Norvick and Smith, 2001]. Although the break up history of the Tasman region is complex, rifting began in the latest Jurassic-early Cretaceous with the initiation of extension between East Antarctica and Australia [Willcox and Stagg, 1990]. Extension throughout the region during the Cretaceous led to formation and development of rift basins within the STR and ETP [Hill and Exxon, 2004].

A relative shift in plate motions between Australia and Antarctica to a more N-S direction in the Paleocene [Tikku and Cande, 1999] resulted in seafloor spreading off of western Tasmania [Hill, et al., 1997]. At this time, the STR was transferred from the Antarctic plate to the Australian plate [Royer and Rollet, 1997] while seafloor spreading commenced off of southern margin of the STR [Pyle, et al., 1995; Cande, et al., 2000; Norvick and Smith, 2001]. The changes in the plate configurations during the Paleocene-Eocene resulting in uplift and deformation of the region [Exon, et al., 2002]. Apatite fission track data indicates cooling along the east and west coast of Tasmania at this time [O'Sullivan and Kohn, 1997], and may be

due to uplift of the region coupled with denudation. Rapid denudation is also recorded at 55-50 Ma in Victoria Land and the Transantarctic Mountains [Fitzgerald, 1992].

Fast N-S seafloor spreading commenced at ~43 Ma in the Southern Ocean, resulting in separation of the STR from Antarctica along the Tasman Fracture Zone [Hill and Exxon, 2004]. By 33.5 Ma (Eocene-Oligocene boundary), the STR and Antarctica were completely separated resulting in the opening of the Tasman gateway and formation of the Antarctic Circumpolar Current [Hill and Exxon, 2004]. Structures located in Victoria Land, Antarctica (Bowers Structure) have been shown to line up with the Tasman Fracture Zone [Hill and Exxon, 2004]. This structure was most likely active in the Eocene and Oligocene, at which time the Adare Trough was producing seafloor crust, separating East and West Antarctica with uplifting in northern Victoria Land [Cande, et al., 2000]. Until the Paleocene, the Rennick Graben in Antarctica and the Ninene Basin in the STR were part of the same N-S trending extensional structure.

1-6.1. West Tasmanian Margin

Several large depositional basins result from the extension of the Tasmanian region. To the west of the island of Tasmania is the Sorell Basin. Sub-basins within the Sorell Basin are faulted into half-grabens (Fig. 1-5). Within this basin, Late Cretaceous sediment are syn-rift in nature with significant deformation associated with seaward dipping normal faults, ranging from near-vertical to low-angle listric. Deformation extends only to the top of the Cretaceous formation, with little to no

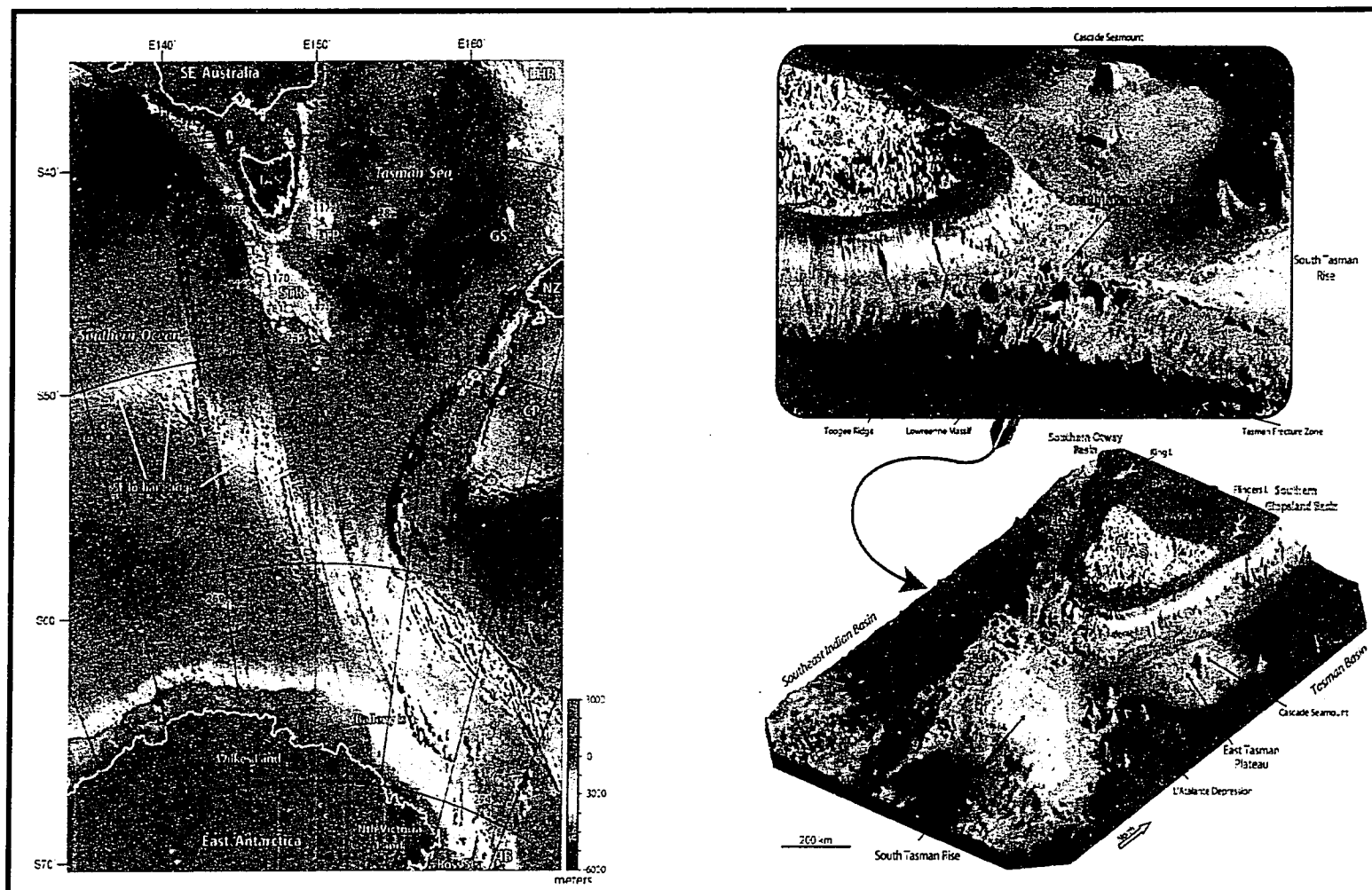


Figure 1-5: The Tasmania region and associated seaways and basins. Colored circles represent DSDP or ODP holes. TAS=Tasmania, STR=South Tasman Rise, ETP=East Tasman Plateau, LHR=Lord Howe Rise, NZ>New Zealand, CP=Campbell Plateau, IB=Island Bank. From Hill and Exxon [2004].

faulting extending into the overlying Paleocene and Eocene strata [Hill and Exxon, 2004]. However, reverse faulting and gentle to moderate folding is interpreted as well [Hill and Exxon, 2004]. Interpretations of seismic profiles across the basin indicate that igneous intrusions are prolific throughout the basement terrane, suggesting the intrusions were emplaced at the time of breakup [Hill and Exxon, 2004].

The sedimentary units of the Sorell Basin include the Late Cretaceous Sherbrook Group which is composed of mainly sandstones and shale. A strong angular mid-Cretaceous unconformity is interpreted throughout the basin within Sherbrook Group [Hill and Exxon, 2004]. Overlying the Sherbrook Group is the Paleocene-middle Eocene Wangerrip Group. The Wangerrip Group is composed of shallow marine quartz sandstones, siltstones, and mudstones [Hill and Exxon, 2004]. Overlying the Wangerrip Group is the middle Eocene to mid-Oligocene Nirranda Group, composed of fine sandstones and calcareous mudstones deposited in a shelf marine environment [Hill and Exxon, 2004]. Finally, the Heytesbury Group (mid-Oligocene to Miocene) cap the sequence and are composed of outer shelf carbonates and fossiliferous limestone [Hill and Exxon, 2004].

1-6.2. South Tasman Rise

Two main structural provinces comprise the STR. The western block of the STR is complexly deformed with mainly N-S trends and a lesser developed E-W trend [Hill and Exxon, 2004]. The eastern block is structurally simpler, characterized by a shallow basement beneath the crest of the STR and flanked by NW-SE trending

rift basins [Hill and Exxon, 2004]. The more complex western block of the STR results from deformation within the Late Cretaceous to Early Tertiary Tasmanian-Antarctic shear zone. The STR was transferred from the Antarctic plate to the Australian plate in the Paleocene, and then deformation resulting from the formation of the Tasman Fracture Zone [Hill and Exxon, 2004].

Sedimentary basins with more than 2 km of sediment are pronounced throughout the STR [Hill and Exxon, 2004]. Seismic interpretations suggest deep basins on the STR contain thick accumulations of Late Cretaceous sediment [Hill and Exxon, 2004]. However, DSDP and ODP drill holes have not recovered Cretaceous sediments from the STR. Paleocene and younger section on the STR is relatively well known from deep sea drilling [Kennett, et al., 1975]. Results from DSDP and ODP drill holes indicate that Paleocene-Eocene siliciclastics are overlain unconformably by Oligocene and younger pelagic carbonates [Hill and Exxon, 2004].

1-7. Integrated History of the Circumpacific Region

1-7.1. Basement rocks and Tectonics

Prior to the rifting of New Zealand and Tasmania from West Antarctica, the region most likely shared a common geologic history. Before the breakup, active collision along the east Gondwana continental margin resulted in terrane accretion onto the New Zealand-Marie Byrd Land margin, along with the emplacement of igneous and metamorphic belts associated with subduction. The Swanson Formation of MBL can be correlated with the Greenland Group in New Zealand, the Lachlan

Group in Australia and to the Robertson Bay Group in northern Victoria Land, Antarctica. This correlation is based on parallel lithology and age of metamorphism. The Ford Granodiorite, in wMBL, are observed intruding into the Swanson Formation and geochemical analysis indicates that the parental magmas were generated by active subduction along the east Gondwana margin during the mid to late Paleozoic [Pankhurst, et al., 1998]. Furthermore, sedimentary rocks found on the South Island of New Zealand are interpreted to represent an accretionary prism that would have been parallel to MBL in Cretaceous times. Based on these data, the sedimentary accretionary prism of the South Island, New Zealand, the Swanson Group of MBL and the correlative Greenland Group of New Zealand most likely represent accretionary prisms from subduction along the active continental margin of East Gondwana prior to its breakup. The Ford Granodiorite represents the magmatic arc that resulted from subduction of the now defunct Phoenix Plate under this area of east Gondwana up to Cretaceous times.

Since the conjugate continental margins to Marie Byrd Land and the Ross Embayment are the Chatham Rise and Campbell Plateau, the basement geology should be similar. Basement rocks of the Chatham Rise are interpreted as Upper Paleozoic and Mesozoic schist and greywacke. These rocks are observed in outcrops on the Chatham Islands, the Canterbury region of the South Island, New Zealand, and have been dredged from the Chatham Rise crest [Wood and Herzer, 1993]. Basement rocks of the Campbell Plateau fall into two groups: silicic to intermediate plutonic rocks and quartzose metasedimentary rocks [Beggs, et al., 1990]. The plutonic

basement of the Campbell plateau comprises Cretaceous granites emplaced into the early Paleozoic metasediments.

The basement of the Chatham Rise is similar to the Swanson Group of MBL and the Greenland Group of New Zealand. All three regions are characterized by schists and greywacke rocks. Similarly, the basement of the South Tasman Rise is also Paleozoic schist [Hill and Moore, 2001] of similar age and rock type to the Swanson Group, Greenland Group, and basement found on the Chatham Rise. Mid-Cretaceous granites of the Byrd Coast Granite in wMBL can be correlated to granites on the Campbell Plateau and are identified on the Colbeck Shelf in the Eastern Ross Sea by Luyendyk, et al. [2001]. Based on the similarities between the basement rock types of the conjugate continental fragments, it is likely the basement of the Ross Embayment is composed primarily early Paleozoic metasedimentary schist intruded by mid-Cretaceous granites emplaced during the extension and rifting of the region, thus forming mylonitic fabrics.

Although little is known about the basement of the Ross Sea, samples of metamorphic basement rocks have been obtained at DSDP Site 270 in the eastern Ross Sea. The basement rocks here show evidence for both ductile and brittle deformation along with early Late Cretaceous fission track ages, indicating faulting and extension of the region took place at this time [Fitzgerald and Baldwin, 1997]. Similarly mylonitic gneisses were dredged from the Colbeck Trough offshore wMBL [Luyendyk, et al., 2001]. U-Pb geochronology and $^{40}\text{Ar}/^{39}\text{Ar}$ and apatite fission track dating of the Colbeck Trough mylonites, the Fosdick Mountains and Edward

VII Peninsula in wMBL indicate two episodes of tectonism in the Ross Sea; i) extension before 90 Ma and ii) extension between 80-71 Ma [Siddoway, et al., 2004]. The close correlation of ages from samples onshore wMBL, offshore Cape Colbeck, and DSDP Site 270 cores, indicate extensional deformation occurred over a wide region [Fitzgerald and Baldwin, 1997; Siddoway, et al., 2004]. Siddoway, et al. [2004] concluded extension of the WARS occurred during detachment style faulting and was completed prior rifting off of the Campbell Plateau from Marie Byrd Land. If so, then the rifted conjugate margins to the Ross Sea and MBL should exhibit similar extensional features and structures.

No basement samples have been recovered from the western Ross Sea. However, the Paleozoic Beacon Supergroup is interpreted from the Cape Roberts core holes in McMurdo Sound, suggesting seismic acoustic basement here may be the Beacon Sandstone [*Cape-Roberts-Science-Team*, 2000]. It is possible that early Paleozoic metasedimentary schist underlies under the Beacon Sandstone in the western Ross Sea. Another possibility for basement rocks in the western Ross Sea may be the Jurassic Kirkpatrick Basalts and the Ferrar Dolerites that are also widespread throughout the TAM. If the TAM is the western boundary of the WARS, then the two regions would likely have the same or similar rock types. Since the TAM contain both Kirkpatrick Basalts/Ferrar Dolerites and Beacon Sandstone, it is possible that these two rock types underlay the sedimentary sequences of the western Ross Sea.

1-7.2. Extensional Structures

Magnetic anomaly data indicates seafloor spreading had commenced by 79.1 Ma between the Chatham Rise and Marie Byrd Land. Rifting between the Campbell Plateau and the Ross Embayment/wMBL had commenced by this time, but production of oceanic lithosphere was not fully underway [Stock and Cande, 2002]. Middle Cretaceous normal fault systems on the Chatham Rise most likely were formed due to the Lord Howe Rise Rift system, resulting in the formation of the Bounty Trough [Laird, 1993]. A similar system of Cretaceous normal faults is observed on the Campbell Plateau that are parallel to the trend of the Late Cretaceous spreading axis formed during the separation of the Campbell Plateau from Antarctica [Laird, 1993]. The Great South Basin contains a northeast trending system of mid-Cretaceous grabens and half-grabens. The rifting event responsible for this is thought to have coincided with the last stages of subduction, just before the Campbell Plateau rifted from West Antarctica [Beggs, 1993].

In wMBL Luyendyk, et al. [2003] interprets NE-SW extension from 104-96 Ma. The faults and dykes associated with this event trend at a high angle to the continental margin and the extension they record is orthogonal to the orientation of seafloor spreading at ~79 Ma [Stock and Cande, 2002]. Therefore, these structures must result from extension that led to the formation of the Ross Sea rift [Luyendyk, et al., 2003]. Also, rift related structures in the eastern Ross Sea trend at a high angle and tend to be abruptly truncated at the passive margin edge [Luyendyk, et al., 2001]. Since fault trends in wMBL and the eastern Ross Sea are oblique to the continental

shelf edge [Luyendyk, et al., 2001; Luyendyk, et al., 2003], this orientation implies these extensional features are not related to the rifting of the Campbell Plateau from West Antarctica 79 Ma. Furthermore, middle Cretaceous grabens and half-grabens in Greater New Zealand and on the Campbell Plateau are oblique to the trend of the rifted margin, while the Late Cretaceous grabens are parallel to it. Even though evidence of rifting during the Late Cretaceous in the Ross Embayment and MBL sectors of WANT has not been found, it seems likely that margin parallel extensional structures, in the form of grabens and faults, should exist in the Ross Sea and would most likely be directly related to the Late Cretaceous rifting off of the Campbell Plateau. It is surprising that these structures have not yet been found.

1-7.3. Basin Stratigraphy

In general, Cretaceous rift basins in the Tasmanian-South Tasman Rise region, the Campbell Plateau and the Ross Sea share similar features. The most noticeable similarity between each of these basins is the basement structure. The structure of the GSB on the Campbell Plateau, the basins of the STR and the four major basins of the Ross Sea all result from stretching of continental lithosphere that formed fault bounded horsts and grabens interpreted as Cretaceous age. It is very possible that each of these features formed during the same phase of tectonism. Luyendyk, et al. [2003] suggests that the formation and extension of the Ross Sea occurred at 104-96 Ma based on fault and dyke trends and associated ages in wMBL. If this event did extend the Ross Sea, it is highly likely that it would have formed

extensional basins on the Campbell Plateau and on the Tasmanian rise, which were still connected to the Ross Sea at that time.

Another similarity between the three basins is the Cretaceous age syn-rift sediments. In each of the basins, Cretaceous sediments are interpreted to have deposited and deformed during continental extension and are offset by normal faults (Fig. 1-6). Although there are no samples of Cretaceous units in the Ross Sea, these units are interpreted as non-marine terrestrial sand and silts and breccia [Hayes, et al., 1975; Luyendyk, et al., 2001]. Similarly core holes on the STR indicate Cretaceous syn-rift sediments are composed of sands, silts and breccia basement clasts [Hill and Moore, 2001]. The Cretaceous syn-rift units interpreted in the GSB are interpreted as coarse clastic sediment [Sherwood, et al., 1999]. The similar composition and deformation patterns interpreted in the three basins, suggest they may share a parallel depositional and tectonic history. The geologic parallels of the Ross Sea with the STR and GSB suggest that Cretaceous Ross Sea sediments may also be composed of non-marine brecciated sandstone.

Un-deformed sediment of Paleocene age can be found on both the Campbell Plateau and the STR and is capped by un-deformed Eocene sediment (Fig. 1-6) [Sherwood, et al., 1999; Hill and Exon, 2004]. No evidence of Paleocene age sediment has been found in the Ross Sea to date. However, deformed strata thought to

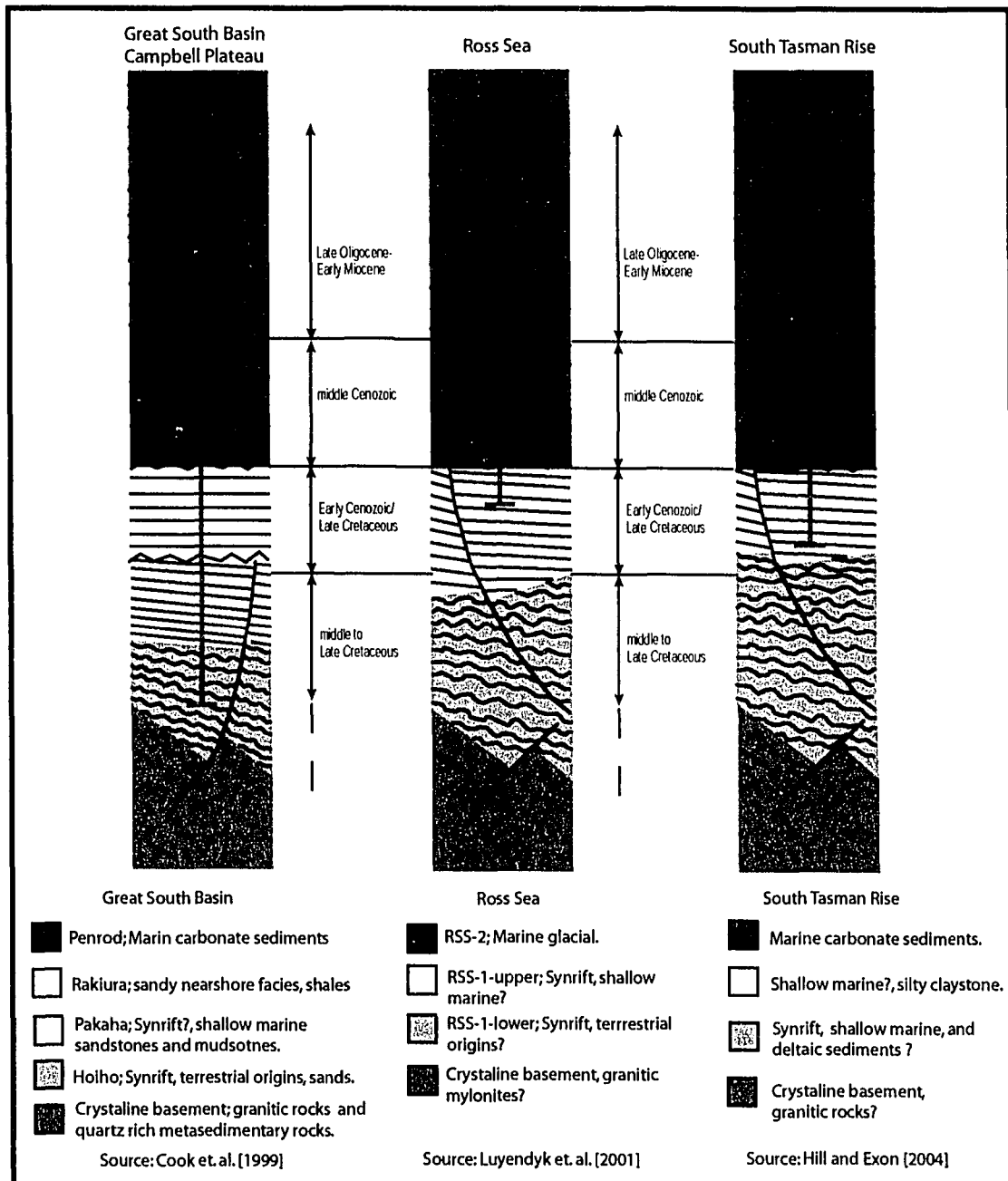


Figure 1-6: Comparison of stratigraphy interpreted in the Great South Basin/Campbell Plateau, Ross Sea, and South Tasman Rise. All basins are characterized by faulted basement structure overlain by syn-rift Cretaceous syn-rift sediments. Stratigraphy is based on seismic interpretations and core samples. Red lines indicate units sampled in each basin.

be Eocene in age is interpreted throughout the Ross Sea [Decesari, et al., 2004]. Since the STR has Paleocene sediment capped by Eocene strata, and did not break away from the western Ross Sea until Eocene time, one would expect Paleocene strata in the Ross Sea as well. Because significant glaciation did not occur until the Oligocene, it is problematic to suggest that Paleocene strata in the Ross Sea were eroded by glaciation prior to the deposition of Eocene strata. Furthermore, if this did occur, the Paleocene strata almost certainly would have been eroded on the STR, which is not the case. It is possible Paleocene strata are preserved in the Ross Sea and have not been imaged or interpreted as of yet. It is also possible Eocene Ross Sea strata may be older than interpreted and was deposited in the Paleocene before being deformed.

McMurdo Sound but cannot be correlated into the Victoria Land Basin [Hannah, 1994; Wilson, et al., 1998]. The problem with having a syn-rift Paleocene unit in the Ross Sea is there are no known tectonic events that occurred to deform the strata at this time. In the Ross Sea a syn-rift unit is interpreted within basement half-grabens and truncated by an angular unconformity overlain by another syn-rift unit above [Luyendyk, et al., 2001; Decesari, et al., 2004]. The deformation of these units is possibly linked to two known tectonic episodes in the Ross Sea. First, the Cretaceous extension of the Ross Embayment and second, the Eocene Adare Trough spreading event [Cande, et al., 2000]. If Paleocene strata are present in the Ross Sea it may have been deformed from Eocene extension or it may remain un-deformed as it is on the STR.

1-8. Outstanding Problems

Although many geologic parallels can be drawn between the Ross Sea region, the Tasman region, and the New Zealand region, many outstanding questions remain. These questions include:

- 1) Can the Beacon Sandstone, found in the TAM, also be found throughout the Ross Sea? Does the Beacon Sandstone correlate to sedimentary units on the STR, Campbell Plateau or the New Zealand region?
- 2) Are there Paleocene sediments similar to those sampled on the STR in the Ross Sea? Could the RSS-1-upper unit be the missing Paleocene section?
- 3) Can stratigraphy between the different Ross Sea basins be correlated? Were the sedimentary depositional environments uniform across the Ross Sea?
- 4) What types of rocks compose the Ross Sea basement? Is it characterized everywhere by mylonitized granite and gneiss?
- 5) Does the WAES span the Ross Sea region? Does the WAES indicate that the Ross Sea region was an elevated prior to Cretaceous extension?
- 6) Do the Ross Sea, STR, and Campbell Plateau share a similar Cretaceous tectonic history?
- 7) What is the affect of Tertiary Adare Trough seafloor spreading on the Ross Sea?

To answer these questions cores sampling pre-Oligocene Ross Sea strata and basement are needed. Also, a more detailed stratigraphic correlation between the western and eastern Ross Sea is needed to better understand the relationship between

stratigraphic units between the basins. Not only will drilling test this correlation, but it will allow for more detailed geologic comparisons of the Ross Sea to the Tasman and New Zealand regions. Drilling will shed more information on the tectonic events of the Ross Sea as well as its climatic and glacial history. Finally, subsidence modeling of the Ross Sea basins will help to answer questions regarding the timing and magnitude of tectonic events, resulting in the formation of the Ross Sea.

References Cited

- Adams, C. J. (1986), Geochronological studies of the Swanson Formation of Marie Byrd Land, West Antarctica, and correlation with Northern Victoria Land, East Antarctica, and South Island, New Zealand, *N. Z. J. Geol. Geophys.*, 29, 345-358.
- Adams, C. J. (1987), Geochronology of granite terranes in the Ford Ranges, Marie Byrd Land, West Antarctica, *N. Z. J. Geol. Geophys.*, 30, 51-72.
- Adams, C. J. D., and P. J. Oliver (1979), Potassium-argon dating of Mt Somers Volcanics, South Island, New Zealand: Limitations in dating Mesozoic Volcanic Rocks, *New Zealand Journal of Geophysics*, 20, 287-301.
- Adams, C. J. D., and P. Robinson (1977), Age of metamorphism of schists, Chatham Island, South-west Pacific, *N. Z. J. Geol. Geophys.*, 20, 287-301.
- Anderton, P. W., N. H. Holloway, J. C. Engstrom, H. M. Ahmad, and B. Chong (1982), Great South and Campbell Basins, New Zealand: Evaluation of Geology and Hydrocarbon Potential, edited, New Zealand Geological Survey.
- Balance, P. F. (1993), The Paleo-Pacific, Post-subduction Passive Margin Thermal Relaxation Sequence (Late Cretaceous-Paleogene) of the Drifting of New Zealand Continent, in *South Pacific Sedimentary Basins*, edited, pp. 93-110.
- Barley, M. E., S. D. Weaver, and J. R. De Laeter (1988), Strontium Isotope Composition and Geochronology of Intermediate Silicic Volcanics, Mt Somer and Banks Peninsula, New Zealand, *New Zealand Journal of Geophysics*, 21, 197-206.
- Beggs, J. M. (1993), Depositional and tectonic history of Great South Basin, in *South Pacific Sedimentary Basins*, edited by P. F. Balance, pp. 365-373, Elsevier, Amsterdam.
- Beggs, J. M., G. A. Challis, and R. A. Cook (1990), Basement Geology of the Campbell Plateau; Implications for Correlation of the Campbell Magnetic Anomaly System, *N. Z. J. Geol. Geophys.*, 33, 401-404.
- Bradshaw, J. D. (1989), Cretaceous geotectonic patterns in the New Zealand region, *Tectonics*, 8, 803-820.
- Bradshaw, J. D., P. B. Andrews, and B. D. Field (1983), Swanson Formation and related rocks of Marie Byrd Land and a comparison with the Robertson Bay Group of Northern Victoria Land, in *Antarctica Earth Science*, edited by R. L. Oliver and others, pp. 274-279, Australian Academy of Sciences, Canberra.

Bradshaw, J. D., R. J. Pankhurst, S. D. Weaver, B. C. Storey, R. J. Muir, and T. R. Ireland (1997), New Zealand superterranea recognized in Marie Byrd Land and Thurston Island, in *The Antarctic Region: Geological Evolution and Processes*, edited by C. A. Ricci, pp. 429-436, Terra Antarctica Pub., Siena.

Campbell, H. J., and a. others (1993), Cretaceous-Cenozoic geology and biostratigraphy of the Chatham Islands, New Zealand, *Institute of Geological and Nuclear Sciences Monograph*, 2, 269.

Cande, S. C., J. M. Stock, D. Müller, and T. Ishihara (2000), Cenozoic Motion between East and West Antarctica, *Nature*, 404, 145-150.

Cape-Roberts-Science-Team (2000), Summary of Results, Initial Report on CRP-3, Cape Roberts Project, Antarctica, *Terra Antarctica*, 7, 185-209.

Carter, R. M. (1988), Plate Boundary Tectonics, Global Sea Level Changes and the Development of the Eastern South Island Continental margin, New Zealand, Southwest Pacific, *Marine and Petroleum Geology*, 5, 90-107.

Coney, P. J., A. Edwards, R. Hine, F. Morrison, and D. Windrim (1990), The regional tectonics of the Tasman orogenic system, eastern Australia, *J. Struct. Geol.*, 12, 519-543.

Cook, R. A., R. Sutherland, and H. Zhu (1999), Cretaceous-Cenozoic Geology and Petroleum Systems of the Great South Basin, New Zealand, *Institute of Geological and Nuclear Sciences Monograph*, 20, 188.

Cooper, A. K., P. F. Barker, and G. Brancolini (Eds.) (1995), *Geology and Seismic Stratigraphy of the Antarctic Margin, atlas, CD-ROMs*, 301 pp., Amer. Geophys. Union, Washington, D.C.

Cooper, A. K., F. J. Davey, and K. Hinz (1991), Crustal extension and the origin of sedimentary basins beneath the Ross Sea and Ross Ice Shelf, Antarctica, in *Geological Evolution of Antarctica*, edited by M. R. A. Thompson, J. A. Crame and J. W. Thompson, pp. 285-291, Cambridge Univ. Press, New York.

Cooper, R. P., and A. J. Tulloch (1992), Early Paleozoic terranes in New Zealand and their relationship to the Lachlan Fold Belt, *Tectonophysics*, 214, 129-144.

Davey, F. J., and G. Brancolini (1995), The Late Mesozoic and Cenozoic structural setting of the Ross Sea region, in *Geology and Seismic Stratigraphy of the Antarctic Margin*, edited by A. K. Cooper, P. F. Barker and G. Brancolini, pp. 167-182, Amer. Geophys. Union, Washington, D.C.

Dean, A. A. (1993), Analysis and correlation of igneous clast geochemistry and petrography from four Mesozoic conglomerates, 263 pp, University of Canterbury, Christchurch, New Zealand.

Decesari, R. C., B. P. Luyendyk, L. R. Bartek, C. C. Sorlien, D. S. Wilson, J. B. Diebold, and S. E. Hopkins (2004), Ice shelf drill sites proposed to study Pre-Late Oligocene climate and tectonic history, Coulman High, Southwestern Ross Sea, Antarctica, *EOS Trans. AGU*, 85, Fall Meet. Suppl., Abstract T11A-1244.

DiVenere, V. J., D. V. Kent, and I. W. D. Dalziel (1994), Mid-Cretaceous Paleomagnetic Results From Marie Byrd Land, West Antarctica: A Test of Post-100 Ma Relative Motion Between East and West Antarctica, *J. Geophys. Res.*, 99, 15,115-115,139.

Elliot, D. H. (1992), Jurassic magmatism and tectonism associated with Gondwanaland break-up: An Antarctic perspective, in *Magmatism and the Causes of Continental Break-up*, edited by B. C. Storey, T. Alabaster and R. J. Pankhurst, pp. 165-184, Geol. Soc. Spec. Publ.

Exon, N. F., P. J. Hill, J. Keene, G. Chaproniere, R. Howe, P. Harris, A. Heap, and A. Leach (2002), Basement rocks and younger sediments on the southeast Australian continental margin: RV Franklin Cruise, *Geoscience Aust. Rec.*

Field, B. D., and G. H. Browne (1989), Cretaceous and Cenozoic Geological Development of the Canterbury Region, South Island, New Zealand, *New Zealand Geological Survey Basin Studies*, 2.

Fitzgerald, P. G. (1999), Nature and evolution of the Antarctic landscape since Gondwana breakup, paper presented at 8th International Symposium on Antarctic Earth Sciences, Victoria Univ., Wellington, New Zealand.

Fitzgerald, P. G. (1994), Thermochronologic constraints on post-Paleozoic tectonic evolution of the central Transantarctic Mountains, Antarctic, *Tectonics*, 13, 818-836.

Fitzgerald, P. G. (1992), The Transantarctic Mountains of Southern Victoria Land: The application of apatite fission track analysis to a rift shoulder uplift, *Tectonics*, 11, 634-662.

Fitzgerald, P. G., and S. L. Baldwin (1997), Detachment Fault Model for the Evolution of the Ross Embayment, in *The Antarctic Region: Geological Evolution and Processes*, edited by C. A. Ricci, pp. 555-564, Terra Antarctica Pub., Siena.

Fitzgerald, P. G., S. L. Baldwin, K. A. Farley, and P. B. O'Sullivan (2000), Landscape evolution and exhumation of the Transantarctic Mountains in the Kukri Hills of

southern Victoria Land: Constraints from Apatite Fission Track Thermochronology and (U-Th)/He dating of apatites, *EOS Trans. AGU*, 81, F1102.

Grindley, G. W., C. J. D. Adams, Lumb J.T., and W. A. Watters (1977), Paleomagnetism, K-Ar Dating, and Tectonic Interpretations of Cretaceous and Cenozoic Volcanic Rocks from Chatham Islands, New Zealand, *N. Z. J. Geol. Geophys.*, 20, 425-467.

Hamilton, R. J., B. P. Luyendyk, C. C. Sorlien, and L. R. Bartek (2001), Cenozoic Tectonics of the Cape Roberts Rift Basin, and Transantarctic Mountains Front, Southwestern Ross Sea, Antarctica, *Tectonics*, 20, 325-342.

Hannah, M. J. (1994), Eocene dinoflagellates from the CIROS-1 drill hole, McMurdo Sound Antarctica, *Terra Antarctica*, 1, 371.

Hayes, D. E., and L. A. Frakes (1975), General synthesis: Deep Sea Drilling Project 28, in *Initial Reports of the Deep Sea Drilling Project, Leg 28*, edited by D. E. Hayes and L. A. Frakes, pp. 919-942, U.S. Government Printing Office, Washington, D.C.

Hayes, D. E., L. A. Frakes, and S. S. Party (1975), Sites 270, 271, 272, in *Initial Reports of the Deep Sea Drilling Project, Leg 28*, edited by D. E. Hayes and L. A. Frakes, pp. 211-234.

Herzer, R. H., G. A. Challis, R. H. K. Christie, G. H. Scott, and W. A. Watters (1989), The Urry Knolls, late Neogene alkaline basalt extrusives, southwest Chatham Rise, *Journal of Royal Society of New Zealand*, 19, 181-192.

Hill, P. J., and N. Exon (2004), Tectonics and Basin Development of the Offshore Tasmanian Area Incorporating Results from Deep Ocean Drilling, *Geophysical Monograph Series*, 151, 19-41.

Hill, P. J., A. Meixner, A. M. G. Moore, and N. F. Exon (1997), Structure and Development of the west Tasmanian offshore sedimentary basin: results of recent marine and aeromagnetic surveys, *Australian Journal of Earth Science*, 44, 579-596.

Hill, P. J., and A. M. G. Moore (2001), Geological Framework of the South Tasman Rise and East Tasman Plateau, *Geoscience Aust. Rec.*, 2001.

Houtz, R. E., J. E. Ewing, M., and A. G. Lonardi (1976), Seismic Reflection Profiles of the New Zealand Plateau, *J. Geophys. Res.*, 72, 4713-47298.

Kamp, P. J. J. (1986), Late Cretaceous-Cenozoic tectonic development of the Southwest Pacific region, *Tectonophysics*, 121, 225-251.

Kennett, J. P., R. E. Houtz, and E. al. (1975), *Initial Reports of the Deep Sea Drilling Program, leg 29*, 1197 pp., U.S. Government Printing Office, Washington D.C.

Kyle, P. R., D. H. Elliot, J. F. Sutter, and P. Vella (1981), Jurassic Ferrar Supergroup tholeiites from the Transantarctic Mountains, Antarctica, and their relationship to the initial fragmentation of Gondwana, paper presented at The Fifth International Gondwana Symposium, Victoria Univ., Wellington, New Zealand.

Laird, M. G. (1993), Cretaceous Continental Rifts: New Zealand Region, in *South Pacific Sedimentary Basins: Sedimentary Basins of the World 2*, edited by P. F. Balance, pp. 37-49, Elsevier, Amsterdam.

Larter, R. D. (2003), What Caused Late Cretaceous rifting between New Zealand and Antarctic? Paper presented at 9th International Symposium on Antarctic Earth Sciences, Potsdam, Germany.

Larter, R. D., A. P. Cunningham, and P. F. Barker (2002), Tectonic Evolution of the Pacific Margin of Antarctica 1, late Cretaceous Reconstructions, *J. Geophys. Res.*, 107, 2345.

Lawver, L. A., and L. M. Gahagan (1994), Constraints on timing of extension in the Ross Sea region, *Terra Antarctica*, 1, 545-552.

LeMasurier, W. E., and C. A. Landis (1996), Mantle plume activity recorded by low relief erosion surfaces in West Antarctica and New Zealand, *Geol. Soc. Am. Bull.*, 108, 1450-1466.

LeMasurier, W. E., and D. C. Rex (1989), Evolution of linear volcanic ranges in Marie Byrd Land, West Antarctica, *J. Geophys. Res.*, 94, 7223-7236.

Luyendyk, B. P. (1995), Hypothesis for Cretaceous rifting of east Gondwana caused by subducted slab capture, *Geology*, 23, 373-376.

Luyendyk, B. P., S. Cisowski, C. H. Smith, S. M. Richard, and D. L. Kimbrough (1996), Paleomagnetic study of the northern Ford Ranges, western Marie Byrd Land, West Antarctica: a middle Cretaceous pole, and motion between West and East Antarctica? *Tectonics*, 15, 122-141.

Luyendyk, B. P., S. M. Richard, C. H. Smith, and D. L. Kimbrough (1992), Geological and geophysical investigations in the northern Ford Ranges, Marie Byrd Land, West Antarctica, in *Recent Progress in Antarctic Earth Science: Proceedings of the 6th Symposium on Antarctic Earth Science, Saitama, Japan, 1991*, edited by Y. Yoshida, K. Kaminuma and K. Shiraishi, pp. 279-288, Terra Pub., Tokyo, Japan.

Luyendyk, B. P., and C. H. Smith (1994), Geological Expedition to King Edward VII Peninsula and the Ford Ranges, Marie Byrd Land, Antarctic, *Antarctic J. of the US*, 28, 10-13.

Luyendyk, B. P., C. H. Smith, and G. Druivenga (2003), Gravity measurements on King Edward VII Peninsula, Marie Byrd Land, West Antarctica, during GANOVEX VII, *Geolog. Jahrb.*, B 95, 101-126.

Luyendyk, B. P., C. C. Sorlien, D. S. Wilson, L. R. Bartek, and C. H. Siddoway (2001), Structural and tectonic evolution of the Ross Sea rift in the Cape Colbeck region, Eastern Ross Sea, Antarctica, *Tectonics*, 20, 933-958.

Luyendyk, B. P., D. S. Wilson, and C. S. Siddoway (2003), Eastern margin of the Ross Sea Rift in western Marie Byrd Land, Antarctica: Crustal structure and tectonic development, *Geochem. Geophys. Geosyst.*, 4, 1090, doi:1010.1029/2002GC000462.

Moore, P. R. (1989), Stratigraphy of the Waipawa Black Shale, *New Zealand Geological Survey Recourses*, 38, 19.

Mukasa, S. B., I. W. D. Dalziel, and R. J. Pankhurst (1994), U-Pb and (super 40) Ar/(super 39) Ar age constraints on the development and subsequent fragmentation Gondwanaland's Pacific margin, Marie Byrd Land, Antarctica, *Eos, Transactions, American Geophysical Union*, 75, 692.

Nathan, S., H. J. Anderson, R. A. Cook, R. H. Herzer, R. H. Hoskins, J. I. Raine, and S. D (1986), Cretaceous and Cenozoic basins of the West Coast region, South Island, New Zealand, *New Zealand Geological Survey Basins Study*, 1.

Norvick, M. S., and M. A. Smith (2001), Mapping the plate tectonic reconstruction of southern and southeastern Australia and implications for petroleum systems, *APPEA Journal*, 41, 15-35.

O'Sullivan, P. B., and B. P. Kohn (1997), Apatite fission track thermochronology of Tasmania, *Geoscience Aust. Rec.*, 61.

Pankhurst, R. J., and P. D. Rowley (1991), Rb-Sr Study of Cretaceous Plutons from Southern Antarctic Peninsula and Eastern Ellsworth land, Antarctica, in *Geological Evolution of Antarctica*, edited by M. R. A. Thomson, J. A. Crame and J. W. Thomson, pp. 387-394.

Pankhurst, R. J., S. D. Weaver, J. D. Bradshaw, B. C. Storey, and T. R. Ireland (1998), Geochronology and geochemistry of pre-Jurassic superterrane in Marie Byrd Land, Antarctica, *J. Geophys. Res.*, 1033, 2529-2547.

Pyle, D. G., D. M. Christie, J. J. Mahoney, and R. A. Duncan (1995), Geochemistry and geochronology of ancient southeast Indian and southwest Pacific seafloor, *J. Geophys. Res.*, *100*, 22261-22282.

Richard, S. M., C. H. Smith, D. L. Kimbrough, P. G. Fitzgerald, B. P. Luyendyk, and M. O. McWilliams (1994), Cooling history of the northern Ford Ranges, Marie Byrd Land, West Antarctica, *Tectonics*, *13*, 837-857.

Royer, J. Y., and N. Rollet (1997), Plate tectonic setting of the Tasmanian region, *Australian Journal of Earth Science*, *44*, 543-560.

Sherwood, A., R. Sutherland, and R. Cook (1999), Great South Basin, New Zealand, might hold considerable potential, *Oil & Gas J.*, *97*, 78-82.

Siddoway, C., S. Richard, C. M. Fanning, and B. P. Luyendyk (2004), Origin and emplacement mechanisms for a middle Cretaceous gneiss dome, Fosdick Mountains, West Antarctica (Chapter 16), in *Gneiss domes in orogeny*, edited by D. L. Whitney, C. T. Teyssier and C. Siddoway, pp. 267-294, Geological Society of America.

Siddoway, C. S., S. L. Baldwin, P. G. Fitzgerald, C. M. Fanning, and B. P. Luyendyk (2004), Ross Sea mylonites and the timing of continental extension between East and West Antarctica, *Geology*, *32*, 57-60.

Smith, C. H. (1995), Cordierite gneiss and high temperature metamorphism in the Fosdick Mountains, West Antarctica, with implications for breakup processes in the Pacific sector of the Mesozoic Gondwana margin, Ph.D. dissertation thesis, 313 pp, University of California, Santa Barbara.

Stock, J. M., and S. C. Cande (2002), Tectonic History of Antarctic Seafloor in the Australia-New Zealand-South Pacific Sector: Implications for Antarctic Continental Tectonics, in *Antarctica at the Close of a Millennium: Proceedings of the 8th International Symposium on Antarctic Earth Sciences, Wellington, 1999*, edited by J. A. Gamble, D. N. B. Skinner and S. Henrys, pp. 251-259, The Royal Society of New Zealand, Wellington, New Zealand.

Storey, B. C., P. T. Leat, S. D. Weaver, R. J. Pankhurst, J. D. Bradshaw, and S. Kelley (1999), Mantle Plumes and Antarctica - New Zealand rifting: evidence from mid-Cretaceous mafic dykes, *J. Geol. Soc. Lond.*, *156*, 659-671.

Sutherland, R. (1999), Basement geology and tectonic development of the greater New Zealand region: an interpretation from regional magnetic data, *Tectonophysics*, *308*, 341-362.

Sutherland, R., P. King, and R. A. Wood (2001), Tectonic Evolution of Cretaceous Rift Basins in South-Eastern Australia and New Zealand: Implications for

Exploration Risk Assessment, in *PESA Eastern Australian Basins Symposium*, edited, Melbourn, Australia.

Tikku, A. A., and S. C. Cande (1999), The oldest magnetic anomalies in the Australian-Antarctic basin: are they isochrons? *J. Geophys. Res.*, 104, 661-677.

Weaver, S. D., J. D. Bradshaw, and C. J. Adams (1991), Granitoids of the Ford Ranges, Marie Byrd Land, Antarctica, in *Geological Evolution of Antarctica*, edited by M. R. A. Thompson, et al., pp. 345-351, Cambridge Univ. Press, Cambridge, Mass.

Weaver, S. D., B. C. Storey, R. J. Pankhurst, S. B. Mukasa, V. J. DiVenere, and J. D. Bradshaw (1994), Antarctica-New Zealand rifting and Marie Byrd Land lithospheric magmatism linked to ridge subduction and mantle plume activity, *Geology*, 22, 811-814.

Willcox, J. B., and H. M. Stagg (1990), Australia's southern margin: a product of oblique extension, *Tectonophysics*, 173, 269-281.

Wilson, G. S., A. P. Roberts, K. L. Verosub, F. Florindo, and L. Sagnotti (1998), Magnetobiostrati-graphic chronology of the Eocene-Oligocene transition in the CIROS-1 core, Victoria Land margin, Antarctica: Implications for Antarctic glacial history, *Geol. Soc. Am. Bull.*, 110, 35-47.

Wood, R. A., P. B. Andrews, and R. H. Herzer (1989), Cretaceous and Cenozoic Geology of the Chatham Rise Region, South Island, New Zealand, *New Zealand Geological Survey Basin Studies*, 3.

Wood, R. A., and R. H. Herzer (1993), The Chatham Rise, New Zealand, in *South Pacific Sedimentary Basins*, edited by P. F. Balance, Elsevier, Amsterdam.



Chapter 2

Regional Seismic Correlations of the Ross Sea; Implications for the Tectonic History of the West Antarctic Rift System

Abstract

Previous studies of the Ross Sea were not able to correlate seismic stratigraphic units between the basins. Late Oligocene-early Miocene RSS-2 sequence has been correlated from DSDP sites 270 and 272, in the eastern Ross Sea, across structural highs, into the central Ross Sea. Also, the late Oligocene-early Miocene V4 unit has been correlated from the Roberts Ridge drill sites of the Cape Roberts Project (CRP), in the western Ross Sea, to the central Ross Sea. The tops of both late Oligocene-early Miocene RSS-2 and V4 units tie in the central Ross Sea, suggesting the units are equivalent. Two unconformities below RSS-2/V4 have been identified in front of the ice shelf in both the western and eastern Ross Sea. These unconformities are interpreted as RSU6 (Oligocene) and RSU7 (Late Cretaceous?). Unconformity RSU6 was jump correlated from the CRP drill sites to a site survey along the Coulman High sector of the Ross Ice Shelf front.

Correlation of late Oligocene-early Miocene units across the Ross Sea, support the interpretations of Davey, et al. [2000], Barrett, et al. [2000], Hamilton, et

al. [2001], and Luyendyk, et al. [2001], that stratigraphic units throughout the Ross Embayment can be linked. The eastern and western Ross Sea may have similar tectonic histories during Cretaceous time, based on deformation styles interpreted in units below unconformity RSU7. Extension related to Adare Trough spreading may be expressed by deformation of pre-RSU6 strata, most likely resulting in the deposition and deformation of Eocene strata in the Victoria Land Basin. Paleocene strata may also be present here and would most likely be deformed as a result of extension related to Adare Trough spreading. Evidence for post-RSU6 extension is not observed. Major subsidence of the western Ross Sea most likely occurred in the Oligocene.

2-1. Introduction

The goal of this study is to correlate the stratigraphic record of the eastern Ross Sea to the western Ross Sea to better understand the nature, structure, and tectonic history of the West Antarctic Rift System (Fig. 2-1a). More specifically, correlating the stratigraphy will better constrain the timing, pattern, distribution, and magnitude of tectonic events, as well as climatic changes in the Ross Sea. The relation between the strata in the eastern Ross Sea to strata of the western Ross Sea is uncertain because they have not been correlated between basins with confidence [Brancolini, et al., 1995; DeSantis, et al., 1995]. This paper attempts to physically correlate stratigraphic sequences across the Ross Sea using new and existing seismic reflection data.

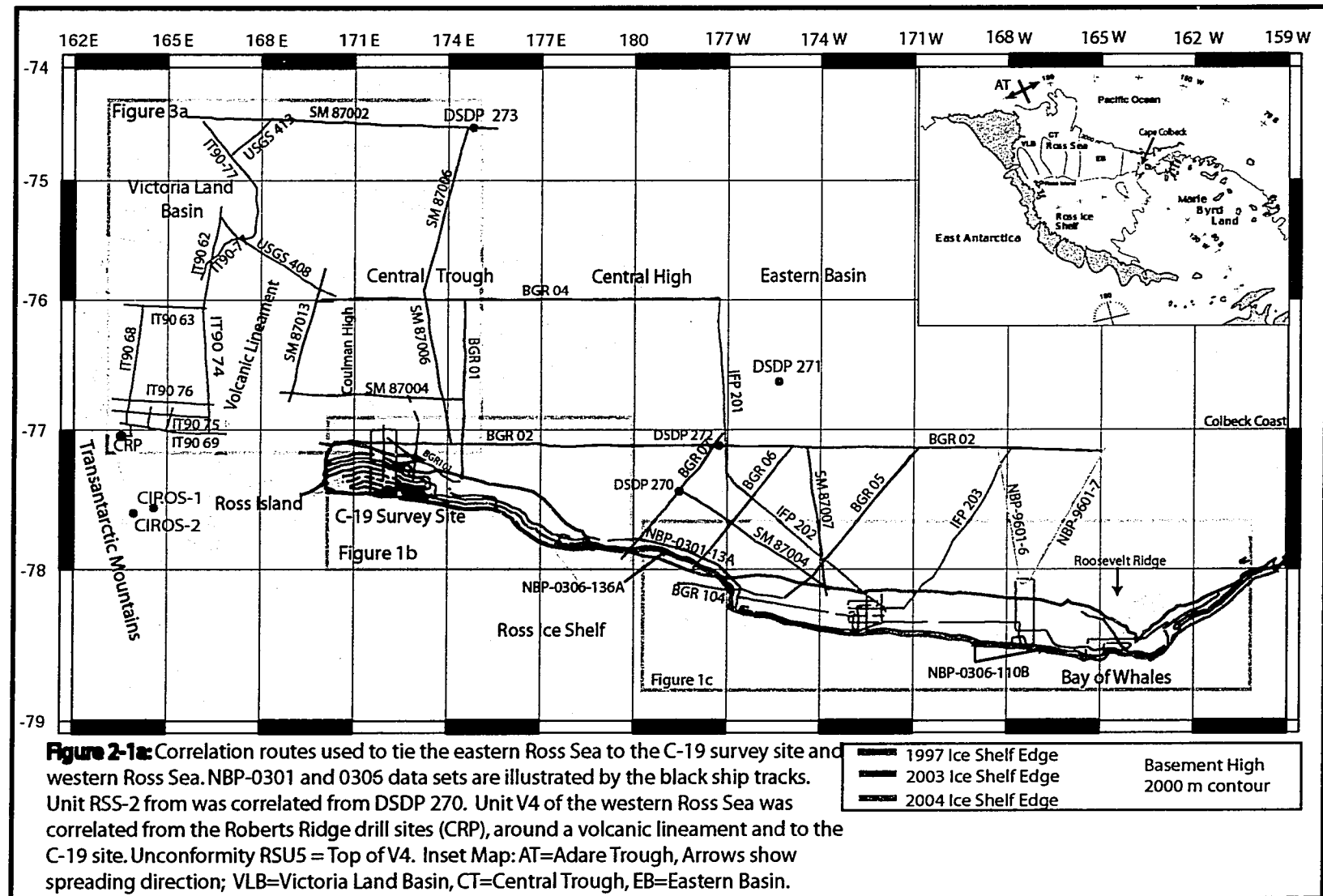
2-1.1. Ross Sea Seismic Stratigraphy

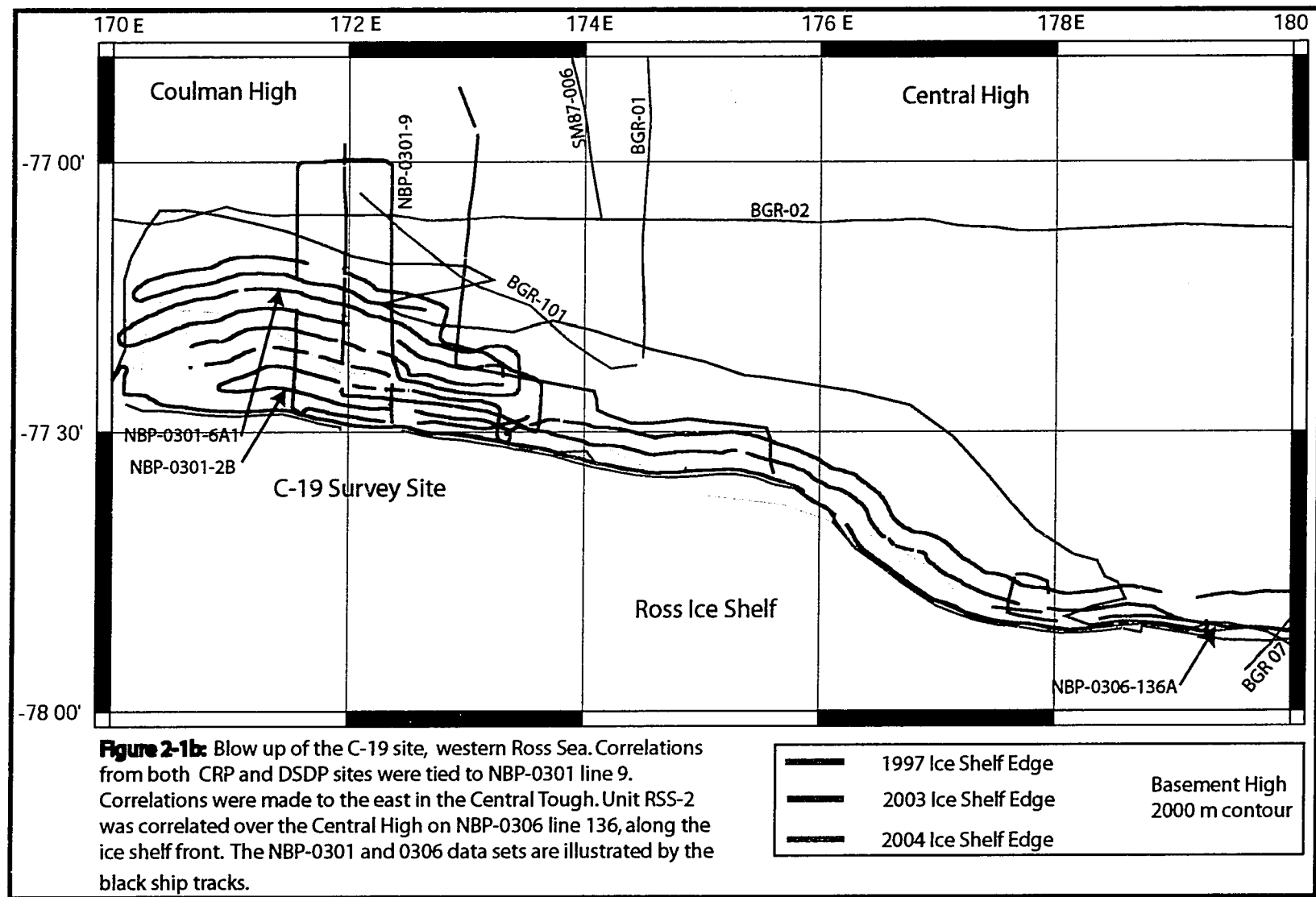
The RSS units of the eastern Ross Sea (discussed in dissertation Chapter 1-3.2) are suggested to correspond to the V seismic units identified earlier in the western Ross Sea by Cooper et al. [1987]. However, the relation between the RSS units of the eastern Ross Sea and the V sequences of Cooper et al. [1987] is uncertain because they have not been correlated across the Central High [Brancolini, et al., 1995; DeSantis, et al., 1995]. Attempts have been made by Cooper et al. [1987], DeSantis et al. [1995], Barrett et al. [2000], Davey et al. [2000], Hamilton et al. [2001], and Luyendyk et al. [2001] at correlating the western and eastern Ross Sea based on age of the units and seismic character (Table 2-1).

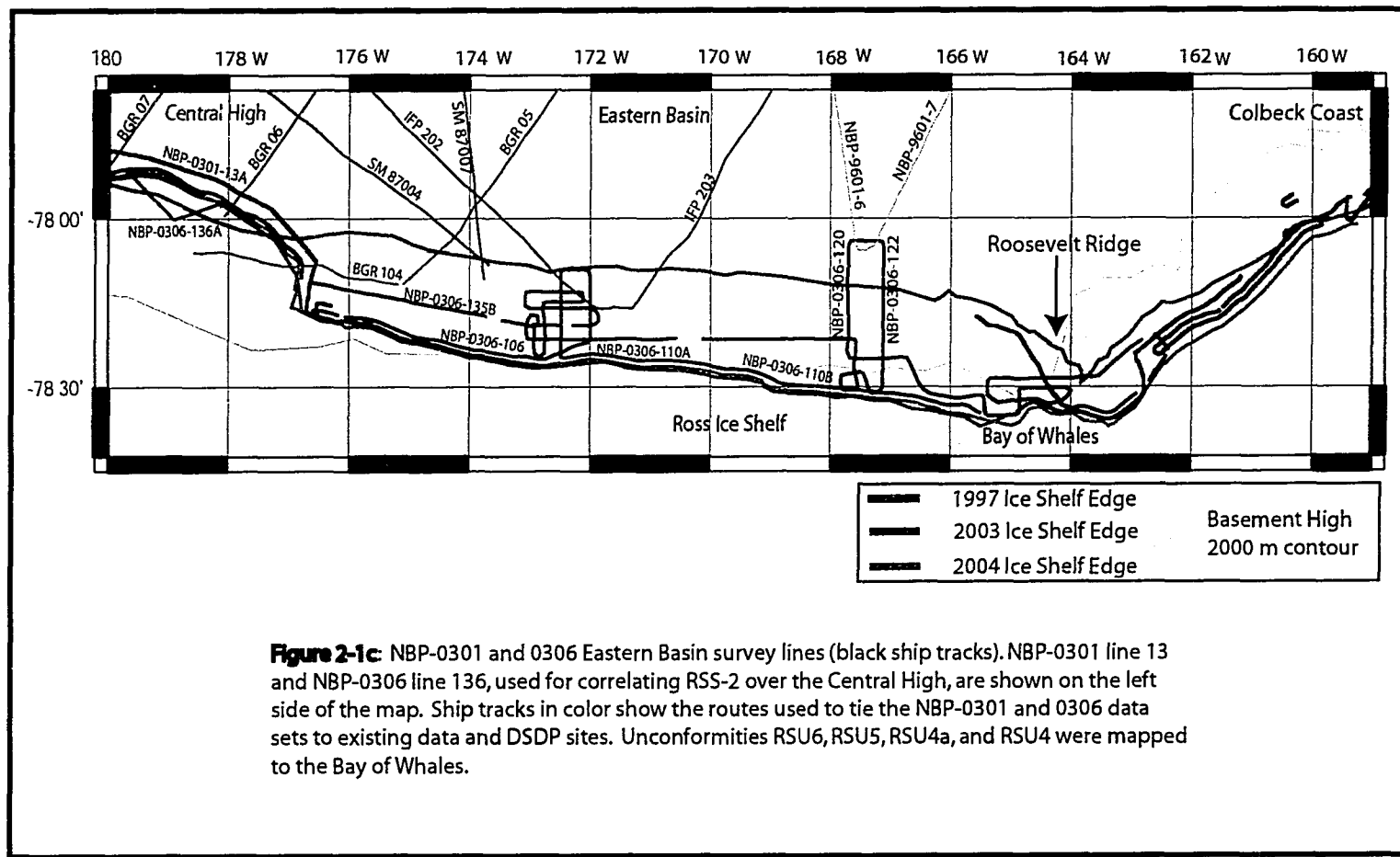
<i>R sequence</i>	<i>Unconformity</i>	<i>Age</i>	<i>Environment</i>	<i>V sequence</i>
RSS-8		Pleistocene		V1
-----	RSU1			
RSS-7		Pliocene	Full WAIS	?
-----	RSU2			
RSS-6		Late Miocene?		V2?
-----	RSU3			
RSS-5		Middle Miocene		V3?
-----	RSU4		Transitional to WAIS?	V3
RSS-4		Early Miocene		
-----	RSU4A			
RSS-3		Early Miocene		V3
-----	RSU5			
RSS-2-upper		L. Oligocene - Early Miocene		V4
-----	Local unconf.			
RSS-2-lower			Pre-WAIS	
-----	RSU6			
RSS-1-upper		>E. Oligocene?		V5?
-----	RSU7			
RSS-1-lower		Late Cretaceous?		??

*DeSantis et al. [1995; 1999]; Barrett et al. [2000]; Hamilton et al. [2001]; Luyendyk et al. [2001]

Table 2-1: Proposed correlation* of eastern Ross Sea RSS units, western Ross Sea V units, age, and depositional environment.







The V units of the western Ross Sea, proposed by Cooper et al. [1987], are numbered from V1 (youngest sedimentary) to V5 (oldest sedimentary) and V6 (volcanic) above acoustic basement, V7 (Table 2-1). The V sequences have been correlated from the VLB to the Cape Roberts Project drill sites (CRP) by Davey et al. [2001], using Italian and RVIB *Nathaniel B. Palmer* seismic reflection data (Fig. 2-1a). An unconformity between early and late Miocene glacial-marine sediments was interpreted by Davey et al. [2000] and Hamilton et al [2001] as the V3/V4 boundary. It was sampled at CRP and dated at ~21 Ma [Fielding and Thompson, 1999]. Within unit V4, an angular unconformity separating V4a and V4b was sampled. Hamilton et al [2001] interprets the overlying V3/V4a units, above the V4a/V4b unconformity, to display much less tilting. They infer this to indicate major exhumation of the TAM in southern Victoria Land was completed by this time. Below the V4 units is unit V5a. An angular unconformity separating units V4 and V5a has been interpreted by Davey et al. [2001] as unconformity RSU6 (>26 Ma in the Eastern Basin). Davey et al. [2001] suggest Late Oligocene/Early Miocene (V4) and Early Oligocene-late Eocene (?) (V5) units in the western VLB correspond to units RSS-2 and RSS-1, respectively, of the eastern Ross Sea. Unit V7 was sampled at the base of the drilled section and may correspond with the Mesozoic-Paleozoic Beacon Sandstone found throughout the TAM [Cape-Roberts-Science-Team, 2000]. Davey et al. [2001] suggest the sedimentary sequences within the VLB are younger than previously thought.

At the southern end of McMurdo Sound are the CIROS-1 and CIROS-2 drill sites (Fig. 2-1a) [Hannah, 1994; Wilson, et al., 1998]. The oldest sediments recovered

at CIROS-1 are glacial and glacial-marine strata of early-late Eocene age [Barrett, 1989; Hannah, 1997; Hannah, et al., 1997; Wilson, et al., 1998]. Correlation of Eocene and Oligocene strata from CIROS-1 to the VLB remains problematic because of faulting, unconformities, and shallow water bottom multiples between McMurdo Sound and VLB [Bartek, et al., 1996; Henrys, et al., 1998].

2-2. Seismic Reflection Data and Methods

2-2.1. Survey Areas and Methods

Two marine geological and geophysical surveys were conducted during January of 2003 and 2004 along the Ross Ice Shelf front of both the western and eastern Ross Sea, during RVIB *Nathaniel B. Palmer* cruises 03-01 (NBP-0301) and 03-06 (NBP-0306). The primary objectives of the surveys were to collect detailed grids of seismic data to select drill sites designed to investigate the climatic and tectonic history of the Ross Sea. Surveys were located in regions where large sections of the ice shelf have recently broken off, exposing previously unexplored seafloor [Decesari, et al., 2003; Decesari, et al., 2004]. NBP03-01 collected ~2,253 km of new multichannel seismic reflection (MCS) data and ~2,500 km of single channel (SCS) reflection data. NBP03-06 collected ~1,400 km of new MCS /SCS seismic reflection data.

In the western Ross Sea, a survey site was chosen where giant iceberg C-19 broke off the ice shelf in 2002. This site is adjacent to Ross Island, 120 km NE from McMurdo Station, and spans the structural provinces of the east flank of the VLB,

across the Coulman High and into the Central Trough (Fig. 2-1a & 2-1b). In the eastern Ross Sea, seismic data were collected where giant iceberg B-15 broke off the ice shelf in 2000, and spans the structural province of the Eastern Basin to the southeastern Ross Sea, offshore southwestern Marie Byrd Land (Fig. 2-1a & 2-1c).

NBP-0301 employed 46-channel (out of 48) seismic reflection profiling and NBP-0306 employed 48-channel seismic reflection profiling. The primary sound source used for both cruises was a 105 in³ generator injector (GI) air gun array. NBP-0301 also used a Bolt 1500C air gun array, consisting of six guns ranging in volume from 80 in³ to 850 in³, totaling 3000 in³. Switching from the GI gun array to the Bolt gun array was done in an effort to maximize sound penetration depths. However, little improvement of the data quality was observed. Both cruises had a hydrophone spacing of 25 m, with shots equally spaced at 25 m intervals while using the GI air guns. This resulted in up to 23-fold stacks for NBP-0301 and 24-fold stacks for NBP-0306. NBP-0301 also had 37.5 m shots while using the Bolt air gun array because the larger volume guns required more time to charge. Both cruises employed single channel reflection profiling by alternating shooting a single gun (SCS) and the GI/Bolt gun array (MCS), followed by recording the alternating shots on separate systems (Appendix A).

2-2.2. Seismic Processing Methods

The suppression of water bottom and peg-leg multiples was the primary goal of processing the seismic data. Multiple attenuation was successful in part due to the

source power being strong enough and streamer offset being long enough. Seismic stratigraphy was imaged below 2.5 seconds two-way-travel-time (TWTT) throughout the data set. Initial processing of seismic data included an interactive velocity analysis at 2 km intervals on shot gathers to choose velocities that were intermediate between primary and multiple reflectors. These velocities were used for a normal moveout (NMO) correction that separated primary reflections from multiple energy. Multiples were filtered out in frequency-wave number (F-K) space and the NMO was removed from the filtered gather. Interactive velocity analysis at 1 km intervals was preformed on filtered CDP gathers to obtain stacking velocities. Other processing steps include Butterworth band pass frequency filtering and near trace muting prior to stacking. (See Fig. 2-2a & 2-2b for a FK de-multiple example). An interval velocity model derived from stacking velocities was compiled and used in a 2-D finite difference depth migration. The 2-D finite difference migration is capable of locating reflectors in their correct positions even with steeply dipping reflectors, as well as producing an output in both time and depth sections [Claerbout, 1985]. Most of the processed data have been migrated using this method, and fault plane reflections have been imaged.

A better multiple suppression method has prompted the modification of the processing technique. The parabolic Radon Transform [Hampson, 1991] was used in later processing rather than the F-K filtering method for multiple suppression. Parabolic Radon Transforms use offset curvature rather than just the apparent velocity, used by F-K filtering, which results in multiple attenuation even on near traces. An interactive velocity analysis was performed at 1 km intervals on CDP

Figure 2-2a-c: Processing comparisons on NBP-0301 Line 2B
(see figure 2-1b for location)

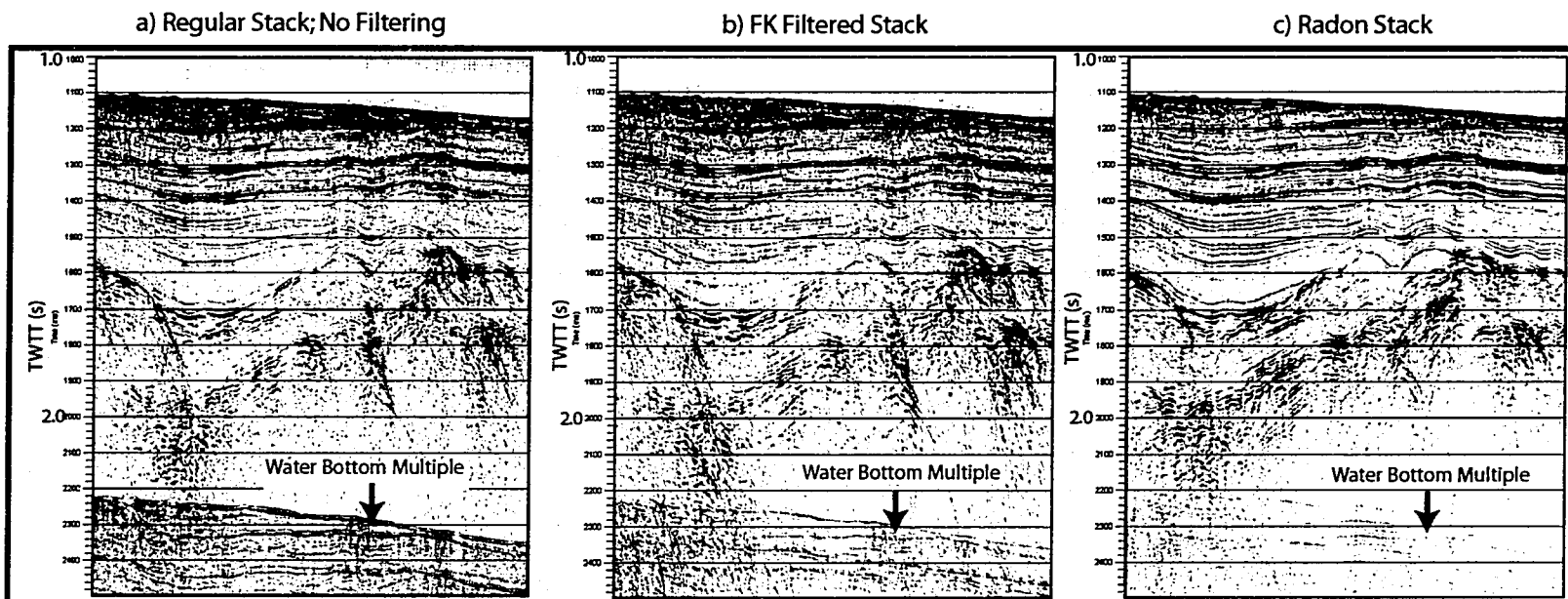


Figure 2-2a: Regular stack without any multiple attenuation. The sea floor multiple is at twice

Figure 2-2b: FK filtered stack. The water bottom multiple has been attenuated using a FK filter. A majority of the multiple has been removed, but some still remains.

Figure 2-2c: Radon Stack. The multiple was highly attenuated using the Radon Transform multiple attenuation method. Little multiple energy remains.

gathers, prior to the parabolic Radon Transform, to determine the stacking velocities. After a NMO correction on the CDP gathers, the parabolic Radon Transform is applied and a multiple model is produced. The multiple model is subtracted from the original CDP gathers, resulting in the attenuation of multiple reflections. The de-multiple CDP gathers are then stacked. This multiple suppression method has resulted in the imaging of reflections from strata below 3 s TWTT in the eastern Ross Sea. (See Fig. 2-2d for a Radon de-multiple stack; Appendix B).

2-3. Correlation Results

2-3.1. Correlation of RSS Sequences to V Sequences in the Ross Sea

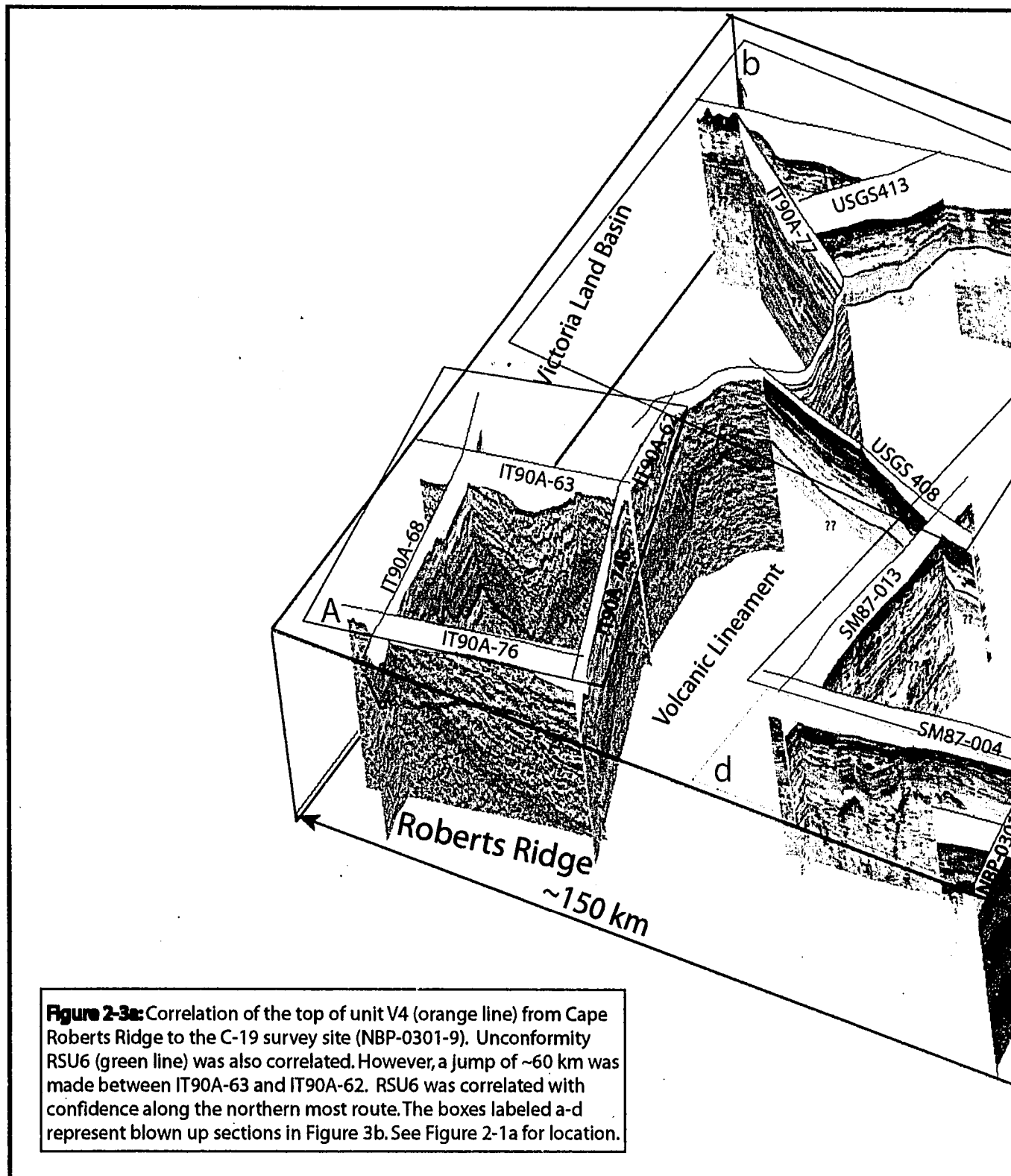
An angular unconformity representing the top of seismic unit V4 (Late Oligocene-Early Miocene; > 23.7 Ma) was correlated from CRP core holes in the VLB to the C-19 survey site using multiple paths along Italian, Russian, German, and USGS seismic lines (Fig. 2-1a & 2-1b; Table 2-2) [Cooper, et al., 1995]. The top of unit V4 was correlated north in the VLB before heading east and then south in the Central Trough to the C-19 site on the Coulman High. Multiple routes were used to correlate the top of V4 to C-19 in order to increase confidence levels in the correlation (Fig. 2-3a & 2-3b). Rather than correlate directly east from CRP, the correlation route was taken to the north to tie around a volcanic lineament, associated with the late Cenozoic Terror Rift that extends northward from Ross Island to Beaufort and Franklin Islands (Fig. 2-1b) [Brancolini, et al., 1995]. Stratigraphic units, including the top of V4, are cut by the volcanic lineament between Beaufort

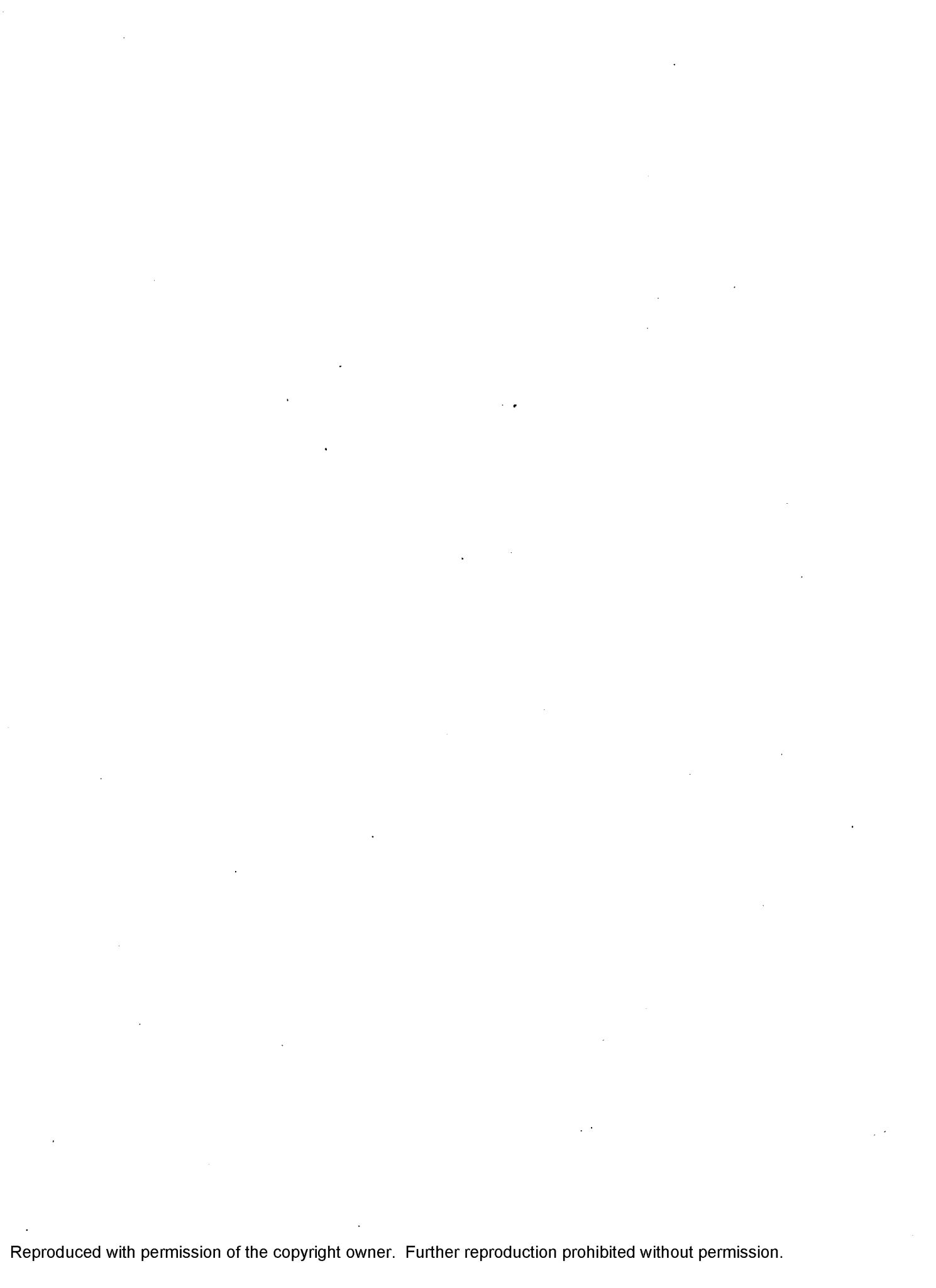
and Franklin Islands. The top of unit V4 is the oldest continuous horizon that was able to be correlated to the C-19 survey site. Unfortunately, multiples in the Italian data make reflectors beneath the top of V4 hard to correlate through the eastern VLB and to C-19.

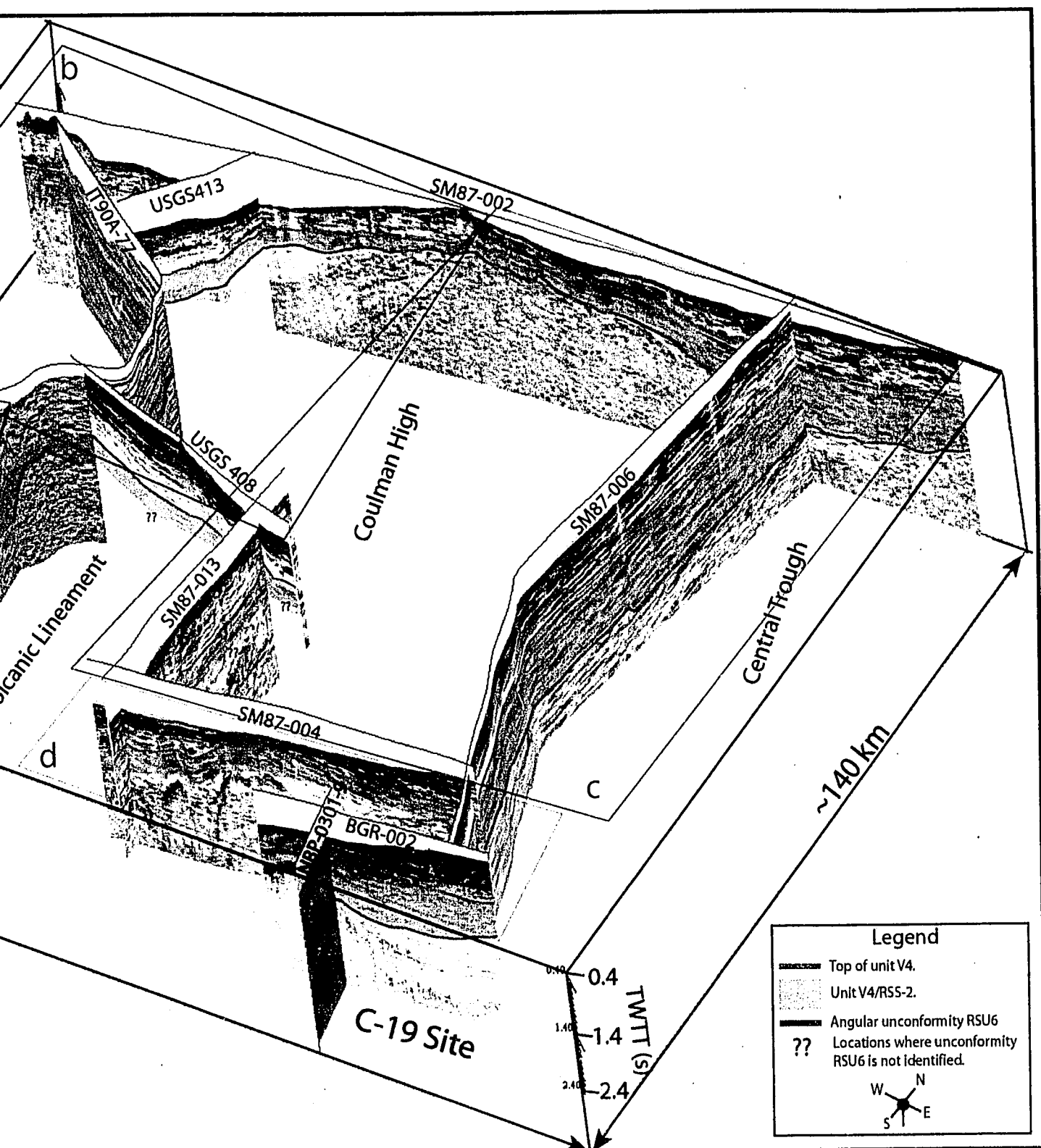
CRP to C-19			Eastern Basin to C1-9		
Line Number	Organization	Year	Line Number	Organization	Year
IT90-62	OGS ¹	1990	BGR 01	BGR ⁴	1980
IT90-68	OGS ¹	1990	BGR 02	BGR ⁴	1980
IT90-69	OGS ¹	1990	BGR 04	BGR ⁴	1980
IT90-71	OGS ¹	1990	BGR 05	BGR ⁴	1980
IT90-72	OGS ¹	1990	BGR 06	BGR ⁴	1980
IT90-74	OGS ¹	1990	BGR 07	BGR ⁴	1980
IT90-75	OGS ¹	1990	BGR 101	BGR ⁴	1980
IT90-76	OGS ¹	1990	BGR 104	BGR ⁴	1980
IT90-77	OGS ¹	1990	IFP 201	IFP ⁵	1982
USGS 408	USGS ²	1984	IFP 202	IFP ⁵	1982
SM 87013	MAGE ³	1987	IFP 203	IFP ⁵	1982
SM 87004	MAGE ³	1987	SM 87004	MAGE ³	1987
SM 87006	MAGE ³	1987	SM 87006	MAGE ³	1987
BGR 02	BGR ⁴	1980	SM 87007	MAGE ³	1987
			NBP 9601-6	UCSB ⁶	1996
			NBP 9601-7	UCSB ⁶	1996
			NBP 0301-13	UCSB ⁶	2003
			NBP 0306-136	UCSB ⁶	2004

Table 2-2: MCS data used in Correlation used for correlating seismic stratigraphy interpreted at CRP to the C-19 survey site and eastern Ross Sea strata over the Central to the C-19 site. 1) Osservatorio Geofisico Sperimentale di Trieste (Italy), 2) U. S. Geological Survey, 3) Joint Stock Company Marine Arctic Geological Expedition (Russia), 4) Bundesanstalt fur Geowissenschaften und Rohstoffe (Germany), 5) Institute Francaise du Petrole (France), 6) University of California, Santa Barbara (USA)

Correlation of an older reflector, interpreted as angular unconformity RSU6 (~30 Ma), was attempted from CRP to the C-19 site. Unconformity RSU6 can be correlated to the north from CRP on the western side of the VLB along lines IT90-68 and IT90-63, where it becomes too difficult to differentiate from multiples (Fig. 2-1a, 2-3a & 2-3b). Although RSU6 is within multiples along this route, the unconformity









Reproduced with permission of the copyright owner. Further reproduction prohibited without permission.

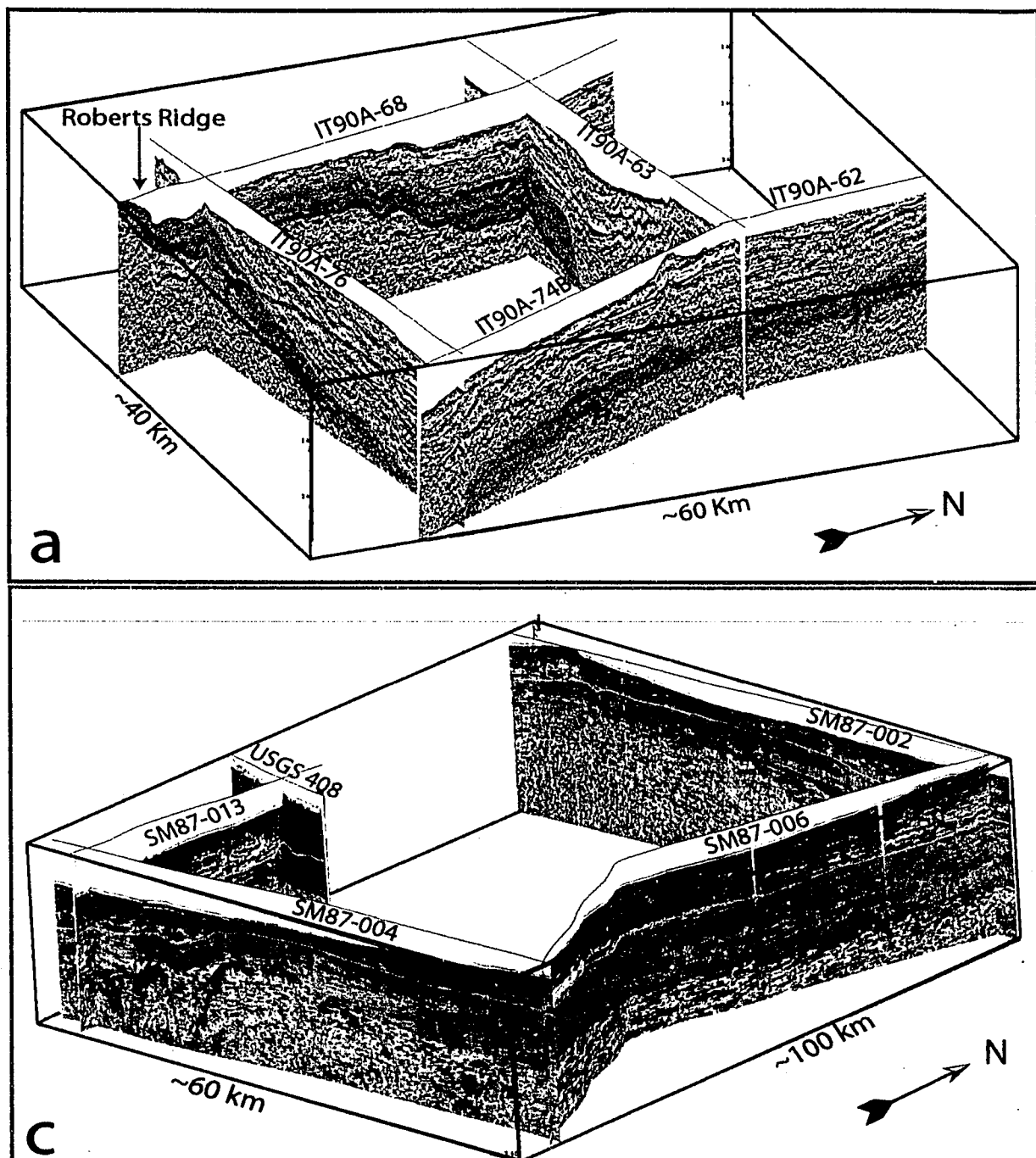
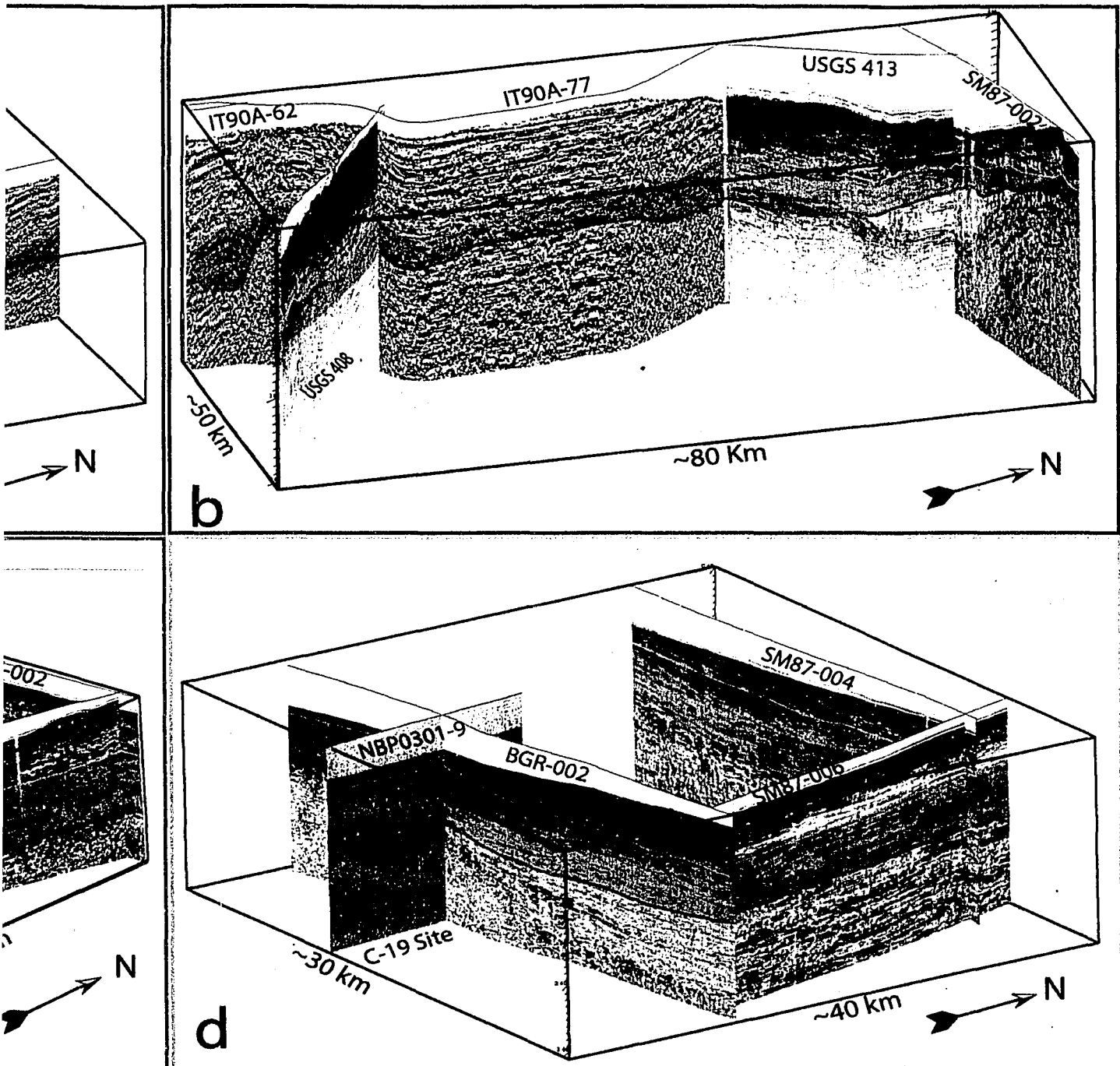


Figure 2-3b: Blow up sections from Figure 2-3a of the C-19 Site. See Figure 1a for location of the smaller diagram interpreted as the top of unit V4 was corelated from Roberts Ridge survey site (Box d). Angular unconformity RSU6 (~30 Ma) to the C-19 site



ions from Figure 2-3a of the correlation from Roberts Ridge to the location of the smaller diagrams. An angular unconformity unit V4 was correlated from Roberts Ridge (Box a) to the C-19 unconformity RSU6 (~30 Ma) was correlated from Roberts

Legend	
—	Top of unit V4.
■	Unit V4/RSS-2. ?? RSU6 not Identified.
—	Unconformity RSU-6.



can be interpreted through. An attempt was made to correlate an existing interpretation of unconformity RSU6, on Russian line SM87-002 in the northern VLB (see Antarctic Research Series (ARS) vol. 68 plate 8), south to our interpretation of RSU6 on IT90-63 (Fig. 2-1a, 2-3a & 2-3b). Unconformity RSU6 can be correlated from the Russian line south to the end of IT90-77, where it becomes too deep to interpret (Fig. 2-1a & 2-3a). The gap between RSU6 on IT90-77 to IT90-63 is ~60 km. RSU6 most likely ties across the gap, but given the data quality, its location cannot be resolved at this time. Unconformity RSU6 ties into the Central Trough along SM87-002 and to the C-19 site (Fig. 2-1a, 2-3a & 2-3b). RSU6 onlaps the western flank of the Central High and cannot be correlated across into the eastern Ross Sea.

Interpretations of NBP-0301 and NBP-0306 seismic data indicate the late Oligocene-early Miocene RSS-2 unit of the Eastern Basin can be correlated across the Central High, along the Ross Ice Shelf front. A correlation of the RSS-2 unit from DSDP Site 270 to NBP-0301 and NBP-0306 reflection data was made using a combination of routes on French (IFP 201, 202, 203), German (BGR 02, 05, 06, 07, 104), and Russian (SM 87004, 87007) seismic lines (Fig. 2-1a & 2-1c; Table 2-2) [Cooper, et al., 1995]. Unconformities RSU6, RSU5 and unit RSS-2 were correlated west onto the Central High from the Eastern Basin on NBP-0301 line 13A and NBP-0306 line 136A. Existing interpretations of the Eastern Basin were used to tie to the NBP-0301 and NBP-0306 data (ARS vol. 68 plates 10 and 14) [Cooper, et al., 1995]. Unconformity RSU5 merges into younger unconformities above, pinching out unit

RSS-3 at ~175.5 ° W on NBP-0306 lines 106, 135, and German Line BGR-104 (Fig. 2-1a). Unconformity RSU6 onlaps the eastern flank of the Central High. Unconformity RSU5 eventually daylights, leaving only a thin layer (60 to 80 m) of RSS-2 over the axis of the Central High on NBP-0306 line 136A (Fig. 2-4). At this location, the eroded RSS-2 unit is resting directly on top of acoustic basement and can be correlated into the Central Trough. On NBP-0301 line 13A, the RSS-2 sequence pinches out on acoustic basement. A jump correlation of approximately 6 km was made across the Central High between 77.8° S, 179.8 ° E and 77.8° S, 179.8° W (Fig. 2-1a & 2-5).

To increase the confidence of the correlation, existing correlations of the RSS-2 sequence across the northern Central High, along German seismic line BGR-04 (see ARS vol. 68 plate 9), where reinterpreted [Cooper, et al., 1995]. Interpretations on BGR-04 (plate 9 of ARS vol. 68) show that unconformities RSU5, RSU4a and RSU4, as well as units RSS-2, RSS-3 and RSS-4, can be correlated across this portion of the Central High. The reinterpretations of RSU6, RSU5, RSU4a, and RSU4 north from DSDP Site 272 along IFP-201 to BGR-04 (Fig. 2-1a) corresponded with the existing interpretations with one exception; unconformity RSU4 could not be mapped across the Central High. Seismic unit RSS-2 and unconformity RSU5 correlate across the Central High into the Central Trough on line BGR-04. However, unconformity RSU6 onlaps the Central High, resulting in RSS-2 resting on top of the basement structure over the high. An array of German (BGR 01, 02, 101) and Russian (SM 87004, 87006) seismic lines were used to tie unconformity RSU5 from the western flanks of

NBP-0306 line 136

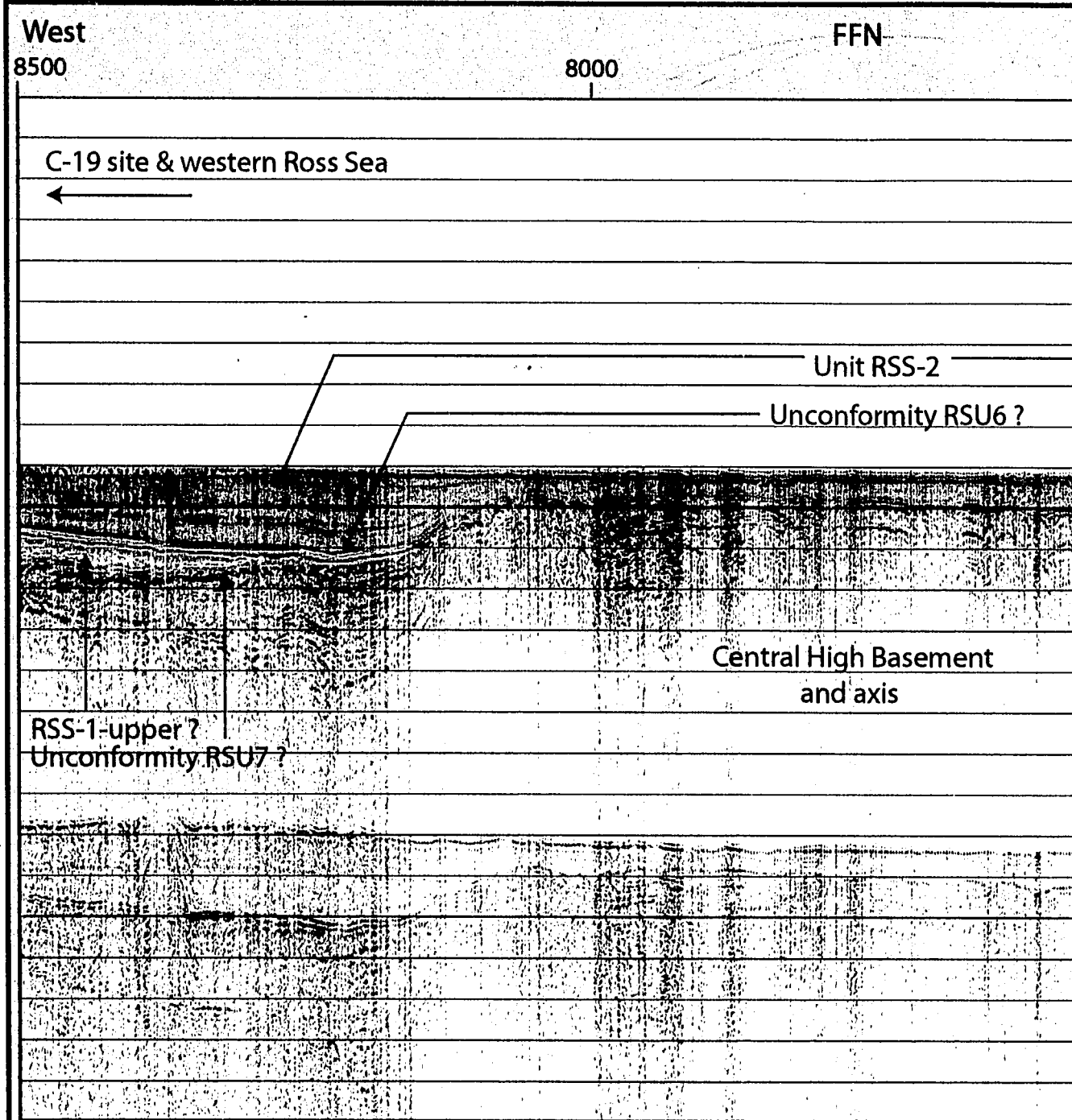
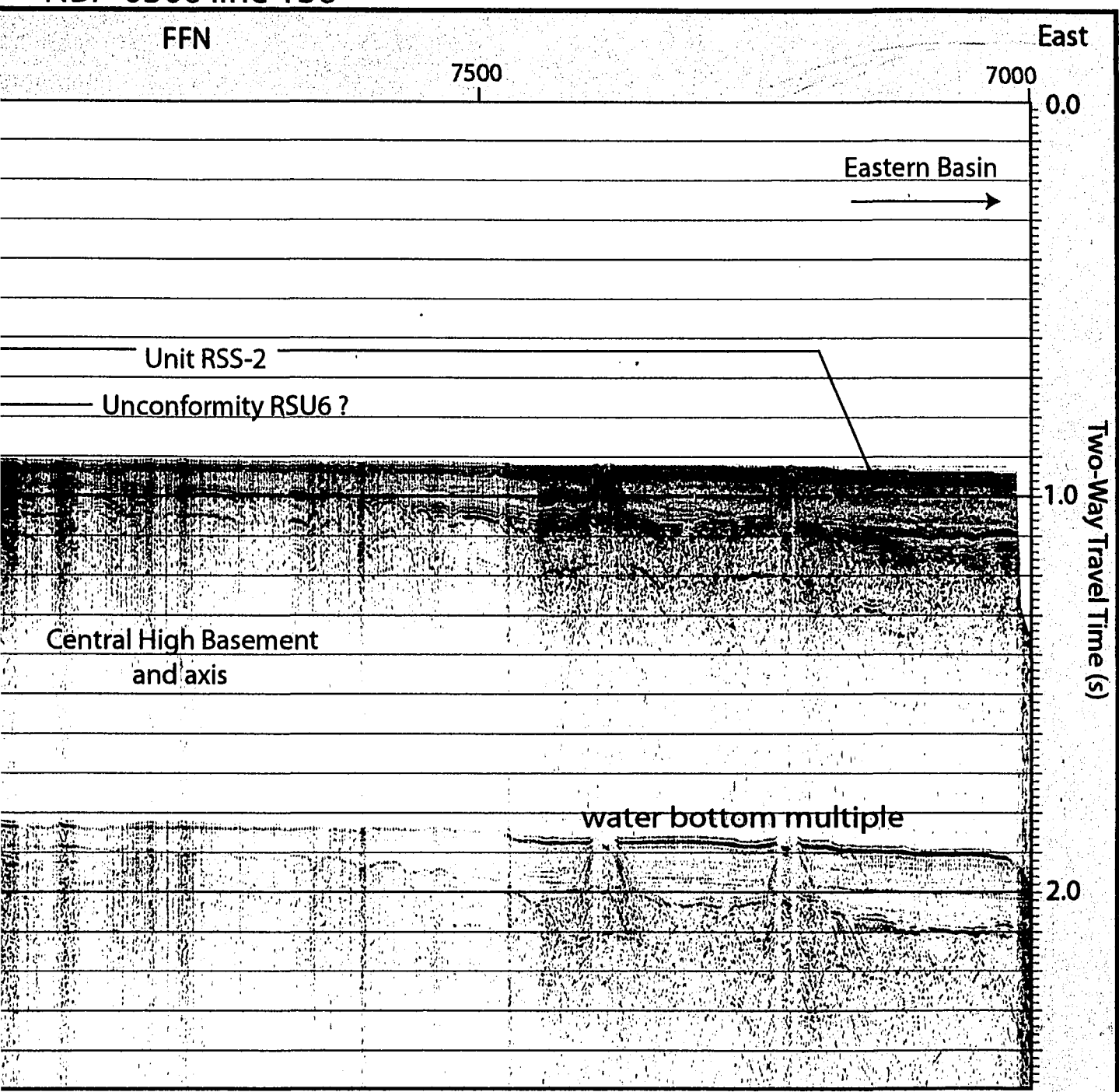


Figure 2-4: Seismic line NBP-0306-136 along the ice shelf front over the axis of the Central High. unit RSS-2. A thin layer of RSS-2 is interpreted crossing the Central High without pinching out. In acoustic basement structure of the Central High. Unit RSS-1-upper is interpreted within basement (RSU6 ?) separating it unit from overlying RSS-2. Below RSS-1-upper is an angular unconformity beneath. Because the water bottom multiple is deep, no de-multiple processing was done on this

NBP-0306 line 136



ce shelf front over the axis of the Central High. Green shade shows the interpretation of
ssing the Central High without pinching out. Interpreted under unit RSS-2 is the
Unit RSS-1-upper is interpreted within basement grabens with an unconformity
Below RSS-1-upper is an angular unconformity (RSU7 ?) with possible RSS-1-lower
eep, no de-multiple processing was done on this line.

← 5 km →

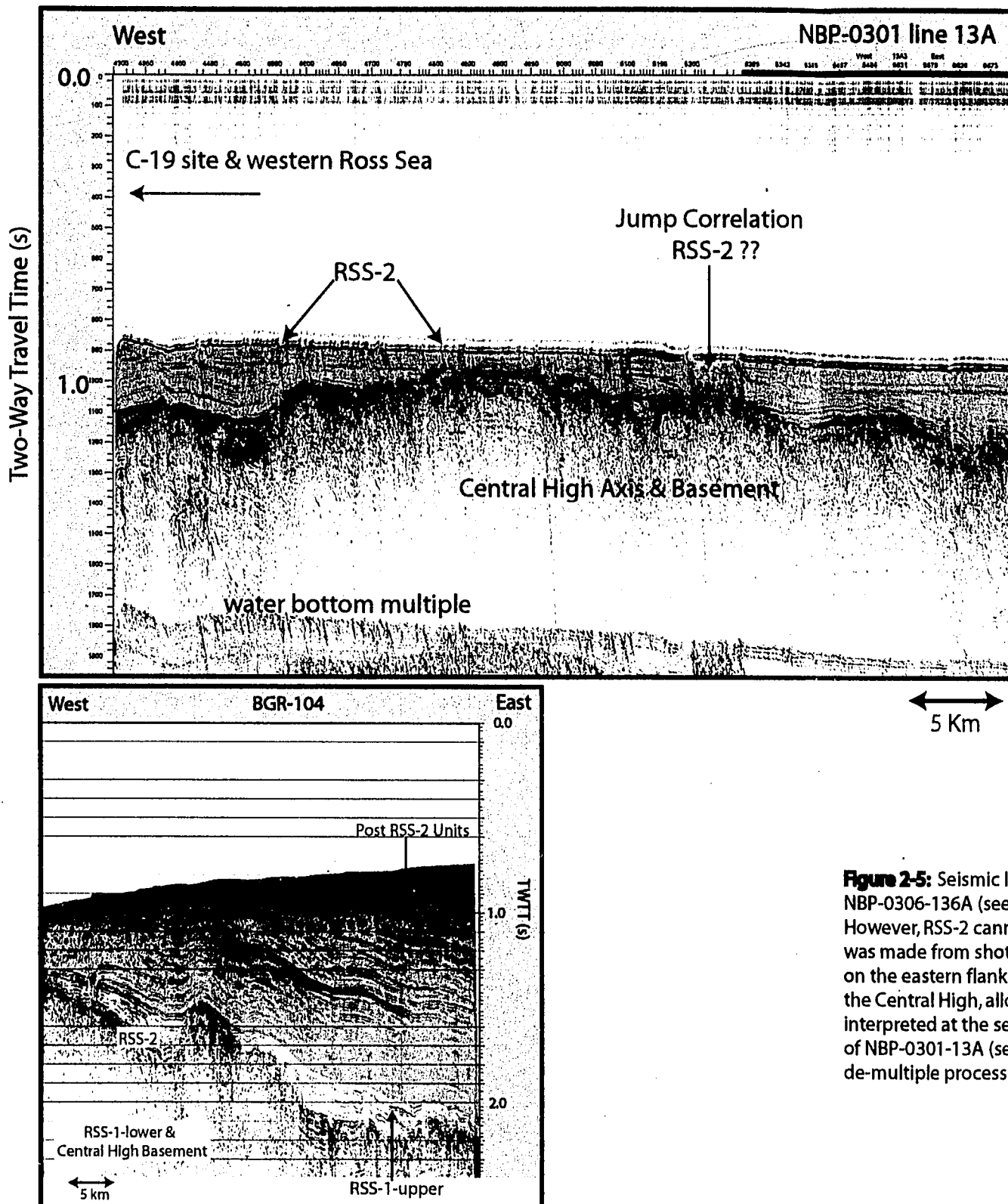


Figure 2-5: Seismic I NBP-0306-136A (see However, RSS-2 cannot was made from shot on the eastern flank the Central High, all interpreted at the se of NBP-0301-13A (see de-multiple processi



Reproduced with permission of the copyright owner. Further reproduction prohibited without permission.

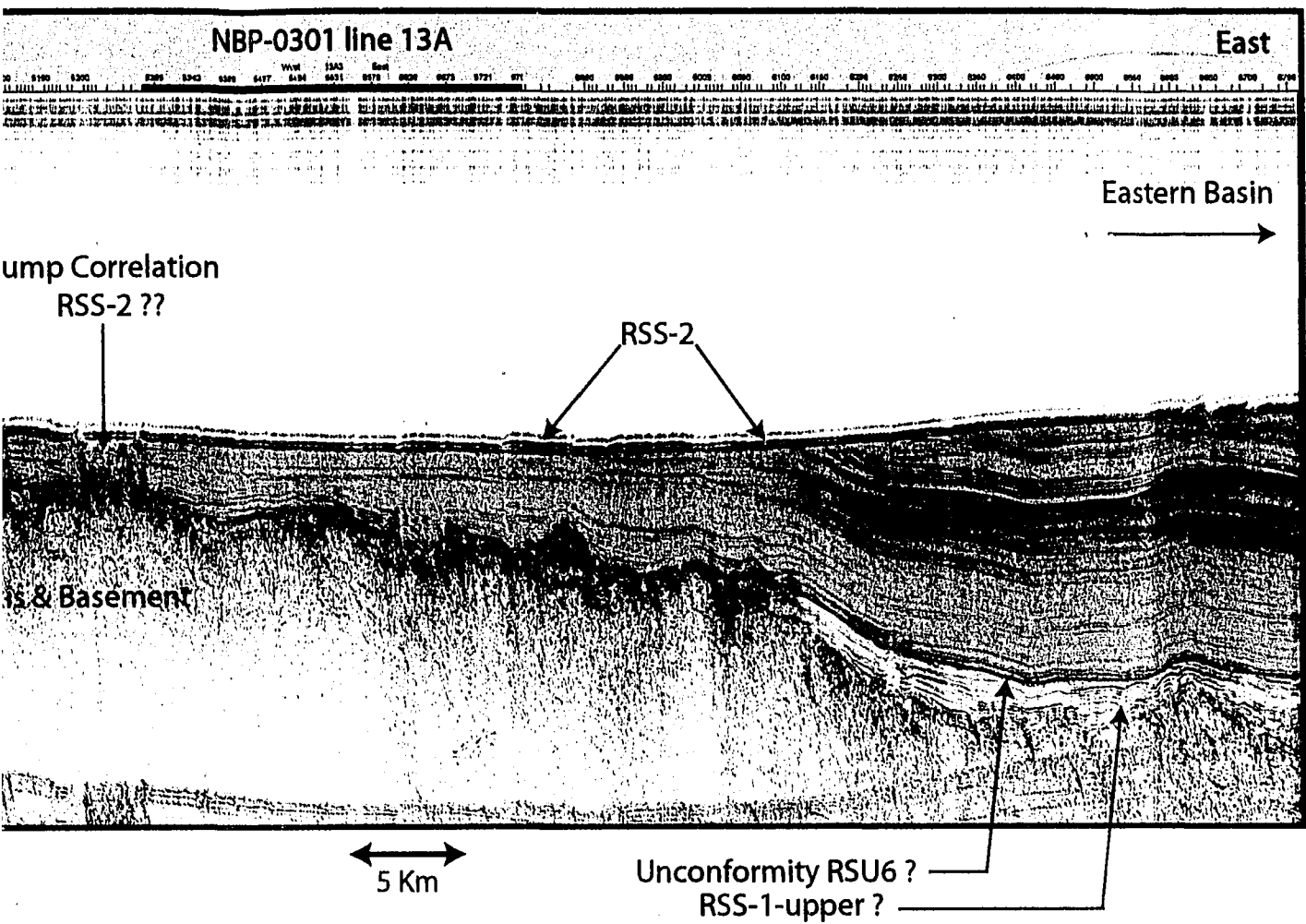


Figure 2-5: Seismic line NBP-0301-13A across the axis of the Central High. This line is north of NBP-0306-136A (see figure J2-1a & 2-1c). RSS-2 is interpreted overlying Central High basement. However, RSS-2 cannot be confidently correlated across the high. A jump correlation of ~6 km was made from shot point 5200 to 5250. Unconformity RSU6 and unit RSS-1 upper pinch out on the eastern flank of the Central High. Post RSS-2 units pinched out on the eastern flank of the Central High, allowing unit RSS-2 to daylight. A thin veneer of post RSS-2 units are interpreted at the sea floor (See BGR-104 line segment to the left). BGR-104 is located to the east of NBP-0301-13A (see figure 1A for location). Because the water bottom multiple is deep, no de-multiple processing was done on this line.



South

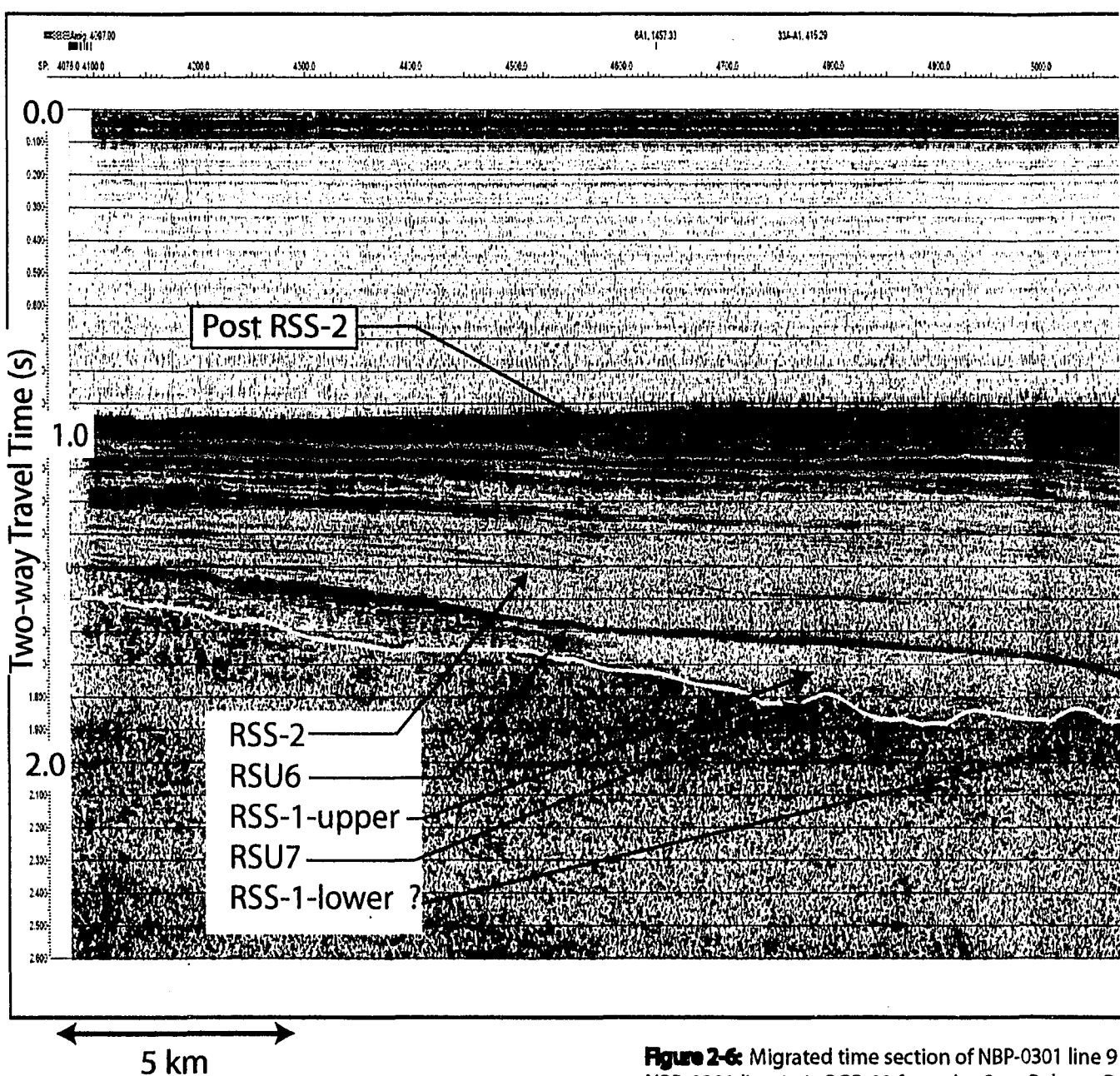


Figure 2-6: Migrated time section of NBP-0301 line 9 NBP-0301 line 9 via BGR-02 from the Cape Roberts Di NBP-0301 line 9 via BGR-02 from the Eastern Basin. Th reflectors is 0.04 s or one seismic cycle. A thickening s RSS-1-upper is interpreted on top of unconformity RS may be RSS-1-lower and or basement.

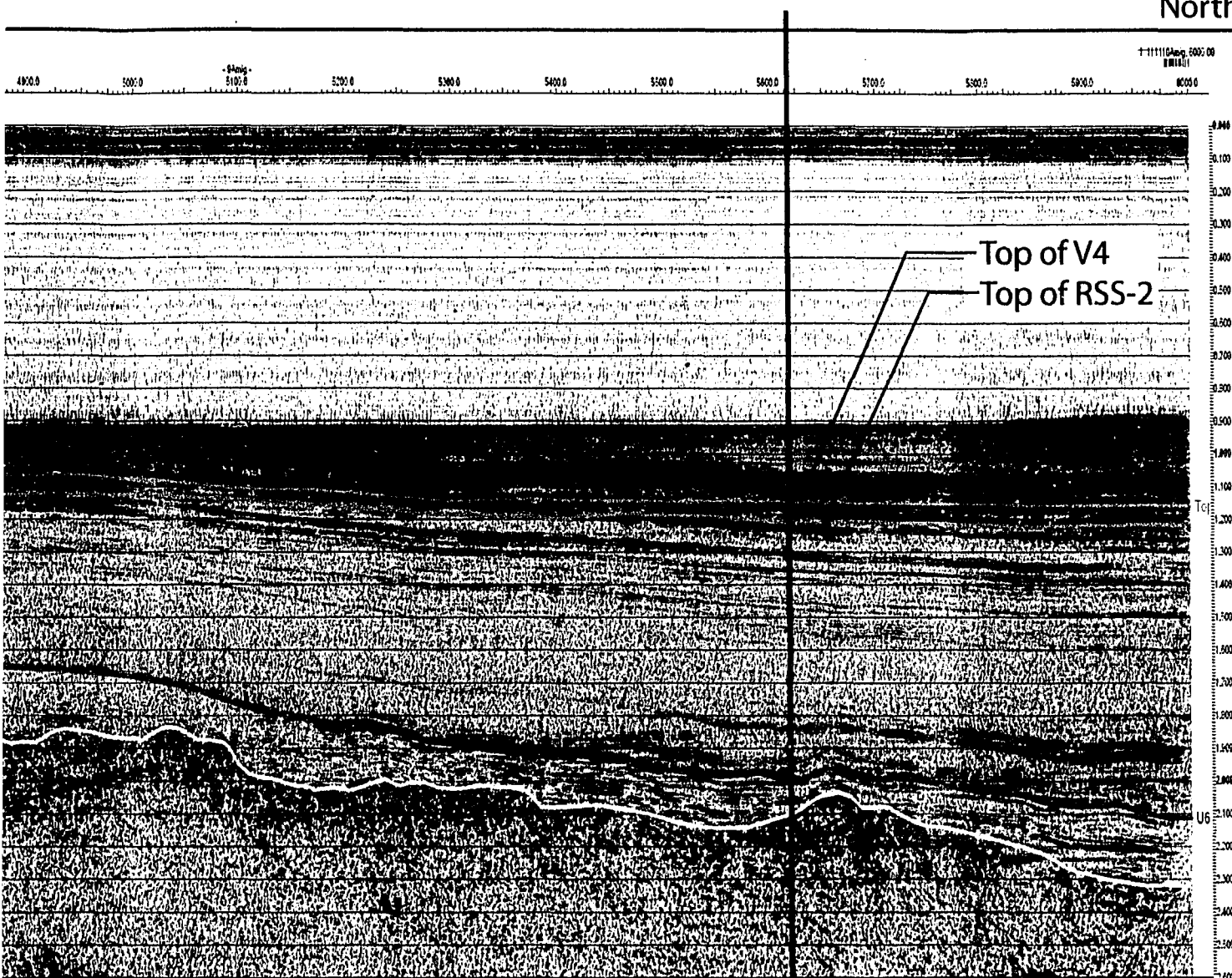


Reproduced with permission of the copyright owner. Further reproduction prohibited without permission.

NBP-0301 line 9

Tie with BGR-02

North



tion of NBP-0301 line 9 from the C-19 site. The top of V4 was tied to
om the Cape Roberts Drill sites. Unconformity RSU5 was also tied to
om the Eastern Basin. The difference between RSU5 and Top of V4
mic cycle. A thickening section of RSS-2 is interpreted here. Unit
n top of unconformity RSU7. Highly disrupted reflectors below RSU7
asement.

the Central High into the C-19 survey site (Fig. 2-1a & 2-1b). Unconformity RSU5 tied 0.04 s, or one seismic cycle, from the top of the V4 reflector (Fig. 2-6). This suggests the reflector marking unconformity RSU5 in eastern Ross Sea is the same reflector marking the Top of V4 in western Ross Sea.

Unconformities RSU7, RSU6, RSU5, RSU4a, and RSU4 were correlated along the ice shelf front to the Bay of Whales region of the eastern Ross Sea. Units between unconformities, RSU5, RSU4a, and RSU4 thin to the east and merge together, before daylighting in the eastern Bay of Whales. Unconformity RSU6 is prominent along the ice shelf front and onlaps Roosevelt Ridge, a newly discovered basement high in the Bay of Whales. Unconformity RSU7 is interpreted along the Ross Ice Shelf front within basement half-grabens.

2-3.2. Seismic Stratigraphy of the Eastern Ross Sea

2-3.2.1. Unconformity RSU7 and Sequences RSS-1-upper and RSS-1-lower. Dipping and offset reflectors are interpreted on top of acoustic basement and below relatively flat and undisturbed strata throughout the Eastern Basin. This strata is interpreted as the RSS-1 unit. Within the RSS-1 unit is a faulted, angular unconformity, interpreted to separate slightly dipping and offset reflectors from more highly deformed reflectors within basement half-grabens (Fig. 2-7). Based on similarities in reflection characteristics with the RSS-1-lower and upper unit of Luyendyk et al. [2001], the highly deformed synrift unit within basement half-

grabens is interpreted as RSS-1-lower, and the less deformed synrift unit above is interpreted as RSS-1-upper. Unconformity separates the RSS-1-lower and upper.

Both RSS-1 sequences are interpreted along the ice shelf front throughout the Eastern Basin (Fig. 2-1a & 2-1c). RSS-1-upper has a gentle westward tilt and drops below 3 s TWTT around 178 ° W, along the ice shelf front, where it is too deep to image. Similar dipping and offset reflectors, overlying an angular unconformity, are interpreted on the eastern flanks of the Central High. These reflectors are interpreted as RSS-1-upper and unconformity RSU7, respectively. Grabens within the acoustic basement on the Central High are filled with highly disrupted and offset reflectors, characteristic of RSS-1-lower.

2-3.2.2. Unconformities RSU6, RSU5 and Unit RSS-2. An angular unconformity separates the synrift RSS-1-upper unit from un-deformed stratigraphy above. This unconformity is not deformed and has been tied to existing interpretations of unconformity RSU6 (>26 Ma) in the Eastern Basin. In the Bay of Whales, RSU6 merges with unconformity RSU7 (Fig. 2-7), before onlapping the basement of the Roosevelt Ridge. To the east of Roosevelt Ridge, unconformities RSU6 and RSU7 separate into two distinct reflectors. Strata above RSU6 is mainly flat lying and un-deformed. This strata is interpreted as late-Oligocene-early Miocene RSS-2. A majority of the flat lying and undisturbed strata interpreted in the Eastern Basin are of unit RSS-2. The unit is gently tilted and thickens to the west to over 2,000 m [Cooper, et al., 1995] throughout most of the Eastern Basin, with the exception of the eastern flanks of the Central High, where it tilts and thickens to the

NBP-0306 line 110B sp# 2020-3020

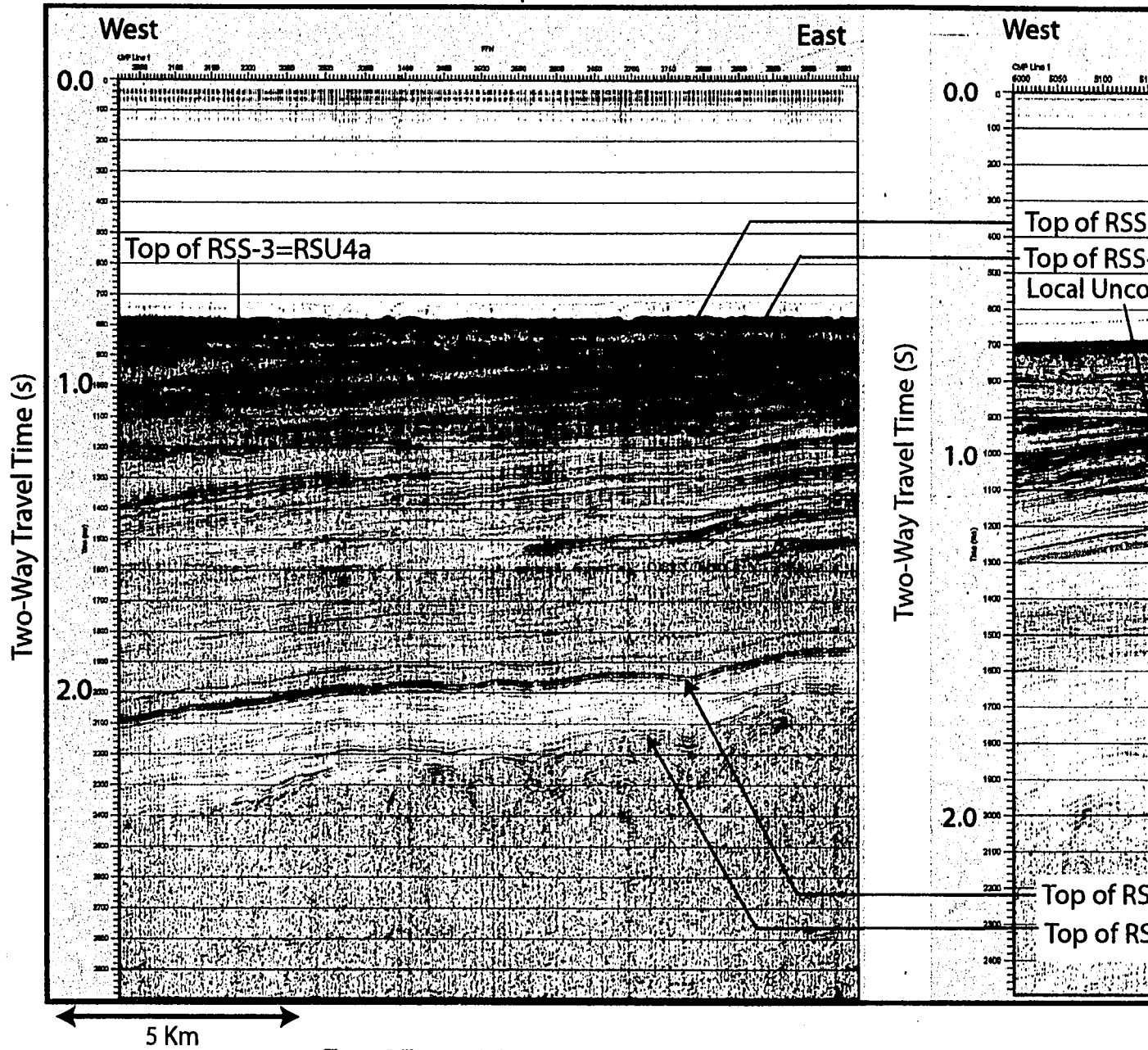
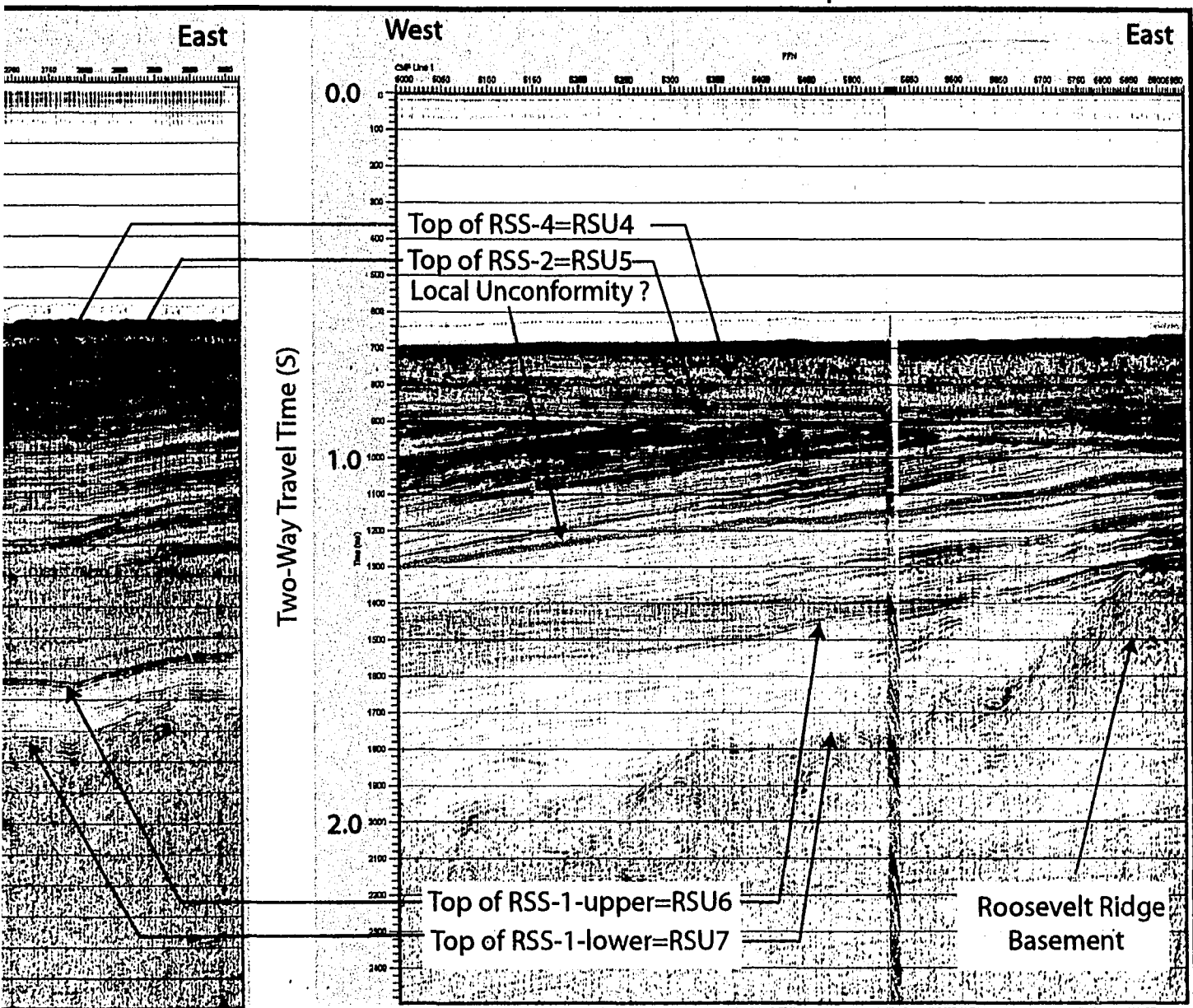


Figure 2-7: Seismic line NBP-0306-110B in the Eastern Basin along the ice shelf front (see figure 1). The figure on the left is from ~169 degrees W longitude and the figure on the right is from ~166 degrees W longitude. Units RSS-1-lower through RSS-3 are interpreted. Late Cretaceous unit RSS-1-lower is characterized by basement grabens (orange shade). Less deformed strata above RSS-1-lower is RSS-1-upper (left) or onlap acoustic basement of the Roosevelt Ridge in the Bay of Whales (right figure). Within RSS-1-lower/upper is angular unconformity RSU6 and the Oligocene RSS-2 is relatively flat with a slight dip to the west. Local unconformities are observed in RSS-2, but cannot be clearly defined. The post RSS-2 units of RSS-3 (purple shade) and RSS-4 (pink shade) are interpreted above RSU6.



Reproduced with permission of the copyright owner. Further reproduction prohibited without permission.



5-110B in the Eastern Basin along the ice shelf front (see figure 2-1a & 2-1c). Displayed are two segments of line 110B. 59 degrees W longitude and the figure on the right is from ~ 166 degrees W longitude in the Bay of Whales. Seismic are interpreted. Late Cretaceous unit RSS-1-lower is characterized by highly deformed reflectors and is preserved in e). Less deformed strata above RSS-1-lower is RSS-1-upper (yellow shade). RSS-1-lower and upper are interpreted e Roosevelt Ridge in the Bay of Whales (right figure). Within basement grabens, unconformity RSU7 separates upper is angular unconformity RSU6 and the Oligocene RSS-2 unit (green shade). RSS-2 is not faulted and is mainly Local unconformities are observed in RSS-2, but cannot be correlated throughout the unit (green line on right figure). purple shade) and RSS-4 (pink shade) are interpreted above RSS-2.



Reproduced with permission of the copyright owner. Further reproduction prohibited without permission.

east. The RSS-2 sequence is characterized by intervals of transparent layers sandwiched between distinct, stronger reflections and onlap surfaces. This suggests local unconformities are present within the sequence (Fig. 2-7). Luyendyk et al. [2001] identified a local unconformity within RSS-2 off Cape Colbeck, in the eastern Ross Sea. At this location, RSS-2 is divided into an lower and upper unit [Luyendyk, et al., 2001]. Along the ice shelf front, a local unconformity is interpreted, but cannot be correlated throughout the data set (Fig. 2-7). It is possible the local unconformity may be similar to the unconformity identified by Luyendyk et al. [2001], separating RSS-2 into lower and upper units.

An unconformity capping the RSS-2 unit is interpreted and mapped across the Eastern Basin, along the ice shelf (Fig. 2-1c & 2-7). This unconformity was tied to unconformity RSU5. Unconformity RSU5 is described as a marine-subglacial unconformity, having been formed under an ice sheet or glacier during a sea level fall [DeSantis, et al., 1995]. DeSantis et al. [1999] suggests that RSU5 may only be of subglacial origin for areas on or near structural highs and is of marine origin elsewhere in the eastern Ross Sea.

2-3.2.3. Post RSS-2 units. Ross Sea seismic units RSS-3 through RSS-5 have been interpreted and mapped across the ice shelf front in the Eastern Basin (Fig. 1c & 2-7). For the purposes here, RSS-3 through RSS-5 are termed post RSS-2 units. In front of the ice shelf in the Bay of Whales the post RSS-2 units are thin, discontinuous, and are not definable as separate units. To the west of the Bay of Whales, RSS-3 through RSS-5 separate into thin slivers and may be correlated as

distinct stratigraphic units. Post RSS-2 units pinch out on the eastern flanks of the Central High, allowing RSS-2 to daylight (Fig. 2-5-BGR-104 inset).

2-3.3. Seismic Stratigraphy of the C-19 Site; Western Ross Sea

Acoustic basement reflections are interpreted throughout the C-19 site. Internal reflections within the acoustic basement are also interpreted (Fig. 2-8). Cooper et al. [1987] interprets basement reflections offshore Cape Roberts as Paleozoic Beacon Supergroup. Cores from CRP-3 bottomed in sandstone interpreted as the Devonian Arena Sandstone of the Beacon Supergroup [Cape-Roberts-Science-Team, 2000]. Therefore, the acoustic basement at C-19 may be composed of the Beacon Supergroup.

Half-grabens within the basement are filled with strata similar in character to unit RSS-1-lower. This unit is disrupted, discontinuous, highly deformed, and offset by numerous faults that cannot be clearly mapped. This unit is interpreted as synrift RSS-1-lower (Fig. 2-6 & 2-8). Overlying the highly deformed strata is an angular unconformity. The unconformity is offset by normal faults and primarily caps only units filling basement grabens. This unconformity is interpreted as RSU7. A less deformed unit above the angular unconformity is interpreted as tilted and offset by a few faults. Although the unit displays synrift characteristics, it is not deformed to the degree of RSS-1-lower, below. This unit is interpreted as RSS-1-upper and is not continuous throughout the survey site, forming lenses where unconformities above

West

NBP 0301 Line 6A

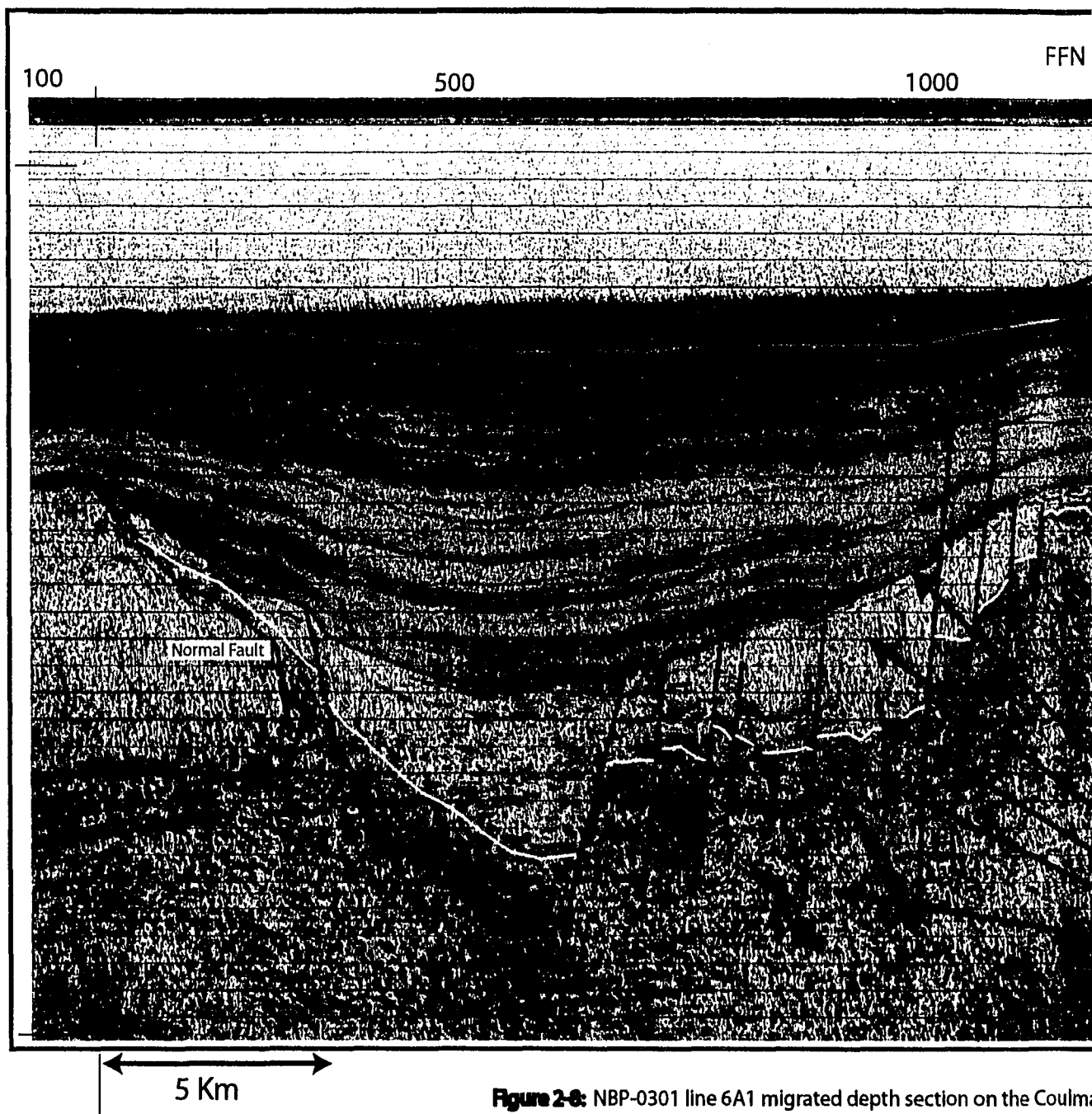
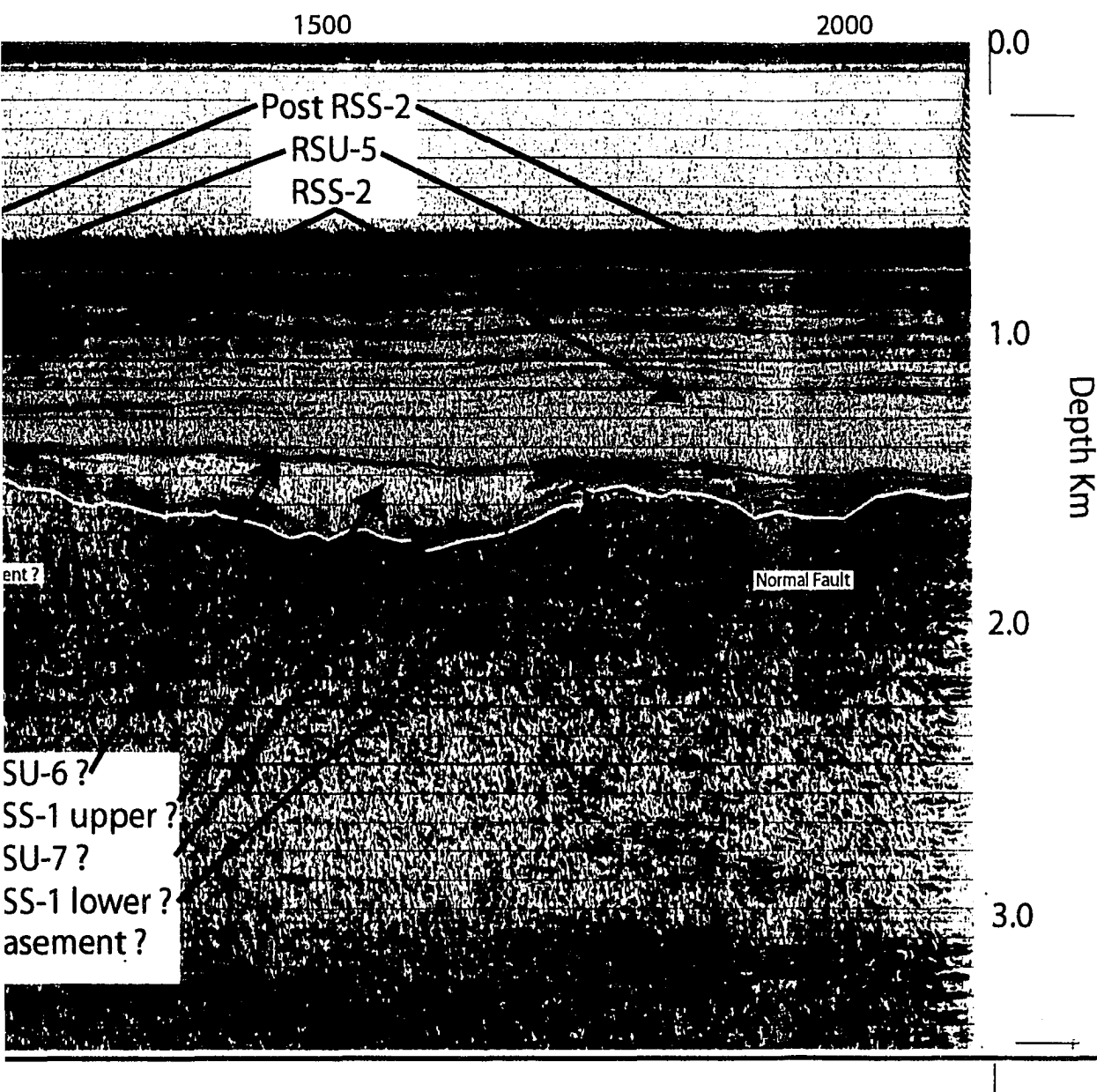


Figure 2-8: NBP-0301 line 6A1 migrated depth section on the Coulman High. The section shows thickening of the section throughout the Coulman High and has an approximately N-S trend. Unit RSS-1 is interpreted to have deposited a "U" shaped sag associated with it and thickens to ~ 1200 meters before terminating just below the seafloor. Unit RSS-2 is interpreted to onlap unit RSS-1 before the deposition of RSS-2 and may have been active during its deposition.

Migrated Depth

East



h, C-19 survey site (see figure 2-1b). A fault bounded graben is interpreted the graben, unit RSS-1-lower, RSS-1-upper and RSS-2 thicken. Unit RSS-2 -1-lower/upper are cut by normal faults. Several Faults cut into RSS-2 and formity RSU-6 on the edges of the graben, suggesting the graben formed tion.

and below the unit merge (Fig. 2-8). A second angular unconformity caps synrift RSS-1-upper and is offset by a few, graben bounding faults. This angular unconformity is interpreted as RSU6 and for the most part it is not faulted. Overlying RSU6 is late Oligocene-Early Miocene RSS-2, which has been tied to this survey. The RSS-2 unit is flat lying, un-deformed, and thickens within basement grabens. Graben bounding faults offsetting unconformity RSU6 are also interpreted to cut into and in some cases through the RSS-2/V4 unit (Fig. 2-8).

A majority of strata imaged on C-19 seismic lines are of unit RSS-2. The unit thickens in a “U” shape pattern within large fault bounded grabens, indicating subsidence occurred during the deposition of RSS-2 (Fig. 8). On top of the Coulman High, RSS-2 is thinner, but its reflector spacing is constant, indicating a constant unit thickness (Fig. 2-8). In the northern portion of the C-19 site, post RSS-2 units are thin, with little separation between reflectors. These are interpreted as units RSS-3, RSS-4a and RSS-4. In the southern portions of the survey site, near the ice shelf, these units merge into very thin unidentifiable reflectors. To the east, along the ice shelf, post RSS-2 units separate into individual units, thickening into the Central Trough. These units cannot be tied to the post RSS-2 units identified in the northern sector of C-19.

2-4. Discussion: Implications for the Tectonic History of the Ross Sea

2-4.1. The Regional Correlation

Correlating the stratigraphic units of the eastern Ross Sea to the western Ross Sea is crucial for understanding the timing and magnitude of tectonic and climatic events in the region. Although many authors have attempted to link the RSS units to the V units, these links have been speculation and not a direct correlation.

Lithological comparisons of RSS-2, cored at DSDP Site 270 in the eastern Ross Sea, to V4, cored at Roberts Ridge (CRP) in the western Ross Sea, indicate both units are composed of similar strata of a similar age. At DSDP Site 270, RSS-2 was divided into four sub-units. Sub-units 1 and 2 (youngest) are interpreted as glacial-marine in origin. Sub-units 3 and 4 (oldest) are of shallow marine or near shore origin, but do not show any evidence of glacial influence [Hayes and Frakes, 1975]. The sediment composing RSS-2 is mostly a diamictite with mud, silty clay, and mixtures of sand and silt [Hayes and Frakes, 1975]. Unit V4 at CRP is also a diamictite composed of mainly mud, silt, and sand [Cape-Roberts-Science-Team, 2000]. Strata recovered from the younger sections of unit V4 at CRP, are interpreted to have glacial-marine origins, while the older sub-units are interpreted as originating in a shallow marine environment [Cape-Roberts-Science-Team, 2000]. Biostratigraphic analysis of RSS-2 and V4 constrains both units to span the Oligocene-Miocene boundary. Unconformity RSU5 was not sampled at any of the DSDP sites. However, DSDP Site 272 sampled the base of RSS-3 and DSDP Site 270 sampled the top of RSS-2. Based on diagnostic benthic foraminifera assemblages, the

top of RSS-2 is constrained to the early Miocene, between ~19.2 to 21 Ma [Hayes and Frakes, 1975; Steinhauff, et al., 1987; DeSantis, et al., 1995; DeSantis, et al., 1999]. Similarly, the top of V4 at Roberts Ridge is constrained to the early Miocene. Marine diatoms were the most abundant diagnostic assemblages recovered in the CRP cores, and were used to date the top of V4 to ~21 Ma [Cape-Roberts-Science-Team, 2000].

The similarities between the lithologies of RSS-2 and V4, as well as the age of the unit tops (early Miocene; ~21 Ma), suggest the correlation of unit RSS-2 to unit V4 is robust. The regional correlation strengthens this relationship because the top of RSS-2 (unconformity RSU5) can be correlated across the Central High and tied to the top of unit V4 in the C-19 survey site. Therefore, the unconformity marking the V3/V4 boundary is most likely unconformity RSU5 and can be constrained to the CRP drill site. Since the age of RSU5 in the eastern Ross Sea is currently bracketed between the bottom of RSS-3 and the top of RSS-2, the regional correlation indicates the age suggested by DeSantis et al. [1995] for RSU5 of 21 Ma (Early Miocene) is correct.

DeSantis et al [1999] interprets the deposition of RSS-2 to represent a period in which valley glaciers cutting into the Central High during Oligocene time. This created glacial deposits while deep water deposits were being formed in the Eastern Basin. The correlation suggests a similar depositional/climatic environment most likely existed in the western Ross Sea at the time RSS-2/V4 was being deposited.

Evidence for this stems from the fact that both RSS-2 and V4 are composed of glacial-marine sediments of similar composition and age.

Although unconformity RSU6 was not correlated across the Central High, the preliminary correlation of RSU6 from CRP to the C-19 site, strengthens the interpretations of Davey et al. [2000] regarding the age and location of RSU6 in the western Ross Sea. This correlation suggests unconformity RSU6 is Oligocene age throughout the Ross Sea. Reflectors above and below RSU6 throughout the Ross Sea are relatively parallel to the unconformity. There is a possibility that RSU6 is not a true angular unconformity. Rather, RSU6 may be a change in depositional patterns or possibly diagenesis of sediments. This would produce a large reflection that could be interpreted as a sequence boundary. However, widespread reflections within RSS-1-upper are truncated by RSU6, indicating that RSU6 is an angular unconformity throughout the Ross Sea. The interpretation of unconformity RSU7 at the C-19 site suggests both the eastern and western Ross Sea share a common Late Cretaceous tectonic history.

2-4.2. Tectonics of the Eastern Ross Sea

The seismic data indicates two different extensional events may have taken place in the southern sector of the eastern Ross Sea. The first event was most likely during the Late Cretaceous and recorded by RSS-1-lower. The second event probably occurred during the deposition of RSS-1-upper, possibly corresponding with Eocene Adare Trough seafloor spreading [Cande, et al., 2000]. The different styles of

deformation interpreted by Luyendyk et al. [2001] off Cape Colbeck, in the eastern Ross Sea, between RSS-1-lower, RSS-1-upper, and RSS-2 are striking. Very similar deposition styles of RSS-1-lower, RSS-1-upper, and RSS-2 along the ice shelf in the eastern Ross Sea are interpreted. Extension-related faulting is interpreted to be constrained within the RSS-1 units and is capped by unconformity RSU6 (Fig. 2-7). This suggests extension within this sector of the Ross Sea was completed by RSU6 time (~30).

Basement grabens were most likely formed during Late Cretaceous crustal extension, followed by basin subsidence and accompanied by the infill of Late Cretaceous RSS-1-lower [Trey, et al., 1999; Luyendyk, et al., 2001]. Faulting continued to deform RSS-1-lower, followed by a hiatus in extension, and the onset of erosion during the Late Cretaceous, forming unconformity RSU7. Luyendyk et al. [2001] interprets the tilted and disrupted nature of RSS-1-lower in the northeastern Ross Sea to indicate basin-and-range style normal faulting and extension.

Interpretation of RSS-1-lower along the ice shelf shows the unit is also tilted and disrupted. This indicates that basin-and-range style faulting and extension is characteristic of the Ross Sea. Prior studies have proposed that regional extension in the eastern Ross Sea began at ~105 Ma, with the onset of Gondwana rifting [Bradshaw, 1989; Richard, et al., 1994; Luyendyk, 1995; Luyendyk, et al., 1996; Siddoway, et al., 2004]. RSS-1-lower was deposited in approximately N-S trending basement grabens formed during this period of extension, and the basin-and-range topography was beveled by erosion before the end of extension. Thus, the synrift

tilted strata of RSS-1-lower was preserved primarily within basement half-grabens, before the onset of widespread deposition of RSS-1-upper [Luyendyk, et al., 2001].

Luyendyk et al. [2001] proposed that unconformity RSU7 is equivalent to the West Antarctic Erosion Surface (WAES) and was formed well above sea level. The WAES is currently found at elevations of up to ~3 km in western Marie Byrd Land [LeMasurier and Landis, 1996]. Also, the shelf of the eastern Ross Sea does not contain a significant marine sediment thickness of early Tertiary age that would be expected for a subsiding Cretaceous margin if the WAES were formed at sea level [Luyendyk, et al., 2001]. Furthermore, it is more straightforward to accept the WAES forming at elevation rather than forming at sea level and rising 3 km [Luyendyk, et al., 2001].

The formation of unconformity RSU7 was followed by the onset of subsidence of the margin and the deposition of RSS-1-upper in the Early Cenozoic. Renewed faulting of RSS-1-upper suggests further extension at this time. A eustatic sea level drop occurred in the Oligocene exposing the continental margin and eroded RSS-1-upper to form unconformity RSU6. Continued subsidence and sea level rise occurred with the onset of RSS-2 deposition in the late Oligocene. Unit RSS-2 was then tilted westward with continued subsidence. Tilting must have occurred in the Oligocene and early Miocene and is most likely the result of subsidence of the Eastern Basin [Luyendyk, et al., 2001].

2-4.3. Tectonics of the Western Ross Sea

The major exhumation of the TAM during the Eocene and Oligocene coincides with widespread subsidence of the VLB [Hamilton, et al., 2001]. Seismic correlations of strata from the Cape Roberts drill sites into the VLB indicate more than one half of the sediment fill may be of latest Eocene and younger in age [Davey, et al., 2001]. Hamilton, et al. [2001] suggest Eocene strata are widespread in the VLB. Eocene strata was recovered south of Cape Roberts in McMurdo Sound (CIROS) but could not be correlated into the VLB. Regardless, the likelihood of large volumes of Eocene strata in the western Ross Sea is high. Therefore, it is probable that strata of Eocene age extends east into the Central Trough and Eastern Basin as RSS-1-upper.

Cande, et al. [2000] interprets 180 km of E-W seafloor spreading north of the western Ross Sea, across the Adare Trough spreading center, between the middle Eocene-late Oligocene. The spreading pattern requires that the extension must have been transferred south into the Ross Sea. However, Eocene extension of this magnitude has not yet been identified in the Ross Sea. It seems likely that Adare Trough spreading can account for the extension and resulting accommodation space needed for the large thickness of Oligocene and older sediments in the VLB [Hamilton, et al., 2001]. It is possible that some, if not all, of the extension resulting from the Adare Trough may be preserved within RSS-1-upper (Fig 2-6 & 2-8). Although RSS-1-lower is interpreted as deposited and deformed in the Late Cretaceous, it is plausible that subsequent extension in Eocene times may have

reactivated faults, thus deforming the unit further and allowing for further deposition. If unit V5c is the same as RSS-1-upper and is Eocene in age as suggested by Hamilton, et al. [2001], then this scenario is plausible. If this were not the case, then the interpretation that extension resulting from this spreading episode extended into the Ross Sea would be problematic. The possibility that the extension below RSU6 is of both Cretaceous and Eocene age, suggest synrift strata of the RSS-1 sequence may record both Cretaceous and Cenozoic extension events.

RSS-1-upper is prominent to the north, but pinches out towards the south as unconformities RSU6 and RSU7 merge on the Coulman High. As in the eastern Ross Sea, RSS-1-upper is offset by widely spaced normal faults, which are constrained to be older than the late Oligocene-early Miocene RSS-2 sequence. Unconformity RSU6 is a mostly continuous reflector at C-19; however a few moderately dipping normal faults offset the unconformity and extend into the overlying RSS-2 unit. Offsets are fairly small on RSU6 and grow with depth, suggesting that these are growth faults (Fig. 2-8). This extensional event may be related to a similar event in the eastern Ross Sea, in which RSS-1-upper was offset by NNE-SSW trending faults and capped by RSU6 [Luyendyk, et al., 2001]. However, in the C-19 region faults offsetting RSS-1 trend NNW-SSE and offset unconformity RSU6. This suggests a different strain relationship in this sector of the Ross Sea, which may have persisted into the early Oligocene. Faulting here may result from the continued subsidence of the VLB during this period. Several faults extend from RSS-1-lower, cutting through RSS-1-upper, RSS-2 and into post RSS-2 units, terminating just below the seafloor.

Hamilton, et al. [2001] interprets all TAM tilting to have been completed by formation of the V3/V4 (unconformity RSU5). Because faults cut through this boundary, these faults may be growth faults that originally formed from Cretaceous extension and were reactivated during Adare Trough spreading/TAM tilting. Further motion along these faults may have resulted from the onset of the Late Cenozoic Terror Rift or loading resulting from the nearby McMurdo volcanic group.

2-4.4. An Elevated Ross Sea Basement?

Interpretation of unconformities RSU6 and RSU7 at the C-19 site suggest the western Ross Sea may share a common Mesozoic rifting history with the eastern Ross Sea. Studinger et al. [2004] speculates that the TAM was originally the edge of a high plateau that comprised the Ross Sea region. The hotter and weaker central part of the plateau collapsed to form the Ross Sea while the cooler, stronger and thicker western edge formed the TAM [Studinger, et al., 2004]. Upward tilting of the TAM, due to unloading of the footwall (western Ross Sea) [Stern and Ten Brink, 1989; ten Brink, et al., 1997], most likely occurred as the Ross Sea founded and was completed by the formation of RSU5. Luyendyk, et al. [2001] interprets unconformity RSU7 as an extension of the West Antarctic Erosion Surface (WAES) and argues it formed above sea level in the Late Cretaceous during a hiatus in extension. This indicates the region could have been significantly above sea level in the Cretaceous because RSU7 is interpreted in the western Ross Sea.

The stratigraphic record interpreted at C-19 and the eastern Ross Sea suggests the Ross Sea region was once well above sea level. Based on interpretations at C-19, unit RSS-1-lower was deposited and deformed in basement half-grabens during Cretaceous extension. This was followed by subsidence and the formation of unconformity RSU7. Therefore, unconformity RSU7 in the western Ross Sea may represent an extension of the WAES. Renewed extension at a later time and continued subsidence was accompanied by the deposition of RSS-1-upper. By unconformity RSU6 time, the region was at sea level, and continued subsidence allowed for the deposition of RSS-2. The model interpreted for the formation of the western Ross Sea indicates that the entire Ross Sea shares a common tectonic history.

2-5. Summary and Conclusions

The Oligocene-early Miocene RSS-2 unit of the eastern Ross Sea can be confidently correlated across the Central High and into the western Ross Sea in multiple locations. A regional correlation of unit RSS-2 and unconformity RSU5 was made from DSDP Sites 270 & 272, in the eastern Ross Sea, to the Cape Roberts Project drilling sites, in the western Ross Sea. A jump correlation of early Oligocene angular unconformity RSU6, interpreted at CRP [Davey, et al., 2001], was made to an existing interpretation of RSU6 in the northern VLB and Central Trough. This jump correlation indicates unconformity RSU6 can be correlated from CRP drill sites to the Central Trough. Based on the correlations, unit ages, and unit composition, this study concludes the glacial-marine RSS-2 unit of the eastern Ross Sea is the same sequence

as the glacial-marine V4 unit of the western Ross Sea. To test this correlation, new cores are needed in the western and eastern Ross Sea, sampling pre-Oligocene strata and basement.

Highly deformed, syn-tectonic RSS-1-lower strata filling basement half-grabens throughout the Ross Sea imply a uniform Cretaceous extension history. Interpretations of unconformity RSU7 across the Ross Sea suggest the Late Cretaceous WAES may have been Ross Sea wide. Therefore, the Ross Sea was most likely a region of significant elevation prior to the Cenozoic.

Deposition of synrift RSS-1-upper may have been coeval with Eocene Adare Trough seafloor spreading. If this is the case, then unit RSS-1-upper would have to be Eocene in age. Extension of the Ross Sea at this time would be recorded by deformation of RSS-1-upper and further deformation of RSS-1-lower. Interpretations of RSS-1-upper in the Central Trough and Eastern Basin indicate extension associated with Adare Trough spreading was not just focused in the VLB. Rather, Tertiary extension may have affected the Central Trough and Eastern Basin as well. Correlation of the RSU6 unconformity indicates that the Ross Sea remained above sea level prior to ~30 Ma. Regional subsidence resulted in the necessary accommodation space for the deposition of the glacial-marine RSS-2 sequence.

References Cited

- ANTOSTRAT (1995), Seismic Stratigraphic Atlas of the Ross Sea, in *Geology and Seismic Stratigraphy of the Antarctic Margin*, edited by A. K. Cooper, Barker, P. F., Brancolini, G., p. 22 plates, American Geophysical Union, Washington, D.C.
- Barrett, P. J. (Ed.) (1989), *Antarctic Cenozoic history from CIROS-1 drill hole, McMurdo Sound*, 254 pp., DSIR, Wellington.
- Barrett, P. J., M. Massimo Sarti, and S. Wise (Eds.) (2000), *Studies from the Cape Roberts Project, Ross Sea, Antarctica: Initial report on CRP-3*, 209 pp., Terra Antarctica Pub., Siena.
- Bartek, L. R., S. A. Henrys, J. B. Anderson, and P. J. Barrett (1996), Seismic stratigraphy of McMurdo Sound, Antarctica: Implications for glacially influenced Early Cenozoic eustatic change? *Mar. Geol.*, 130, 79-98.
- Bradshaw, J. D. (1989), Cretaceous geotectonic patterns in the New Zealand region, *Tectonics*, 8, 803-820.
- Brancolini, G., A. K. Cooper, and F. Coren (1995), Seismic Facies and Glacial History in the Western Ross Sea (Antarctica), in *Geology and seismic stratigraphy of the Antarctic margin*, edited by A. K. Cooper, P. F. Barker and G. Brancolini, pp. 209-234, Amer. Geophys. Union, Washington, D. C.
- Busetti, M., and A. K. Cooper (1994), Possible ages and origins of unconformity U6 in the Ross Sea, Antarctica, *Terra Antarctica*, 1, 341-343.
- Busetti, M., G. Spadini, F. M. Van der Wateren, S. Cloetingh, and C. Zanolla (1999), Kinematic Modeling of the West Antarctic Rift System, Ross Sea, Antarctica, *Global Plan. Ch.*, 23, 79-103.
- Busetti, M., and I. Zayat (1994), Ross Sea Regional Working Group, Distribution of Seismic Units in the Ross Sea, *Terra Antarctica*, 1, 345-348.
- Cande, S. C., J. M. Stock, D. Müller, and T. Ishihara (2000), Cenozoic Motion between East and West Antarctica, *Nature*, 404, 145-150.
- Cape-Roberts-Science-Team (2000), Summary of Results, Initial Report on CRP-3, Cape Roberts Project, Antarctica, *Terra Antarctica*, 7, 185-209.

Claerbout, J. F. (1985), *Imaging the earth's interior*, 398 pp., Blackwell Scientific, Boston.

Cooper, A. K., P. F. Barker, and G. Brancolini (Eds.) (1995), *Geology and Seismic Stratigraphy of the Antarctic Margin, atlas, CD-ROMs*, 301 pp., Amer. Geophys. Union, Washington, D.C.

Cooper, A. K., F. J. Davey, and J. C. Behrendt (1987), Seismic stratigraphy and structure of the Victoria Land Basin, western Ross Sea, Antarctica, in *The Antarctic Continental Margin: Geology and Geophysics of the Western Ross Sea*, edited by A. K. Cooper and F. J. Davey, pp. 27-65, Circum-Pacific Council for Energy and Mineral Resources, Houston, Texas.

Cooper, A. K., F. J. Davey, and K. Hinz (1991), Crustal extension and the origin of sedimentary basins beneath the Ross Sea and Ross Ice Shelf, Antarctica, in *Geological Evolution of Antarctica*, edited by M. R. A. Thompson, J. A. Crame and J. W. Thompson, pp. 285-291, Cambridge Univ. Press, New York.

Davey, F. J., P. J. Barrett, M. B. Cita, F. Tessensohn, M. Thomson, K. J. Woolfe, P.-N. Webb, and C. R. S. Team (2001), Drilling for Antarctic Cenozoic climate and tectonic history at Cape Roberts, southwestern Ross Sea, *EOS Trans. AGU*, 82, 589-590.

Davey, F. J., G. Brancolini, R. J. Hamilton, S. A. Henrys, C. C. Sorlien, and L. R. Bartek (2000), A revised correlation of seismic stratigraphy at the Cape Roberts drill sites with the seismic stratigraphy of the Victoria Land basin, in *Studies from the Cape Roberts Project, Ross Sea, Antarctica; scientific results of CRP-2/2A; Part I, Geophysics and physical properties studies for CRP-2/2A*, edited by F. J. Davey and R. D. Jarrard, pp. 215-220, Terra Antarctica.

Decesari, R. C., B. P. Luyendyk, L. R. Bartek, C. C. Sorlien, D. S. Wilson, J. B. Diebold, and S. E. Hopkins (2004), Ice shelf drill sites proposed to study Pre-Late Oligocene climate and tectonic history, Coulman High, Southwestern Ross Sea, Antarctica, *EOS Trans. AGU*, 85, Fall Meet. Suppl., Abstract T11A-1244.

Decesari, R. C., C. C. Sorlien, B. P. Luyendyk, L. R. Bartek, J. B. Diebold, and D. S. Wilson (2003), Tectonic evolution of the Coulman High and Central Trough along the Ross Ice Shelf, Southwestern Ross Sea, Antarctica, *EOS Trans. AGU*, 84, Fall Meeting Suppl. Abstract T12A-0447.

DeSantis, L., J. B. Anderson, G. Brancolini, and I. Zayatz (1995), Seismic record of Late Oligocene through Miocene glaciation on the central and eastern continental shelf of the Ross Sea, in *Geology and seismic stratigraphy of the Antarctic margin*, edited by A. K. Cooper, P. F. Barker and G. Brancolini, pp. 235-260, Amer. Geophys. Union, Washington, D. C.

DeSantis, L., S. Prato, G. Brancolini, M. Lovo, and L. Torelli (1999), The Eastern Ross Sea continental shelf during the Cenozoic: Implications for the West Antarctic ice sheet development, *Global Plan. Ch.*, 23, 173-196.

Fielding, C. R. A., and M. R. A. Thompson (1999), *Initial Report on CRP-2/2A, Cape Roberts Project, Antarctica*, 173 pp., Terra Antarctica.

Hamilton, R. J., B. P. Luyendyk, C. C. Sorlien, and L. R. Bartek (2001), Cenozoic Tectonics of the Cape Roberts Rift Basin, and Transantarctic Mountains Front, Southwestern Ross Sea, Antarctica, *Tectonics*, 20, 325-342.

Hampson, D. (1991), Inverse velocity stacking for multiple elimination, *J. Canadian Soc. Explor. Geophys.*, 22, 44-55.

Hannah, M. J. (1997), Climate controlled dinoflagellate distribution in late Eocene/earliest Oligocene strata from the CIROS-1 drill hole, McMurdo Sound, Antarctica, *Terra Antarctica*, 4, 73-78.

Hannah, M. J. (1994), Eocene dinoflagellates from the CIROS-1 drill hole, McMurdo Sound Antarctica, *Terra Antarctica*, 1, 371.

Hannah, M. J., M. B. Cita, R. Coccioni, and S. Monechi (1997), The Eocene/Oligocene boundary at 70 degrees south, McMurdo Sound, Antarctica, *Terra Antarctica*, 4, 79-87.

Hayes, D. E., and L. A. Frakes (1975), General synthesis: Deep Sea Drilling Project 28, in *Initial Reports of the Deep Sea Drilling Project, Leg 28*, edited by D. E. Hayes and L. A. Frakes, pp. 919-942, U.S. Government Printing Office, Washington, D.C.

Henrys, S. A., L. R. Bartek, G. Brancolini, B. P. Luyendyk, R. J. Hamilton, C. C. Sorlien, and F. J. Davey (1998), Seismic stratigraphy of the pre-quaternary strata off Cape Roberts and their correlation with strata cored in the CIROS-1 drill hole, McMurdo sound, *Terra Antarctica*, 5, 273-279.

Hinz, K., and M. Block (1984), Results of geophysical investigations in the Weddell Sea and in the Ross Sea, Antarctica, paper presented at 11th World Petrol. Congress, Wiley, London.

Kamp, P. J. J., and P. G. Fitzgerald (1987), Geologic constraints on the Cenozoic Antarctica-Australia-Pacific relative plate motion circuit, *Geology*, 15, 694-697.

LeMasurier, W. E., and C. A. Landis (1996), Mantle plume activity recorded by low relief erosion surfaces in West Antarctica and New Zealand, *Geol. Soc. Am. Bull.*, 108, 1450-1466.

Luyendyk, B. P. (1995), Hypothesis for Cretaceous rifting of east Gondwana caused by subducted slab capture, *Geology*, 23, 373-376.

Luyendyk, B. P., C. C. Sorlien, and L. R. Bartek (1996), Early Tertiary Rifting in the Eastern Ross Sea and Offshore Western Marie Byrd Land, Antarctica, *EOS, Transactions of the American Geophysical Union, Fall Meeting Supplement*, 77, F312.

Luyendyk, B. P., C. C. Sorlien, D. S. Wilson, L. R. Bartek, and C. H. Siddoway (2001), Structural and tectonic evolution of the Ross Sea rift in the Cape Colbeck region, Eastern Ross Sea, Antarctica, *Tectonics*, 20, 933-958.

Richard, S. M., C. H. Smith, D. L. Kimbrough, P. G. Fitzgerald, B. P. Luyendyk, and M. O. McWilliams (1994), Cooling history of the northern Ford Ranges, Marie Byrd Land, West Antarctica, *Tectonics*, 13, 837-857.

Siddoway, C. S., S. L. Baldwin, P. G. Fitzgerald, C. M. Fanning, and B. P. Luyendyk (2004), Ross Sea mylonites and the timing of continental extension between East and West Antarctica, *Geology*, 32, 57-60.

Steinhauff, D. M., M. E. Renz, D. M. Harwood, and P.-N. Webb (1987), Miocene diatom biostratigraphy of DSDP hole 272: Stratigraphic relationship to the underlying Miocene of DSDP hole 270, Ross Sea, *Antarctic J. of the US*, 22, 123-125.

Stern, T. A., and U. S. Ten Brink (1989), Flexural uplift of the Transantarctic Mountains, *J. Geophys. Res.*, 94, 10,315-310,330.

Studinger, M., R. E. Bell, W. R. Buck, G. Karner, and D. Blankenship (2004), Sub-ice geology inland of the Transantarctic Mountains in light of new aerogeophysical data, *Earth Planet. Sci. Lett.*, 220, 391-408.

ten Brink, U. S., R. I. Hackney, S. Bannister, T. A. Stern, and Y. Makovsky (1997), Uplift of the Transantarctic Mountains and the bedrock beneath the East Antarctic ice sheet, *J. Geophys. Res.*, **102**, 27, 603-627, 621.

Trey, H., A. K. Cooper, G. Pellis, B. Della Vedova, G. Cochrane, G. Brancolini, and J. Makris (1999), Transect across the West Antarctic rift system in the Ross Sea, Antarctica, *Tectonophysics*, **301**, 61-74.

Wilson, G. S., A. P. Roberts, K. L. Verosub, F. Florindo, and L. Sagnotti (1998), Magnetobiostrati-graphic chronology of the Eocene-Oligocene transition in the CIROS-1 core, Victoria Land margin, Antarctica: Implications for Antarctic glacial history, *Geol. Soc. Am. Bull.*, **110**, 35-47.



Chapter 3

A Model for Two Stage Mesozoic and Cenozoic Extension of the Ross Sea

Abstract

The timing and magnitude of extension in the Ross Sea between East and West Antarctica has remained largely problematic. Outstanding questions include, did extension occur in both Cretaceous and Cenozoic time, why is there so much Oligocene and younger sediment in the Ross Sea, and what tectonic history accounts for the necessary accommodation space? The basins of the Ross Sea are interpreted to have formed during Cretaceous extension, and are now filled with kilometers of sediment. A 1-D backstripped subsidence model was computed for the deepest parts of the Central Trough and Eastern Basin to infer periods of extension. Stratigraphic units were decompacted and tectonic subsidence calculated. Corrections for paleobathymetry and eustatic sea level changes were applied. Cooling curves were predicted for a single extension event and dual extension events using combinations of stretching factors. Predicted subsidence curves were computed from cooling curves

and compared to observed subsidence to determine tectonic history of the basins. This model assumes unconformity RSU6 (30 Ma) formed in shallow water near sea level.

The results support a two stage extension of the Ross Sea. Cretaceous extension began around ~95 Ma at a stretching factor of ~2 across the Ross Sea. Tertiary extension occurred at a stretching factor of ~ 2 in the Central Trough and Eastern Basin. However, stretching factors were also probably between 2 and 3 in the Victoria Land Basin in Tertiary time. All extension in the Central Trough and Eastern Basin was completed by the formation of unconformity RSU6 and deposition of early Oligocene sediments. Tertiary extension was likely simultaneous with seafloor spreading along the Adare Trough, northwest of the Ross Sea. An alternative model with only Cretaceous extension of the basins requires most thermal subsidence throughout the Ross Sea to predate Oligocene sedimentation. This timing requires that unconformity RSU6 formed many of hundreds of meters below sea level, implying that it is not a wave-cut feature.

3-1. Introduction

The four major sedimentary basins of the Ross Sea, the Northern Basin (NB), Victoria Land Basin (VLB), Central Trough (CT), and Eastern Basin (EB) (Fig. 3-1), are interpreted to have formed during Cretaceous extension of the region [Davey and Brancolini, 1995]. A long-standing problem is whether the Antarctic plate was separated into two plates during the Cenozoic [Molnar, et al., 1975; Stock and Molnar, 1987]. The details of the uplift history of the TAM and the subsidence of the

major Ross Sea basins are most likely related to motion between East and West Antarctica. Between 43 and 26 Ma, approximately 180 km of E-W rifting occurred across the Adare Trough spreading center directly north of the western Ross Sea (Fig. 3-1) [Cande, et al., 2000]. Seafloor spreading is recorded by magnetic anomalies and is thought to have influenced Tertiary extension of the western Ross Sea, especially the VLB [Hamilton, et al., 2001].

Several questions about the formation of the Ross Sea have gone unanswered. First, what is the timing and magnitude of Ross Sea extension? Second, did Tertiary extension affect the Central Trough and Eastern Basin as well as the Victoria Land Basin? Third, why is there so much late Oligocene-early Miocene RSS-2 strata and what created the necessary accommodation space for its accumulation? The objectives of this study are to answer these questions by determining the subsidence history of the Central Trough and Eastern Basin. We hypothesize that Tertiary extension associated with Adare Trough spreading affected the Central Trough and Eastern Basin, creating the necessary accommodation space needed for the deposition of Oligocene RSS-2 and younger strata. An alternative hypothesis limits Tertiary extension to the VLB, suggesting the CT and EB were only affected by Cretaceous extension [Karner, et al., 2005]. To test these hypotheses we use the backstripping method to determine the observed tectonic subsidence and fit it to predicted tectonic subsidence curves using different combinations of stretching factors.

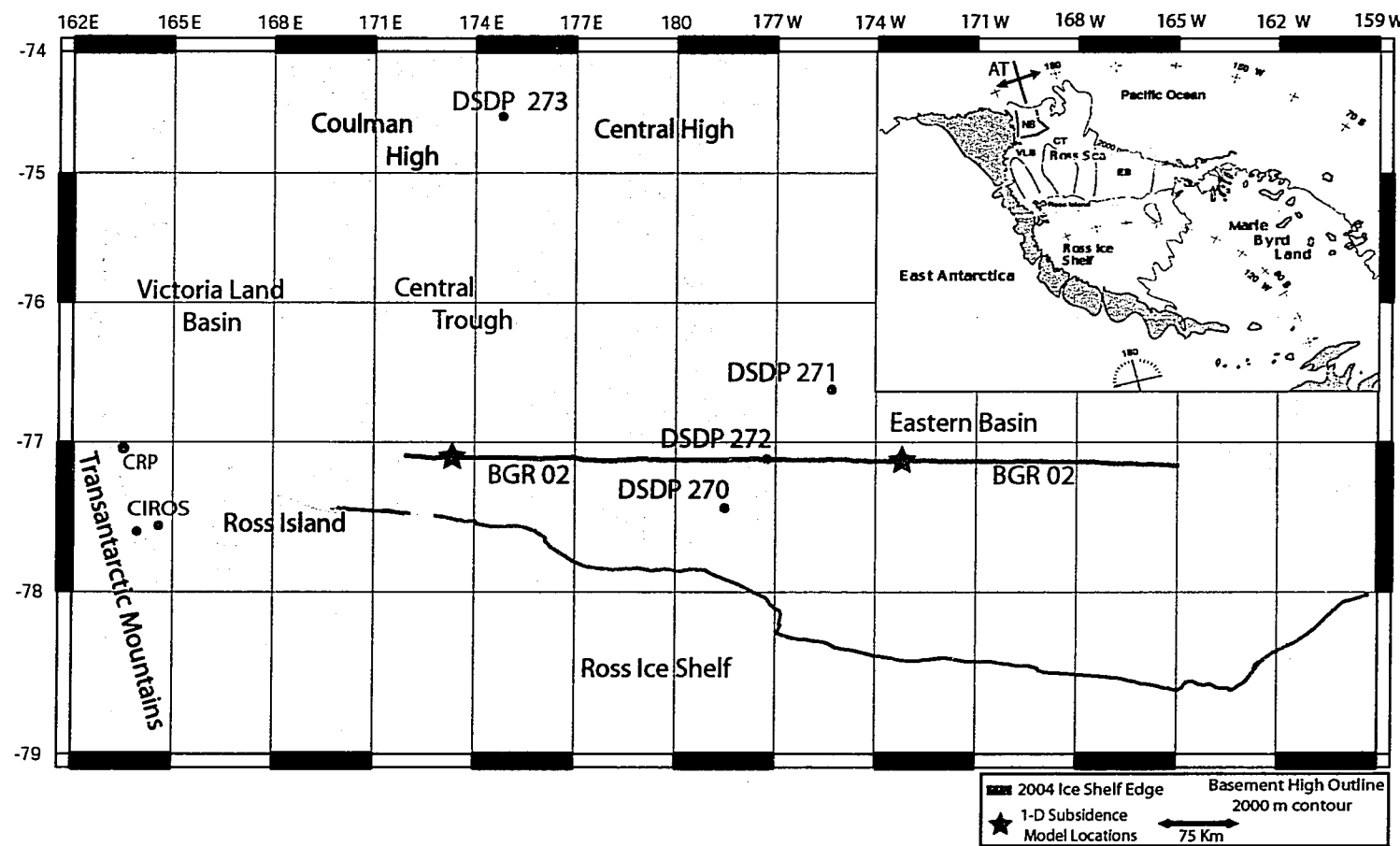


Figure 3-1: Inset: the Ross Sea region map showing locations of the major sedimentary basins and the Transantarctic Mountains. AT, Adare Trough (arrows indicate former spreading direction [Cande et.al. 2000]); NB, Northern Basin; VLB, Victoria Land Basin; CT, Central Trough; EB, Eastern Basin. Yellow box in is the approximate location of the large map. Lithologic information for the Ross Sea strata was obtained from core reports for DSDP Sites 270, 271, 272, and 273. Red stars indicate locations of the 1-D subsidence study along German seismic profile BGR-02. The Coulman High and the Central High are outlined in light blue (2,000 m contour).

3-2. Geohistory and Backstripping Methods

The goal of a geohistory analysis is to describe the subsidence of a basin and sedimentation accumulation through time based on present-day stratigraphic data. This is done to identify the timing of extensional events from the geohistory curve. In order to do this, three corrections are applied to the present stratigraphic thickness. These steps include:

- 1) Decompaction: Starting with the youngest unit, each layer is removed at prescribed time steps and the units beneath are decompacted to account for progressive loss of porosity with depth of burial. Also known as backstripping.
- 2) Isostatic Compensation: Correcting the depth of each unit for the isostatic uplift after removing the upper sediment load and replacing it with water.
- 3) Paleobathymetric and Eustatic Corrections: Correcting for the paleowater depth at the time of unit deposition and the long term global eustatic sea level changes relative to today's sea level.

The result is the tectonic subsidence, or that which is due to effects other than sediment loading or sea level change. A one dimensional (1-D) subsidence history was produced at two points along German seismic profile BGR-02 [ANTOSTRAT, 1995; Brancolini, et al., 1995] (Fig. 3-1). The Victoria Land Basin was not included due to uncertainties regarding basement depth, unit age and thicknesses, and Neogene-Quaternary volcanic influences. The 1-D model assumes Airy isostacy (i.e. any vertical load column is locally compensated) to attempt to determine the tectonic

subsidence of the basins. This subsidence history assumes instantaneous, pure-shear rifting [McKenzie, 1978]. However, in reality rifting events occur over a finite period of time. Work by Jarvis and McKenzie[1980] indicate for stretching events ≤ 2 , the instantaneous rifting model is valid if the duration of rifting is less than 60 Myrs.

3-2.1. Stratigraphic Analysis

To better understand the subsidence history of a basin, the sedimentary infill and unit thickness must be interpreted. Seismic stratigraphic interpretations of BGR-02 are only published in terms of two-way-travel-time and therefore needed depth conversion prior to obtaining unit thicknesses. Published stratigraphic depth maps are available in the ANTOSTRAT [1995] compilation. However, these maps were computed using stacking velocities rather than interval velocities. Interval velocities compute the average velocity over a depth interval containing more than one unit. Therefore, depth conversion of BGR-02 using an interval velocity model was favored over the ANTOSTRAT [1995] depth maps. Due to the lack of published velocity data necessary for depth conversion, a velocity model for BGR-02 was obtained from crossovers with RVIB Nathaniel B. Palmer cruises NBP96-01 and NBP03-01 seismic profiles. In the CT, BGR-02 crosses NBP-0301 lines 9, 11A and 38A and in the EB, it crosses NBP96-01 lines 4, 6 and 7.

Reinterpretation of the BGR-02 depth section identified unconformities RSU6-RSU4 in the CT and unconformities RSU6-RSU3 in the EB (Fig. 3-2). These unconformities are interpreted to have formed at or close to sea level

Ross Sea Cross Section A

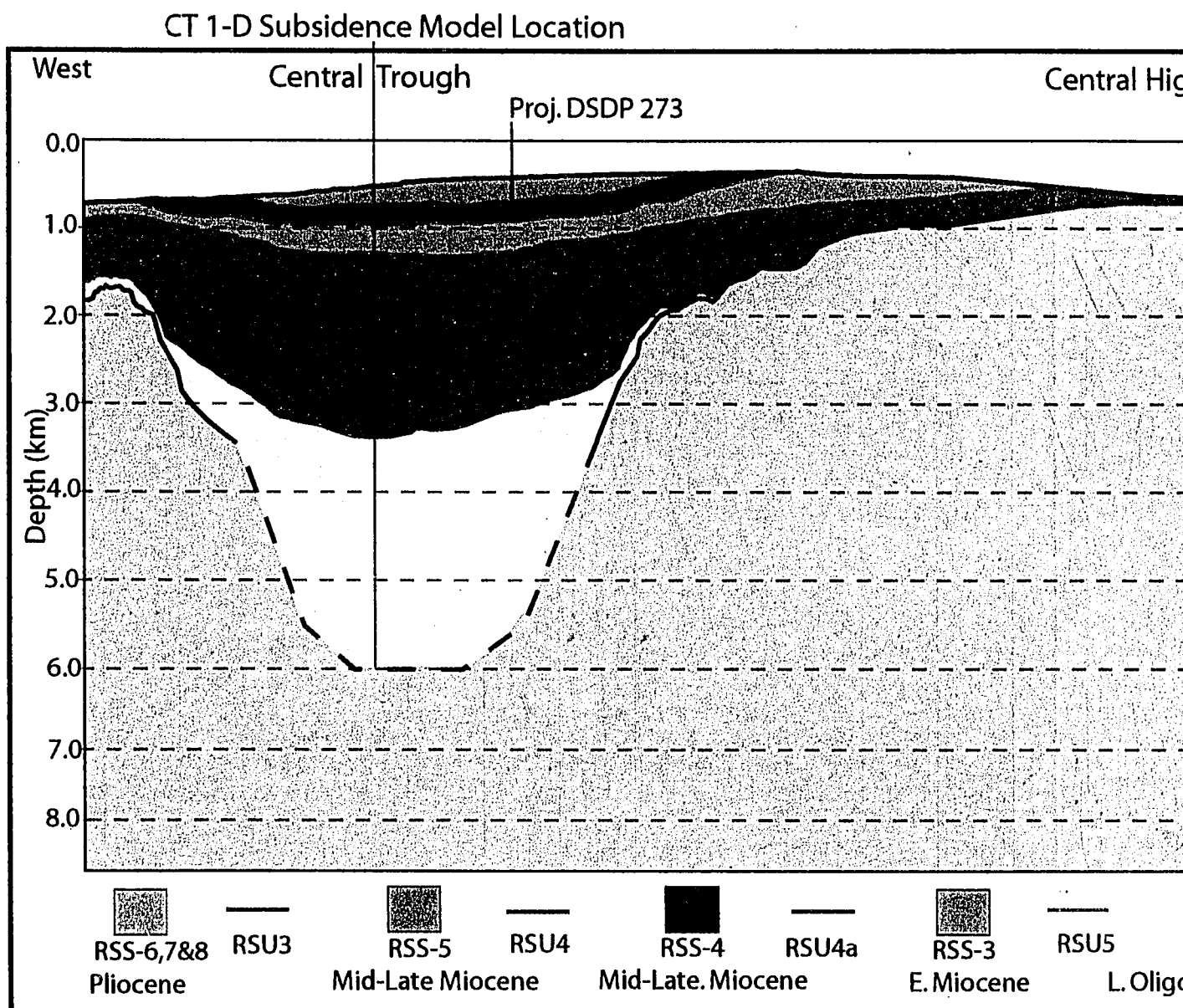
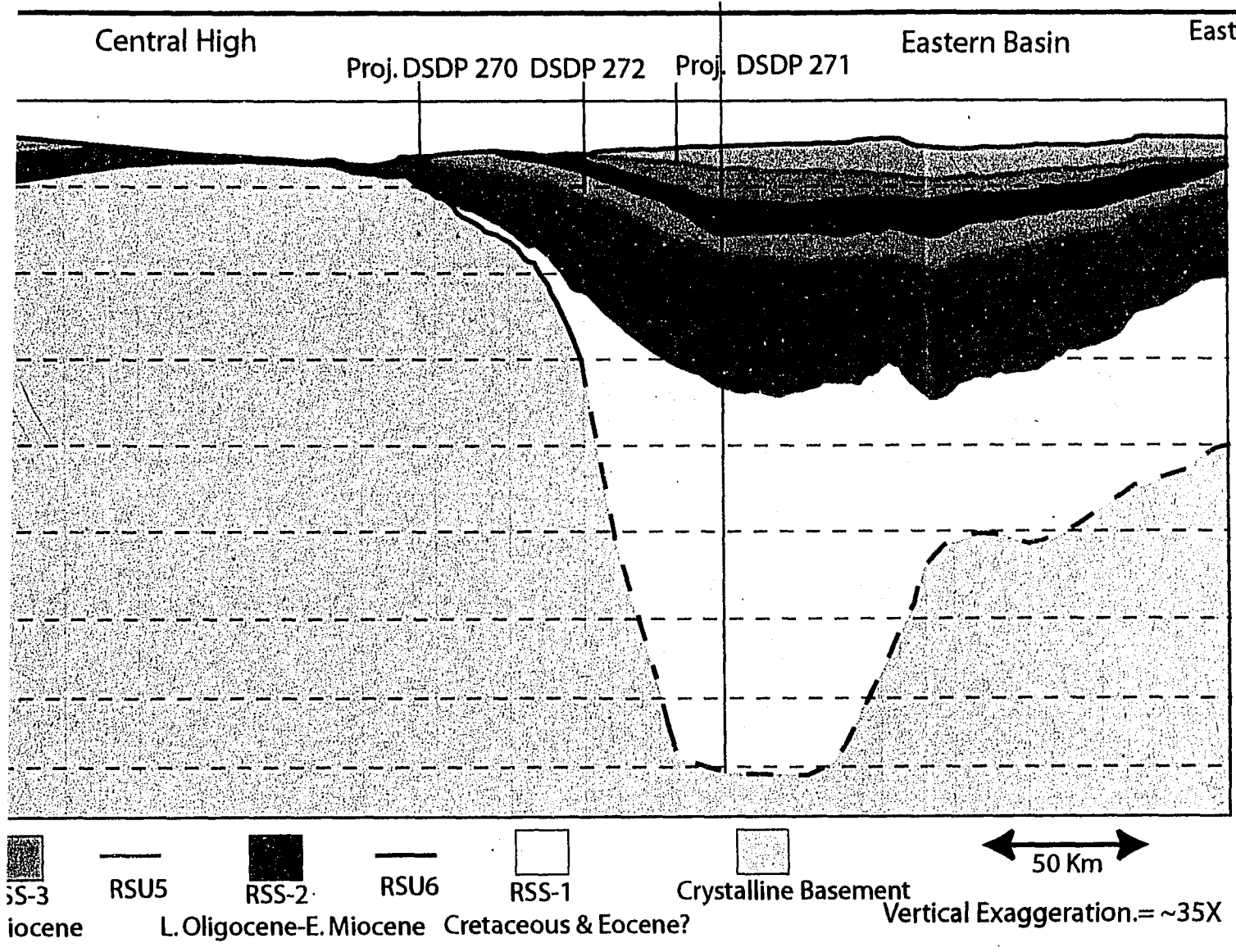


Figure 3-2: Cross section of the Ross Sea along German seismic profile BGR-272, and 273 are projected onto this profile. 1-D subsidence models were computed to ensure computation of maximum extension and thickest sedimentary sequences obtained from crossovers with NBP-9601 and NBP-0301 seismic lines. Because data obtained from Trey et al. [1999] (Dashed gray lines). Solid gray lines represent

Section Along Profile BGR-02

EB 1-D Subsidence Model Location



man seismic profile BGR-02 spanning the Central Trough to Eastern Basin. DSDP Sites 270, 271, subsidence models were computed in the deepest parts of the Central Trough and Eastern Basin to thickest sedimentary sequences. This profile was depth converted using interval velocities 0301 seismic lines. Because basement could not be imaged in the basins, basement depths were). Solid gray lines represent acoustic basement interpreted from the seismic reflection data.

[Hayes and Frakes, 1975; DeSantis, et al., 1995; DeSantis, et al., 1999]. Depth to unconformities and unit thicknesses of RSS-2 through RSS-6, 7 & 8 (grouped as one unit) were calculated at the deepest locations of each basin along the profile, ensuring the most extended crust and thickest sediment accumulation. In the CT, this location was at shot point #10450 on BGR-02 and in the EB at shot point #4200 on BGR-02 (Tables 3-1a & 3-1b; Fig. 3-2).

Although unconformity RSU7 is interpreted in both basins, it was not included in this study because of the lack of control on its age. RSS-1-lower and RSS-1-upper were grouped together as a single RSS-1 unit. Unfortunately, acoustic basement could not be resolved in the deepest part of the CT or EB from seismic reflection data. Depth to basement was obtained from gravity and seismic refraction modeling of Trey, et al. [1999] (dashed gray line in Fig.3-2).

Table 3-1a: Central Trough unit thickness; BGR-02 SP #10450

Seismic Unit	Unit Thickness (meters)	Unconformity	Depth to Unconformity (meters below seafloor)
RSS-5	268	Seafloor	0
RSS-4	175	RSU4	268
RSS-3	264	RSU4a	443
RSS-2	2241	RSU5	707
RSS-1	2530	RSU6	2948
		Basement	5478

Table 3-1b: Eastern Basin unit thickness; SP # 4200

Seismic Unit	Unit Thickness (meters)	Unconformity	Depth to Unconformity (meters below seafloor)
RSS-6,7&8	285	Seafloor	0
RSS-5	400	RSU3	285
RSS-4	370	RSU4	685
RSS-3	230	RSU4a	1055
RSS-2	1550	RSU5	1285
RSS-1	4705	RSU6	2835
		Basement	7540

3-2.2. Porosity and Lithology Relationships

The purpose of decompaction is to remove the progressive effects of rock volume that change over time and depth. The compaction history is likely to be complex being affected by lithology, overpressuring, diagenesis, and other factors (Fig. 3-3a). Therefore, some general relationships are needed which hold over time and depth. Sediment porosity changes with depth (where porosity at depth $z = \phi e^{-cz}$) and depends on the initial (surface) porosity of the sediments (ϕ) and the compaction decay constant (c). The initial porosity, the compaction decay constant, and the sediment matrix density are critical parameters in the decompaction process. These properties can be determined from sediment lithology using the compaction curves of Sclater and Christie [1980]. For this study, the average composition of the sediment in terms of sand, clay, silt, and diatoms were determined for each stratigraphic unit. Lithological descriptions of each unit were obtained from core logs for DSDP Sites 270, 271, 272, and 273 [Hayes, et al., 1975]. The average initial porosity and compaction decay constant were calculated by taking a weighted percentage of these parameters for the individual components (Table 3-2 & 3-3; Appendix E).

	Initial Porosity (ϕ_0)	Decay Cons. (c)	Grain Density
Sand	49	0.27	2.65
Clay/Shale	63	0.51	2.72
Silt	56	0.39	2.71
Diatomaceous	77	0.30	2.20
<0.5 km depth	87	0.66	2.20
>0.5 km depth	70	0.25	2.20

Table 3-2: Initial porosity, compaction decay constant and grain density of varying lithologies (from [Sclater and Christie, 1980; Compton, 1991]).

Seismic Unit	%Clay	%Silt	%Sand	%Diatoms	Avg. Initial Porosity	Avg. Decay Cons.	Avg. Density
RSS-8	58.0	28.0	6.33	7.67	61.23	0.45	2.67
RSS 6&7	48.1	23.4	26.6	1.90	57.90	0.41	2.69
RSS-5	49.76	29.56	7.11	13.56	61.83	0.43	2.64
RSS-4	26.13	18.34	4.27	51.27	68.30	0.37	2.45
RSS-3	46.0	23.60	5.0	25.47	64.26	0.42	2.58
RSS-2	51.2	35.17	12.98	0.80	58.92	0.44	2.71
RSS-1	50.0	0.0	50.0	0.0	56.0	0.39	2.71

Table 3-3: Average lithology and compaction parameters of RSS units from DSDP 270, 271, 272, 273.

The compaction curves of Sclater and Christie [1980] do not give the compaction properties for diatomaceous sediment. These were determined from work done by Compton [1991] on the diatomaceous Monterey Shale in California. Diatomaceous sediments were dealt with separately as they have much lower densities and higher porosities than other lithologies. Since unit RSS-1 has not been sampled, an average lithology of 50% sand and 50% clay is assumed. This is consistent with the interpretation that RSS-1 is of shallow marine origin [Brancolini, et al., 1995].

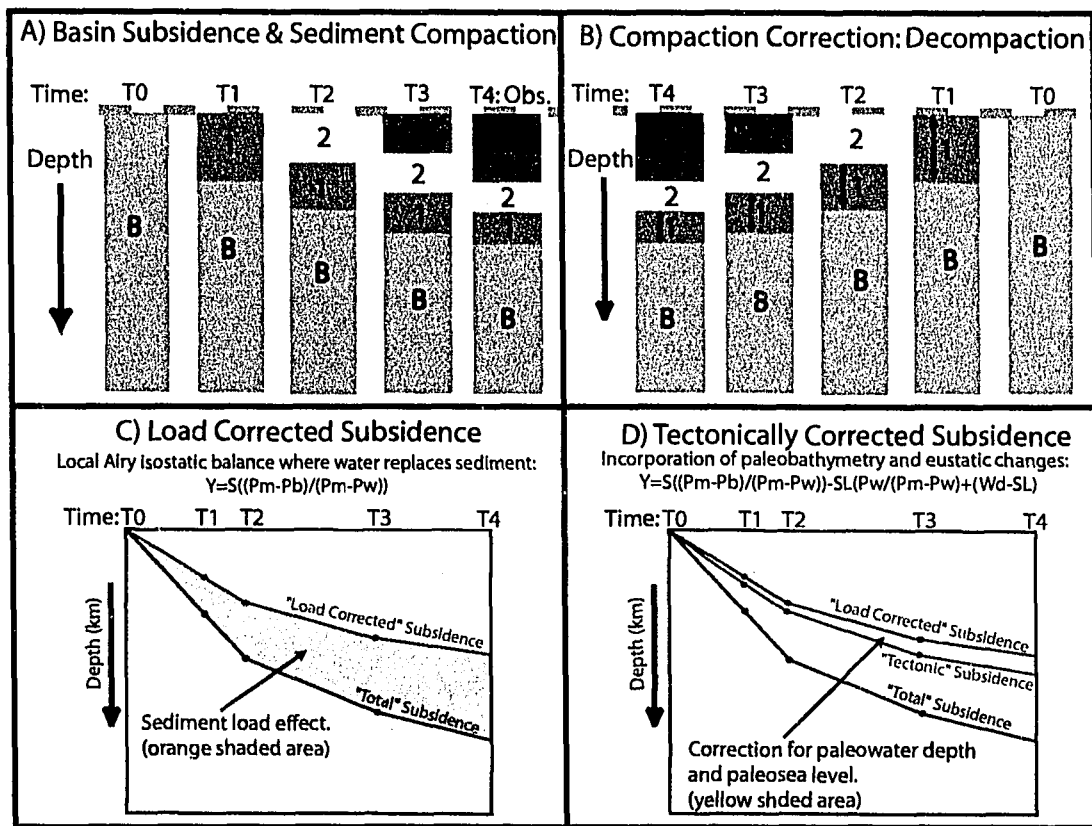


Figure 3-3: The decompaction method: **A)** After basement extension, sediment (unit 1) fill the newly formed basin. Over time, younger sediments (units 2-4) are deposited and compact the older sediment (unit 1), effectively reducing its thickness. By the observed time T4, unit 1 is fully compacted by overburden weight. **B)** The compaction correction decompacts sedimentary units by removing younger sediments starting at the observed time T4, restoring each unit to its original thickness at time of deposition. **C)** Load corrected subsidence is determined assuming Airy isostatic balance, where sediment is replaced by water, thus removing the subsidence due to sediment loading (orange shaded area) from the total subsidence. **D)** Paleobathymetry and eustatic changes (yellow shaded area) are added to the load corrected subsidence to compute the total tectonic subsidence.

Initial porosities used in this study (58%-63%) are higher than those used in DeSantis, et al. [1999] (45%). The reason for this is that DeSantis, et al.[1999] used a seismic velocity model to determine porosity-depth relationships. This method fails to take into account the high initial porosity of diatomaceous sediment, as well as underestimates initial sediment porosity due to overcompaction of present-day near surface sediment by Plio-Pliestocene glacial advances. These glacial advances were not a significant factor in the earlier Tertiary sequences [Accaino, et al., 2005].

3-2.3. Decompaacted Thickness and Load Corrected Subsidence

The thickness of a sedimentary layer at a given time in the past is determined by moving the layer up on the appropriate porosity-depth curve. This is equivalent to sequentially removing overlying layers and allowing the layer of interest to decompress (Fig. 3-3b). Mass is kept constant and only changes in sediment volume, in terms of layer thickness, are determined. For this study, the general decompression equation was used:

$$y'_2 - y'_1 = y_2 - y_1 - \phi_o/c \{ \exp(-cy_1) - \exp(-cy_2) \} + \phi_o/c \{ \exp(-cy'_1) - \exp(-cy'_2) \}$$

where y_1 and y_2 are the present unconformity depths, and y'_1 and y'_2 are the decompaacted depths [Allen and Allen, 2005]. The calculated decompaacted subsidence curve of each horizon is plotted with respect to present-day sea level.

Once the decompaacted subsidence curve is known, the sediment loading effect is treated as a problem of local Airy isostatic balance (Fig. 3-3c). The porosity and bulk density of each layer at its decompaacted depth is taken into account. Load-

corrected tectonic subsidence is the subsidence that would have occurred if the basin was filled with water and no sedimentation had taken place. As a result, the component of basement subsidence due to sediment loading is removed, thereby isolating the tectonic component of subsidence. The corrected tectonic subsidence resulting from the sediment load is calculated by:

$$Y_L = S(\rho_m - \rho_s / \rho_m - \rho_w)$$

where Y_L is the basement depth corrected for the sediment load, S is the total thickness of the column corrected for compaction, and ρ_m , ρ_s , ρ_w are the mantle, mean sediment, and water densities, respectively [Allen and Allen, 2005] (Appendix F).

3-2.4. Tectonic Subsidence: Eustatic and Paleobathymetry Corrections

Global sea level changes over time must be taken into account to obtain the total tectonic subsidence. Global eustasy is accounted for using the curves of Kominz, et al. [1998] and Miller et al. [2005]. Late Tertiary lowstands of -10 m (± 20 m) were approximated from the global sea level curves. Even though paleobathymetric data is poorly known for the Ross Sea, DSDP Site 270 contains benthic faunal assemblages that can be used as a proxy for water depth. Faunal assemblages within Oligocene RSS-2 record an upward deepening sequence, from shallow marine conditions to depths of several hundred meters, similar to present-day water depths [Leckie and Webb, 1986]. Due to the lack of accurate and available paleobathymetric data, paleobathymetry at each unconformity was estimated so that the observed subsidence

matched predicted subsidence curves for reasonable stretching factors (Table 3-4). This study uses the assumption that unconformity RSU6 (30 Ma) formed at sea level by wave cutting processes during a prominent sea level fall at 30 Ma [DeSantis, et al., 1999]. Unconformities RSU5, RSU4a, RSU4, and RSU3 are interpreted to have been cut by a combination of eustatic sea level falls, grounded ice and subglacial currents [DeSantis, et al., 1995; DeSantis, et al., 1999].

Unconformity	Age (Ma)	Paleobathymetry (W_d) (meters)	Eustatic Correction (Δ_{sl}) (meters)
RSU6	30 ± 4	100 ± 50	0
RSU5	19 ± 2	200 ± 200	-10 ± 20
RSU4a	17 ± 1	200 ± 200	-10 ± 20
RSU4	14.5 ± 1	200 ± 200	-10 ± 20
RSU3	11 ± 3	200 ± 200	-10 ± 20
Seafloor	0	500 ± 200	0

Table 3-4: Paleobathymetry and eustatic corrections applied in this study for Ross Sea unconformities. Eustatic corrections estimated from Kominz, et al. [1998] and Miller, et al.[2005].

To obtain the total tectonic subsidence, paleobathymetry and eustatic corrections were applied to the load corrected subsidence using:

$$Y_T = S(\rho_m - \rho_s / \rho_m - \rho_w) - \Delta_{sl}(\rho_m / \rho_m - \rho_w) + (W_d - \Delta_{sl})$$

where $S(\rho_m - \rho_s / \rho_m - \rho_w)$ is the load corrected term, Δ_{sl} is the eustatic correction, and W_d is the paleobathymetry (Fig. 3-3d) [Allen and Allen, 2005].

3-2.5. Predicted Tectonic Subsidence for Given Stretching Factors (β)

Predicted tectonic subsidence curves were calculated for different lithosphere stretching factors (β) in an effort to fit them to observed backstripped tectonic

subsidence curves. This was done to determine the timing and amount of extension the Ross Sea has undergone based on the subsidence results. Predicted curves were calculated for a single Cretaceous rifting event and two phase Cretaceous and Tertiary extensional events using multiple combinations of β values.

Predicted subsidence was calculated from forward modeling of temperature vs. depth profiles assuming instantaneous, pure-shear extension [McKenzie, 1978]. McKenzie [1978] solves for thermal contraction for a single extension event by Fourier expansion. For this study, thermal contraction was solved for by a finite difference heat flow calculation in Excel. This method permits a more complex extension history to be considered. An initial lithosphere thickness of 125 km (consistent with McKenzie [1978]), thermal expansion coefficient of $3.28 \times 10^{-5} \text{ }^{\circ}\text{C}^{-1}$, mantle temperature of $1330 \text{ }^{\circ}\text{C}$, and mantle density of 3.33 g cm^{-3} were used for this calculation. For the single Cretaceous extension model, rifting was set to have occurred at 95 Ma and then thermally cooled to present-day (Fig. 3-4a). For the two phase Cretaceous and Tertiary extension model, rifting initiated at 95 Ma, followed by thermal cooling to 35 Ma when a second extension event occurred, also followed by thermal cooling to the present-day (Fig. 3-4b). This method takes into account any thermal subsidence that may result from the Cretaceous event during Cenozoic time. The tectonic subsidence from thermal cooling was calculated and plotted against observed tectonic subsidence curves for comparison of results.

3-3. Observations and Results

Decompacted subsidence curves show the total tectonic subsidence and sediment accumulation over time. The subsidence history prior to 30 Ma is poorly constrained due to the absence of dated stratigraphic indicators between the Late Cretaceous and early Oligocene. However, since 95 Ma, more than 5.5 km of sediment accumulation has occurred in the Central Trough (Fig. 3-5a) and more than 7.5 km in the Eastern Basin (Fig. 3-5b). Both the CT and EB indicate a similar subsidence history for unconformity RSU6 (30 Ma). However, post RSU6 unconformities (RSU5, RSU4a, and RSU4) are deeper in the EB than in the CT. This may be due to compaction of the units in the EB resulting from deposition of the overlying RSS-7&8 units that are not present in the Central Trough or possibly the more extension in the EB.

3-3.1. Load Corrected and Total Tectonic Subsidence Curves Since 30 Ma

The results from the load corrected and total tectonic subsidence curves differ significantly. However, this is expected as the load corrected subsidence does not take into account eustasy and paleo-water depth. Ignoring the effects of eustasy and paleobathymetry, the load corrected curves indicate that the CT subsided an additional 780 m (± 100 m) since 30 Ma (RSU6 time) while the EB subsided an additional 690 m (± 100 m) (Fig. 3-6). Adding in the effects of eustasy and paleobathymetry, to determine the total tectonic subsidence, results in 1,180 m (± 220 m) of additional tectonic subsidence in the CT and 1,090 m (± 220 m) in the EB since

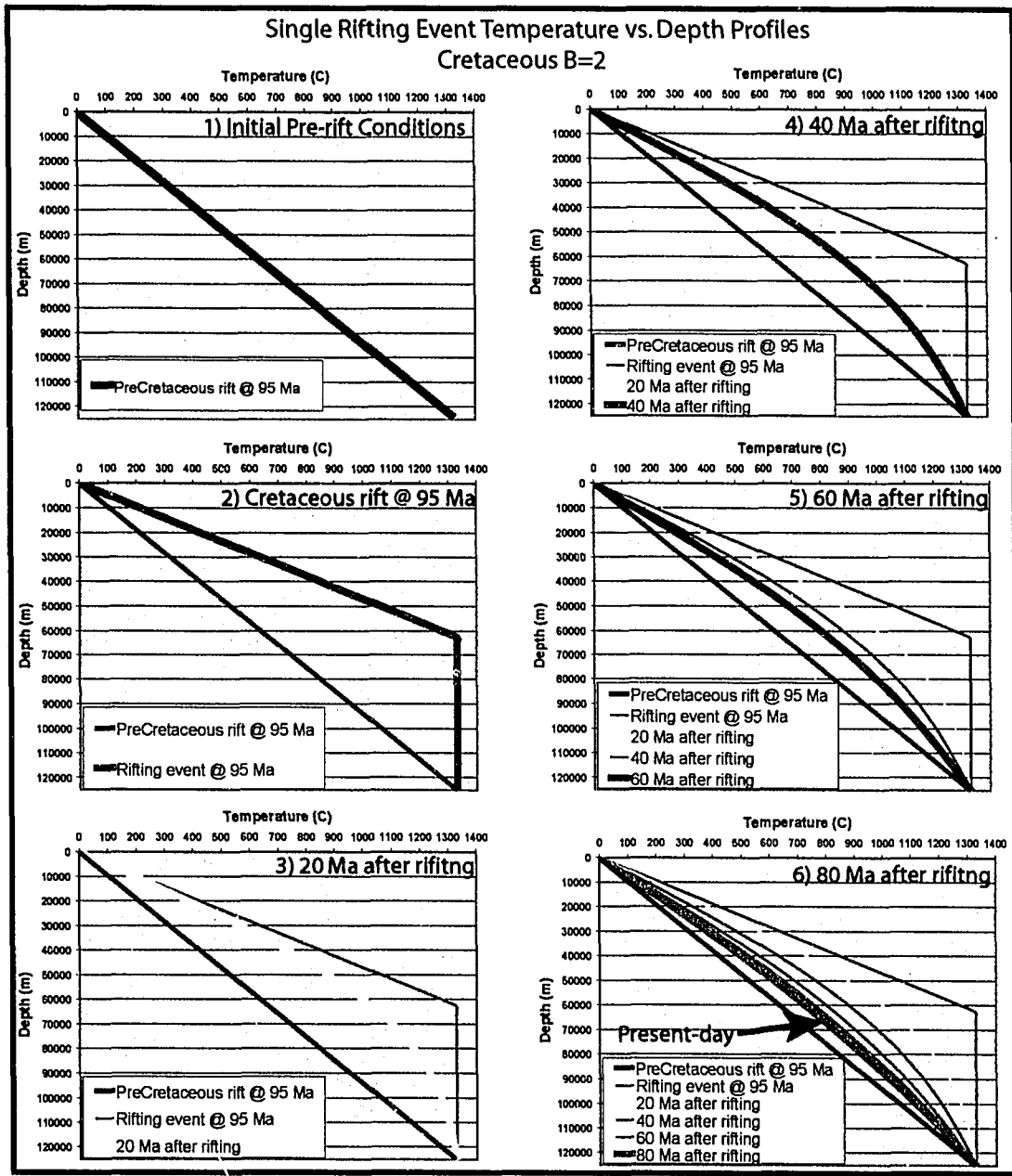


Figure 3-4c: Predicted temperature vs. depth curves for a single Cretaceous extension event at $\beta=2$ for 125 km thick lithosphere assuming instantaneous, pure-shear rifting [McKenzie 1978]. **1)** Initial pre-rift conditions. **2)** Cretaceous rift conditions at 95 Ma. **3-6)** Thermal cooling at 20, 40, 60, and 80 Ma, respectively. Thermal profiles relax back to equilibrium or pre-rift conditions. Predicted present-day conditions are close to equilibrium conditions, indicating that thermal subsidence of the Ross Sea would be near completion from a Cretaceous only rifting event.

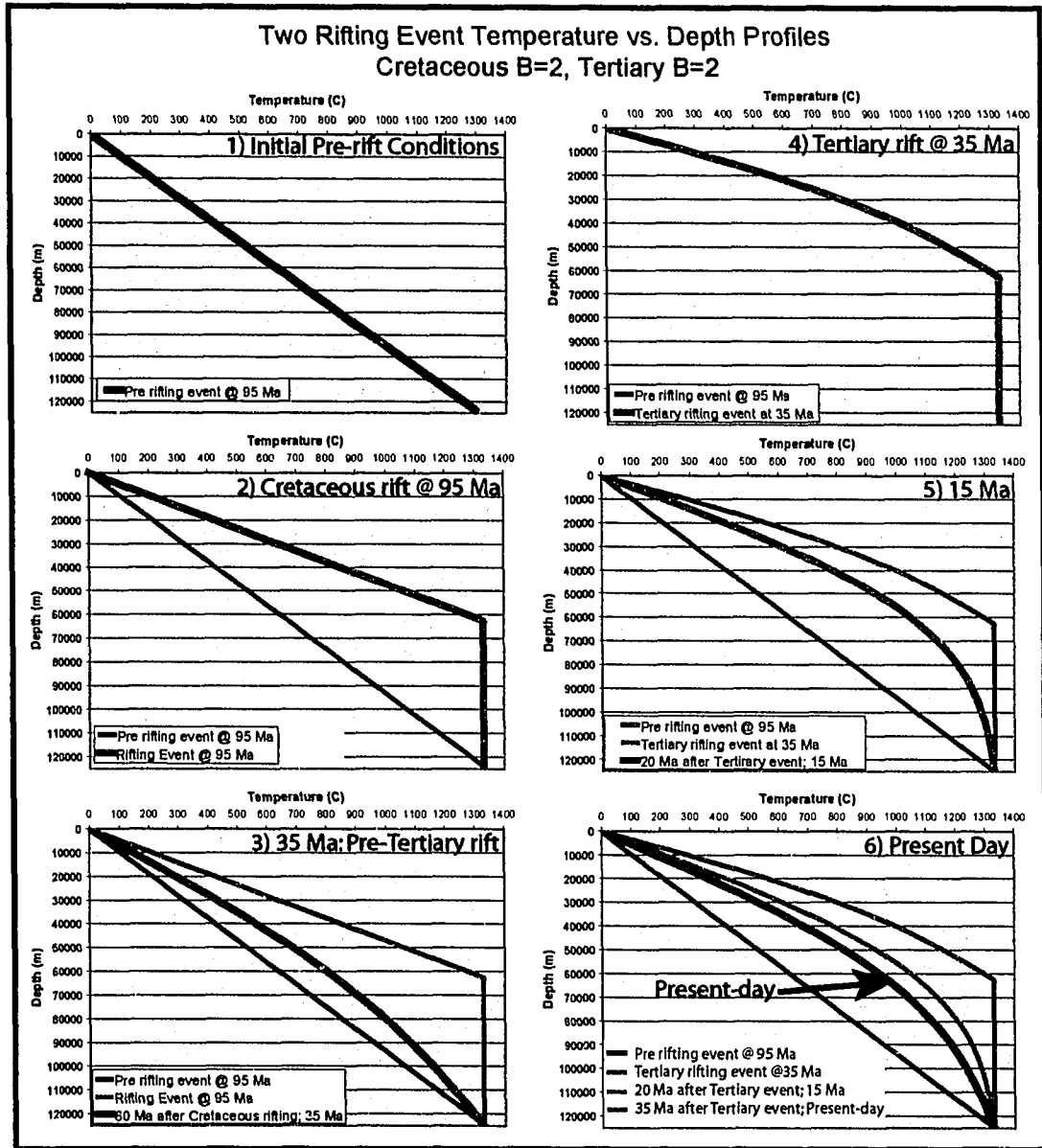


Figure 3-4b: Predicted temperature vs. depth curves for two stage extension, a Cretaceous event and a Tertiary event both at stretching factors of 2 for 125 km thick lithosphere assuming instantaneous, pure-shear rifting [McKenzie 1978]. **1)** Initial pre-rift conditions. **2)** Cretaceous rift conditions at 95 Ma. **3)** Cretaceous thermal cooling to 35 Ma. **4)** Tertiary extension event at 35 Ma. **5)** Thermal cooling at 20 Ma after Tertiary rifting event (15 Ma). **6)** Thermal cooling at 35 Ma after Tertiary rifting event or present-day. Predicted present-day conditions are not at equilibrium indicating that tectonic subsidence of the Ross Sea is still occurring.

30 Ma (Fig. 3-7). The curves for both basins show subsidence rapidly occurred to ~15 Ma, before slowing from 15 Ma to present.

3-3.2. Predicted vs. Observed Tectonic Subsidence

If the Ross Sea was extended by a single rifting event in the Cretaceous, then most of the thermal tectonic subsidence has been completed by now. However, if the Ross Sea was extended in two stages, temperature vs. depth profiles should show that the basins are still subsiding due to thermal cooling. Present-day temperature vs. depth relationships suggest the accommodation space of the Ross Sea Embayment may be presently enlarging, possibly resulting from continued tectonic subsidence of extended continental crust.

Thermal tectonic subsidence is directly affected by the amount of stretching. Predicted subsidence curves can be fitted to the observed tectonic subsidence curves for the Central Trough and Eastern Basin to determine the amount of crustal stretching (β) that has affected the Ross Sea. A single Cretaceous extension event is considered first. Predicted tectonic subsidence for stretching values of $\beta=2$, $\beta=4$, and $\beta=5$ were plotted against the observed load corrected (Fig. 3-6a) and total tectonic subsidence (Fig. 3-7a). None of the subsidence curves fits the single Cretaceous event curves. At 100% ($\beta=2$) extension in the Cretaceous, only ~280 m of additional subsidence would be expected since 30 Ma. This leaves over 800 m of unaccounted subsidence in both the CT and EB. Similarly, if a larger Cretaceous extensional event ($\beta=4$) affected the Ross Sea, the predicted subsidence would be on the order of ~400

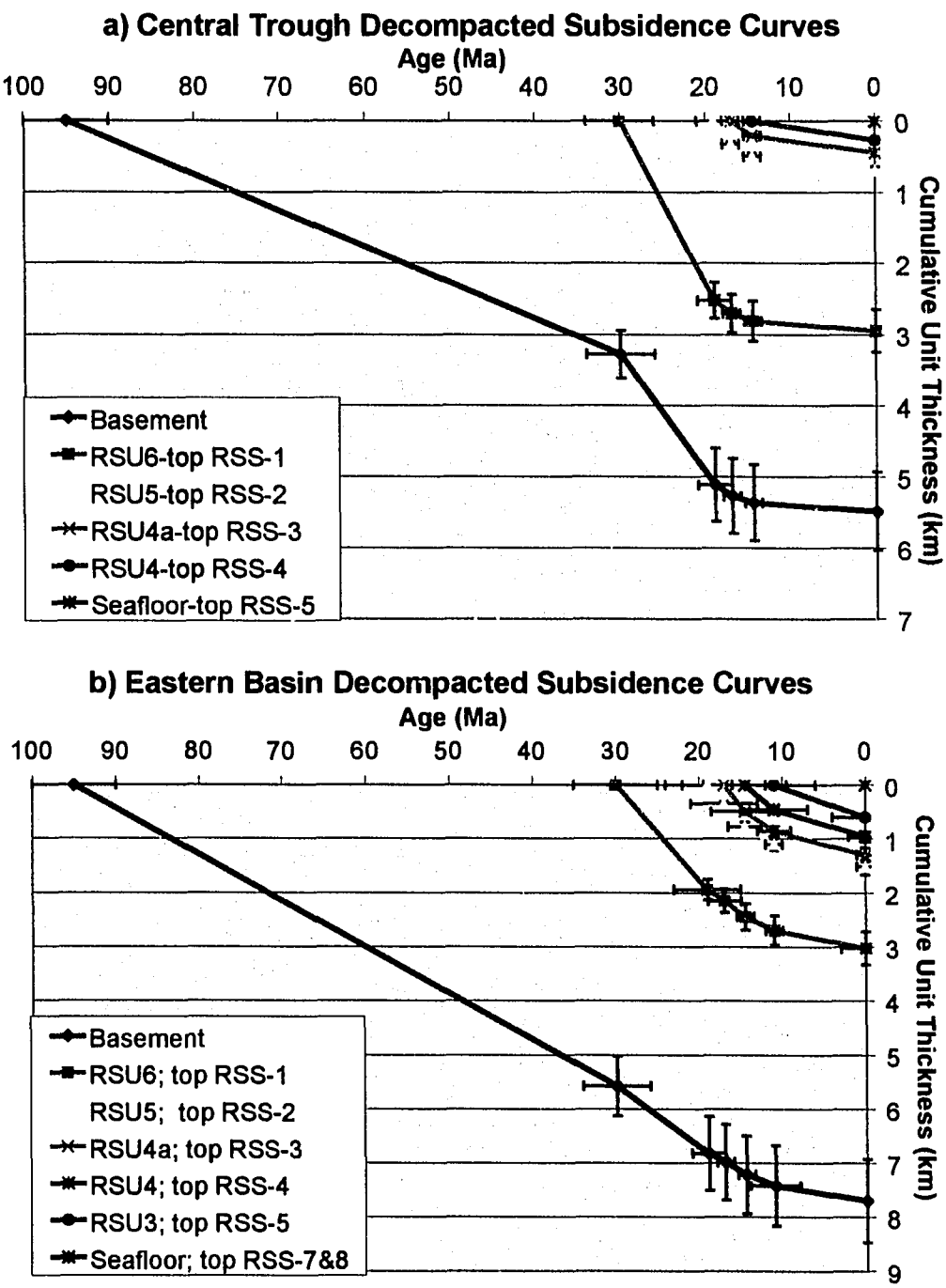
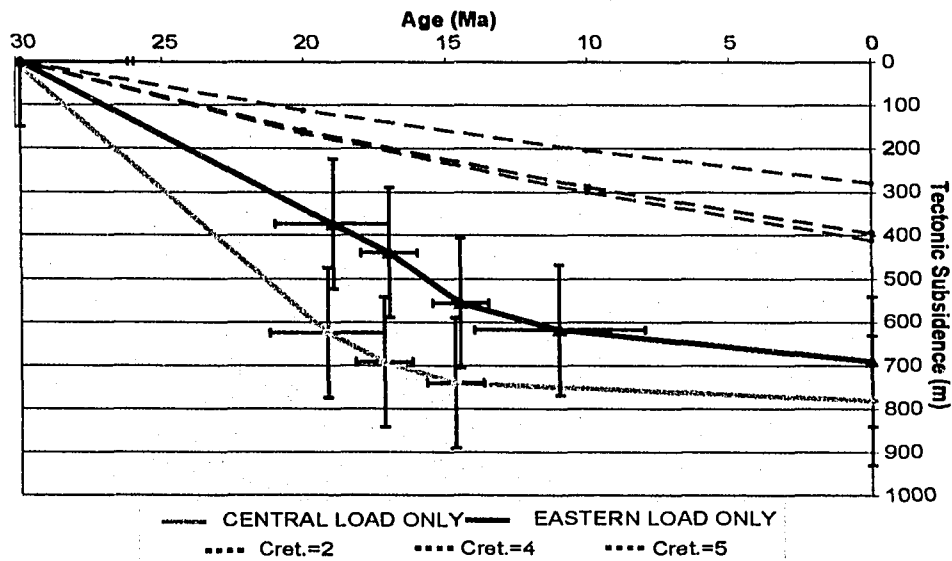


Figure 3-5: Decompacted total subsidence of the Central Trough and Eastern Basin basement and unconformities RSU6-RSU3. **a)** Total subsidence of the Central Trough indicates ~5.5 km of basement subsidence and ~3 km of RSU6 subsidence. **b)** Total subsidence of the Eastern Basin indicates ~7.5 km of basement subsidence and ~3 km of RSU6.

a) Cretaceous Rifting Event Only:
Central Trough and Eastern Basin Load Only Subsidence



b) Cretaceous and Tertiary Rifting Events:
Central Trough and Eastern Basin Load Only Subsidence

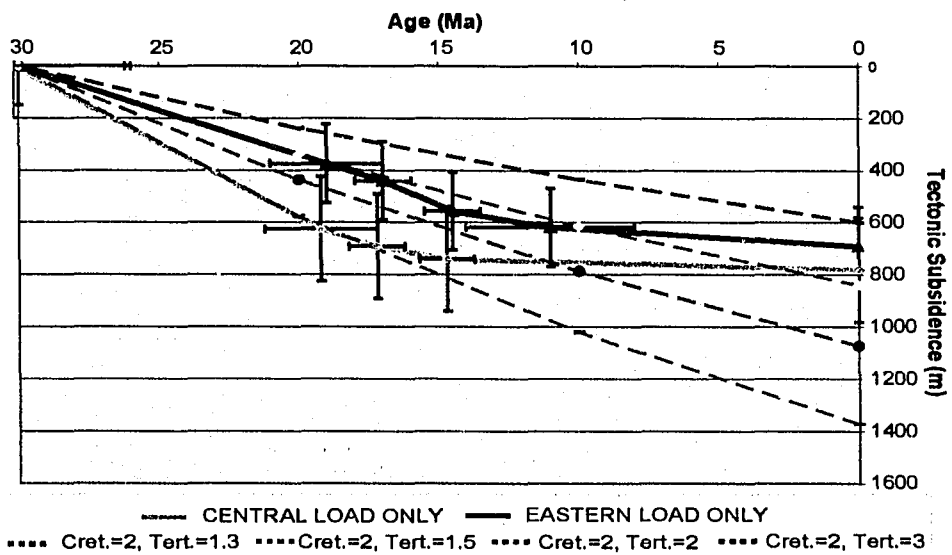


Figure 3-6: Load only tectonic basement subsidence curves for the Central Trough (orange) and Eastern Basin (purple). The Central Trough has subsided ~780 m and the Eastern Basin has subsided ~690 m since 30 Ma. **a)** Cretaceous rifting event: dashed lines are predicted subsidence curves for a single Cretaceous rifting event with $\beta=2, 4$, and 5 . **b)** Cretaceous and Tertiary rifting event: dashed lines are predicted subsidence for a Cretaceous and Tertiary rifting event using different combination of β values.

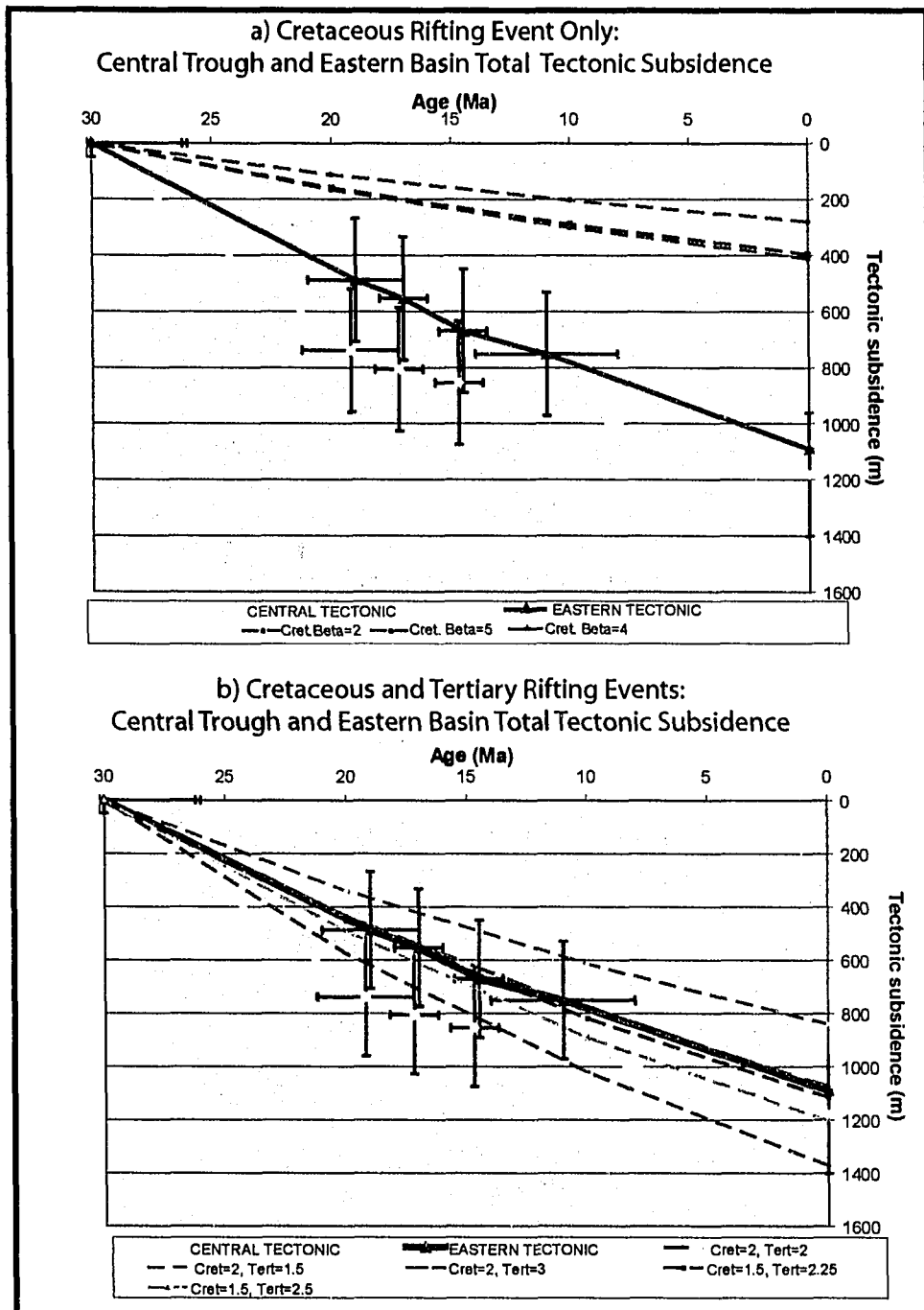


Figure 3-7: Total tectonic basement subsidence curves for the Central Trough (yellow) and Eastern Basin (pink). The Central Trough has subsided ~1200 m and the Eastern Basin has subsided ~1100 m since 30 Ma. **a)** Cretaceous rifting event: dashed lines are predicted subsidence curves $\beta=2, 4$, and 5 . **b)** Cretaceous and Tertiary rifting event; dashed lines are predicted subsidence for different combination of β values. A Cretaceous event at $\beta=2$ followed by a Tertiary event at $\beta=2$ fits observed Eastern Basin subsidence closely. Other combinations of Cret.=1.5, Tert.=2.25 or 2.5 also can explain both the CT and EB observed subsidence.

m. Over 700 m of unaccounted subsidence would remain in both the CT and EB if this were the case. These results indicate that no amount of Cretaceous-only extension in the Ross Sea can account for the tectonic subsidence of the basement from 30 Ma to the present, assuming that unconformity RSU6 formed at sea level.

A two stage Cretaceous and Tertiary extension was modeled and compared to the observed data. The results show that observed tectonic subsidence for the Central Trough and Eastern Basin can be explained by an initial rifting event in the Cretaceous, followed by a second rifting event in the Tertiary. A range of stretching factors were used to produce several predicted subsidence curves to best estimate the amount of extension the Ross Sea underwent as a result of two rifting events. The load corrected tectonic subsidence curves for both the CT and EB are bracketed by predicted subsidence curves using stretching factors of Cretaceous $\beta=2$, Tertiary $\beta=1.3$ and Cretaceous $\beta=2$, Tertiary $\beta=1.5$ (Fig. 3-6b). However, this would assume there were no eustatic changes over time and that paleobathymetry did not change, which is very unlikely given the major glaciation events that have occurred since 30 Ma.

The total tectonic subsidence curves for both the CT and EB are bracketed by predicted subsidence curves using stretching factors of Cretaceous $\beta=2$, Tertiary $\beta=1.5$ and Cretaceous $\beta=2$, Tertiary $\beta=3$ (Fig. 3-7b). Further refinement reveals that predicted subsidence resulting from a stretching factor of Cretaceous $\beta=2$, Tertiary $\beta=2$ fits the EB observed total tectonic subsidence very closely (Fig. 3-7b). The observed subsidence of the CT does not fit a Cretaceous $\beta=2$, Tertiary $\beta=2$ curve, but

does fit within the error limits. Both the CT and EB observed subsidence can be explained by alternative combinations of stretching factors that are within error limits. These combinations include Cretaceous $\beta=1.5$, Tertiary $\beta=2.25$ and Cretaceous $\beta=1.5$, Tertiary $\beta=2.5$ (Fig. 3-7b). It is possible that the CT may have a slightly lower Cretaceous stretching factor combined with a slightly higher Tertiary stretching factor that would produce similar results as the EB with stretching factors of Cretaceous $\beta=2$, Tertiary $\beta=2$. Regardless, these results indicate that two stages of significant extension may account for the observed subsidence of the Central Trough and Eastern Basin.

3-4. Discussion

3-4.1. Can a Single Cretaceous Extension Event Explain Ross Sea Subsidence?

An alternative model for the formation of the Ross Sea basins limits Tertiary extension only to the Victoria Land Basin, resulting in Cretaceous-only extension in the Central Trough and Eastern Basin [Karner, et al., 2005]. The Cretaceous-only model requires that most thermal subsidence throughout the Ross Sea predates Oligocene sedimentation. This timing requires that Cretaceous extension created deep paleo-basins for the deposition of Oligocene strata [Karner, et al., 2005].

For a single Cretaceous extension event to explain the subsidence history, Tertiary Ross Sea unconformities would have to had formed at depths of hundreds of meters rather than at or near sea level, where wave cutting or glacial processes could have cut the unconformities. The total tectonic subsidence of the Eastern Basin was

fitted to a Cretaceous $\beta=4$ predicted subsidence curve by changing the paleo-water depth at each unconformity until the observed subsidence curve fit the predicted subsidence (Fig. 3-8). The results show that unconformity RSU6 would have to form at 900 m depth, RSU5 at 680 m, RSU4a at 640 m, RSU4 at 555 m, and RSU3 at 540 m. If this is the case, then unconformities RSU5-RSU3 formed close to the present-day seafloor depth. It is possible that grounded ice could have cut these unconformities. However, no evidence exists for a major and long-lasting ice sheet advance in the Ross Sea at the time of RSU5 and RSU4a formation [DeSantis, et al., 1995; DeSantis, et al., 1999].

How would the results for Cretaceous-only extension be different had flexural compensation been assumed as opposed to local Airy compensation? A local sediment load produces a broader area subsidence response in a flexural process than an Airy process. In a flexural response the accommodation space for sediment is less than a local isostatic response. The backstripping analyses accounts for the observed sediment thickness by combining effects including tectonic subsidence, isostatic response and paleobathymetry. Therefore, less isostatic response at a basin center in a flexural compensation model requires deeper bathymetry to account for an assumed subsidence history than a local compensation model. The paleobathymetry for RSU6 in flexural compensation would be significantly deeper than 900 m found for the 1-D model. This in fact is a consequence of the analysis of Karner et al. [2005] that requires the basins to be deep when RSU6 is formed.

If unconformity RSU6 formed at 900 m or greater depths, then the unconformity cannot be a wave-cut erosion feature and other processes, such as glaciation or deep water currents, would have formed the unconformity. Unconformity RSU6 has been suggested to have formed as a deepwater unconformity resulting from strong currents related to the opening of the Drake Passage around 29 Ma [Hinz and Block, 1984]. Deep water Oligocene unconformities are interpreted in the Indian Ocean and the western Pacific Ocean. These unconformities may have resulted from aggressive erosive Antarctic Bottom Water currents that formed during the Oligocene cool down of Antarctica [Davies, et al., 1975]. Therefore, it is possible RSU6 formed from erosive bottom water currents in the Ross Sea. Anderson and Bartek [1992] suggest subglacial erosion processes may have formed RSU6. However, DeSantis, et al. [1999] argue that RSU6 was not formed by subglacial processes based on the improbability that a large-sized ice sheet was grounded on the seafloor at significant depth without leaving any signs of erosion or deposition.

If unconformity RSU6 was cut at 900 m or more by grounded ice, significant erosion of RSS-1 would be expected. Rather, relatively parallel reflectors are interpreted above and below RSU6 [DeSantis, et al., 1995]. This is characteristic of gentle slopes, typical of shallow shelves. Therefore, it seems unlikely that unconformity RSU6 formed at deep water depths from glaciation. Formation of RSU6 at depth fits less well with current interpretations of the unconformity as a wave-cut erosion surface [DeSantis, et al., 1995; DeSantis, et al., 1999]. We favor an origin of Ross Sea Tertiary unconformities as shallow water unconformities that were

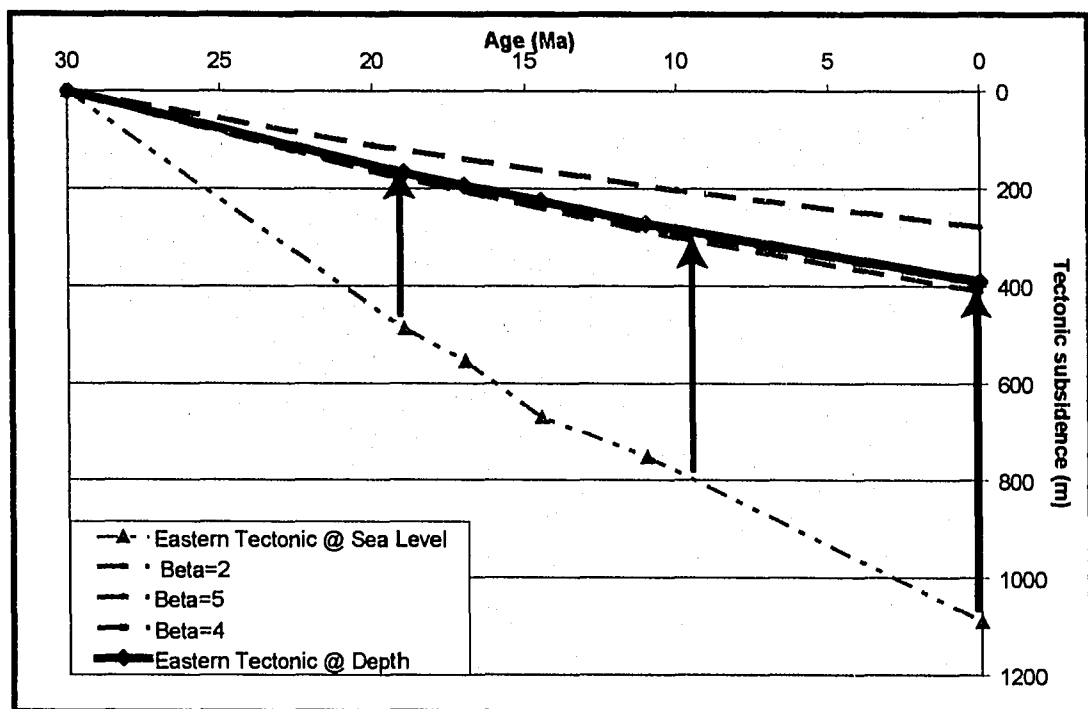


Figure 3-8: If the Tertiary Ross Sea unconformities formed at sea level, then the observed total tectonic subsidence (dashed pink line) cannot be explained by a single Cretaceous extension event. If Tertiary unconformities formed at a depth of hundreds of meters, then the observed subsidence (solid blue line) can be explained by a single Cretaceous event. In this case, unconformity RSU6 would have to form at a depth of ~900 m.

formed from a combination of sea level changes and erosion from grounded ice. Therefore, we propose a two stage extension model initiating with Cretaceous extension and followed by an early Tertiary event consistent with the shallow water unconformity assumption.

3-4.2. Two Stages of Extension in the Ross Sea

A time series of crustal models spanning the Central Trough and Eastern Basin along profile BGR-02 were made showing the evolution of the Ross Sea (Fig. 3-9a-f). The models were constructed starting with the present-day crustal structure of the Ross Sea working backwards in incremental time steps to determine the structure in the past. Thermal subsidence was taken into account to determine the vertical position as well as horizontal position due to stretching, required by the stretching factor, to reconstruct the crustal thickness at each time step. Present-day crustal thickness were obtained from Trey, et al. [1999], who calculated crustal thicknesses along seismic profile BGR-02 from seismic refraction and gravity data.

3-4.2.1. Cretaceous time: Prior to initial extension at 95 Ma, the Ross Sea was probably an elevated region high above sea level (Fig. 3-9a). At this time the pre-rift crust of the Ross Sea was approximately 50 km thick. The observed subsidence of the Central Trough and Eastern Basin can be explained by a two stage extension model with an initial Cretaceous extension event at 95 Ma. This is in agreement with proposed plate reconstructions for the region that suggest Late Cretaceous motion between East and West Antarctica around 95-90 Ma [Lawver and Gahagan, 1994;

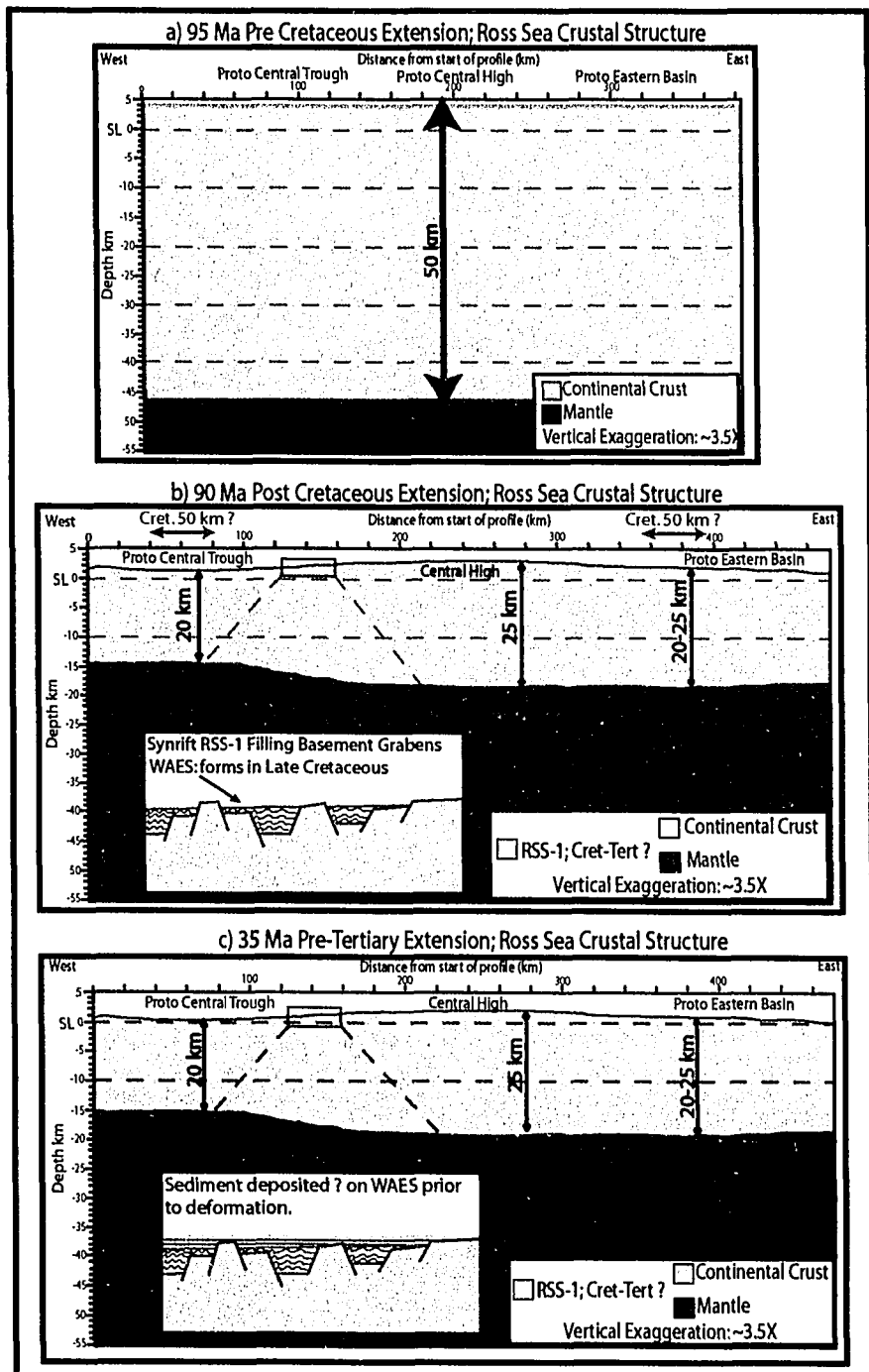


Figure 3-9 Model of Ross Sea formation. SL= Sea Level, insets not to scale **a)** 95 Ma Pre-Cretaceous extension: The Ross Sea may have been an elevated region with crustal thickness of ~50 km. **b)** 90 Ma Post Cretaceous extension: Crust thins to 20-25 km, graben formation accommodates a combined ~100 km of E-W extension. Formation of the proto-basins and deposition of syn-rift RSS-1. **c)** 35 Ma, Pre-Tertiary extension: Thermal subsidence of the region, but remains above sea level. Continued RSS-1 deposition onttop of the West Antarctic Erosion Surface (WAES). The WAES formed in the Late Cretaceous, post-90 Ma.

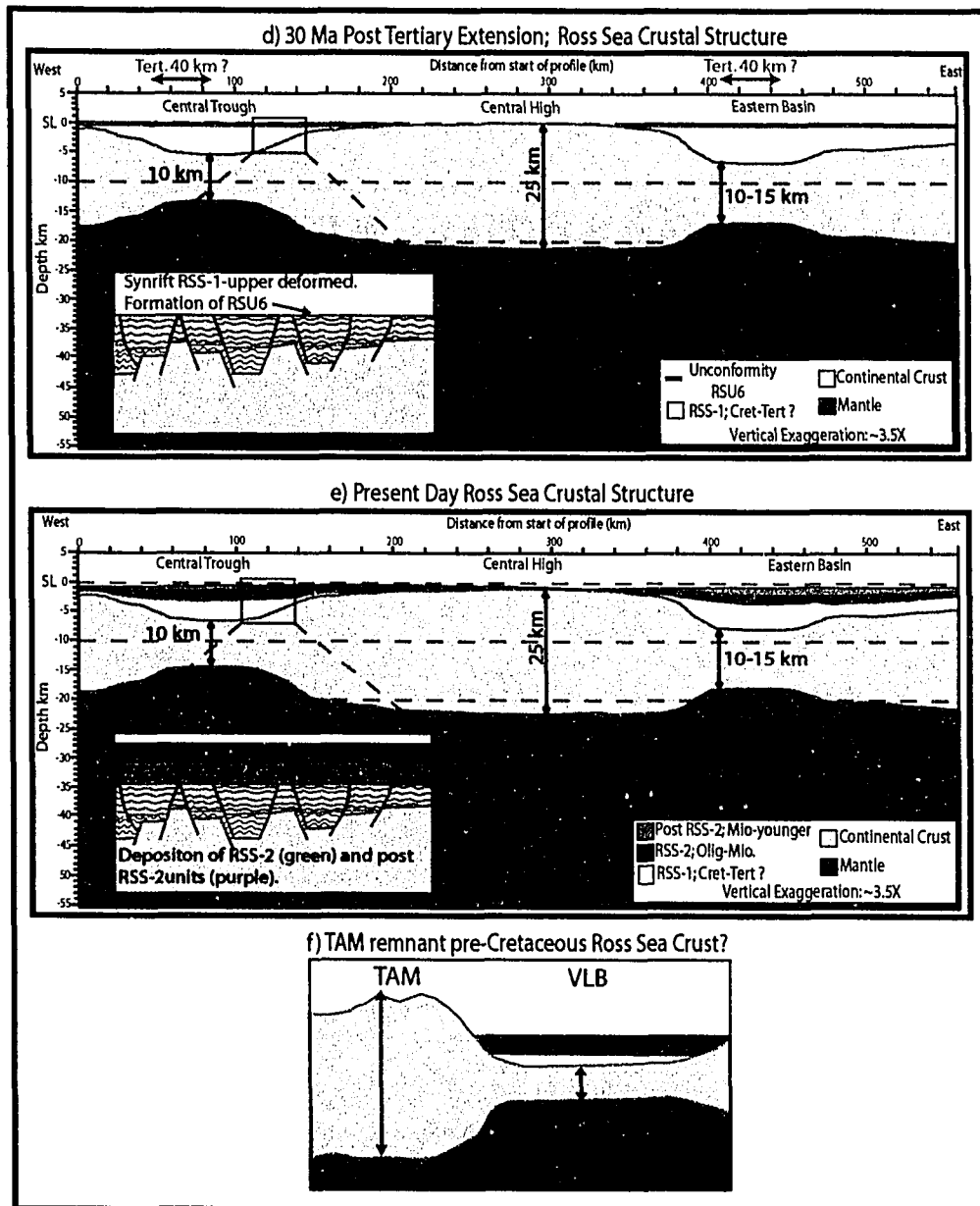


Figure 3-9: SL=Sea Level, insets not to scale. **d)** 30 Ma, post Tertiary extension: localized crustal thinning of the proto-basins to 10 km thick and the formation of present-day Ross Sea basins. The Central High does not extend and remains 25 km thick. The region is largely below sea level except for the Central High. Formation of unconformity RSU6. **e)** Present-day: thermal subsidence from 30 Ma to present results in submergence of the Central High and development of the necessary accommodation space for the deposition of Oligocene RSS-2 and post RSS-2 glacial units. **f)** The TAM may be a remnant of the original 50 km thick Ross Sea crust that was not extended in Cretaceous or Tertiary rifting events.

Davey and Brancolini, 1995]. Extension commenced at ~95 Ma, at which time the Ross Sea region underwent ~100% ($\beta=2$) extension in a roughly east-west direction. This is consistent with interpreted Cretaceous N-S trending basement faults in the Central Trough as well as interpreted Cretaceous NE-SW and E-W trending faults offshore Cape Colbeck in the eastern Ross Sea and onshore western Marie Byrd Land [Luyendyk, et al., 2001; Luyendyk, et al., 2003; Decesari, et al., 2004]. These fault trends suggest an overall E-W Cretaceous extensional pattern.

During Cretaceous extension, the crust was thinned to ~20 km in the locations of the proto-Victoria Land Basin, proto-Central Trough, and proto-Eastern Basin, and ~25 km in the locations of the present-day basement highs such as the Central High (Fig. 3-9b). North-south trending fault bounded grabens formed in the basement helping to accommodate the ~100 km of combined E-W extension between the Central Trough and Eastern Basin sectors of the Ross Sea. The lower sequences of sedimentary unit RSS-1 were deposited and deformed within the grabens. Tectonic subsidence of the region occurred due to the extension event, but the region remained significantly above sea level.

Cretaceous extension in the eastern Ross Sea is proposed to have been controlled by detachment fault systems [Fitzgerald and Baldwin, 1997; Luyendyk, et al., 2001; Siddoway, et al., 2004]. Extension along low-angle detachment faults is a common mechanism in crustal terrains where the amount of extension approaches or exceeds 100% [Fitzgerald and Baldwin, 1997]. Mylonitic gneisses were recovered from offshore Cape Colbeck and are dated at 95-98 Ma [Luyendyk, et al., 2001;

Siddoway, et al., 2004]. Further to the west at DSDP Site 270 in the Eastern Basin, basement mylonites were also recovered with similar Late Cretaceous cooling ages. These mylonites show a brittle upon ductile textural overprint, interpreted as evidence of exhumation in a detachment system [Fitzgerald and Baldwin, 1997]. Fitzgerald and Baldwin [1997] proposed detachment faulting accommodated Cretaceous rifting and multiple detachment faults likely occur within the Ross Sea. Although no evidence for detachment faults has been found in the VLB or CT, Cretaceous extension throughout the Ross Sea was most likely controlled by detachment systems that were located in the present-day basins.

In western Marie Byrd Land, the Late Cretaceous West Antarctic Erosion Surface (WAES) is observed at ~3 km above sea level [LeMasurier and Landis, 1996]. Luyendyk, et al. [2001] interprets the WAES to have formed at significant elevation and has correlated it into the eastern Ross Sea as angular unconformity RSU7. Here the WAES separates the lower and upper components of RSS-1 and has subsided below sea level [Luyendyk, et al., 2001]. The initial high elevation of the WAES may result from an elevated thermal profile due to significant magmatic input approximately 105 to 94 Ma [Richard, et al., 1994; Smith, 1995; Luyendyk, et al., 2001]. The WAES has also been interpreted separating the lower and upper RSS-1 unit in the western sector of the Eastern Basin and the Central Trough [Decesari, et al., 2004]. Therefore, it is possible that the Ross Sea region was topographically high at the time of formation of the WAES.

We propose the WAES formed after the main phase of Cretaceous rifting in the Ross Sea (Fig. 3-9b inset). Once the crust was thinned from 50 km to 25 km the region tectonically subsided, including western Marie Byrd Land. At this time Cretaceous RSS-1 was beveled in the Ross Sea, along with rocks in Marie Byrd Land, forming the WAES. The Ross Sea, and WAES, remained at significant elevation above sea level until Tertiary rifting occurred.

3-4.2.2. Tertiary time: Between Late Cretaceous extension and ~35 Ma, the Ross Sea region was thermally subsiding (Fig. 3-9c). At this time, the region remained largely above sea level (~1-3 km) and deposition of RSS-1 most likely continued in the continental basin on top of the WAES. The subsidence history indicates that a second, Tertiary extension event occurred around ~35 Ma which correlates with the Eocene Adare Trough seafloor spreading event. Hamilton, et al. [2001] suggested that seafloor spreading across the Adare Trough must have affected extension in the western Ross Sea. Furthermore, it is likely that Adare Trough rifting can account for extension inferred for the VLB and the large thickness of Oligocene and older sediments in it [Hamilton, et al., 2001]. Magnetic lineations suggest that at least 180 km of E-W seafloor spreading occurred across the Adare Trough [Stock and Cande, 1999; Cande, et al., 2000; Stock and Cande, 2002; Cande and Stock, 2004]. However, the VLB is only 130 to 150 km wide. Therefore an excess of at least 30-50 km, or more, of extension from the Adare Trough must have been accommodated elsewhere. Cande and Stock [2006] proposes two models for the accommodation of Adare Trough extension into the Ross Sea. The first model partitions Adare Trough

extension between the Northern Basin and the Central Trough. The second model has the Northern Basin accommodating all of the Adare Trough extension. We favor the first model, but suggest the extension was partitioned over all of the Ross Sea basins.

The subsidence history of the CT and EB indicates Tertiary extension affected these locations as well as the VLB. This extension is likely the excess Adare Trough extension. Tertiary extension of ~100% extended the Ross Sea further but in only localized areas corresponding to the proto-Central Trough and proto-Eastern Basin (Fig. 3-9d). These areas may have been zones of pre-existing weakness from Cretaceous extension. This model suggests ~40 km of E-W extension occurred in the Central Trough and ~40 km in the Eastern Basin, resulting in the formation of the present-day Ross Sea basins. The Central High is most likely a zone of relatively strong continental crust, compared to the weakened proto-basins, that was not affected by Tertiary extension and remained ~25 km thick. Syn-extension deposition of the Eocene shallow marine component of RSS-1, along with deformation of the WAES, occurred during this time and is interpreted from seismic data [Luyendyk, et al., 2001; Decesari, et al., 2003; Decesari, et al., 2004]. North-South trending normal faults are interpreted to offset both the Cretaceous and Eocene components of RSS-1 in the Central Trough and Eastern Basin suggesting fault reactivation [Decesari, et al., 2003; Decesari, et al., 2004]. Tertiary extension resulted in the subsidence of the WAES below sea level in the Ross Sea. However, the WAES remained considerably above sea level (~3 km) in western Marie Byrd Land, because this region was not significantly affected by Tertiary extension.

By 30 Ma, the entire RSS-1 unit was deposited and angular unconformity RSU6 was being cut at or near sea level. At this time, the Central High was at or slightly above sea level (Fig. 3-9d). Unconformity RSU6 onlaps the Central High, suggesting the axis of the high was not submerged at this time [Decesari, et al., 2004]. All extension must have been completed by the formation of unconformity RSU6 and before the deposition of RSS-2. If RSS-2 was deposited during extension, then it would exhibit syn-rift characteristics. In fact, RSS-2 is not faulted or deformed in the Central Trough or the Eastern Basin [Luyendyk, et al., 2001; Decesari, et al., 2003]. Between 30 Ma and present, on-going thermal cooling resulted in subsidence of the region, sending the Central High below sea level (Fig. 3-9e). The necessary accommodation space needed for the deposition of the late Oligocene-early Miocene glacial-marine RSS-2 developed as a result of this subsidence. Gentle westward tilting of RSS-2 in the Eastern Basin is interpreted to indicate thermal subsidence of the basin [Luyendyk, et al., 2001]. Post RSS-2 glacial units (RSS-3, RSS-4a, RSS-4, RSS-5 and RSS-6, 7, & 8) were also deposited in this accommodation space.

These results indicate that the Ross Sea region may represent founded continental crust resulting from the collapse of thick, elevated crust (Fig. 3-9f). The TAM may be the preserved edge of the collapsed crust. Studinger, et al. [2004] speculates West Antarctic structure, geologic history and heat flow may be consistent with the collapse of a high plateau of thick crust. In this scenario, extensional collapse of the hotter, weaker central part of the elevated region would thin the crust producing the Ross Sea. The cooler, stronger edges would be left behind and would

not be extended. The TAM would correspond to the remnant stronger edge. Bialas, et al. [2005] proposes a model of a ~50 km thick plateau that retains significant elevation on its flanks as the plateau is extended and lowered. The present-day TAM represents the edge. Our results support these hypotheses; however, there is no evidence that the region was a plateau. Instead, it may have been an elevated, thickened block of crust with significant surface topography.

3-4.3. Tertiary Ross Sea Extension in Three Major Bands

Free Air and Bouguer gravity grids of the Ross Embayment [Luyendyk, et al., 2002] indicate the basins of the Ross Sea are characterized by positive anomalies. Free Air anomalies of 0 to >+20 mGal and Bouguer anomalies of approximately +40 mGal characterize the basins (Fig. 3-10). The Coulman High and Central High are characterized by negative (>-40 mGal) Free Air anomalies and negative (0 to -40 mGal) Bouguer anomalies. Both Free Air and Bouguer gravity show a strong Moho signal. Because the positive gravity anomalies correspond to the basins, they can be used as a proxy for thinned continental crust.

If the VLB, CT and EB formed as a result of Adare Trough spreading, then the gravity data can show the extent and location of Tertiary extension in the Ross Sea. The Adare Trough is interpreted as a very negative (<-60 mGal) anomaly on the Free Air grid (Fig. 3-10). Extension from the Adare Trough branches into the Ross Sea in three locations. As a result, the VLB, CT, and westernmost EB deepened

Ross Sea Free Air Gravity

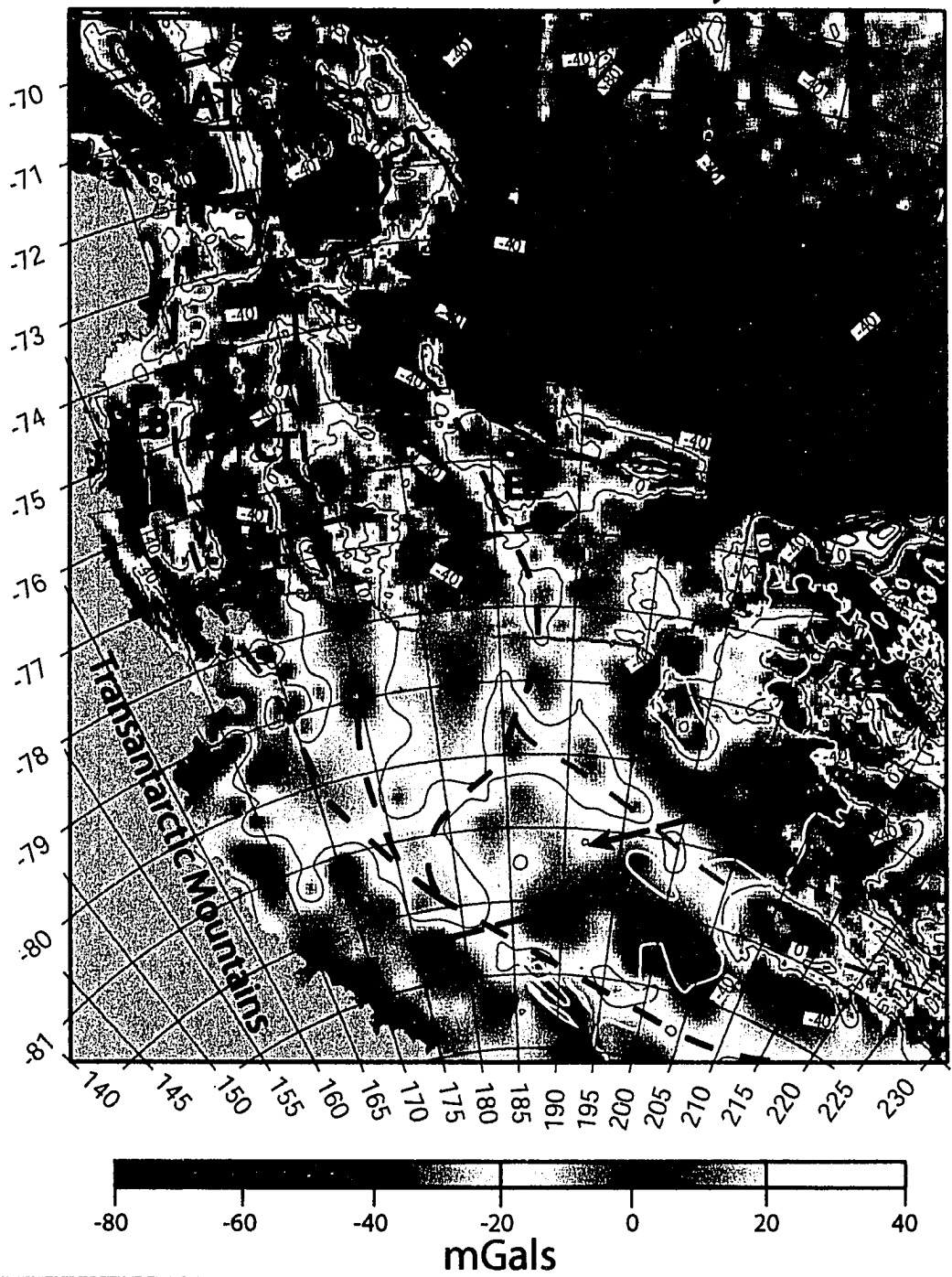
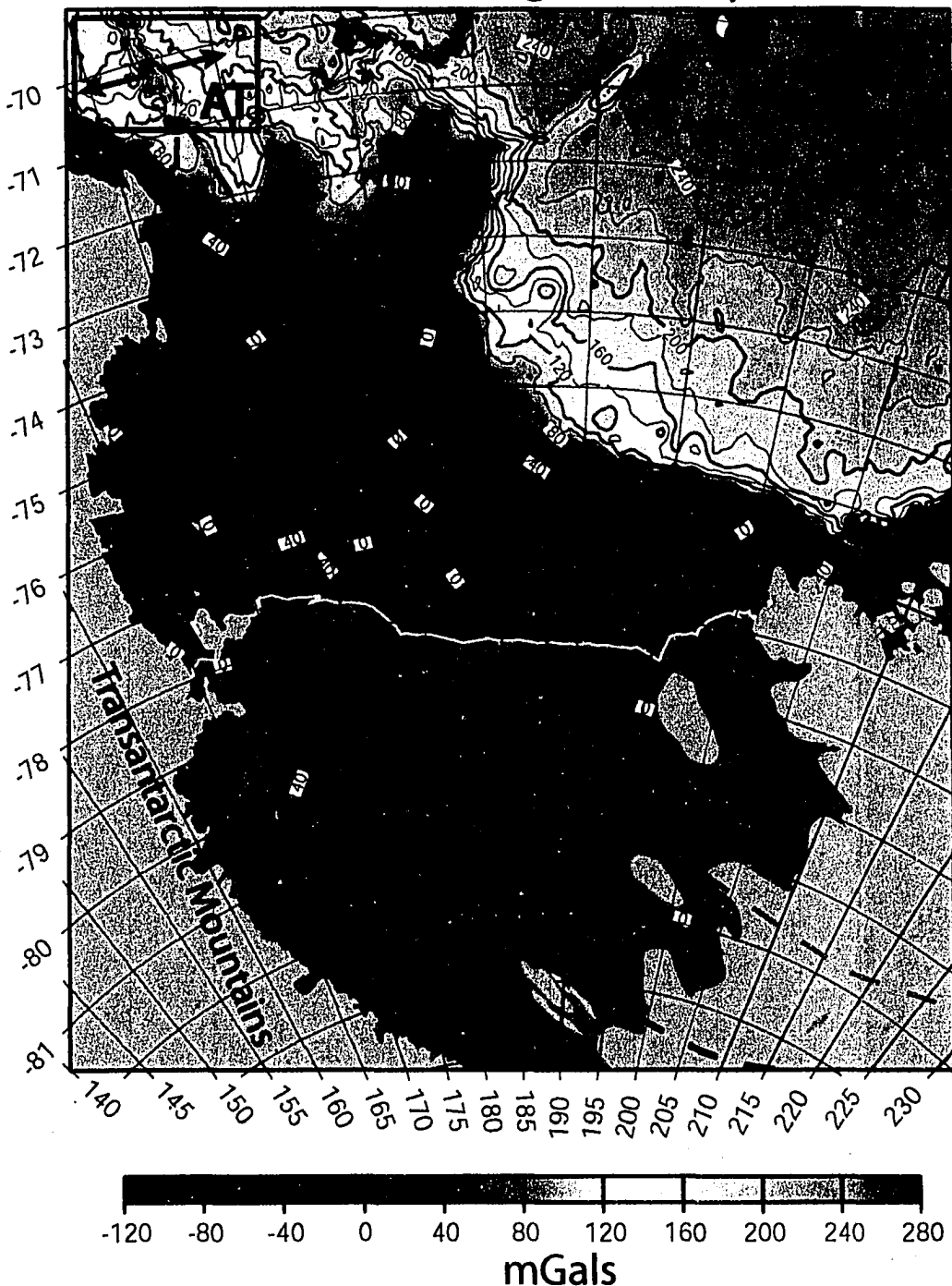


Figure 3-10: The VLB, CT and EB are characterized by bands of positive anomalies, Trough extension. Positive anomalies outlining the basins are indicated by black trend to the southeast. A possible second zone of motion into West Antarctica is c dark gray line=2000 m continental shelf break, white line=ice grounding line.

Ross Sea Bouguer Gravity



anomalies, reflecting highly extended crust, possibly resulting from Tertiary Adare
and by black dashed lines. In the southern Ross Sea the anomalies connect and then
Antarctica is outlined by the gray dashed line. Solid light gray line=Ross Ice Shelf front,
line.



Reproduced with permission of the copyright owner. Further reproduction prohibited without permission.

producing the thinnest crust (~10 km) in the Ross Sea. The positive gravity anomalies outlining the basins continue south under the ice shelf. The VLB and CT anomalies appear to merge at about 80° S and then trend to the southeast. The EB anomaly may also merge with the VLB and CT anomalies at about 81° S. However, a linear positive gravity anomaly is also interpreted to trend to the southeast from the EB anomaly trend, just north of the VLB-CT trend (Fig. 11).

The magnitude of the linear positive gravity anomalies under the ice shelf decreases to the south (Fig. 3-10). This may indicate that E-W extension became less further to the south in the Ross Sea. The southeast linear trend also follows the TAM front. Since major exhumation of the TAM was at 55 Ma [Fitzgerald, et al., 1986; Fitzgerald, 1992; Fitzgerald, et al., 2000], E-W extension in the southern Ross Sea would have run into the TAM front, which would have been a relatively strong body of thicker crust compared to the thinned Ross Sea. Therefore, rifting between East and West Antarctica would have been forced to follow the TAM front to the southeast. The linear southeast trending positive gravity anomalies may represent a transition zone from E-W extension in the northern Ross Sea to more oblique extension in the southern Ross Sea before transitioning into dextral strike-slip motion into southern Marie Byrd Land. This may have occurred in two bands, a northern band splaying from the EB and a more southern splay from the VLB and CT (Fig. 3-10).

3-5. Conclusions

The observed subsidence of the Ross Sea basins indicate extension was focused in two major episodes during the evolution of the Ross Sea Embayment. The first event commenced in Cretaceous time and was followed by an early Tertiary event, with ~100% extension for both events. All extension was completed by RSU6 time (~30 Ma) as required by the seismic stratigraphic record of RSS-2. Tertiary rifting of the Ross Sea corresponds to extension that occurred as seafloor spreading along the Eocene Adare Trough (43-26 Ma) [Cande, et al., 2000]. Pre-rift Ross Sea crust was probably an elevated feature well above sea level with thicker than normal continental crust on the order of 50 km. Cretaceous rifting extended the crust resulting in the formation of the West Antarctic Rift System. Early Tertiary extension resulted in thinning of localized sections of the crust resulting in the formation of the present-day Ross Sea basins. Post Tertiary rift thermal subsidence resulted in the necessary accommodation space for the deposition of Oligocene RSS-2 and post RSS-2 units.

A single Cretaceous extension event requires deepwater formation for unconformity RSU6 that is not consistent with the stratigraphic record at DSDP Site 270. A single Cretaceous extension event also requires that all of unit RSS-1 was deposited and deformed in the Cretaceous. This interpretation is not consistent with the stratigraphic record. Therefore, a shallow water formation for unconformity RSU6 and a two stage extension model is favored, consistent with the stratigraphic record.

The Campbell Plateau would have been attached to the Ross Sea and western MBL prior to and during Cretaceous extension. Therefore, the Campbell Plateau most likely would have been a region of elevated topography well above sea level. Cretaceous rifting would have thinned Campbell Plateau crust to ~ 25 km. In fact, present-day Campbell Plateau crust is ~ 25 km [Cook, et al., 1999]. Furthermore, the Late Cretaceous Waipounamu Erosion Surface is interpreted across the Campbell Plateau and New Zealand region [LeMasurier and Landis, 1996]. LeMasurier and Landis [1996] suggest the Waipounamu Erosion Surface and the WAES are the same erosion surface and formed at sea level. However, the results from this study indicate both erosion surfaces would have formed at significant elevation above sea level after Cretaceous extension, based on the parallel geological histories of the region.

Sea floor spreading of the Iselin Trough, north of the Ross Sea, between 80 and 55 Ma may have resulted in up to 100 km of extension in the Ross Sea [Cande and Stock, 2004]. Although the observed subsidence of Ross Sea basins study does not indicate additional extension corresponding to this event, it is possible that Iselin Trough rifting further extended the Ross Sea. Due to poor stratigraphic constraints of pre-Oligocene strata, the resolution of Ross Sea subsidence between 90 and 30 Ma is uncertain.

Better subsidence models for the Campbell Plateau are needed to further compare the tectonic histories of the Ross Sea and the New Zealand region. This will help test the hypothesis that the Campbell Plateau was an elevated region of thicker than normal continental crust prior to Cretaceous extension. Also, better subsidence

modeling of the Campbell Plateau will help to resolve the dispute of whether the Waiponamu Erosion Surface formed at sea level or is the conjugate erosion surface to the WAES, thus forming at elevation following Cretaceous rifting. Better stratigraphic control is also needed to refine the subsidence history of the Ross Sea. Constraining the age and origin of unconformity RSU6 in the Ross Sea, through future drilling, would significantly improve uncertainties in the timing of this model. Better stratigraphic constraints of both the lower and upper section of unit RSS-1 would help to improve the resolution of the subsidence model prior to 30 Ma. Finally, work needs to be done to better constrain the paleobathymetry of the unconformities in the Ross Sea. Expansion of the 1-D subsidence model into a 2-D model, applying decompaction corrections and subsidence calculations to a grid of the Ross Sea, will better determine how all the basins respond in 2-D.

Referenced Cited

- Accaino, F., G. Bohm, and G. Brancolini (2005), Analysis of Antarctic glaciations by seismic reflection and refraction tomography, *Mar. Geol.*, 126, 145-154.
- Allen, P. A., and J. R. Allen (2005), *Basin Analysis: Principles and Applications*, Blackwell Scientific.
- Anderson, J. B., and L. R. Bartek (1992), Cenozoic glacial history of the Ross Sea revealed by intermediate resolution seismic reflection data combined with drill site information, in *The Antarctic Paleoenvironment: A perspective on global change*, edited by J. P. Kennett and D. A. Warnke, pp. 231-263, Amer. Geophys. Union, Washington, D.C.
- ANTOSTRAT (1995), Seismic Stratigraphic Atlas of the Ross Sea, in *Geology and Seismic Stratigraphy of the Antarctic Margin*, edited by A. K. Cooper, Barker, P. F., Brancolini, G., p. 22 plates, American Geophysical Union, Washington, D.C.
- Barrett, P. J., M. Massimo Sarti, and S. Wise (Eds.) (2000), *Studies from the Cape Roberts Project, Ross Sea, Antarctica: Initial report on CRP-3*, 209 pp., Terra Antarctica Pub., Siena.
- Behrendt, J. C., and A. K. Cooper (1991), Evidence of rapid Cenozoic uplift of the shoulder escarpment of the Cenozoic West Antarctica Rift System and speculation on possible climate forcing, *Geology*, 19, 315-319.
- Bialas, R. W., W. R. Buck, M. Studinger, and P. G. Fitzgerald (2005), Extending thickened continental crust: Implications for the Transantarctic Mountains and West Antarctic Rift System, *EOS Trans. AGU*, 86, Fall Meet. Suppl., Abstract T43B-1407.
- Bradshaw, J. D. (1989), Cretaceous geotectonic patterns in the New Zealand region, *Tectonics*, 8, 803-820.
- Brancolini, G., A. K. Cooper, and F. Coren (1995), Seismic Facies and Glacial History in the Western Ross Sea (Antarctica), in *Geology and seismic stratigraphy of the Antarctic margin*, edited by A. K. Cooper, P. F. Barker and G. Brancolini, pp. 209-234, Amer. Geophys. Union, Washington, D. C.
- Busetti, M., and A. K. Cooper (1994), Possible ages and origins of unconformity U6 in the Ross Sea, Antarctica, *Terra Antarctica*, 1, 341-343.

Busetti, M., and I. Zayat (1994), Ross Sea Regional Working Group, Distribution of Seismic Units in the Ross Sea, *Terra Antarctica*, 1, 345-348.

Cande, S. C., C. A. Raymond, J. M. Stock, and W. F. Haxbe (1995), Geophysics of the Pitman Fracture Zone and Pacific-Antarctic plate motion during the Cenozoic, *Science*, 270, 947-951.

Cande, S. C., and J. M. Stock (2004), Constraints on Late Cretaceous and Cenozoic Extension in the Ross Sea from the Southwest Pacific Plate Circuit, *EOS Trans. AGU*, 85, Fall Meet. Suppl., Abstract T14A-03.

Cande, S. C., J. M. Stock, D. Müller, and T. Ishihara (2000), Cenozoic Motion between East and West Antarctica, *Nature*, 404, 145-150.

Compton, J. S. (1991), Porosity and burial history of siliceous rocks from the Monterey and Sisquoc Formations, Point Pedernales area, California, *American Bulletin*, 103, 625-636.

Cook, R. A., R. Sutherland, and H. Zhu (1999), Cretaceous-Cenozoic Geology and Petroleum Systems of the Great South Basin, New Zealand, *Institute of Geological and Nuclear Sciences Monograph*, 20, 188.

Cooper, A. K., P. F. Barker, and G. Brancolini (Eds.) (1995), *Geology and Seismic Stratigraphy of the Antarctic Margin, atlas, CD-ROMs*, 301 pp., Amer. Geophys. Union, Washington, D.C.

Cooper, A. K., F. J. Davey, and J. C. Behrendt (1987), Seismic stratigraphy and structure of the Victoria Land Basin, western Ross Sea, Antarctica, in *The Antarctic Continental Margin: Geology and Geophysics of the Western Ross Sea*, edited by A. K. Cooper and F. J. Davey, pp. 27-65, Circum-Pacific Council for Energy and Mineral Resources, Houston, Texas.

Davey, F. J., and G. Brancolini (1995), The Late Mesozoic and Cenozoic structural setting of the Ross Sea region, in *Geology and Seismic Stratigraphy of the Antarctic Margin*, edited by A. K. Cooper, P. F. Barker and G. Brancolini, pp. 167-182, Amer. Geophys. Union, Washington, D.C.

Decesari, R. C., B. P. Luyendyk, L. R. Bartek, C. C. Sorlien, D. S. Wilson, J. B. Diebold, and S. E. Hopkins (2004), Ice shelf drill sites proposed to study Pre-Late Oligocene climate and tectonic history, Coulman High, Southwestern Ross Sea, Antarctica, *EOS Trans. AGU*, 85, Fall Meet. Suppl., Abstract T11A-1244.

Decesari, R. C., C. C. Sorlien, B. P. Luyendyk, L. R. Bartek, J. B. Diebold, and D. S. Wilson (2003), Tectonic evolution of the Coulman High and Central Trough along the Ross Ice Shelf, Southwestern Ross Sea, Antarctica, *EOS Trans. AGU*, 84, Fall Meeting Suppl. Abstract T12A-0447.

De Santis, L., J. B. Anderson, G. Brancolini, and I. Zayatz (1995), Seismic record of Late Oligocene through Miocene glaciation on the central and eastern continental shelf of the Ross Sea, in *Geology and seismic stratigraphy of the Antarctic margin*, edited by A. K. Cooper, P. F. Barker and G. Brancolini, pp. 235-260, Amer. Geophys. Union, Washington, D. C.

De Santis, L., S. Prato, G. Brancolini, M. Lovo, and L. Torelli (1999), The Eastern Ross Sea continental shelf during the Cenozoic: Implications for the West Antarctic ice sheet development, *Global Plan. Ch.*, 23, 173-196.

Fitzgerald, P. G. (1992), The Transantarctic Mountains of Southern Victoria Land: The application of apatite fission track analysis to a rift shoulder uplift, *Tectonics*, 11, 634-662.

Fitzgerald, P. G., and S. L. Baldwin (1997), Detachment Fault Model for the Evolution of the Ross Embayment, in *The Antarctic Region: Geological Evolution and Processes*, edited by C. A. Ricci, pp. 555-564, Terra Antarctica Pub., Siena.

Fitzgerald, P. G., S. L. Baldwin, K. A. Farley, and P. B. O'Sullivan (2000), Landscape evolution and exhumation of the Transantarctic Mountains in the Kukri Hills of southern Victoria Land: Constraints from Apatite Fission Track Thermochronology and (U-Th)/He dating of apatites, *EOS Trans. AGU*, 81, F1102.

Fitzgerald, P. G., M. Sandiford, P. J. Barrett, and A. J. W. Gleadow (1986), Asymmetric extension associated with uplift and subsidence in the Transantarctic Mountains and the Ross Sea Embayment, *Earth Planet. Sci. Lett.*, 81, 67-78.

Hamilton, R. J., B. P. Luyendyk, C. C. Sorlien, and L. R. Bartek (2001), Cenozoic Tectonics of the Cape Roberts Rift Basin, and Transantarctic Mountains Front, Southwestern Ross Sea, Antarctica, *Tectonics*, 20, 325-342.

Hayes, D. E., and L. A. Frakes (1975), General synthesis: Deep Sea Drilling Project 28, in *Initial Reports of the Deep Sea Drilling Project, Leg 28*, edited by D. E. Hayes and L. A. Frakes, pp. 919-942, U.S. Government Printing Office, Washington, D.C.

Hayes, D. E., L. A. Frakes, and S. S. Party (1975), Sites 270, 271, 272, in *Initial Reports of the Deep Sea Drilling Project, Leg 28*, edited by D. E. Hayes and L. A. Frakes, pp. 211-234.

Hinz, K., and M. Block (1984), Results of geophysical investigations in the Weddell Sea and in the Ross Sea, Antarctica, paper presented at 11th World Petrol. Congress, Wiley, London.

Jarvis, G. T., and D. P. McKenzie (1980), The development of sedimentary basins with finite extension rates, *Earth Planet. Sci. Lett.*, 48, 42-52.

Karner, G. D., M. Studinger, and R. E. Bell (2005), Gravity anomalies of sedimentary basins and their mechanical implications: Application to the Ross Sea basins, West Antarctica, *Earth Planet. Sci. Lett.*, 235, 577-596.

Kominz, M. A., K. G. Miller, and J. V. Browning (1998), Long-term and short-term global Cenozoic sea level estimates, *Geology*, 26, 311-314.

Lawver, L. A., and L. M. Gahagan (1994), Constraints on timing of extension in the Ross Sea region, *Terra Antarctica*, 1, 545-552.

Leckie, R. M., and P. N. Webb (1986), Late Paleogene and early Neogene foraminifers of Deep Sea Drilling Project Site 270, Ross Sea, Antarctica, in *Initial Reports of the Deep Sea Drilling Project*, edited by J. P. Kennett and C. C. von der Borch, pp. 1093-1120, Washington, D. C.

LeMasurier, W. E., and C. A. Landis (1996), Mantle plume activity recorded by low relief erosion surfaces in West Antarctica and New Zealand, *Geol. Soc. Am. Bull.*, 108, 1450-1466.

LeMasurier, W. E., and D. C. Rex (1990), Late Cenozoic volcanism on the Antarctic Plate: An overview, in *Volcanoes of the Antarctic Plate and southern oceans*, edited by W. E. LeMasurier and J. W. Thompson, pp. 1-17, Amer. Geophys. Union, Washington, D. C.

Luyendyk, B. P., C. H. Smith, and G. Druivenga (2003), Gravity measurements on King Edward VII Peninsula, Marie Byrd Land, West Antarctica, during GANOVEX VII, *Geolog. Jahrb.*, B 95, 101-126.

Luyendyk, B. P., C. C. Sorlien, D. S. Wilson, L. R. Bartek, and C. H. Siddoway (2001), Structural and tectonic evolution of the Ross Sea rift in the Cape Colbeck region, Eastern Ross Sea, Antarctica, *Tectonics*, 20, 933-958.

Luyendyk, B. P., D. S. Wilson, and R. De Cesari (2002), New Maps of Gravity and Bedrock-Bathymetry of the Ross Sea Sector of Antarctica, *EOS, Transactions of the American Geophysical Union, Fall Meeting Supplement*, 83, F1357.

McKenzie, D. (1978), Some remarks on the development of sedimentary basins, *Earth Planet. Sci. Lett.*, 40, 25-32.

Miller, K. G., M. A. Kominz, J. V. Browning, J. D. Wright, G. S. Mountain, M. E. Katz, P. J. Sugarman, B. S. Cramer, N. Christie-Blick, and S. F. Pekar (2005), The Phanerozoic Record of Global Sea-Level Change, *Science*, 310, 1293-1298.

Molnar, P., T. Atwater, J. Mammerickx, and S. Smith (1975), Magnetic anomalies, bathymetry, and the tectonic evolution of the south Pacific since the Late Cretaceous, *Geophys. J. R. Astron. Soc.*, 40, 383-420.

Richard, S. M., C. H. Smith, D. L. Kimbrough, P. G. Fitzgerald, B. P. Luyendyk, and M. O. McWilliams (1994), Cooling history of the northern Ford Ranges, Marie Byrd Land, West Antarctica, *Tectonics*, 13, 837-857.

Sclater, J. G., and P. A. F. Christie (1980), Continental stretching: an explanation of the post mid-Cretaceous subsidence of the central North Sea basin, *J. Geophys. Res.*, 85, 3711-3739.

Siddoway, C. S., S. L. Baldwin, P. G. Fitzgerald, C. M. Fanning, and B. P. Luyendyk (2004), Ross Sea mylonites and the timing of continental extension between East and West Antarctica, *Geology*, 32, 57-60.

Smith, C. H. (1995), Cordierite gneiss and high temperature metamorphism in the Fosdick Mountains, West Antarctica, with implications for breakup processes in the Pacific sector of the Mesozoic Gondwana margin, Ph.D. dissertation thesis, 313 pp, University of California, Santa Barbara.

Stock, J. M., and S. C. Cande (2002), Tectonic History of Antarctic Seafloor in the Australia-New Zealand-South Pacific Sector: Implications for Antarctic Continental Tectonics, in *Antarctica at the Close of a Millennium: Proceedings of the 8th International Symposium on Antarctic Earth Sciences, Wellington, 1999*, edited by J.

A. Gamble, D. N. B. Skinner and S. Henrys, pp. 251-259, The Royal Society of New Zealand, Wellington, New Zealand.

Stock, J. M., and S. C. Cande (1999), Tectonic history of Antarctic seafloor in the Australia-New Zealand-South Pacific sector: Implications for Antarctic continental tectonics (abstract), paper presented at 8th International Symposium on Antarctic Earth Sciences, July 5-9, 1999, Victoria Univ., Wellington, New Zealand.

Stock, J. M., and P. Molnar (1987), Revised early Tertiary history of plate motion in the southwest Pacific, *Nature*, 325, 495-499.

Studinger, M., R. E. Bell, W. R. Buck, G. Karner, and D. Blankenship (2004), Sub-ice geology inland of the Transantarctic Mountains in light of new aerogeophysical data, *Earth Planet. Sci. Lett.*, 220, 391-408.

Tesssensohn, F., and G. Worner (1991), The Ross Sea rift system, Antarctica: structure, evolution, and analogs, in *Geological evolution of Antarctica*, edited by M. R. A. Thompson, J. A. Crame and J. W. Thompson, pp. 273-278, Cambridge Univ. Press, Cambridge, Mass.

Trey, H., A. K. Cooper, G. Pellis, B. Della Vedova, G. Cochrane, G. Brancolini, and J. Makris (1999), Transect across the West Antarctic rift system in the Ross Sea, Antarctica, *Tectonophysics*, 301, 61-74.



Chapter 4

The Tectonic Framework of the Coulman High and Central Trough; Implications for Ice Shelf Drill Sites Proposed to Study pre-Oligocene Ross Sea Climate and Tectonic History

Abstract:

A dense grid of new seismic data along the C-19 sector of the Ross Ice Shelf, spanning the Coulman High and part of the Central Trough, provides a unique location for studying the tectonic and climate history of the Ross Sea. Interpretations of seismic data show faulted basement, filled with synrift sedimentary units interpreted as Cretaceous in age, capped by an angular unconformity (RSU7). Another synrift unit overlies RSU7 and is capped by an angular unconformity (RSU6) and late Oligocene-early Miocene glacial-marine strata. The synrift strata are interpreted to indicate two episodes of extension in the Ross Sea; one in the Cretaceous, and one in the Eocene resulting from spreading of the Adare Trough. Gravity and magnetic data were also collected throughout the region. Gravity data shows a strong Moho signal, indicating that the bulk of the Coulman High is underlain by thick crust, while the Central Trough is underlain by thinned crust. New seismic data now covers several high amplitude magnetic anomalies previously

interpreted as Cenozoic volcanic centers extending to the seafloor. Seismic data suggests this is not the case and the magnetic anomalies may result from volcanic activity during Cretaceous and or Eocene extension of the Ross Sea.

The C-19 site provides one of the best locations in the Ross Sea for sampling pre-Oligocene strata using the Ross Ice Shelf as a drilling platform. In 2008 the ice shelf will have advanced ~3.5 km to the north, covering the southern section of the C-19 survey grid. Drill sites have been selected along the ice shelf front and are designed to target a complete section of pre-Oligocene Ross Sea strata along a transect of E-W core holes. Drilling here may obtain samples that record the Eocene-Oligocene global climate cooling event. Recovery of Oligocene and Miocene sediments will also provide a climate record and test for climate oscillations. Drilling will test the hypothesis that Eocene age strata is present in the Ross Sea and records the Adare Trough extensional event as well as possibly sample sediment of Paleocene age. Drilling here may also recover stratigraphy as old as Cretaceous in age that has never been sampled in the Ross Sea and obtain samples of Ross Sea basement rocks that will help constrain the timing and magnitude of extension in the Ross Sea.

4-1. Introduction

Piecing together the tectonic history of the Ross Sea Rift has been problematic because of the lack of data coverage across the region. The majority of what is known about the tectonic history of the Ross Sea comes from work focused primarily on the Victoria Land Basin (VLB) and the Transantarctic Mountains (TAM) in the western

Ross Sea. Several studies have worked on the tectonic history of the eastern portion of the rift [Luyendyk, et al., 2001; Luyendyk, et al., 2003]. Even so, the relationship between the eastern and western Ross Sea is poorly understood. Since the West Antarctic Rift System (WARS) [LeMasurier and Rex, 1990; Behrendt, et al., 1991] divides the Antarctic continent into East and West Antarctica, understanding the development of the entire Ross Sea is crucial for comprehending the global implications of the Antarctic plate tectonic system.

The tectonic history of the eastern WARS and its relation the western side has remained largely unknown. This study uses newly acquired geophysical data, to investigate the tectonic framework of the Coulman High and Central Trough sectors of the southwest Ross Sea. The tectonic history of this region is important for understanding the WARS and for providing links between the tectonic history of the eastern and western Ross Sea (Fig. 4-1). This study also proposes drill sites along the Ross Ice Shelf front that will sample pre-Oligocene strata, designed to constrain the timing and magnitude of major tectonic events of the Ross Sea. Drilling here will also help to constrain the climatic evolution of the Antarctic climate since the Cretaceous.

4-2. Geophysical Data

A marine geophysical survey was conducted along the Ross Ice Shelf front during RVIB Nathaniel B. Palmer cruises 03-01 (NBP-0301) and 03-06 (NBP-0306). Surveys were located in regions where large sections of the ice shelf have recently broken off, exposing previously unexplored seafloor [Decesari, et al., 2003;

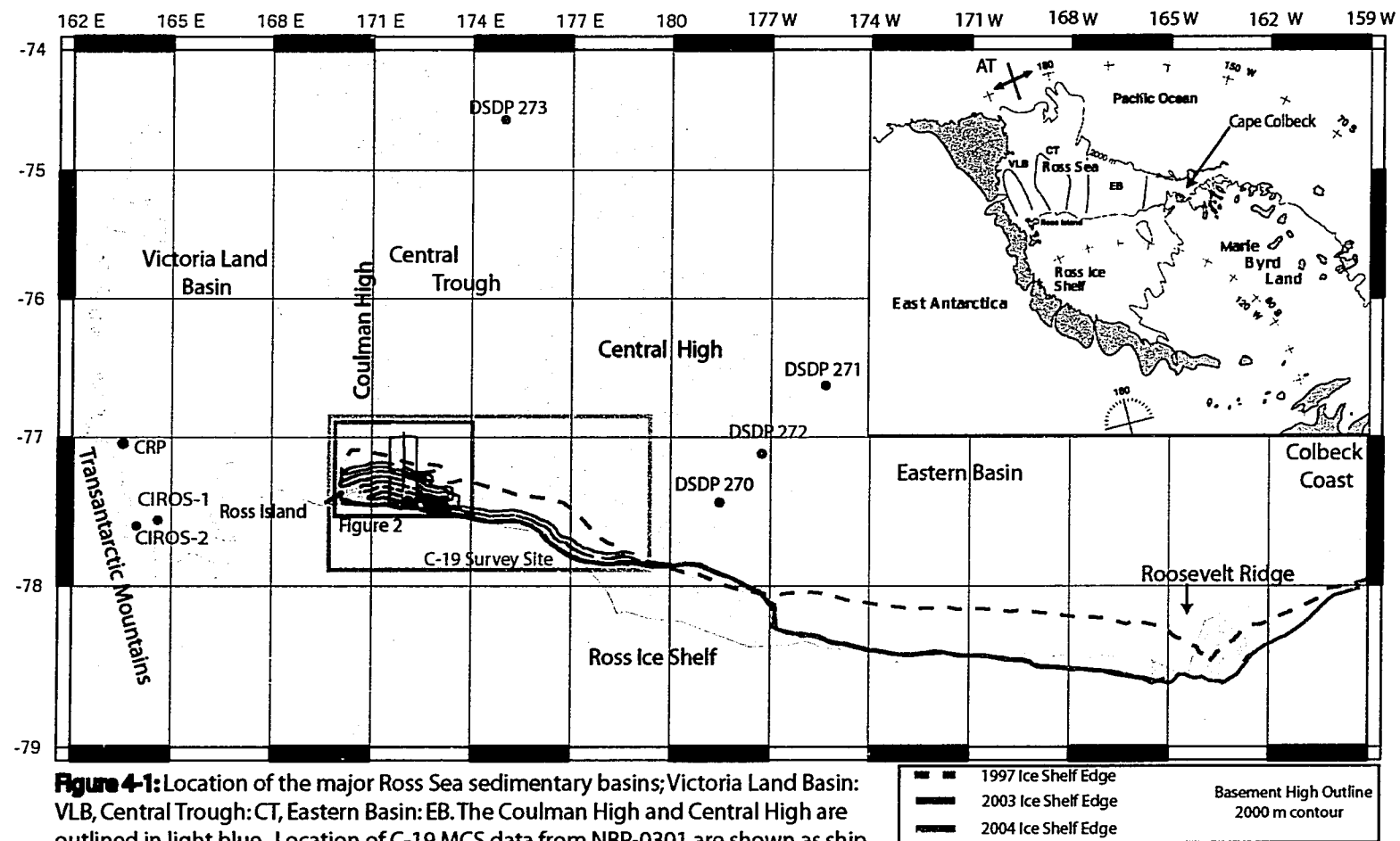
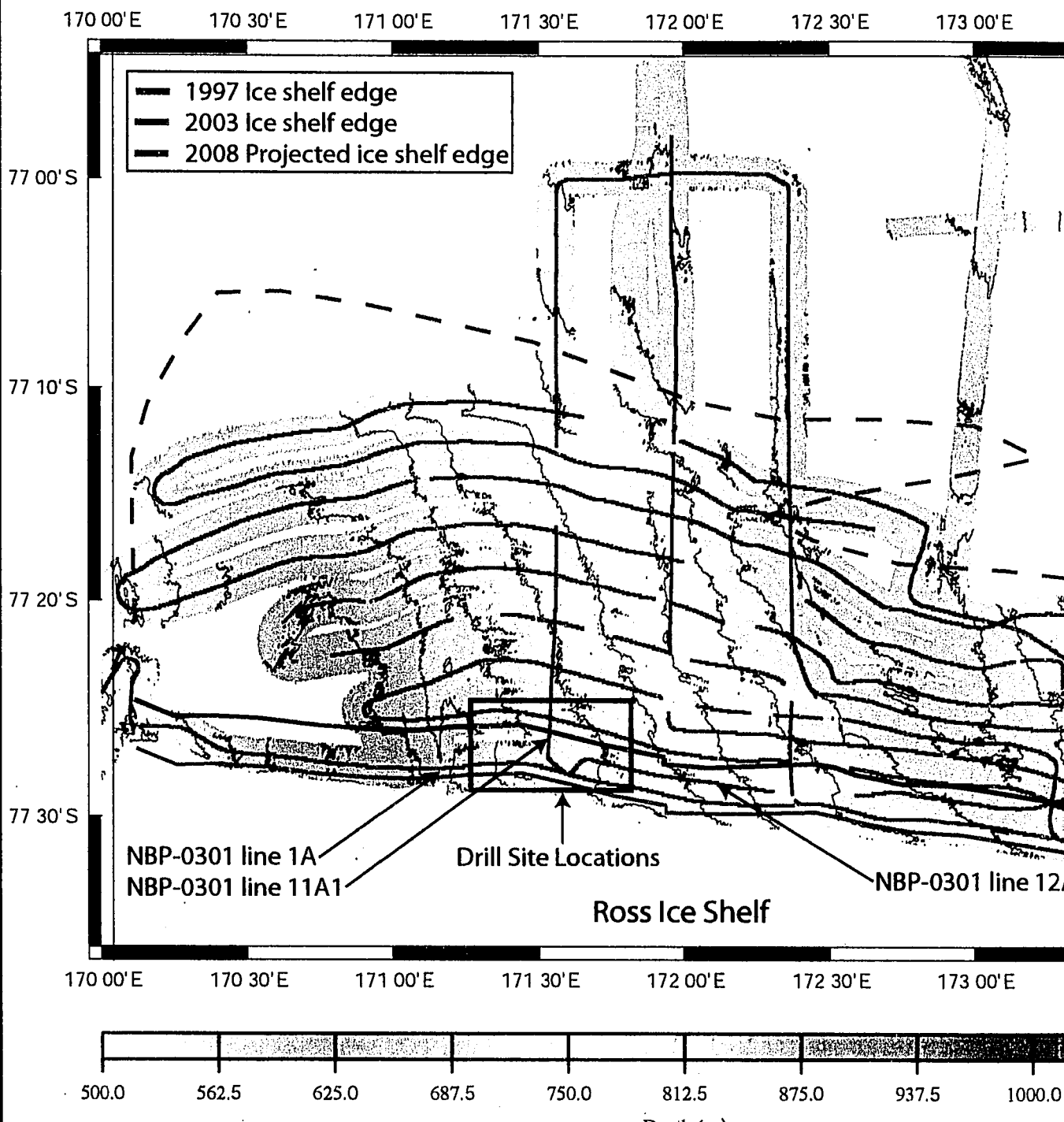
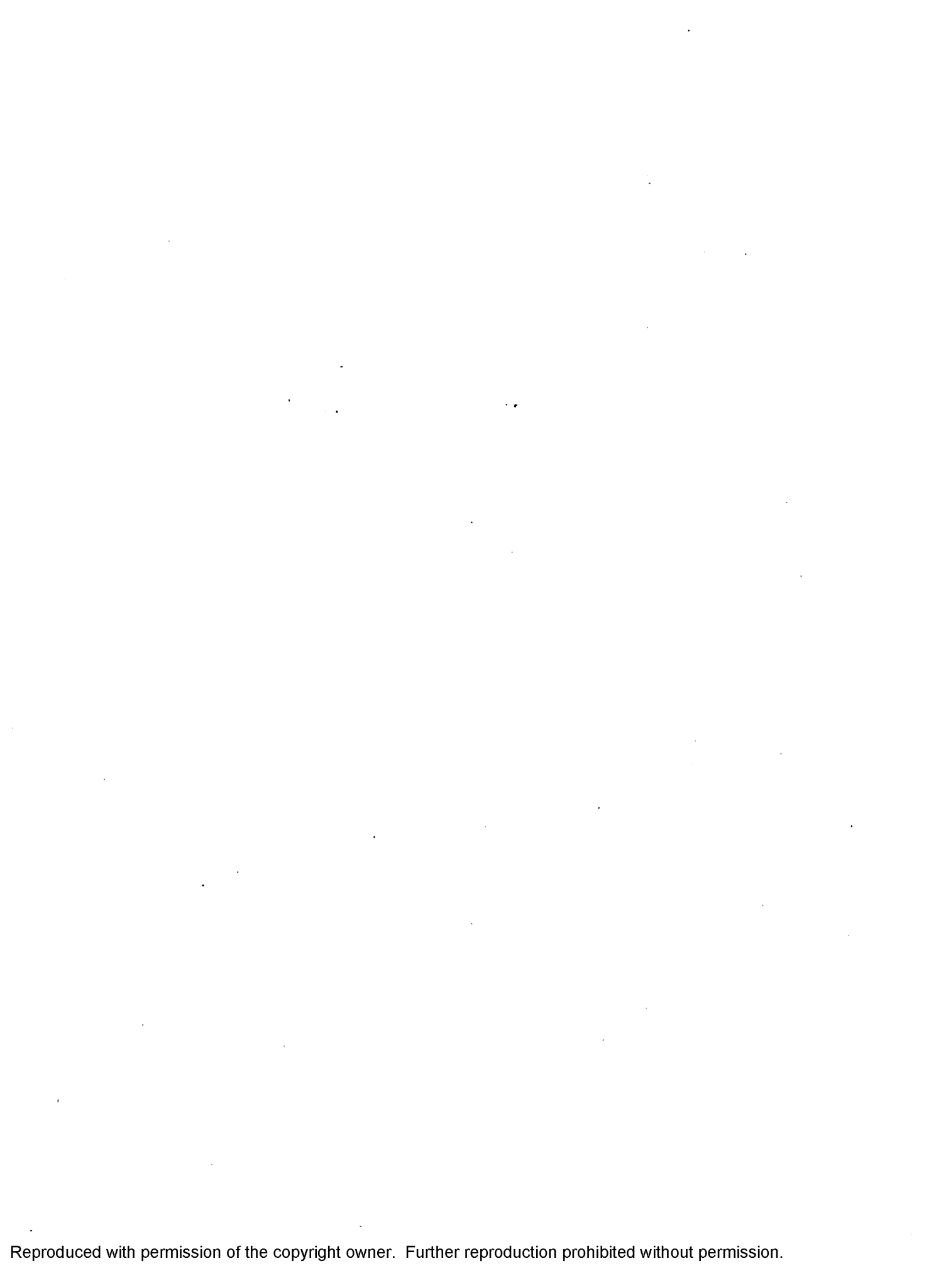


Figure 4-1: Location of the major Ross Sea sedimentary basins; Victoria Land Basin: VLB, Central Trough: CT, Eastern Basin: EB. The Coulman High and Central High are outlined in light blue. Location of C-19 MCS data from NBP-0301 are shown as ship tracks (black lines). The C-19 survey site is ~90 km NE from McMurdo Station on Ross Island and is located in a region where the C-19 iceberg broke off from the Ross Ice Shelf in 2002. Red dashed line indicates the ice shelf location in 1997. Blue and green lines represent the ice shelf location in 2003 and 2004 respectively. Inset box: The Ross Sea Region. AT=Adare Trough showing extinct spreading center.

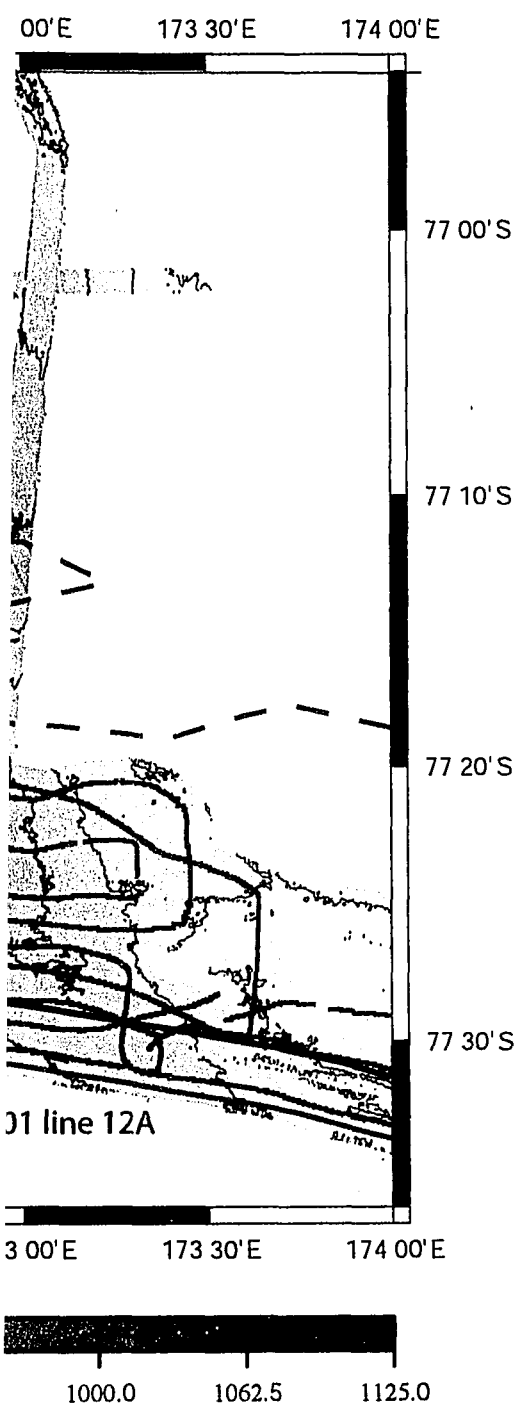
C-19 Multibeam Bathymetry and MCS Basemap





Reproduced with permission of the copyright owner. Further reproduction prohibited without permission.

map



Drill Site Locations

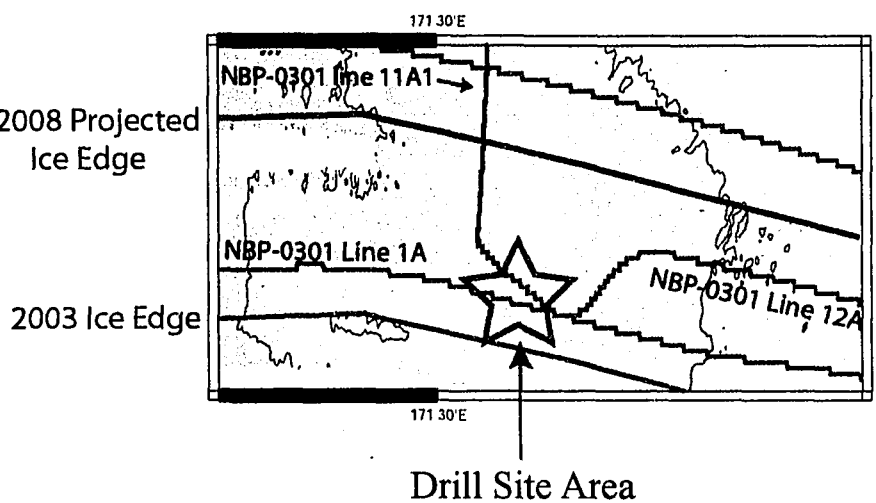


Figure 4-2: The Coulman High sector of the C-19 site. NBP-0301 MCS data is superimposed on multibeam seafloor bathymetry. Water depth ranges from ~600 m to ~900 m. The general trend of the seafloor topography is deepening to the west. Three lines have been targeted for potential drill sites (see boxed area and inset). NBP-0301 lines 1A0, 11A1 and 12A are directly north of the 2003 Ross Ice Shelf (blue line). Because the ice shelf is advancing at ~700 m/yr, these lines will be covered by 2008 (purple line). Water depths at the proposed drill sites are ~800m.



Decesari, et al., 2004]. The surveys were conducted under the premise that the ice sheet, advancing at ~ 1000 m/year, will in time cover the survey sites, thereby allowing drilling into the mapped seabed from the ice shelf (Fig. 4-2). NBP-0301 collected 2,253 km of new multichannel seismic reflection (MCS) data and 2,500 km of single channel (SCS) reflection data. A detailed survey grid was completed in the western Ross Sea where giant iceberg C-19 broke off the ice shelf in 2002. This site is adjacent to Ross Island, covering ~3,600 km², and spans the structural provinces of the east flank of the Victoria Land Basin (VLB), across the Coulman High and into the Central Trough (CT) (Fig. 4-1 & 4-2). The grid pattern consisted of a series of east-west profiles along strike and several north-south dip lines that also doubled as tie lines to existing seismic data in the region. Line spacing was approximately 2 km. Data acquisition and processing were completed using methods outlined in dissertation Chapter 2. (Appendix 1 & 2).

4-3. Interpretations and Observations

4-3.1. Correlation and Identification of Seismic Sequences

Seismic data at C-19 was tied to DSDP Site 270, in the eastern Ross Sea and to the CRP drill sites in the western Ross Sea (dissertation chapter 2) [Decesari, et al., 2003; Decesari, et al., 2004]. Unconformities RSU5 (top of RSS-2) and RSU6 were identified and correlated to DSDP Site 270 and CRP [Decesari, et al., 2004]. Units below unconformity RSU6 were identified based on comparisons of reflection characteristics with existing interpretations in the eastern Ross Sea [Luyendyk, et al.,

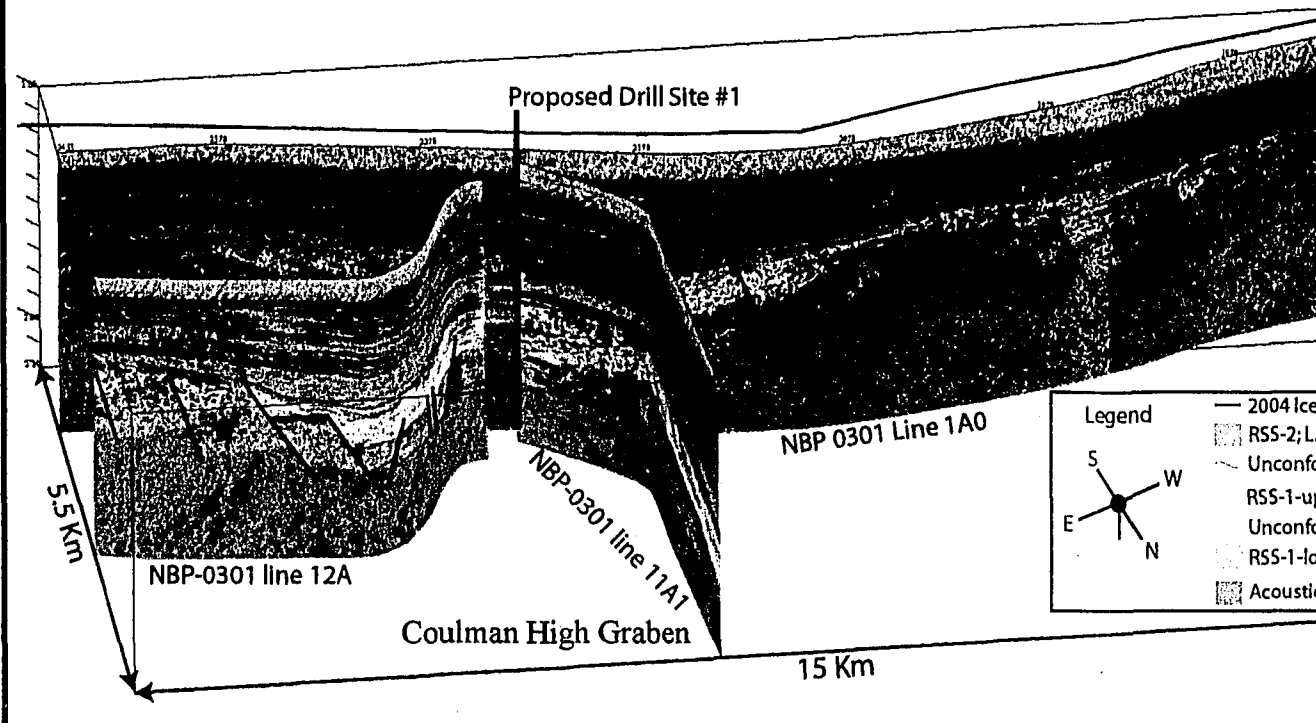
2001] and mapped throughout the C-19 site. Stratigraphy mapped at the C-19 site was also tied to existing interpretations in the Central Trough whenever possible.

4-3.2. Structure within the Seismic Stratigraphy; Acoustic Basement to Seafloor

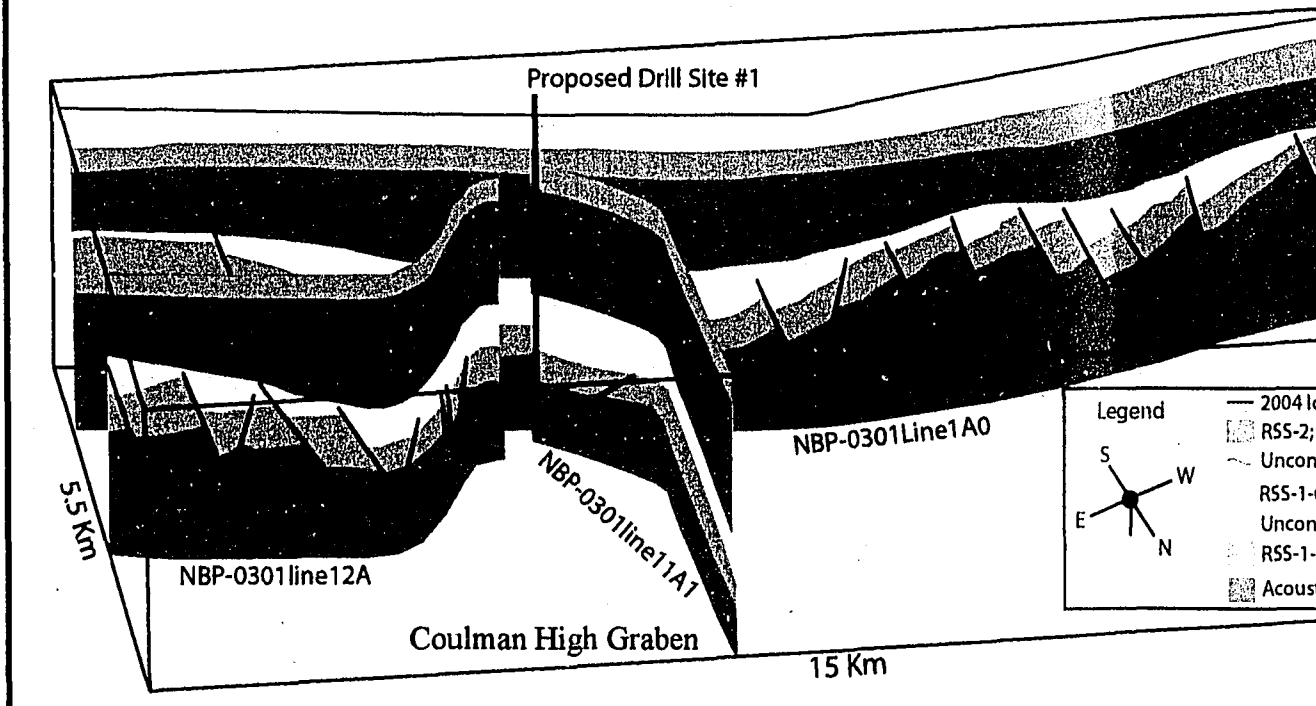
Although it is difficult to image acoustic basement throughout the C-19 survey site, low amplitude and long wavelength (low frequency) reflections are interpreted to represent the top of the Coulman High basement structure (Fig. 4-3 & 4-4). The acoustic basement is interpreted as faulted into tilted blocks forming N-S trending horst and half-grabens, approximately 0.5 km in width. A larger north-south trending graben is interpreted within the Coulman High basement and is called the Coulman High Graben (CHG). The CHG is ~20 km wide in the northern sector of the C-19 survey and narrows to the south becoming ~5 km along NBP-0301 line 1A0 (Fig. 4-3). The CHG extends north through the survey for ~50 km, past the bounds of the seismic grid. The graben is bounded by a large north-south trending normal separation faults, with a series of smaller normal faults forming tilted blocks and smaller horst and grabens within the CHG (Fig. 4-3 & 4-4). Stratigraphic sequences within the graben thicken.

Half-grabens are interpreted within the acoustic basement. Infilling the half-grabens is a highly disrupted and dipping sedimentary layer, typical of synrift deposition. This unit is interpreted as RSS-1-lower based on similarities with the RSS-1-lower unit in the eastern Ross Sea [Luyendyk, et al., 2001]. Cooper, et al. [1987] interprets half-grabens within basement elsewhere in the western Ross Sea and

a) Seismic Interpretations at Proposed Drill Sites



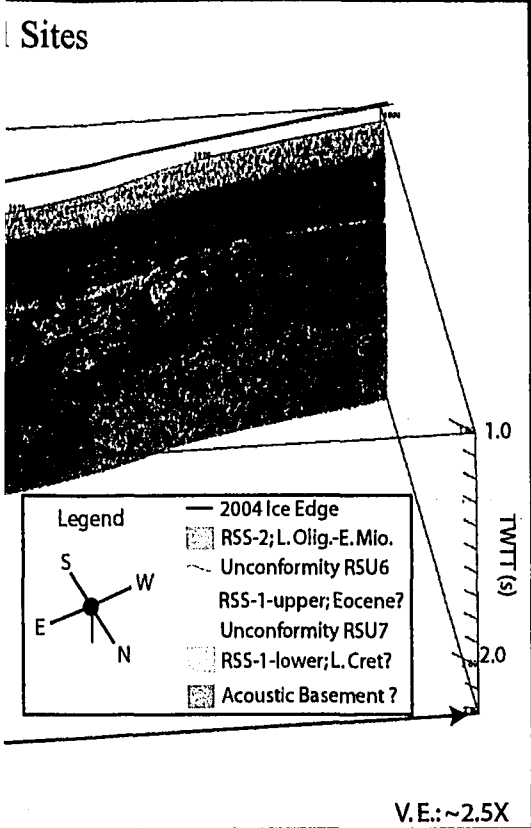
b) Stratigraphic and Structural Model





Reproduced with permission of the copyright owner. Further reproduction prohibited without permission.

Sites



lel

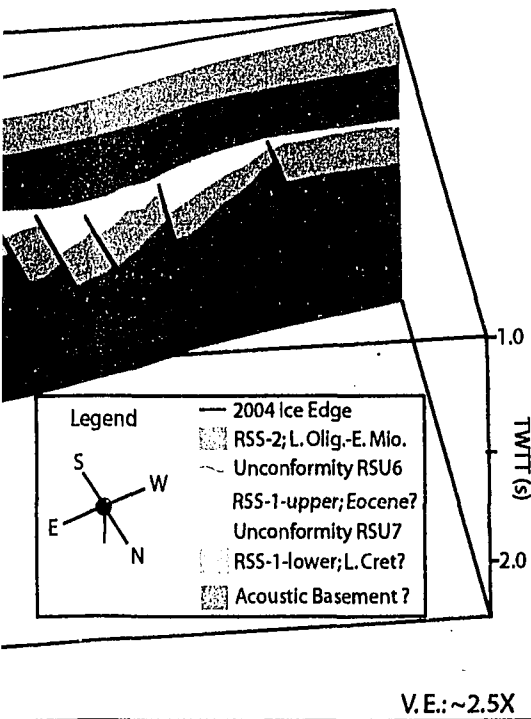


Figure 4-3: a) 3-D seismic section in front of the Ross Ice Shelf looking to the south. The basement is faulted into tilted blocks, filled with synrift sediments (RSS-1-lower; orange) and capped by an angular unconformity (RSU7). Another synrift unit, RSS-1-upper (yellow; Eocene?), overlies RSS-1-lower. Capping this unit is an angular unconformity (RSU6). Overlying are glacial-marine sediments of the RSS-2 sequence. This stratigraphy is characteristic of the C-19 site. b) 3-D model of C-19 faulting and stratigraphy. The proposed drill sites are along these three seismic lines in the Coulman High Graben. Location #1 offers the best potential for recovering a complete section of pre-Oligocene strata, including basement.

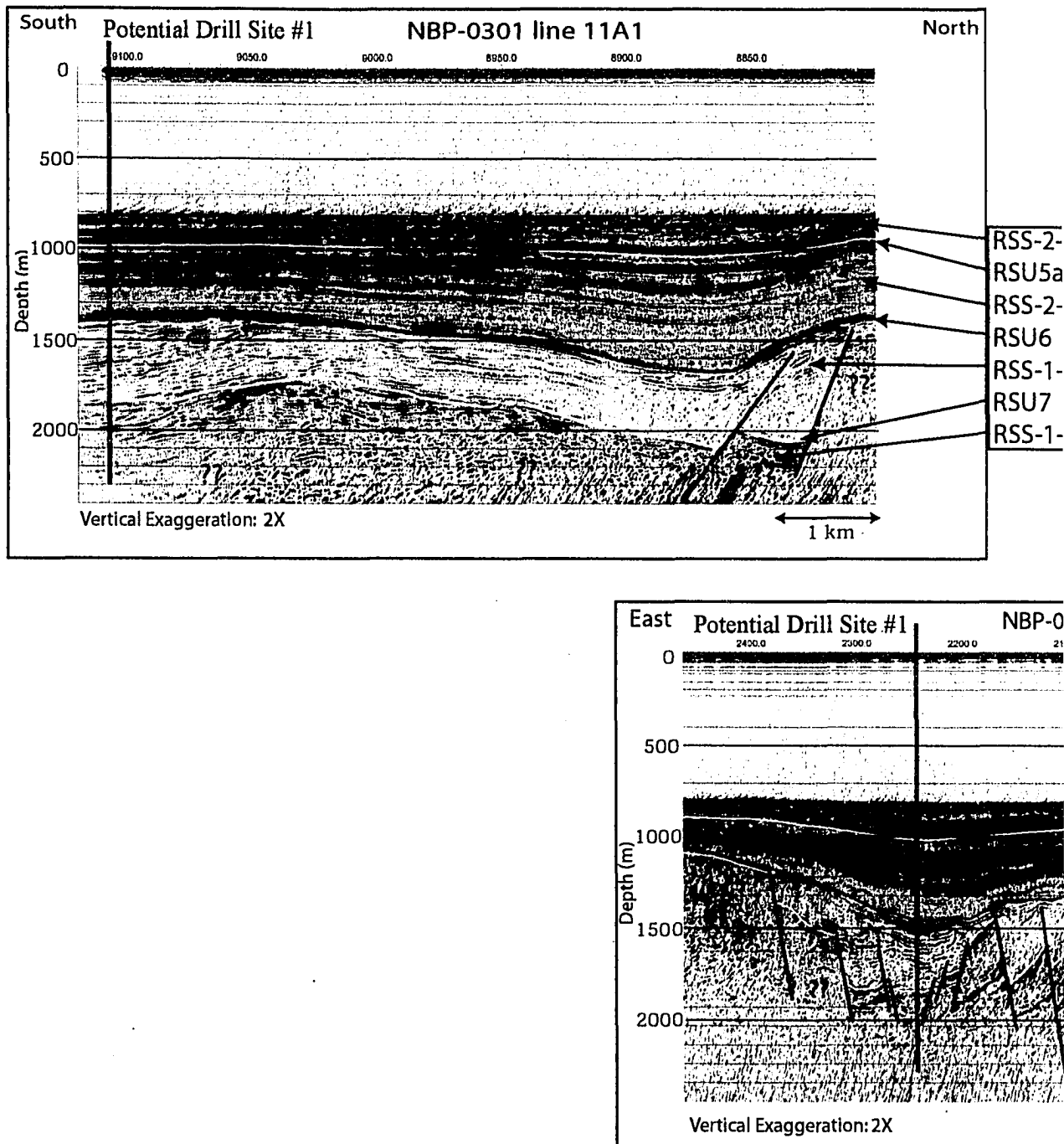
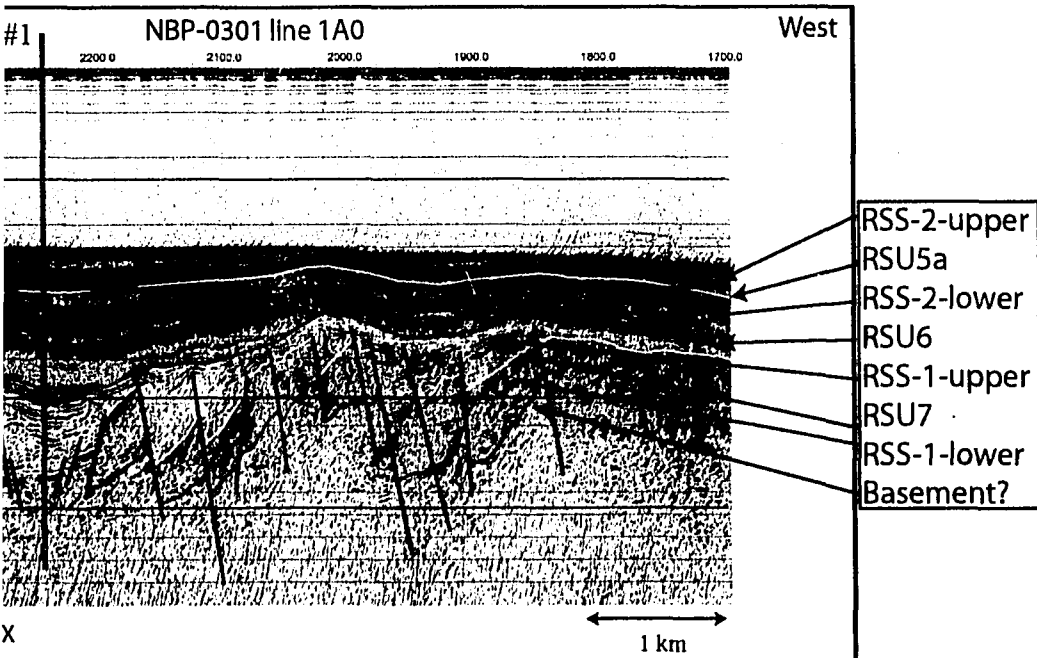
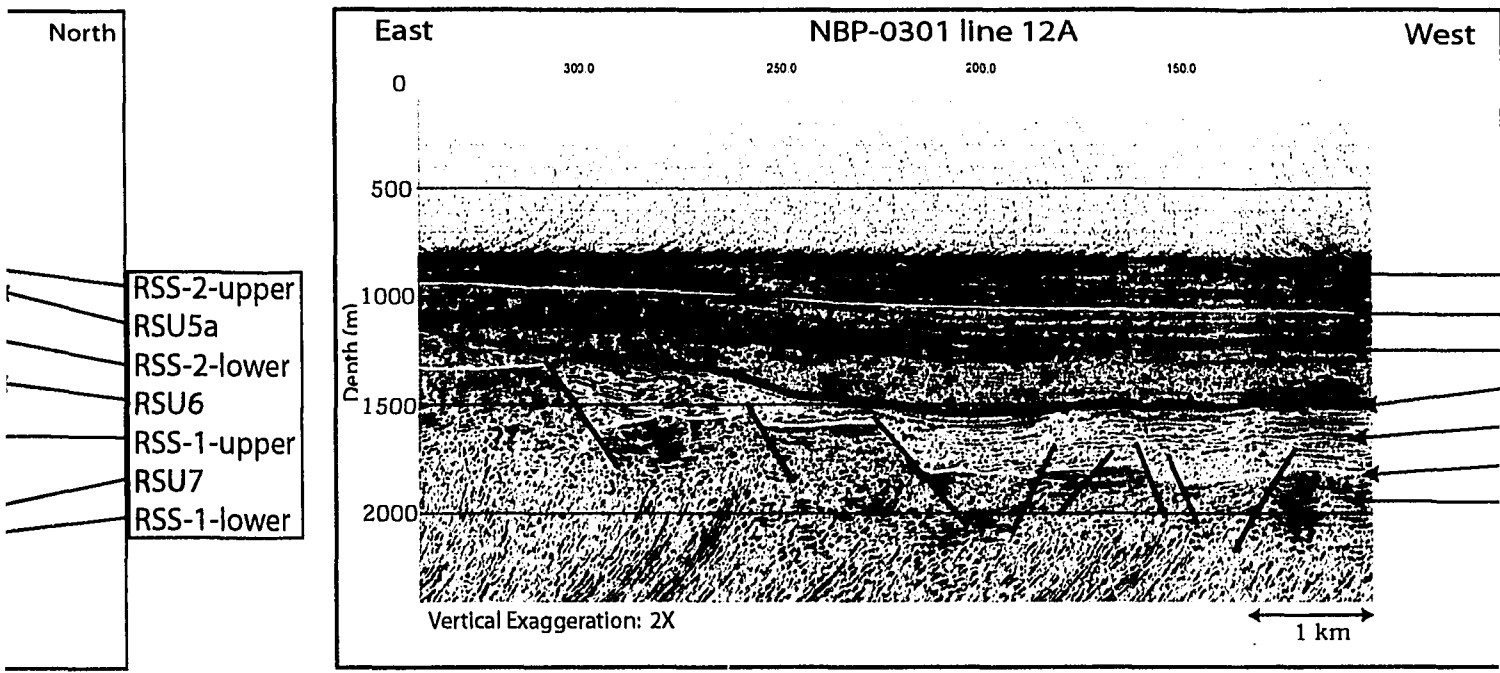
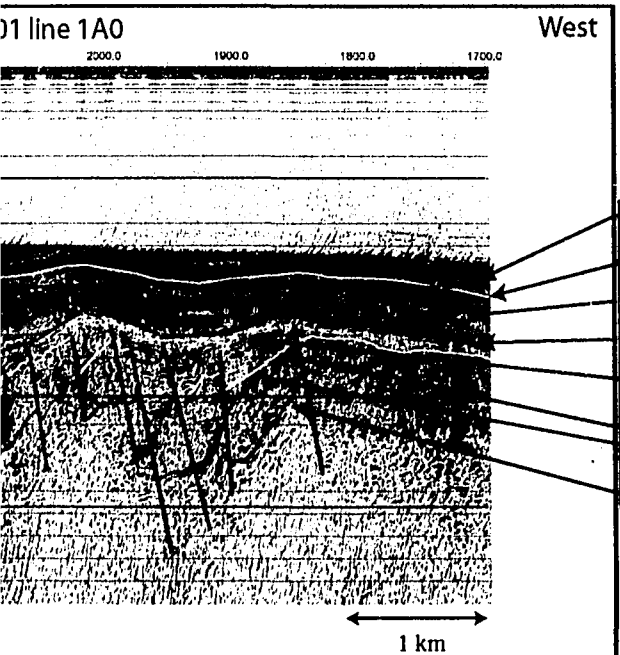
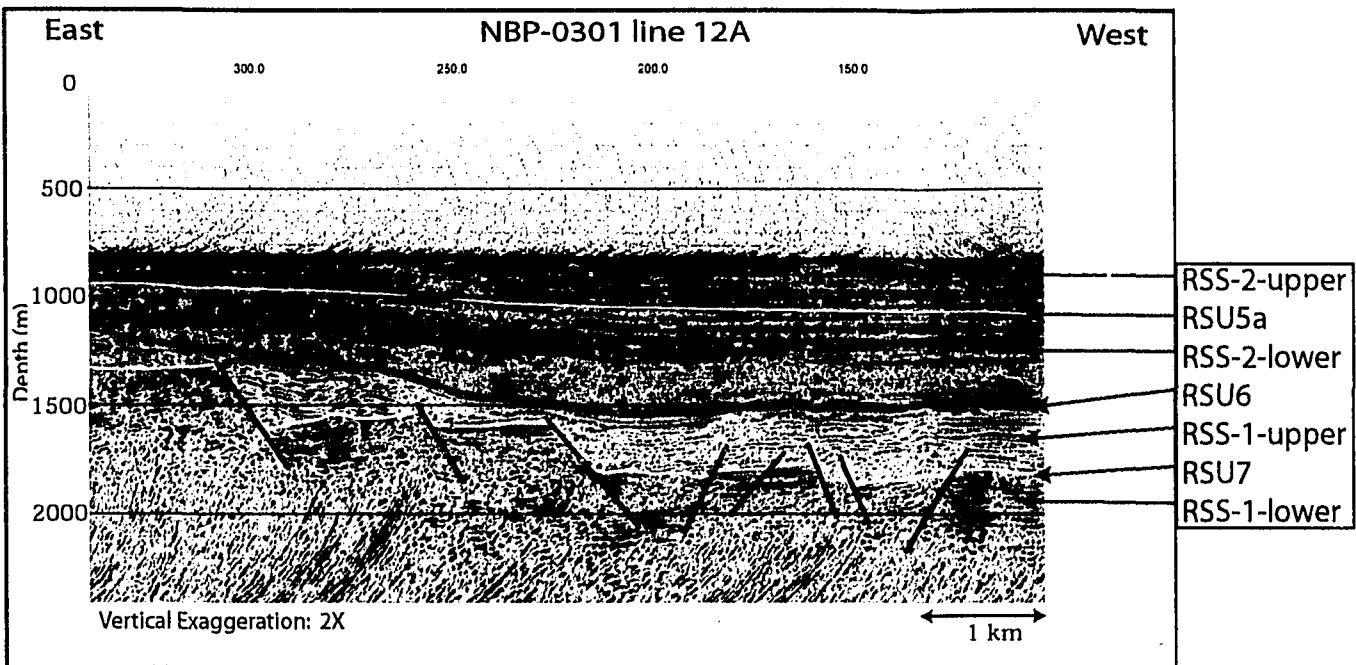


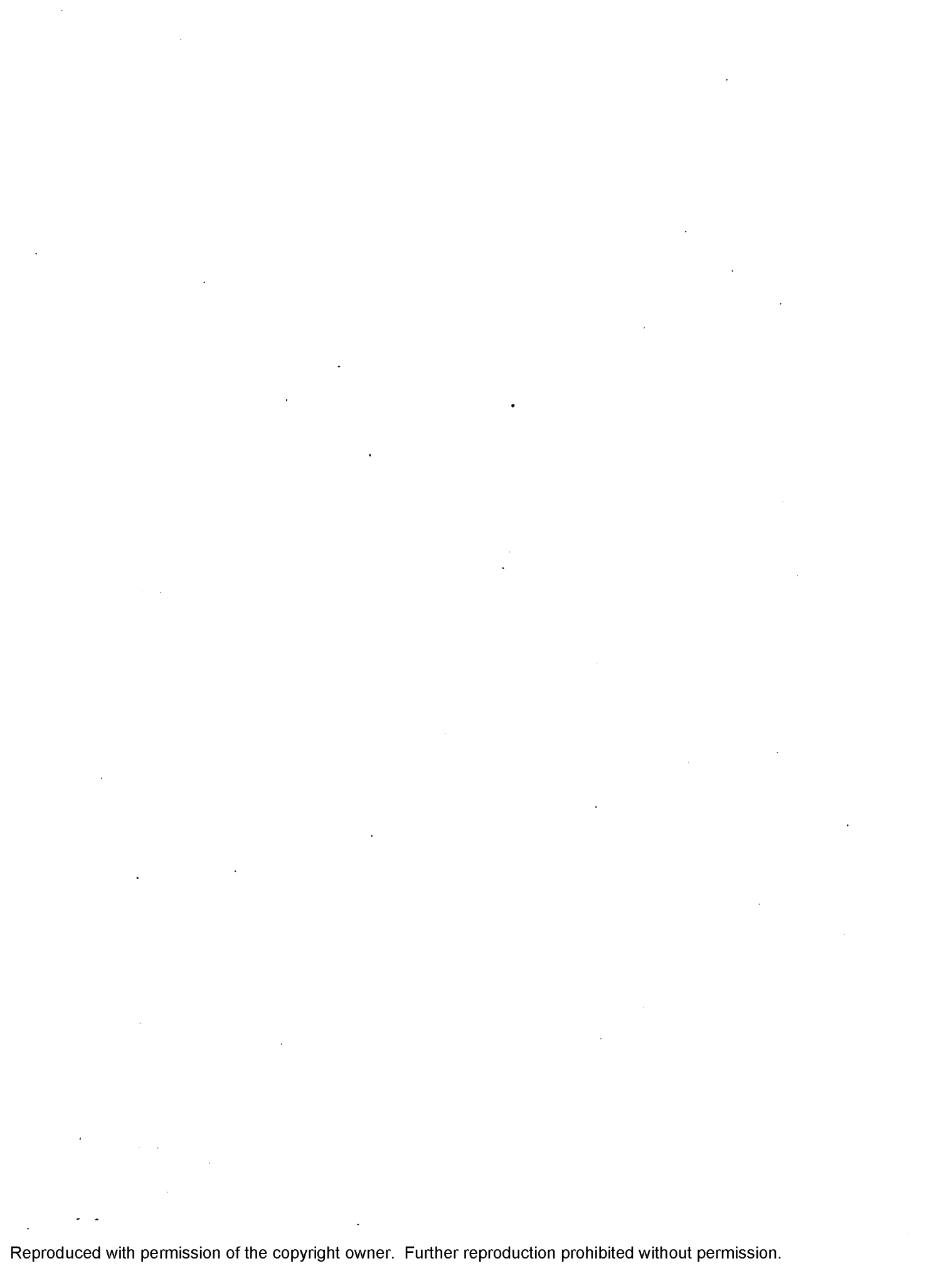
Figure 4-4: Seismic profiles of the proposed long wavelength deep reflections are interpreted. RSS-1-lower (Cretaceous?) fills basement high cut into synrift unit RSS-1-upper (Eocene?). Newly recognized (this study) unconformity separates lower from RSS-2-upper.



files of the proposed drill locations (also shown in Fig. 4-3). Low amplitude, reflections are interpreted as basement faulted into tilted blocks. Synrift (is?) fills basement half-grabens. Faults offsetting unconformity RSU7-1-upper (Eocene?). Capping synrift units are RSS-2-lower and RSS-2-upper. (study) unconformity RSU5a separates slightly steeper dipping RSS-2-r.



drill locations (also shown in Fig. 4-3). Low amplitude, tilted as basement faulted into tilted blocks. Synrift f-grabens. Faults offsetting unconformity RSU7 mapping synrift units are RSS-2-lower and RSS-2-upper. RSU5a separates slightly steeper dipping RSS-2-



Reproduced with permission of the copyright owner. Further reproduction prohibited without permission.

proposed they formed during Cretaceous rifting. Luyendyk, et al. [2001] also proposes RSS-1-lower was deposited during Cretaceous extension. At C-19 numerous normal faults offset stratal units within RSS-1-lower, making fault trends difficult to map (Fig.4-3 & 4-4).

Capping RSS-1-lower is an angular unconformity interpreted as unconformity RSU7 [Decesari, et al., 2003; Decesari, et al., 2004]. Strata above the unconformity is less deformed and tilted than synrift RSS-1-lower below and is interpreted as unit RSS-1-upper (Pre-Oligocene; Eocene?). RSS-1-upper is also interpreted as a syn-extensional unit because of north-south trending normal faults cutting the unit. RSS-1-upper is well preserved within large basement graben such as the CHG. But in regions where the acoustic basement is topographically high, RSS-1-upper is not well preserved (Fig. 4-3 & 4-4). Dipping reflectors within RSS-1-upper are much more subtle than RSS-1-lower and generally dip into the basement grabens within the Coulman High.

Overlying RSS-1-upper is the late Oligocene-early Miocene RSS-2 unit. Angular unconformity RSU6 (~30 Ma; [De Santis, et al., 1995]) separates RSS-1-upper from RSS-2. In the eastern Ross Sea interpretations of unconformity RSU6 show it is not offset by faults, indicating extension was completed by its formation [Luyendyk, et al., 2001]. At the C-19 site unconformity RSU6 is mostly not faulted. However, a few widely spaced north-south normal faults bounding the CHG cut through RSU6 and also offset the overlying RSS-2 unit (Fig. 4-3 & 4-4). Within the CHG, RSS-2 thickens suggesting this unit was deposited as accommodation space

was growing within the graben. An unconformity within RSS-2 separates the unit into a lower and upper sequence (RSS-2-lower and RSS-2-upper). The new unconformity has been named RSU5a and was correlated to the CRP drill holes using the route of Decesari, et al. [2003] (dissertation chapter 2). Unconformity RSU5a ties to an unconformity between the V4a and V4b units of the western Ross Sea. Within the CHG and Central Trough sectors of the C-19 survey, RSS-2-lower has a steeper dip than RSS-2-upper, which is more flat lying (Fig. 4-4). Unconformity RSU5a appears to mark the change in dips between the lower and upper RSS-2 units. Hamilton, et al. [2001] interprets strata above the V4a/V4b unconformity at Cape Roberts to display much less tilting than strata below. They infer this to indicate the major uplift of the TAM, which may be related to Adare Trough spreading, was completed by this time.

Capping RSS-2-upper is unconformity RSU5 and post RSS-2 units (RSS-3 and RSS-4). Unconformity RSU5 is prominent in the northern portions of the survey but merges with the seafloor to the south causing the post RSS-2 units to daylight. In the southern portion of the C-19 site, younger sections of RSS-2 are interpreted to have been eroded away and are exposed at the seafloor. Where unconformity RSU5 is preserved, in the northern portion of the C-19 site, units RSS-3 and RSS-4 are interpreted to overlie the RSS-2 sequence. Early Miocene glacial-marine unit RSS-3 and overlying unconformity RSU5 were mapped throughout the northern portions of the survey site. This unit is characterized by flat lying, undisrupted strata. Capping RSS-3 is unconformity RSU4a, overlain by Middle and Late Miocene glacial marine RSS-4.

4-3.2.1. Central Trough Sector of the C-19 Site: The stratigraphy interpreted on the Coulman High was mapped into the Central Trough along the ice shelf front. Unconformity RSU7 and unit RSS-1-lower become too deep in the middle of the basin to interpret on seismic data with confidence, but it is interpreted to pinch out on the western flank of the Central High. Where RSS-1-lower is interpreted, the unit is indicative of a synrift unit characterized by highly faulted, disrupted, and tilted reflectors. Unit RSS-1-upper and unconformity RSU6 are interpreted across the basin and onlap the western flank of the Central High. RSS-2-lower is interpreted to thicken within the basin, but is still flat lying. This indicates subsidence of the basin, most likely from thermal cooling, was taking place at this time.

In the southwestern Central Trough, a N-S trending structural high was mapped within the basin. This high was named the Central Trough High (CTH) and it extends north to German seismic line BGR-01 (Fig. 4-5). The CTH corresponds with a magnetic anomaly (Fig. 4-6c; see sections 3.4 & 4.2) and is approximately the same width (~16 km) as the maximum amplitude of the magnetic high. Both unconformities, RSU7 and RSU6 are interpreted over the CTH.

4-3.3. Gravity Anomalies and Crustal Structure

Gravity data collected on NBP-0301 consistently contained noise of about 5 milligals (mGals) amplitude of unknown origin that required filtering to remove. Gravity data from NBP-0301 was combined with gravity data from other cruises

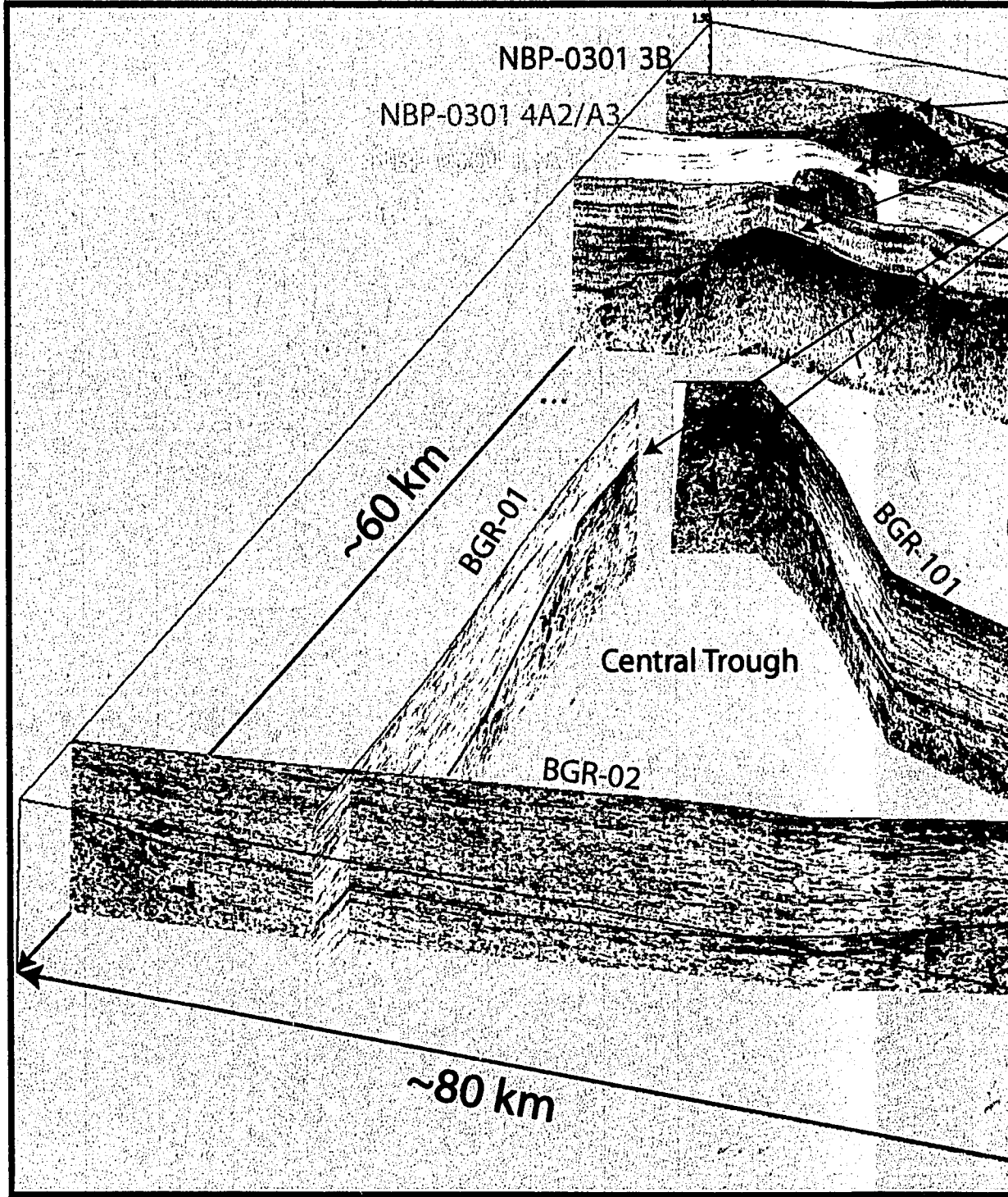
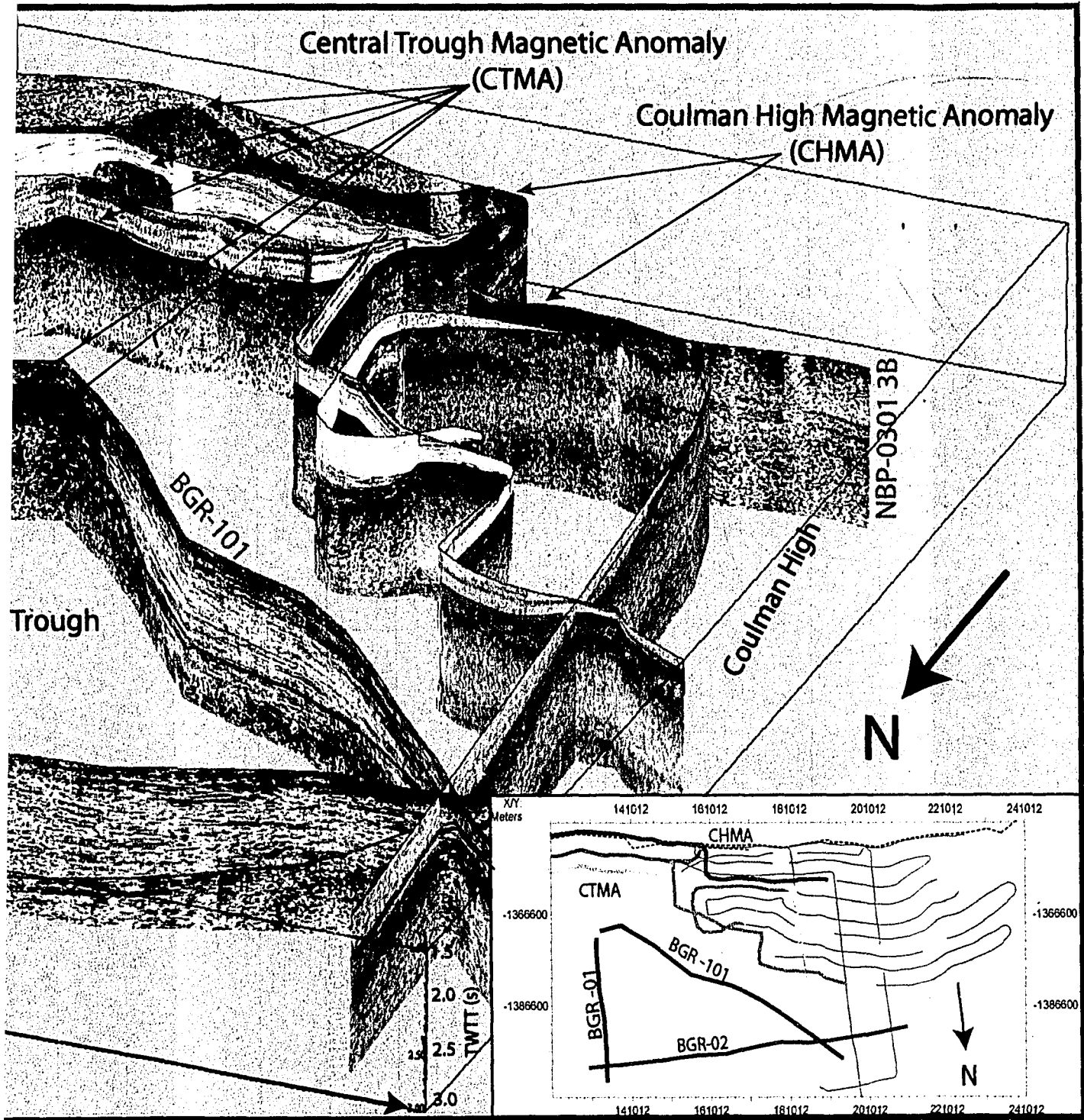


Figure 4-5: Central Trough and eastern Coulman High seismic data in 3-D view showing the map shows the location of survey lines in the 3-D diagram. The Central Trough is imaged on 13A1, fault bounded basement high is interpreted in the Central Trough. The high corresponds to BGR-101 and BGR-01. Fault zones are indicated by dashed black lines. Note



seismic data in 3-D view showing the spatial relationship of structures below unconformity RSU6 (green line). The inset shows the same area as the main figure, but with a different vertical scale. The Central Trough is imaged on seismic profile BGR-02. However, to the south along lines NBP-0301 lines 3B, 4A2/A3, and 5A2/A3, a magnetic low is imaged in the Central Trough. This low corresponds to the Central Trough Magnetic Anomaly (CTMA) and is interpreted to indicate the presence of a magnetic low. The high corresponds to the Central Trough Magnetic Anomaly (CTMA) and is interpreted to indicate the presence of a magnetic high. The dashed black lines indicate the locations of the seismic profiles. Note: seismic data in this image starts at 1.5 s TWTT.



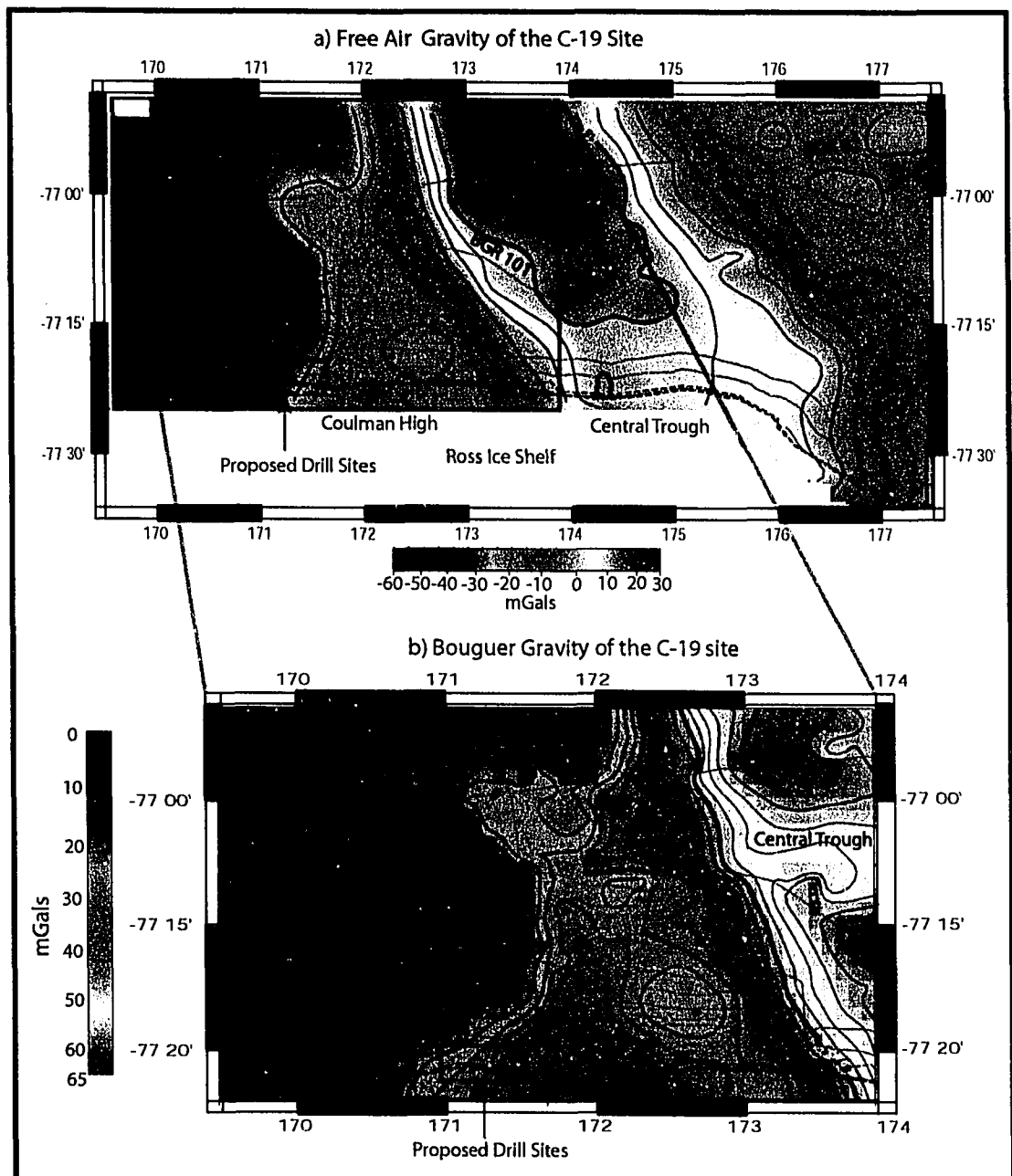


Figure 4-6: **a)** Free Air gravity. The Central Trough is characterized by a large positive ($> +25$ mGals), indicating thinned crust. Large negative anomalies (> -40 mGals) correspond to sediment filled grabens within the Coulman High, indicating the grabens are surface structures. **b)** Bouguer anomaly subset map of the western Central Trough and Coulman High. The Central Trough has a Bouguer anomaly of $>+60$ mGals and the Coulman High is characterized by anomalies ranging from 0 to $+25$ mGals. The Bouguer anomaly may represent Moho topography.

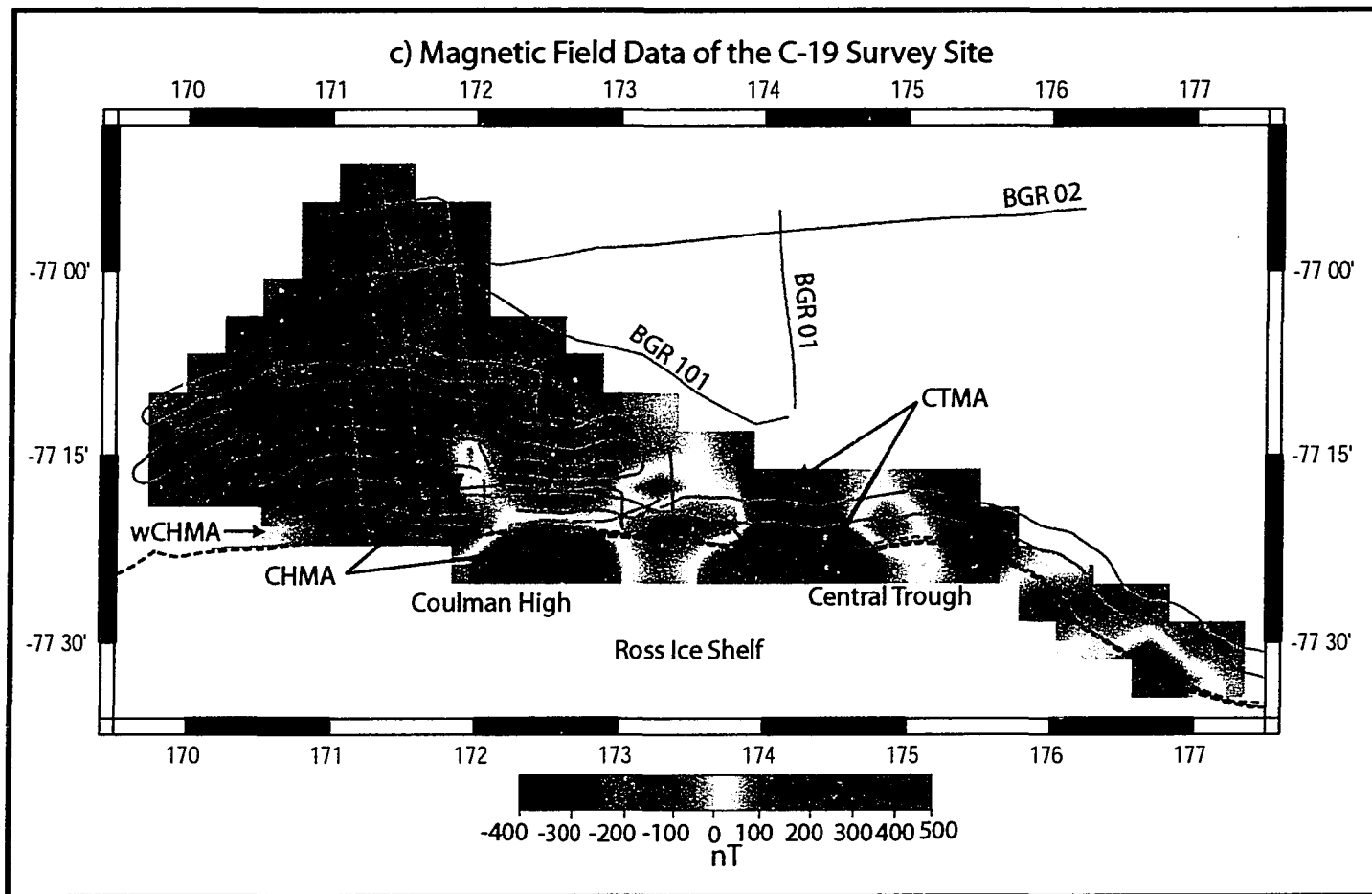


Figure 4-6c) Magnetic anomaly map showing a highs in the Central Trough (CTMA) and on the eastern flank of the Coulman High (CHMA). The CHMA corresponds to a trough (-25 mGals) in the gravity data, suggesting a thickening of the crust, possibly due to volcanic intrusions. The CTMA is most likely a volcanic intrusion possibly forming during Cretaceous extension of the Ross Sea.

throughout the sector [Luyendyk, et al., 2002] and was used to produce Free Air and Bouguer gravity grids of the C-19 region at 2 km grid intervals (Fig. 4-6a & 4-6b). Both the Free Air and Bouguer gravity fields show roughly the same contour patterns throughout the C-19 region. The Central Trough is characterized by large positive anomalies (~30 mGals Free Air and >60 mGals Bouguer) while to the west, the Coulman High is characterized by negative Free Air anomalies (0 to -60 mGals) and Bouguer anomalies (0 to +30 mGals). Several large, approximately circular Free Air gravity lows (~ -49 to -59 mGals) are observed in the western sector of the survey and are also observed in the Bouguer anomaly (<+10 mGals) (Fig. 4-6a & 4-6b).

The similarity of the gravity contours on both the Free Air and Bouguer grids are attributed to reflect the underlying Moho topography. The large positive anomalies within the Central Trough most likely reflect a shallow Moho, resulting from highly thinned continental crust. The negative Free Air anomaly and low positive Bouguer anomaly over the Coulman High most likely reflect thicker continental crust. The roughly circular gravity anomalies observed over the western Coulman High correspond with localized basins within the Coulman High and areas of thicker sediment accumulation. This is attributed to reflect sediment filled grabens within the Coulman High basement that are not in regions of highly thinned crust.

4-3.4. Magnetic Field Data

A Cesium magnetometer was deployed behind the ship at varying distances due to ice conditions and other logistic reasons throughout the cruise. High quality

magnetic data were collected on most profiles. The first step in processing was the removal of the IGRF 2000 (the spherical harmonic summation approximation to the Earth's normal background field) in order to produce the magnetic anomaly. Diurnal variations were accounted for using the Scott Base magnetic observatory as the reference point. The cross over error method was used to correct for the diurnal variations. Manual editing was used to correct cross over errors not accounted for by the diurnal variation.

Overall, the majority of the C-19 site is characterized by non-magnetic rocks and sediments. However, several high amplitude anomalies ($> +300$ nT) are observed in front of the Ross Ice Shelf in the southeast portions of the survey (Fig. 4-6c). These high amplitude anomalies are observed in aeromagnetic surveys conducted over the western Ross Sea and ice shelf [Behrendt, et al., 1996; Chiappini, et al., 2002].

The bulk of the magnetic anomalies are to the south of the C-19 site, over the Ross Ice Shelf. Only the northern segments of the magnetic highs were recorded. The Ross Ice Shelf (RIS) anomaly of Behrendt, et al. [1996] is located on the eastern sector of the Coulman High. This study renames the RIS anomaly the Coulman High Magnetic Anomaly (CHMA) (Fig. 4-6c). The magnetic data shows the CHMA is characterized by a roughly N-S trending elliptical shaped anomaly with maximum amplitudes of $> +200$ nT. Aeromagnetic data indicates the CHMA continues over the ice shelf, where a larger ($> +400$ nT) circular anomaly exists over the eastern flank of the Coulman High [Behrendt, et al., 1996; Chiappini, et al., 2002]. To the west of the CHMA is another elliptical magnetic anomaly called the western Coulman High

Anomaly (wCHMA) in this study? The survey only recorded the very northern portions of the wCHMA (Fig. 4-6c). The wCHMA has maximum amplitudes of ~300 nT and is clearly observed on the aeromagnetic maps [Behrendt, et al., 1996; Chiappini, et al., 2002].

East of the CHMA is a linear high amplitude magnetic anomaly corresponding to the western flank of the Central Trough. While the survey only recorded the northern sector of the magnetic high at > +200 nT, aeromagnetic surveys indicate that the anomaly continues south, over the Ross Ice Shelf, reaching a maximum amplitude of > +400 nT [Behrendt, et al., 1996; Chiappini, et al., 2002]. Behrendt, et al. [1996] named this linear magnetic high anomaly X. Anomaly X is renamed in this study the Central Trough Magnetic Anomaly (CTMA) (Fig. 4-6c). The CTMA is approximately 16 km wide in the survey region, but increases slightly in width over the ice shelf, and is approximately 100 km in length. The CTMA corresponds to the Central Trough High (Fig. 4-5; see section 3.2.1 & 4.2) interpreted on seismic data.

4-4. Discussion

4-4.1. The Tectonic History of the Coulman High and Central Trough at C-19

The tectonic history of the C-19 survey site is connected to the Mesozoic rifting of the Ross Sea and the formation of the WARS. Gravity data suggests the Coulman High sector of the C-19 site is underlain by thicker continental crust and the Central Trough crust has been highly thinned. This is supported by crustal modeling

to the north of C-19 along profile BGR-02 by Trey, et al. [1999], showing that crustal thicknesses in this region are >20 km for the Coulman High and ~10 km in the Central Trough. Horst and half-grabens are interpreted within the basement structure, indicating the region was affected by significant extension. A generally north-south trend is interpreted for basement grabens and half-grabens, suggesting the over all trend of extension was east-west in nature, resulting in basin-and-range style normal faulting and extension.

At C-19, stratigraphic units characteristic of the Ross Sea are interpreted. These units are separated by angular unconformities RSU6 and RSU7 and are characterized by vastly different styles of deformation. The glacial-marine RSS-2-lower/upper sequences, above unconformity RSU6, are generally not deformed except for gentle tilting of the sequence. Below RSU6, the RSS-1-upper unit is tilted slightly and offset by widely spaced, moderately dipping normal faults. The age of faulting and deposition of the RSS-1-upper unit is constrained as older than the late Oligocene-early Miocene RSS-2 sequence. Angular unconformity RSU7 is interpreted as forming during a hiatus in Cretaceous rifting and is thought to be an extension of the West Antarctic Erosion Surface (WAES), indicating the region was above sea level prior to rifting [Luyendyk, et al., 2001].

RSS-1-lower was most likely deposited and deformed during the main phase of Ross Sea rifting in the Cretaceous. Cooling ages of ~105 to 94 Ma were obtained at DSDP Site 270 [Fitzgerald and Baldwin, 1997], in western Marie Byrd Land [Richard, et al., 1994], and are consistent with the age of the WAES [LeMasurier and

Landis, 1996]. Luyendyk et al. [2001] proposes extension in the eastern Ross Sea began at ~105 Ma and RSS-1-lower, in the eastern Ross Sea, was deposited and deformed at this time. Extension of the C-19 site probably began at this time, along with the deposition of RSS-1-lower in N-S trending basement grabens. Following extension, erosion likely beveled the newly formed structures as the region subsided in the Late Cretaceous. This preserved RSS-1-lower in basement half-grabens and formed angular unconformity RSU7 (WAES) (Fig. 4-3 & 4-4). RSS-1-upper was then deposited on top of RSS-1-lower and a later (Eocene?) phase of E-W extension faulted and tilted the units. Faulting and tilting of RSS-1-upper was minor compared to earlier rifting phases.

Cande, et al. [2000] interprets at least 180 km of E-W seafloor spreading north of the western Ross Sea, across the Adare Trough spreading center from the 43 to 26 Ma. The spreading pattern requires that extension must have been transferred south into the Ross Sea. However, Eocene extension of this magnitude has not yet been identified in the Ross Sea. It seems likely that Adare Trough spreading can account for the extension and the resulting accommodation space needed for the large thickness of Oligocene and older sediments in the VLB [Hamilton, et al., 2001]. It is possible that some, if not all, of the large-scale extension resulting from the Adare Trough may be preserved within RSS-1-upper at C-19 (Fig. 4-3 & 4-4). If unit V5c is the same as RSS-1-upper and is of Eocene age as suggested by Hamilton, et al. [2001], then this scenario is plausible. If this is not the case, then interpretations suggesting extension resulting from Adare Trough spreading extended into the Ross

Sea would be problematic. Further deformation of RSS-1-lower may also have occurred. Although RSS-1-lower is interpreted to have been deposited and deformed in the Late Cretaceous, it is plausible that subsequent extension in the Eocene may have reactivated faults, deforming the unit further. Therefore, the RSS-1 units at C-19 may record Cretaceous and Tertiary extension events in the Ross Sea.

Unconformity RSU6 is a mostly continuous reflector at C-19. However, a few moderately dipping normal faults bounding the CHG offset the unconformity and extend into the overlying RSS-2-lower unit before terminating at unconformity RSU5a. Offsets are fairly small on RSU6 and grow with depth, suggesting these are growth faults (Fig. 4-4). Also, RSS-2-lower thickens more and is tilted slightly more than RSS-2-upper within the CHG and Central Trough. Since the RSS-2-upper/lower boundary is interpreted to represent the end of TAM uplift in the VLB [Hamilton, et al., 2001], the effect of the TAM uplift on the WARS may have been more widespread than previously thought. The TAM uplift not only affected the VLB but most likely affected the Central Trough region. The uplift of the TAM is probably recorded into Oligocene time by faulting within RSS-2-lower and changes in unit thickness and tilting between RSS-2-lower and RSS-2-upper at the C-19 site. Because the faults offset unconformity RSU6 and grow with depth, they probably formed initially during Cretaceous extension and were reactivated during Adare Trough spreading and TAM uplift.

4-4.2. Extension and Volcanic Intrusions

The shape of the magnetic anomalies in the C-19 region, as well as modeling, led Behrendt, et al. [1996] to conclude the magnetic highs resulted from late Cenozoic volcanic centers that extend to the seafloor. However, no volcanic intrusions are interpreted to cut through the Oligocene-Miocene and older stratigraphy to the seafloor over the CHMA and the CTMA on reflection profiles. Units RSS-1-lower, RSS-1-upper, and RSS-2 all overly the anomalies (Fig. 4-5). This indicates the magnetic anomalies were emplaced prior to the deposition and deformation of the RSS-1-lower/upper units, making the magnetic anomalies much older than suggested by Behrendt, et al. [1996]. The CHMA and the CTMA may be volcanic intrusions emplaced during Cretaceous extension of the Ross Sea. It is also possible the magnetic anomalies are due to volcanic intrusions emplaced during continued extension of the Ross Sea in the Eocene, resulting from Adare Trough extension. This scenario seems more likely, as previously thinned crust would have been thinned even further, making it easier for intrusions to penetrate the crust.

Gravity modeling by Trey, et al. [1999] indicates the crust underlying the basins of the Ross Sea must have high densities, indicating mafic intrusions or dikes. This agrees with the magnetic anomalies resulting from intrusions emplaced during extension of the Ross Sea. Normal faults are interpreted on either side of the CTMA, indicating the magnetic anomalies were in place as the basin extended (Fig. 4-5). The CHMA is bounded to the east by a series of normal faults that appear to control the Central Trough. It is possible volcanism intruded into the Central Trough and the

flanks of the Coulman High during basin formation, resulting in the CTMA and CHMA. It is also possible that these anomalies result from much older volcanism related to the Jurassic Kirkpatrick Basalts and Ferrar Dolerites, which are thought to have covered much of the region.

Behrendt, et al. [1996] and Chiappini, et al., [2002] indicate the CHMA and CTMA are truncated to the north by an inferred fault zone, called the Ross Fault. Chiappini, et al., [2002] suggests this fault zone terminates the crustal block containing the source of the magnetic anomalies and that it is different than the crustal blocks to the north containing the Central Trough and the Coulman High. Chiappini, et al., [2002] also indicates the structural provenances of the Coulman High and Central Trough terminate against the inferred Ross Fault and associated magnetic anomalies. Based on seismic interpretations and gravity data, this study disagrees with this interpretation and has mapped the Coulman High and Central Trough south of the inferred Ross Fault, into the region of the CHMA and CTMA. Furthermore, there is no convincing evidence in the seismic data for the existence of the Ross Fault.

4-4.3. Potential Drill Sites at C-19

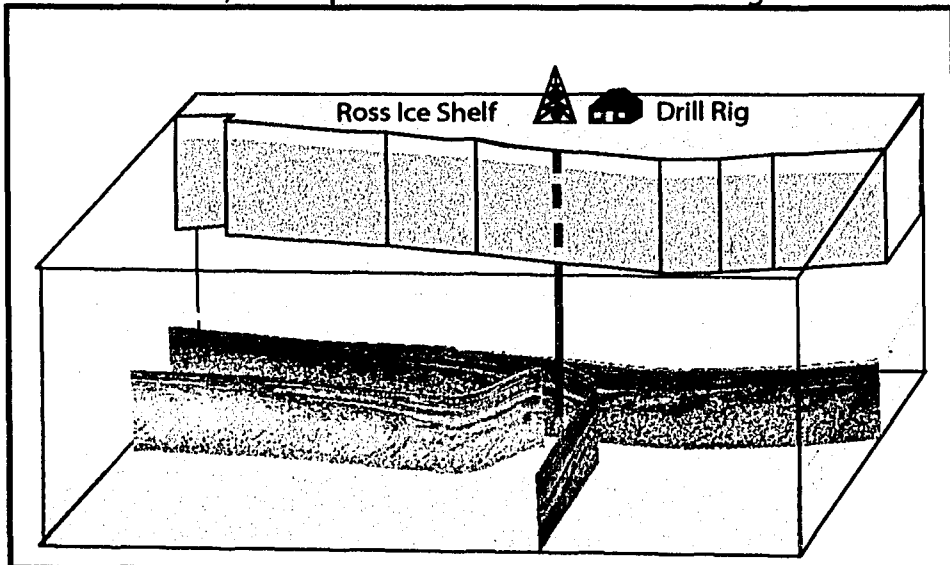
4-4.3.1. ANDRILL: The Antarctic Drilling Program (ANDRILL) is designed to recover stratigraphic records from the Antarctic region by drilling through a floating ice platform (<http://andrill.org>). The program's primary objectives are to investigate Antarctica's role in global climate change over the past 65 My and to

better understand Antarctica's future response to global change. Two test drill sites using the ANDRILL rig are scheduled to drill through the McMurdo Ice Shelf to sample Miocene and younger strata in the austral summers of 2006 and 2007. Future drilling at C-19 would employ the ANDRILL drill rig.

4-4.3.2. Why drill here?: The C-19 site offers one of the best known locations for drilling pre-Oligocene strata in the Ross Sea. At C-19, the ice sheet is moving ~700 m/year to the north [Thomas, et al., 1984]. This means by 2008 the ice shelf will have moved north approximately 3.5 km, covering the first several lines of the survey. The ice shelf can be used as a drilling platform to target strata along the covered lines (Fig. 4-7a). An E-W transect of proposed core holes along the current ice shelf front, on NBP03-01 lines 1A0, 11A1, and 12A, are designed to target a complete section of pre-Oligocene Ross Sea strata within the CHG (Fig. 4-2).

Coring pre-Oligocene strata will test the hypothesis that subaerial, synrift units were filling the Ross Sea during Cretaceous rifting events. It will also test the proposed subsidence model (dissertation chapter 3) for the Ross Sea. Drilling here may record the transition from a warm climate in Eocene time to the drastic cool down of the Oligocene and formation of the Antarctic ice sheets [Zachos, et al., 2001]. Coring will also test the hypothesis that extension related to Adare Trough spreading is recorded in this sector of the Ross Sea. Drilling at DSDP sites, in the eastern Ross Sea, and at Cape Roberts, in the western Ross Sea, only sampled part of the Oligocene RSS-2 unit. DSDP Site 270 did not sample Eocene or older strata [Hayes and Frakes, 1975; Cape-Roberts-Science-Team, 2000]. Considering the shear

a) Conceptual Model of Ice Shelf Drilling



b) ANDRILL Drilling Limits for the Ross Sea

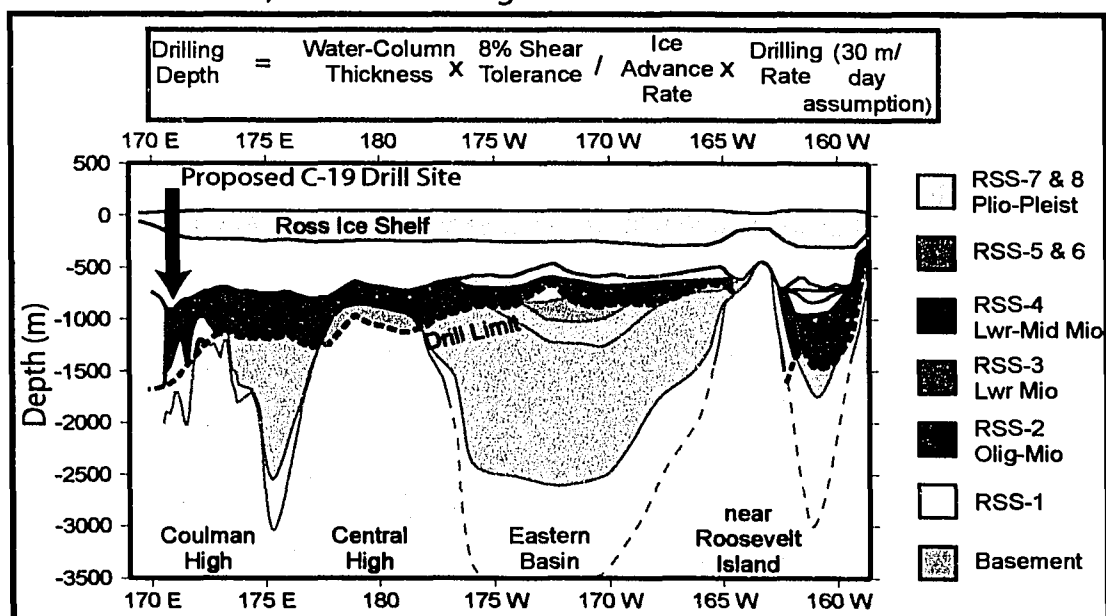


Figure 4-7: A) Drilling concept: Drill through the ice shelf and into the strata below using the ice shelf as the drilling platform. Because the ice shelf is advancing and the angle at which the pipe can be flexed is limited, the water depth beneath the ice shelf is critical. The Ross Ice Shelf is 250-350 m thick and the water thickness under the ice shelf is 550-650 m making drilling here favorable. As the bend in the drill pipe becomes critical, the rig will be picked up and moved back over the core hole so drilling may resume. **B)** The drill limit for the ANDRILL rig is a function of the equation above the figure. Maximum drilling depths are shown for the Ross Sea by the back dashed line. At the proposed C-19 site the maximum depth obtainable is ~1700 m. At this location pre-Oligocene strata and basement can be sampled. Ice shelf drilling will be tested in 2006 & 2007 near McMurdo Station as part of an ANDRILL project.

size of the WARS, the number of samples of Ross Sea basement rock is extremely small. Basement rocks can be obtained at this site and compared to basement rocks obtained at DSDP Site 270 [Hayes and Frakes, 1975] and off Cape Colbeck [Luyendyk, et al., 2001; Siddoway, et al., 2004]. Finally, sampling strata at C-19 will test the hypothesis that unit RSS-2 is equivalent to unit V4 at CRP, as well as test other relationships, such as sediment type, depositional environment, and sediment ages, between the RSS units and the V units.

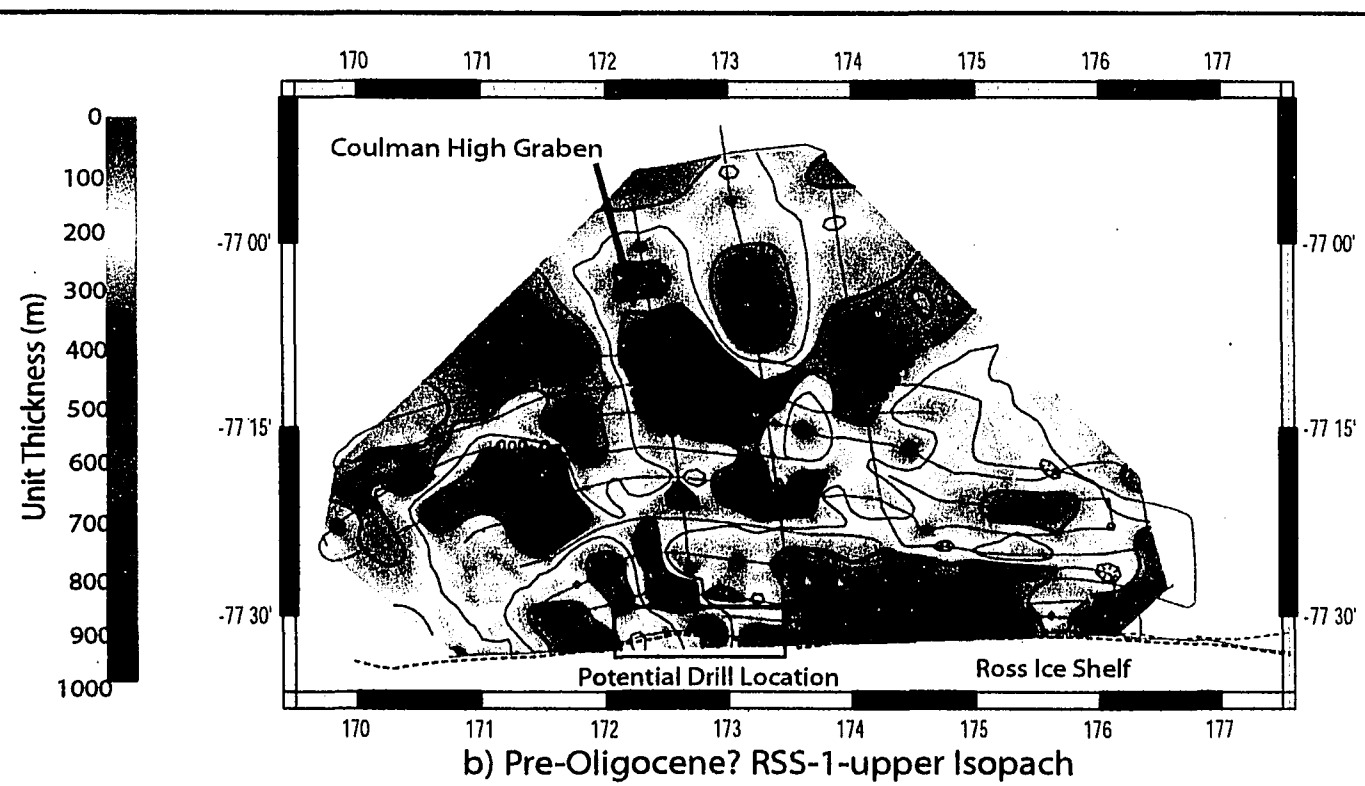
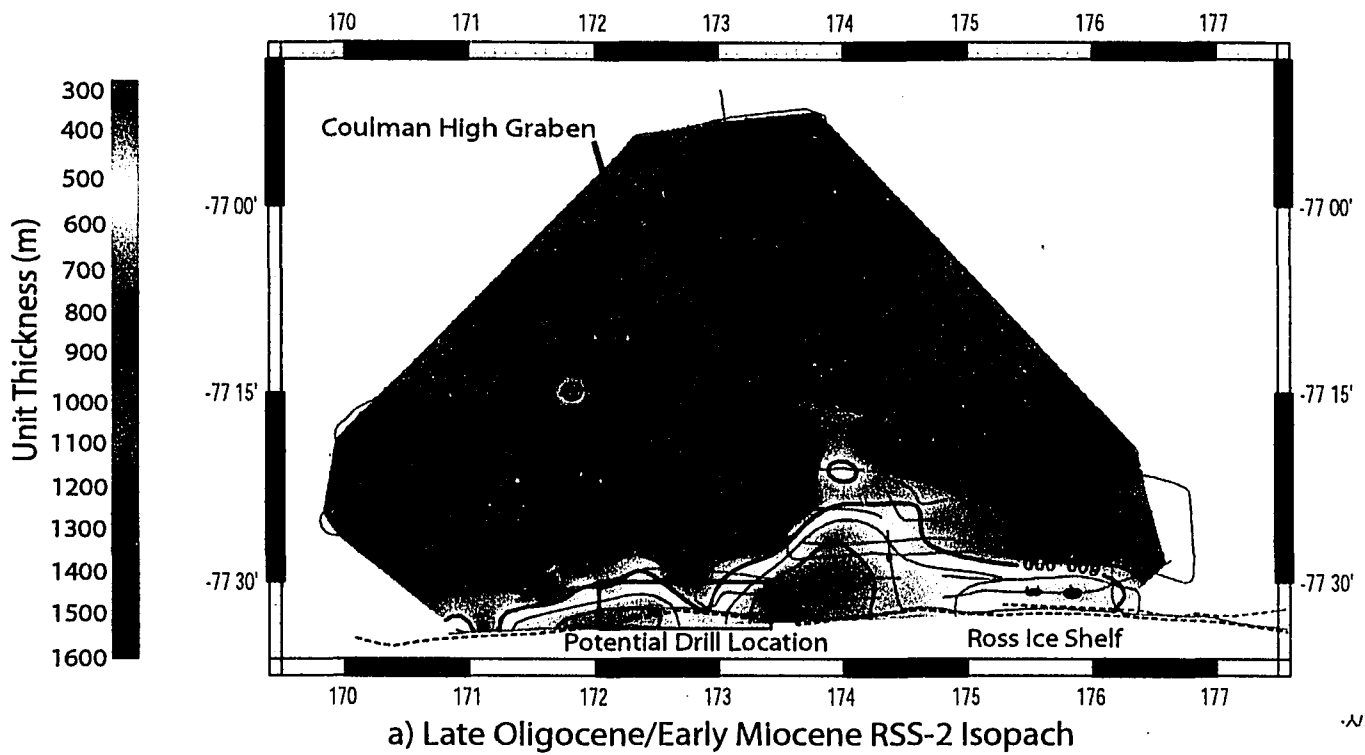
The proposed C-19 drill site is located east of Ross Island, ~90 km. NE from McMurdo Station. Because the ice shelf is advancing, the drilling platform will not be stationary over the target. Since the angle at which the drill pipe can be flexed is limited, the water thickness beneath the ice shelf is critical. The deeper the water, the more flex of the drill stringer can be achieved before the drilling rig must be moved back over the target hole or a new target hole. At the C-19 site, the Ross Ice Shelf is ~200 m thick and the water thickness under the ice shelf is 550-650 m, making drilling here favorable (Fig. 4-2). Using the ANDRILL drill rig, the depth to which drilling is possible is given by: Drilling Depth = (Water Height x 8% Shear Tolerance) / (Ice Advance Rate x Drilling Rate). At the C-19 site, the maximum obtainable depth is ~1,700m from the sea surface, assuming a 30m/day drilling rate (Fig. 4-7b). This depth is just within the range needed to sample pre-Oligocene strata and basement rocks at the C-19 site.

Since unit V4 (RSS-2) was sampled at CRP, why should this unit be resampled at C-19? At the CRP-2 drill site, Naish, et al. [2001] interprets unconformity

bounded sequences in seismic unit V4 and interprets these unconformities as reflecting Milankovitch cycle control of glacial advance and retreat. They concentrate on sequences 9, 10, and 11 within unit V4 and are characterized by upward fining sediment packages from 130-304 meters below sea floor. Ash layers were found in sequences 10 and 11 and were Ar-Ar dated at 23.98 ± 0.13 and 24.22 ± 0.03 , respectively. Sequence 9 is inferred to contain the Oligocene-Miocene boundary. Independent results from Sr-isotope dating and magnetostratigraphy suggest the age gap between sequences 9 and 10 is small. Therefore, Naish, et al. [2001] contend that these sequences reflect 40 kyr oscillations. However, the Oligocene-Miocene boundary is close to 23.0 Ma based on orbital calibrations. Thus the time interval spanned may be ~1 Myr, resulting in a poorly constrained cycle time. Since the CRP core holes are located close to the TAM front, the sedimentary sequences may not be complete due to tectonic activity. Sampling similar age units at greater distance from the TAM front should result in more complete sequences, allowing for a better count of the number of cycles per million years. Therefore, further sampling of RSS-2 at C-19 will gather more evidence to test the conclusions of Naish, et al. [2001].

4-4.3.3. New C-19 Isopach Maps of RSS-1-upper, RSS-2, and post RSS-2

units: In preparation for drilling, new isopach maps were produced for seismic units RSS-1-upper and RSS-2, as well as post RSS-2 units (Fig. 4-9a & 4-9b). Interval velocities were used to calculate unit thickness along seismic lines before interpolating the isopach grid. The NW-SE striking Coulman High Graben is interpreted on the isopach maps, where units RSS-1 and RSS-2 thicken. Unit RSS-2





Reproduced with permission of the copyright owner. Further reproduction prohibited without permission.

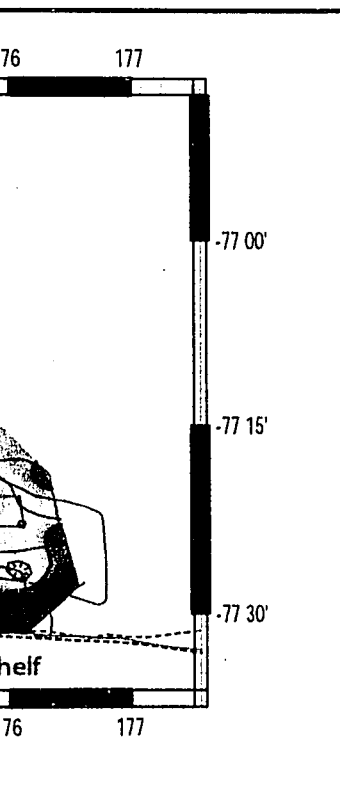
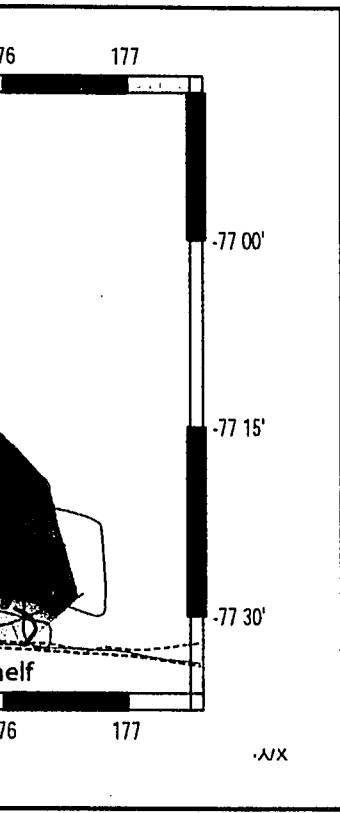


Figure 4-8: **A)** Isopach map of Oliogocene RSS-2 in the C-19 site. Gray lines are ship tracks from cruise NBP-0301. RSS-2 thickens to ~1200 m in the Coulman High Graben (CHG). RSS-2 thins to < 700 m on either side of the CHG, north of the ice shelf. Along the ice shelf front, RSS-2 is thinnest, < 350 m thick. Within CHG at the proposed drill site (black box), RSS-2 is ~600 m thick. **B)** Isopach map of Eocene ? RSS-1-upper. RSS-1-upper thickens to ~800 m within the CHG. Along the ice shelf front RSS-1-upper pinches out (red areas) except within the CHG (black box) where RSS-1-upper is ~450 m thick.



Reproduced with permission of the copyright owner. Further reproduction prohibited without permission.

varies in thickness throughout the survey site from a maximum thickness of ~1200 m in the CHG to ~250 m along the ice shelf front. RSS-1-upper thickens to a maximum of ~800 m in the CHG.

4-4.3.4. Expected drilling results: The proposed drill sites are in a location where pre-Late Oligocene strata have an apparent east dip, infilling tilted basement half-grabens. This location is within the southern portion of the Coulman High Graben. Described below are expected results for proposed drill site #1 (Table 4-1; Fig. 4-3, 4-4 & 4-8). Other potential drill holes in the CHG will have the same stratigraphic sequencing, but will vary in depth and unit thickness from site #1. At drill site #1, approximately 600 m of Late Oligocene-Early Miocene glacial-marine RSS-2 sediments are expected to be cored. It is possible a thin cap of Quaternary sediments overlies RSS-2 at this location. At about 200 meters below sea floor (mbsf) unconformity RSU5a is expected, separating RSS-2-upper from RSS-2-lower. In this region RSS-2-upper is relatively thin, ~200 m, compared to the ~400 m of RSS-2-lower below. Cores from the RSS-2 sequence should be composed of relatively flat lying, undisturbed sediments.

Table 4-1: Expected C-19 Drilling Results

Unit/Unconformity	MBSF (m)	Unit Thickness (m)	Expected Unit Age
Seafloor	0		
RSS-2-upper		200	L. Olig/E. Mio.
RSU5a	250		
RSS-2-lower		400	L. Olig/E. Mio
RSU6	600		
RSS-1-upper		450	Eocene?
RSU7	1000		
RSS-1-lower		>200	Cretaceous?
Basement	1400		Mesozoic?

Drilling through angular unconformity RSU6 should occur at ~600 mbsf (Figs. 4-3, 4-4 & 4-8). Although RSU6 was bracketed by sampling in the eastern Ross Sea, it is inferred to be >26.7 Ma [Busetti and Cooper, 1994] and preferred to be 30 Ma by DeSantis, et al. [1995]. Results from the CRP indicate a major unconformity at 28.5 Ma [Cape-Roberts-Science-Team, 2000] interpreted as unconformity RSU6 [Davey, et al., 2000]. Unconformity RSU6 is interpreted to mark a change between subtropical and polar climates. DeSantis, et al. [1995] interprets RSU6 to have formed at sea level prior to subsiding below sea level in the Oligocene. Sampling unconformity RSU6 at C-19 will test these relationships, as well as better constrain the age, paleobathymetry, and subsidence history of the unconformity.

Below unconformity RSU6 is approximately 450 m of synrift RSS-1-upper. Luyendyk, et al. [2001] suggests RSS-1-upper is of shallow marine origin. No sediments of Eocene age have been sampled in the Ross Sea, except for at the CIROS-1 drill hole, adjacent to the TAM, where early-late Eocene strata were recovered [Hannah, 1997; Hannah, et al., 1997; Wilson, et al., 1998]. Correlation of

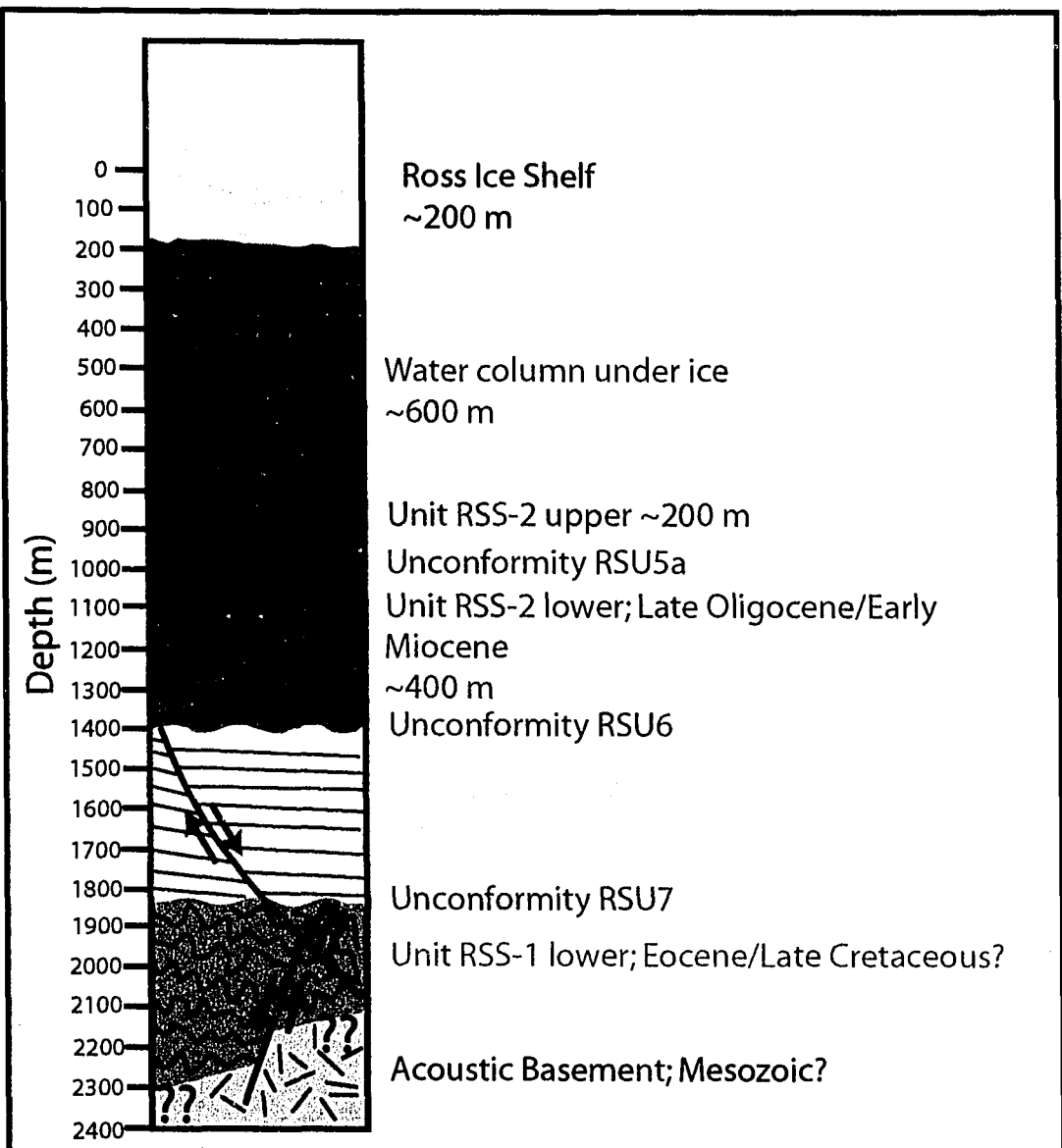


Figure 4-9: Expected results of drilling at site #1 in the southern Coulman High Graben. Depths and thicknesses of units are specific to proposed site #1, but will be similar for other target holes in the area.

strata from CIROS-1 to the VLB remains problematic because of faulting, unconformities, and shallow water bottom multiples between the VLB and McMurdo Sound [Bartek, et al., 1996; Henrys, et al., 1998]. Sampling RSS-1-upper at C-19 will allow for correlation of possible Eocene strata throughout the western Ross Sea. Better constraints are needed for this unit in order to improve subsidence models of the Ross Sea and understanding the timing of tectonic events prior to the Oligocene.

At ~1,000 mbsf angular unconformity RSU7 (WAES) is expected (Figs. 4-3, 4-4 & 4-8). Luyendyk, et al. [2001] interprets the WAES as forming at elevation during a hiatus of rifting events in the Cretaceous before subsiding below sea level. Strata bracketing RSU7 have not yet been sampled anywhere in the Ross Sea and is important for constraining the timing and magnitude of Cretaceous Ross Sea extension, as well as the subsidence history prior to 30 Ma. Below unconformity RSU7 ~200 m or more of Late Cretaceous (?) terrestrial and subaerial synrift RSS-1-lower is expected. This unit may have been sampled at DSDP Site 270 within a basement half-graben [Hayes and Frakes, 1975] and is interpreted by Luyendyk, et al. [2001] in the eastern Ross Sea. At about ~1,400 mbsf drilling of the acoustic basement is expected. Only a few samples of Ross Sea basement have been recovered. Mylonitic basement was sampled at DSDP Site 270 [Hayes and Frakes, 1975] and mylonites were dredged off Cape Colbeck, in the eastern Ross Sea [Luyendyk, et al., 2001]. The C-19 site offers an excellent new location to sample basement rocks, which in this region may consist of the Ferrar Dolerites, Beacon Sandstone, mylonites or another rock type.

4-5. Summary & Conclusions

The Coulman High drill site and C-19 survey site are characterized by N-S trending normal faults interpreted to offset and deform pre-Oligocene (RSS-1) strata. Interpretations of seismic reflection data shows the acoustic basement is faulted into tilted blocks, forming half-grabens filled with terrestrial and subaerial synrift sediments (RSS-1-lower), most likely deposited during Cretaceous Ross Sea extension. Faulting and tilting of RSS-1-upper indicates a second extension event took place prior to the formation of unconformity RSU6 (~30 Ma) and the deposition of Oligocene RSS-2. Extension of this portion of the Ross Sea may correspond to Eocene seafloor spreading of the Adare Trough. The Oligocene RSS-2 sequence can be divided into a lower and upper unit by new unconformity RSU5a. RSU5a has been correlated into the Central Trough and to the Cape Roberts drill site in the Victoria Land Basin where the unconformity is interpreted to mark a change in tilt between the lower and upper unit. Unconformity RSU5a is most likely a regional unconformity throughout the western Ross Sea and may record the end of the TAM uplift.

Gravity maps across the C-19 survey reflect a strong Moho signal, indicating Central Trough crust has been significantly extended compared to the Coulman High. This interpretation agrees with crustal profiles showing the Coulman High crust is >20 km thick and the Central Trough crust is ~10 km thick [Trey, et al., 1999]. Basement reflectors interpreted in the seismic data may correlate to the top of magnetic anomalies observed throughout the C-19 region. The magnetic anomalies have been explained as young Cenozoic volcanic intrusions, outcropping at the

seafloor [Behrendt, et al., 1996]. However, seismic data does not show any evidence for volcanic intrusions penetrating the stratigraphy the seafloor. Therefore, the magnetic anomalies must be older than previously though, possibly corresponding to intrusions emplaced during extensional episodes of the Ross Sea. It seems likely the anomalies were emplaced during Tertiary extension, possibly resulting from Adare Trough spreading. An alternative explanation is the anomalies may result from volcanism that pre-dates Ross Sea extension.

The C-19 site provides an excellent location for sampling Oligocene and older Ross Sea strata using the ice shelf as a drilling platform in the ANDRILL program. The C-19 site offers a location where strata not cored at the DSDP sites or Cape Roberts can be sampled using the ANDRILL drilling rig. This site is logically close to McMurdo Station and provides an opportunity to study the climatic and tectonic history of the Ross Sea away from the TAM, which may influence processes within the Victoria Land Basin.

Strata expected to be recovered at C-19 include subaerial syntectonic Cretaceous (?) and marine Eocene (?) units as well as Oligocene glacial-marine strata. Sampling these units will better constrain the timing of tectonic events and subsidence in the Ross Sea. It will reveal information about the paleoenvironment at the time of deposition, possibly recording a change from a sub-aerial environment, possibly at significant elevation, to a marine setting. Also, re-sampling Oligocene glacial-marine strata will help to better constrain the onset of glaciation between East and West Antarctica.

This drill location will sample Ross Sea basement, which has not been sampled in the western Ross Sea except near the Transantarctic Mountains. Samples of Ross Sea basement have only been recovered at DSDP Site 270 [Hayes and Frakes, 1975] and from dredging off Cape Colbeck [Luyendyk, et al., 2001], both in the eastern Ross Sea. Considering the immense size of the Ross Sea, more basement samples are needed to understand the tectonic evolution of the Ross Sea. Basement at C-19 may be composed or mylonites or some other rock type such as the Beacon Sandstone or Ferrar Dolerites. Coring here will allow for comparing and extending the results of the Cape Roberts Project further east in the Ross Sea. Finally, coring at C-19 will test the hypothesis that unit RSS-2 is equivalent to unit V4 at CRP as well as test other relationships between the RSS units and the V units of the Ross Sea.

References Cited

- Bartek, L. R., B. P. Luyendyk, C. Bi, and S. Kluiving (1996), Initial results of stratigraphic analyses from marine geological and geophysical cruise offshore Marie Byrd Land, Antarctica, *Geol. Soc. Amer. abstracts with programs*, 28, A-422.
- Behrendt, J. C., W. E. LeMasurier, A. K. Cooper, F. Tessensohn, A. Trebu, and D. Damaske (1991), Geophysical studies of the West Antarctic Rift System, *Tectonics*, 10, 1257-1273.
- Behrendt, J. C., R. Saltus, D. Damaske, A. M. McCafferty, C. A. Finn, D. Blankenship, and R. E. Bell (1996), Patterns of late Cenozoic volcanic and tectonic activity in the West Antarctic rift system revealed by aeromagnetic surveys, *Tectonics*, 15, 660-676.
- Busetti, M., and A. K. Cooper (1994), Possible ages and origins of unconformity U6 in the Ross Sea, Antarctica, *Terra Antarctica*, 1, 341-343.
- Cande, S. C., J. M. Stock, D. Müller, and T. Ishihara (2000), Cenozoic Motion between East and West Antarctica, *Nature*, 404, 145-150.
- Cape-Roberts-Science-Team (2000), Summary of Results, Initial Report on CRP-3, Cape Roberts Project, Antarctica, *Terra Antarctica*, 7, 185-209.
- Chiappini, M., F. Ferraccioli, E. Bozzo, and D. Damaske (2002), Regional compilation and analysis of aeromagnetic anomalies for the Transantarctic Mountains–Ross Sea sector of the Antarctic, *Tectonophysics*, 347, 121– 137.
- Cooper, A. K., F. J. Davey, and J. C. Behrendt (1987), Seismic stratigraphy and structure of the Victoria Land Basin, western Ross Sea, Antarctica, in *The Antarctic Continental Margin: Geology and Geophysics of the Western Ross Sea*, edited by A. K. Cooper and F. J. Davey, pp. 27-65, Circum-Pacific Council for Energy and Mineral Resources, Houston, Texas.
- Davey, F. J., G. Brancolini, R. J. Hamilton, S. A. Henrys, C. C. Sorlien, and L. R. Bartek (2000), A revised correlation of seismic stratigraphy at the Cape Roberts drill sites with the seismic stratigraphy of the Victoria Land basin, in *Studies from the Cape Roberts Project, Ross Sea, Antarctica; scientific results of CRP-2/2A; Part I, Geophysics and physical properties studies for CRP-2/2A*, edited by F. J. Davey and R. D. Jarrard, pp. 215-220, Terra Antarctica.

Decesari, R. C., B. P. Luyendyk, L. R. Bartek, C. C. Sorlien, D. S. Wilson, J. B. Diebold, and S. E. Hopkins (2004), Ice shelf drill sites proposed to study Pre-Late Oligocene climate and tectonic history, Coulman High, Southwestern Ross Sea, Antarctica, *EOS Trans. AGU*, 85, Fall Meet. Suppl., Abstract T11A-1244.

Decesari, R. C., C. C. Sorlien, B. P. Luyendyk, L. R. Bartek, J. B. Diebold, and D. S. Wilson (2003), Tectonic evolution of the Coulman High and Central Trough along the Ross Ice Shelf, Southwestern Ross Sea, Antarctica, *EOS Trans. AGU*, 84, Fall Meeting Suppl. Abstract T12A-0447.

DeSantis, L., J. B. Anderson, G. Brancolini, and I. Zayatz (1995), Seismic record of Late Oligocene through Miocene glaciation on the central and eastern continental shelf of the Ross Sea, in *Geology and seismic stratigraphy of the Antarctic margin*, edited by A. K. Cooper, P. F. Barker and G. Brancolini, pp. 235-260, Amer. Geophys. Union, Washington, D. C.

Fitzgerald, P. G., and S. L. Baldwin (1997), Detachment Fault Model for the Evolution of the Ross Embayment, in *The Antarctic Region: Geological Evolution and Processes*, edited by C. A. Ricci, pp. 555-564, Terra Antarctica Pub., Siena.

Hamilton, R. J., B. P. Luyendyk, C. C. Sorlien, and L. R. Bartek (2001), Cenozoic Tectonics of the Cape Roberts Rift Basin, and Transantarctic Mountains Front, Southwestern Ross Sea, Antarctica, *Tectonics*, 20, 325-342.

Hannah, M. J. (1997), Climate controlled dinoflagellate distribution in late Eocene/earliest Oligocene strata from the CIROS-1 drill hole, McMurdo Sound, Antarctica, *Terra Antarctica*, 4, 73-78.

Hannah, M. J., M. B. Cita, R. Coccioni, and S. Monechi (1997), The Eocene/Oligocene boundary at 70 degrees south, McMurdo Sound, Antarctica, *Terra Antarctica*, 4, 79-87.

Hayes, D. E., and L. A. Frakes (1975), General synthesis: Deep Sea Drilling Project 28, in *Initial Reports of the Deep Sea Drilling Project, Leg 28*, edited by D. E. Hayes and L. A. Frakes, pp. 919-942, U.S. Government Printing Office, Washington, D.C.

Henrys, S. A., L. R. Bartek, G. Brancolini, B. P. Luyendyk, R. J. Hamilton, C. C. Sorlien, and F. J. Davey (1998), Seismic stratigraphy of the pre-quaternary strata off Cape Roberts and their correlation with strata cored in the CIROS-1 drill hole, McMurdo sound, *Terra Antarctica*, 5, 273-279.

LeMasurier, W. E., and C. A. Landis (1996), Mantle plume activity recorded by low relief erosion surfaces in West Antarctica and New Zealand, *Geol. Soc. Am. Bull.*, 108, 1450-1466.

LeMasurier, W. E., and D. C. Rex (1990), Late Cenozoic volcanism on the Antarctic Plate: An overview, in *Volcanoes of the Antarctic Plate and southern oceans*, edited by W. E. LeMasurier and J. W. Thompson, pp. 1-17, Amer. Geophys. Union, Washington, D. C.

Luyendyk, B. P., C. H. Smith, and G. Druivenga (2003), Gravity measurements on King Edward VII Peninsula, Marie Byrd Land, West Antarctica, during GANOVEX VII, *Geolog. Jahrb.*, B 95, 101-126.

Luyendyk, B. P., C. C. Sorlien, D. S. Wilson, L. R. Bartek, and C. H. Siddoway (2001), Structural and tectonic evolution of the Ross Sea rift in the Cape Colbeck region, Eastern Ross Sea, Antarctica, *Tectonics*, 20, 933-958.

Luyendyk, B. P., D. S. Wilson, and R. Decesari (2002), New Maps of Gravity and Bedrock-Bathymetry of the Ross Sea Sector of Antarctica, *EOS, Transactions of the American Geophysical Union, Fall Meeting Supplement*, 83, F1357.

Naish, T. R., P. J. Barrett, G. B. Dunbar, K. J. Woolfe, A. G. Dunn, S. Henrys, M. Claps, R. D. Powell, and C. R. A. Fielding (2001), Studies from the Cape Robert Project, Ross Sea, Antarctica; scientific report of CRP-3; Part 1, Sedimentary environments for CRP-3, *Terra Antarctica*, 8, 225-244.

Richard, S. M., C. H. Smith, D. L. Kimbrough, P. G. Fitzgerald, B. P. Luyendyk, and M. O. McWilliams (1994), Cooling history of the northern Ford Ranges, Marie Byrd Land, West Antarctica, *Tectonics*, 13, 837-857.

Siddoway, C. S., S. L. Baldwin, P. G. Fitzgerald, C. M. Fanning, and B. P. Luyendyk (2004), Ross Sea mylonites and the timing of continental extension between East and West Antarctica, *Geology*, 32, 57-60.

Thomas, R. H., D. R. MacAyeal, D. H. Eilers, and D. R. Gaylord (1984), Glaciological studies on the Ross Ice Shelf, Antarctica, 1973-1978, *Ant. Res. Ser.*, 42, 21-53.

Trey, H., A. K. Cooper, G. Pellis, B. Della Vedova, G. Cochrane, G. Brancolini, and J. Makris (1999), Transect across the West Antarctic rift system in the Ross Sea, Antarctica, *Tectonophysics*, 301, 61-74.

Wilson, G. S., A. P. Roberts, K. L. Verosub, F. Florindo, and L. Sagnotti (1998), Magnetobiostrati-graphic chronology of the Eocene-Oligocene transition in the CIROS-1 core, Victoria Land margin, Antarctica: Implications for Antarctic glacial history, *Geol. Soc. Am. Bull.*, 110, 35-47.

Zachos, J., M. Pagani, L. Sloan, E. Thomas, and K. Billups (2001), Trends, rhythms, and aberrations in global climate 65 Ma to present, *Science*, 292, 686-693.



Chapter 5

A Model for the Tectonic Evolution of the Ross Sea

The Ross Sea may be the key for understanding the tectonic evolution of the West Antarctic Rift System. Because the western and eastern sides of the WARS are drastically different in terms of structural style, the Ross Sea plays an important part in linking and understanding the rift system. Due to the lack of data in the Ross Sea, parallels must be drawn with the depositional and tectonic history of the Campbell Plateau and South Tasman Rise. This conclusion chapter integrates stratigraphic evidence, subsidence history, geological evidence from the TAM and western Marie Byrd Land, and evidence from conjugate rift margins of the Ross Sea to develop an overall picture of the Mesozoic and Cenozoic tectonic history and formation of the Ross Sea region.

Crustal reconstructions, based on the subsidence history of the Ross Sea, indicate the region was originally underlain by thickened continental crust on the order of 50 km. The region would have been significantly above sea level during the early and middle Cretaceous. If the TAM are a remnant piece of the original Ross Sea crust, then current crustal thickness of the TAM (~ 40 km) [Studinger, et al., 2004] supports this idea. This suggests the Ross Sea was significantly above sea level prior

to the onset of extension. At this time, the Campbell Plateau and South Tasman Rise would have been attached to the Ross Sea. Therefore, these regions would also have been areas of thickened crust, with topography significantly above sea level. Crustal thickening of the region could have resulted from subduction of the Phoenix Plate under this sector of Gondwana, prior to Cretaceous extension of the region.

At approximately 95 Ma, crustal extension began between East and West Antarctica, most likely along detachment systems in the Ross Sea [Davey and Brancolini, 1995; Fitzgerald and Baldwin, 1997; Siddoway, et al., 2004]. Evidence for Cretaceous extension is widespread throughout the region. This includes extensional structures on the Campbell Plateau, South Tasman Rise, western Marie Byrd Land, and within the Ross Sea. Rift-related Cretaceous volcanism is interpreted in Ford Ranges of Marie Byrd Land [Luyendyk and Smith, 1994]. Also, mylonites were recovered in the eastern Ross Sea and indicate significant Cretaceous extension [Hayes and Frakes, 1975; Luyendyk, et al., 2001; Siddoway, et al., 2004].

Cretaceous synrift sediment is interpreted within basement grabens on the Campbell Plateau, South Tasman Rise, and Ross Sea, indicating active extension of the East Gondwana region during the deposition of these units. Core data from the Campbell Plateau and STR shows the Cretaceous sequences are terrestrial in origin [Beggs, 1993; Hill and Moore, 2001]. Synrift strata filling half-grabens in the Ross Sea are also interpreted as terrigenous in origin [Luyendyk, et al., 2001] and may correspond to synrift units on the Campbell Plateau and STR based on seismic character and stratigraphic position. If this is the case, then the argument that

Cretaceous RSS-1-lower is terrigenous in origin is strengthened, suggesting the Ross Sea was above sea level during its deposition and deformation.

The West Antarctic Erosion Surface offers further evidence that the region was significantly above sea level. The WAES is at significant elevation in Marie Byrd Land [LeMasurier and Landis, 1996] and is interpreted in the Ross Sea [*Luyendyk, et al., 2001; Decesari, et al., 2003; Decesari, et al., 2004*]. Based on these data, it seems likely the Ross Sea was at significant elevation in the Late Cretaceous. The Waipounamu Erosion Surface, found on the Campbell Plateau, is interpreted as an extension of the WAES [LeMasurier and Landis, 1996]. If this is the case, then the Campbell Plateau would also have been significantly above sea level in the Late Cretaceous. By 79 Ma, the Campbell Plateau rifted off from the Ross Sea region and presumably began to subside below sea level.

One result of Cretaceous extension of the Ross Sea is the development of an elevation differential between the un-rifted TAM block and the extended Ross Sea. The Ross Sea would have subsided relative to the TAM block. Continued subsidence due to thermal cooling would only increase the elevation differential between the Ross Sea and the TAM block over time. Therefore, erosion of the TAM block would likely occur as a result of this differential, forming the present-day TAM. Eroded sediment from the TAM would likely be transported into the Ross Sea and deposited there. Major denudation of the TAM occurred in the Paleocene [Fitzgerald, 1992]. If the denudation was the result of TAM erosion, then there would have to be Paleocene sediments in the Ross Sea. This interpretation is problematic because no Paleocene

sediments have been interpreted or sampled in the Ross Sea to date. However, Paleocene sediments have been sampled on the South Tasman Rise. The STR was attached to the western Ross Sea during the Paleocene and did not rift off until 33.5 Ma [*Hill and Exxon*, 2004]. This suggests Paleocene sediment may be in the western Ross Sea.

Paleocene sediments cored on the STR were derived from continental material and contain pollen and spore assemblages indicating a terrigenous origin [Exon, et al., 2001, 2004]. The sediments were deposited in a shallow deltaic setting [Exon, et al., 2001, 2004]. During the Paleocene, the STR was situated off Northern Victoria Land and the TAM. The only possible source of Paleocene continental sediments was from the TAM. The Campbell Plateau had rifted away by this time, and Tasmania was separated from the STR by oceanic crust, making these regions highly unlikely sources of continental sediments. Sedimentation rates, recorded from the fossil record, during the Paleocene on the STR were rapid (4-12 cm/ky) [Exon, et al., 2001]. Similarly, the denudation rate of the northern TAM was also rapid at this time (~12cm/ky) [Fitzgerald, 1994, 2002]. Therefore, it is possible that the elevation differential between the Ross Sea and the TAM block resulted in significant erosion during the Paleocene forming the TAM range. Buried rocks would have been exhumed at this time, explaining the Paleocene exhumation ages of the TAM. The eroded material would have been depositing on the STR and in Ross Sea. Faults interpreted along the TAM front, in the VLB, are interpreted to have controlled the uplift of the TAM [Hamilton, et al., 2001]. These faults may have controlled the

subsidence of the Ross Sea, relative to a stationary TAM front. However, unloading of the footwall (Ross Sea block) could have resulted in upward tilting of the TAM block.

Eocene spreading of the Adare Trough resulted in further extension of the Ross Sea, probably in locations of existing weak crust corresponding to the detachment systems formed during Cretaceous extension. At this time, the present-day basin-and-range structure of the Ross Sea formed, resulting in the subsidence of the basins below sea level. Deposition and deformation of the shallow marine RSS-1-upper unit occurred during this rift phase. After Tertiary extension ended, the Ross Sea continued to thermally subside. A sea level fall at ~30 Ma resulted in the formation of unconformity RSU6, corresponding with a shift to a colder climate and glaciation [DeSantis, et al., 1995]. Extension must have been completed by this time because RSU6 and Oligocene strata above is not faulted in the Ross Sea. Subsidence of the Ross Sea basins occurred after this, resulting in the necessary accommodation space for the deposition of Oligocene glacial-marine RSS-2 and post RSS-2 strata. Predicted thermal cooling curves indicate the Ross Sea should still be subsiding, allowing for further deposition within the basins.

To test this model, more core data is needed from the Ross Sea, Campbell Plateau, and South Tasman Rise, sampling Cretaceous and early Tertiary sediments. Subsidence studies have been done in the Great South Basin on the Campbell Plateau [Cook, et al., 1999]. However, the results were not conclusive and further work needs to be done to better understand and constrain the subsidence and rifting history of the

Campbell Plateau. This would allow for direct comparisons of the Campbell Plateau and Ross Sea subsidence histories. Similarly, a subsidence analysis of the South Tasman Rise would also be useful. Most importantly, locating Paleocene sediments in the Ross Sea is critical for testing this theory. Currently these sediments are not imaged on seismic data, but configuring seismic gear for deeper penetration may help to image these sediments within the VLB. More core data from the Ross Sea may also discover Paleocene sediments in the Ross Sea. Drilling along the Ross Ice Shelf will result in better constraints of pre-Oligocene sediment lithology and age. Understanding the sedimentary infill of the Ross Sea will better constrain the timing and magnitude of tectonic events of the West Antarctic Rift System.

References Cited

- Beggs, J. M. (1993), Depositional and tectonic history of Great South Basin, in *South Pacific Sedimentary Basins*, edited by P. F. Balance, pp. 365-373, Elsevier, Amsterdam.
- Cook, R. A., R. Sutherland, and H. Zhu (1999), Cretaceous-Cenozoic Geology and Petroleum Systems of the Great South Basin, New Zealand, *Institute of Geological and Nuclear Sciences Monograph*, 20, 188.
- Davey, F. J., and G. Brancolini (1995), The Late Mesozoic and Cenozoic structural setting of the Ross Sea region, in *Geology and Seismic Stratigraphy of the Antarctic Margin*, edited by A. K. Cooper, P. F. Barker and G. Brancolini, pp. 167-182, Amer. Geophys. Union, Washington, D.C.
- Decesari, R. C., B. P. Luyendyk, L. R. Bartek, C. C. Sorlien, D. S. Wilson, J. B. Diebold, and S. E. Hopkins (2004), Ice shelf drill sites proposed to study Pre-Late Oligocene climate and tectonic history, Coulman High, Southwestern Ross Sea, Antarctica, *EOS Trans. AGU*, 85, Fall Meet. Suppl., Abstract T11A-1244.
- Decesari, R. C., C. C. Sorlien, B. P. Luyendyk, L. R. Bartek, J. B. Diebold, and D. S. Wilson (2003), Tectonic evolution of the Coulman High and Central Trough along the Ross Ice Shelf, Southwestern Ross Sea, Antarctica, *EOS Trans. AGU*, 84, Fall Meeting Suppl. Abstract T12A-0447.
- DeSantis, L., J. B. Anderson, G. Brancolini, and I. Zayatz (1995), Seismic record of Late Oligocene through Miocene glaciation on the central and eastern continental shelf of the Ross Sea, in *Geology and seismic stratigraphy of the Antarctic margin*, edited by A. K. Cooper, P. F. Barker and G. Brancolini, pp. 235-260, Amer. Geophys. Union, Washington, D. C.
- Exon, N. F., J. P. Kennett, and M. J. Malone (2001), Leg 189 Summary, in *Proceedings of the Ocean Drilling Program, Initial Reports*, edited by J. M. Scroggs.
- Exon, N. F., J. P. Kennett, and M. J. Malone (2004), Leg 189 Synthesis: Cretaceous-Holocene History of the Tasmanian Gateway, in *Proceedings of the Ocean Drilling Program*, edited by N. F. Exon, J. P. Kennett and M. J. Malone.

Fitzgerald, P. G. (2002), Tectonics and landscape evolution of the Antarctic Plate since the breakup of Gondwana with an emphasis on the West Antarctic Rift System and the Transantarctic Mountains, in *Antarctica at the Close of a Millennium: Proceedings of the 8th International Symposium on Antarctic Earth Sciences, Wellington, 1999*, edited by J. A. Gamble, D. N. B. Skinner and S. Henrys, pp. 453-469, The Royal Society of New Zealand, Wellington, New Zealand.

Fitzgerald, P. G. (1994), Thermochronologic constraints on post-Paleozoic tectonic evolution of the central Transantarctic Mountains, Antarctic, *Tectonics*, 13, 818-836.

Fitzgerald, P. G. (1992), The Transantarctic Mountains of Southern Victoria Land: The application of apatite fission track analysis to a rift shoulder uplift, *Tectonics*, 11, 634-662.

Fitzgerald, P. G., and S. L. Baldwin (1997), Detachment Fault Model for the Evolution of the Ross Embayment, in *The Antarctic Region: Geological Evolution and Processes*, edited by C. A. Ricci, pp. 555-564, Terra Antarctica Pub., Siena.

Hamilton, R. J., B. P. Luyendyk, C. C. Sorlien, and L. R. Bartek (2001), Cenozoic Tectonics of the Cape Roberts Rift Basin, and Transantarctic Mountains Front, Southwestern Ross Sea, Antarctica, *Tectonics*, 20, 325-342.

Hayes, D. E., and L. A. Frakes (1975), General synthesis: Deep Sea Drilling Project 28, in *Initial Reports of the Deep Sea Drilling Project, Leg 28*, edited by D. E. Hayes and L. A. Frakes, pp. 919-942, U.S. Government Printing Office, Washington, D.C.

Hill, P. J., and N. Exon (2004), Tectonics and Basin Development of the Offshore Tasmanian Area Incorporating Results from Deep Ocean Drilling, *Geophysical Monograph Series*, 151, 19-41.

Hill, P. J., and A. M. G. Moore (2001), Geological Framework of the South Tasman Rise and East Tasman Plateau, *Geoscience Aust. Rec.*, 2001.

LeMasurier, W. E., and C. A. Landis (1996), Mantle plume activity recorded by low relief erosion surfaces in West Antarctica and New Zealand, *Geol. Soc. Am. Bull.*, 108, 1450-1466.

Luyendyk, B. P., and C. H. Smith (1994), Geological Expedition to King Edward VII Peninsula and the Ford Ranges, Marie Byrd Land, Antarctic, *Antarctic J. of the US*, 28, 10-13.

Luyendyk, B. P., C. C. Sorlien, D. S. Wilson, L. R. Bartek, and C. H. Siddoway (2001), Structural and tectonic evolution of the Ross Sea rift in the Cape Colbeck region, Eastern Ross Sea, Antarctica, *Tectonics*, 20, 933-958.

Siddoway, C. S., S. L. Baldwin, P. G. Fitzgerald, C. M. Fanning, and B. P. Luyendyk (2004), Ross Sea mylonites and the timing of continental extension between East and West Antarctica, *Geology*, 32, 57-60.

Studinger, M., R. E. Bell, W. R. Buck, G. Karner, and D. Blankenship (2004), Sub-ice geology inland of the Transantarctic Mountains in light of new aerogeophysical data, *Earth Planet. Sci. Lett.*, 220, 391-408.

Appendix A

NBP-0301 and NBP-0306 Cruise Details

RVIB *Nathaniel B. Palmer* was used as the geophysical platform for cruises 03-01 (NBP-0301; January, 2003) and 03-06 (NBP-0306; January, 2004) along the Ross Ice Shelf front. Underway geophysical data collected by NBP-0301 and NBP-0306 include multichannel and single channel seismic reflection data, gravity and magnetic field data, multibeam sonar, and deep tow side scan and chirp data. Kasten gravity cores were also recovered on both cruises.

Data Systems Employed: NBP-0301

Data Type	Data Coverage	System Performance
Multichannel Seismic Reflection (MCS)*	2,253 km	Excellent acquisition. Faulty streamer lead in. Gun controller synchronizing problem. Failure of two airguns.
Single Channel Seismic Reflection (SCS)*	2,500 km	Good data acquisition. No problems encountered.
Multibeam Sonar	5,246 km	130-degree swath acquired. Backscatter data of moderate quality. Excellent acquisition, except when pushing through ice. 120 beams.
Gravity	5,246 km	Consistent data coverage. Unknown noise of 5 milligals in data. Removed via filter.
Magnetic Field	3,053 km	Cesium magnetometer. Collected on most profiles. Excellent data acquisition.
Deep Tow Side Scan and Chirp Sonar	Grid at C-19 Site; 5 lines @ 4 km	Functioned without problems

* See text below for details

Data Systems Employed: NBP-0306

Data Type	Data Coverage	System Performance
Multichannel Seismic Reflection (MCS)*	1,400 km	High quality data obtained with excellent resolution. No major problems encountered.
Sonobuoys*	Launched several times a day	Wide-angle reflections obtained. Recorded on OYO aux channel one.
Single Channel Seismic Reflection (SCS)*	1,400 km	High quality data acquisition. No problems encountered.
Multibeam sonar	~2,000 km	126-degree swath acquired. Backscatter data of high quality. Excellent acquisition, except when pushing through ice. 120 beams.
Gravity	~2,000 km	Consistent coverage of good quality. Noise on previous cruises fixed by gyro change-out.
Magnetic field	~2,000 km	Proton magnetometer. Collected on most profiles. Excellent data acquisition.
Deep tow side scan and chirp sonar	Grid at 172° W	Functioned without problems

* See text below for details

A) Seismic Data

1) **NBP-0301:** Multichannel seismic data (MCS) collection was carried out in three phases depending on structure, ice and weather. The first phase, 2003 Julian Day (JD) 008-014, consisted of an array of five 105/105 in³ generator injector (GI) airguns. Originally, six GI guns were deployed, but a manufacturing problem with the array umbilical left only enough intact connectors (three pair required for each GI gun) for five GI guns. A problem with the software synchronizing the GI shooting with the Syntron GCS90 airgun controller meant only four GI guns could be fired at a time. The fifth gun was deployed as a backup. By the end of this phase, two GI guns failed leaving three MCS GI guns firing.

The second phase included entering the deeper basins of the western Ross Sea. The GI gun array was recovered and swapped with an array of six Bolt 1500C Long Life airguns ranging in volume from 80 in³ to 850 in³ totaling 3,000 in³. The tuning of the array was good, matching the modeling upon which the choice of sizes was based. This array was used from JD 015-018, when ice conditions and bad weather necessitated its recovery. From JD 019-021, MCS and SCS were acquired simultaneously with a source consisting of a single GI airgun in 105/105 in³ mode (SCS/MCS alternation explained later). Systems were recovered when it became time to break ice and transit from the eastern Ross Sea back to the western Ross Sea.

The third phase of MCS acquisition occurred between JD 025-026 and included the redeployment of the six-Bolt airgun array. Acquisition ended to leave time for deployment of the deep tow chirp and side scan sonar systems, as well as sediment coring. All sound sourced were towed at 3 m depth. MCS data acquisition

Julian Days	MCS Source	Rep. Rate	Shots recorded	kilometers
008 – 014	4 or 3 105 GI	10 sec	40,650	1,016
015 – 018	6 Bolt 1500C	15 sec	12,305	461
019 - 021	1 105 GI	10 sec	17,365	434
025 – 026	6 Bolt 1500C	15 sec	9,125	342
16 days			79,445	2,253

was carried out with the S/N 48-channel analog streamer towed at 7.5 m depth. The tow leader had a faulty connection with the streamer, resulting in its failure underwater. To solve this problem, the streamer was towed from the shipboard end of

its first active section. This resulted in the loss of 4 useful channels. Despite the problem, the towing characteristics and data quality from the streamer were excellent.

Digitization of MCS data was handled by the OYO DAS-1, which was recorded on 3490 tapes and exported shot gathers to the ship's network in real time via the Triton Elics system. A number of bugs plagued the system for the first half of the leg however, once corrected high level performance was achieved. A total of one hundred thirty five 3490 data tapes were recorded in SEG-D 8048 [32-bit IBM Floating point] format.

Single channel seismic (SCS) data acquisition was conducted by alternately firing between the MCS shots using a gun delay timing unit. The unit worked extremely well synchronizing the timing of the firing of the two systems. SCS sourced varied between a single 25/25 in³ GI gun, two 15 in³ water guns and a single 105/105 in³ GI gun. The GI gun was deployed as a SCS source only in areas with high sea ice concentrations. The strength and frequency spectra of the pair of water guns were analyzed and compared to the single 25/25 in³ GI gun to determine which would be used as the primary SCS source. The frequency content of the data from the water guns ranged from 1.5 to 2 times as high as the GI gun, but the signal level was about 0.5 the amplitude. The single 25/25 in³ GI gun was selected as the primary SCS source.

Two multi-element single channel streamers were used during the survey. The University of North Carolina (UNC) provided an 30 m S/N Technologies 28 element single channel streamer, thought to be more sensitive than the NSF ITI multi-element

single channel streamer on board the *Palmer*. Comparisons were conducted to determine which streamer provided the highest data quality. Quantitative analysis of the data using the same sound source revealed that the signal to noise ratio and dynamic range was higher on the UNC S/N streamer. Therefore, the UNC streamer was used as the primary SCS streamer for the cruise.

2) NBP-0306: Both MCS and SCS systems were deployed in a similar fashion to the NBP-0301 cruise. The source for the MCS system was a six GI airgun array towed at 3 m depth for the entire cruise. The SCS system used a single 25/25 in³ GI gun. The MCS gun array became tangled with the streamer on two occasions, prompting marine technicians to shorten the tow point by 10 meters. MCS data acquisition was carried out with the S/N 48-channel analog streamer towed at 7.5 m depth. The connector problem on the lead in was fixed for this cruise, resulting in the use of all 48 channels. Single channel seismic used the UNC systems as on the NBP-0301 cruise with the 30 m S/N streamer and Erics acquisition system. High quality SCS data was obtained. Shooting interval was 10 seconds with the SCS, delayed by 7 seconds from the MCS. Sonobuoys were launched several times a day and obtained wide-angle reflection data. Sonobouy data were recorded on the OYO aux channel one.

Cruise	Lines	Shot Spacing	Airgun Type
NBP-0301	1A-12A, 27A-30A, 33A-34A	25 m	GI guns
NBP-0301	13A-24, 34B-38A1	37.5 m	Bolt guns*
NBP-0306	101-138A1	25 m	GI guns

* Due to the larger capacity Bolt gun, firing time between shots increased, thus increasing the shot spacing.

B) Ice and Weather Conditions

1) **NBP-0301:** Sea ice coverage was extensive and regulated survey operations. Generally open water offshore eastern Ross Island, at the C-19 calving site, and Edward VII Peninsula, at the B-9 calving site, allowed for good geophysical profiling. The B-15 calving site in the eastern Ross Sea remained filled with sea ice during the cruise. Persistent cloud cover meant that no visual satellite imagery was useful and microwave low-resolution images (85 MHz and NASA interpretation) were the only option to guide operations. Gale winds during part of the eastern Ross Sea survey affected the quality of seismic data collected there.

2) **NBP-0306:** In contrast to the 2002-2003 season, sea ice in the southern Ross Sea, south of 77° S, was largely absent. However, sea ice was thick in most of the Ross Sea north of 77° S compared to most seasons where it has been ice free. Ice was 50% or more in McMurdo Sound. Overall, the weather was good with calm sunny days in McMurdo Sound and overcast conditions in the western Ross Sea. South winds were at 10-15 knots and brief snow flurries occurred. In the eastern Ross Sea winds were 20 knots from the south-east, occasionally rising to 30 knots. These wind speeds did not affect data quality.

C) Survey Coverage and Science Results

1) NBP-0301: Three sites along the ice shelf front were surveyed where giant ice bergs calved off. These include the C-19 site that calved in 2001 located just east of Ross Island, the B-15 site that calved in 2000, and the B-9 site that calved in 1987 located northeast of the Bay of Whales in eastern Ross Sea. Overall project goals were twofold: to survey new exposed seafloor in preparation for drilling into the seabed from the ice shelf when it covers the survey grids in the next few years and to survey the seafloor at these site to compare open ocean and sub ice shelf processes.

Out of the three survey sites, the C-19 site was the most extensively surveyed and covers the eastern flank of the Victoria Land Basin, Coulman High and Central Trough. A grid of geophysical profiles, at a spacing of ~2 km, covering 6,000 sq. km was completed. Profiles were tied to existing seismic lines to the north. In addition, five lowerings of the SIS 1000 deep-tow side scan and chirp sub-bottom sonar system were completed. Five Kasten cores were obtained on the deep-tow survey lines. Multibeam mapping revealed a generally undulating sea floor, grooved with several meters of relief. Side scan sonar profiles were taken both in open water and at sites recently covered by C-19. These revealed scalloped and furrowed sea floor, as well as sites with partially buried grooves. Kasten cores yielded stiff grey clay overlain by green diatomaceous (?) mud. Glacially derived pebbles of volcanic, plutonic, and metamorphic origin were also found in the cores.

NBP-0301 Core #	Latitude	Longitude	Date Recovered
1	77° 08.866' S	171° 51.332' E	1/27/03
2	77° 17.498' S	171° 42.000' E	1/27/03
3	77° 25.011' S	171° 08.028' E	1/28/03
4	77° 26.239' S	171° 32.411' E	1/28/03
5	77° 05.972' S	171° 33.913' E	1/28/03

MCS and SCS profiling was completed east across the Central High and west Eastern Basin into the B-15 calving site. Profiles over the western B-15 site were completed 1 km north of the new ice shelf front. Due to sea ice conditions, this was the only sector of the B-15 site surveyed. In the eastern Ross Sea, at the B-9 site, basement outcrops in the Bay of Whales were imaged. Magnetic anomalies of several hundred nanotesla were profiled in the region. Ties were made to NBP-9601 lines 11, 25, and 26.

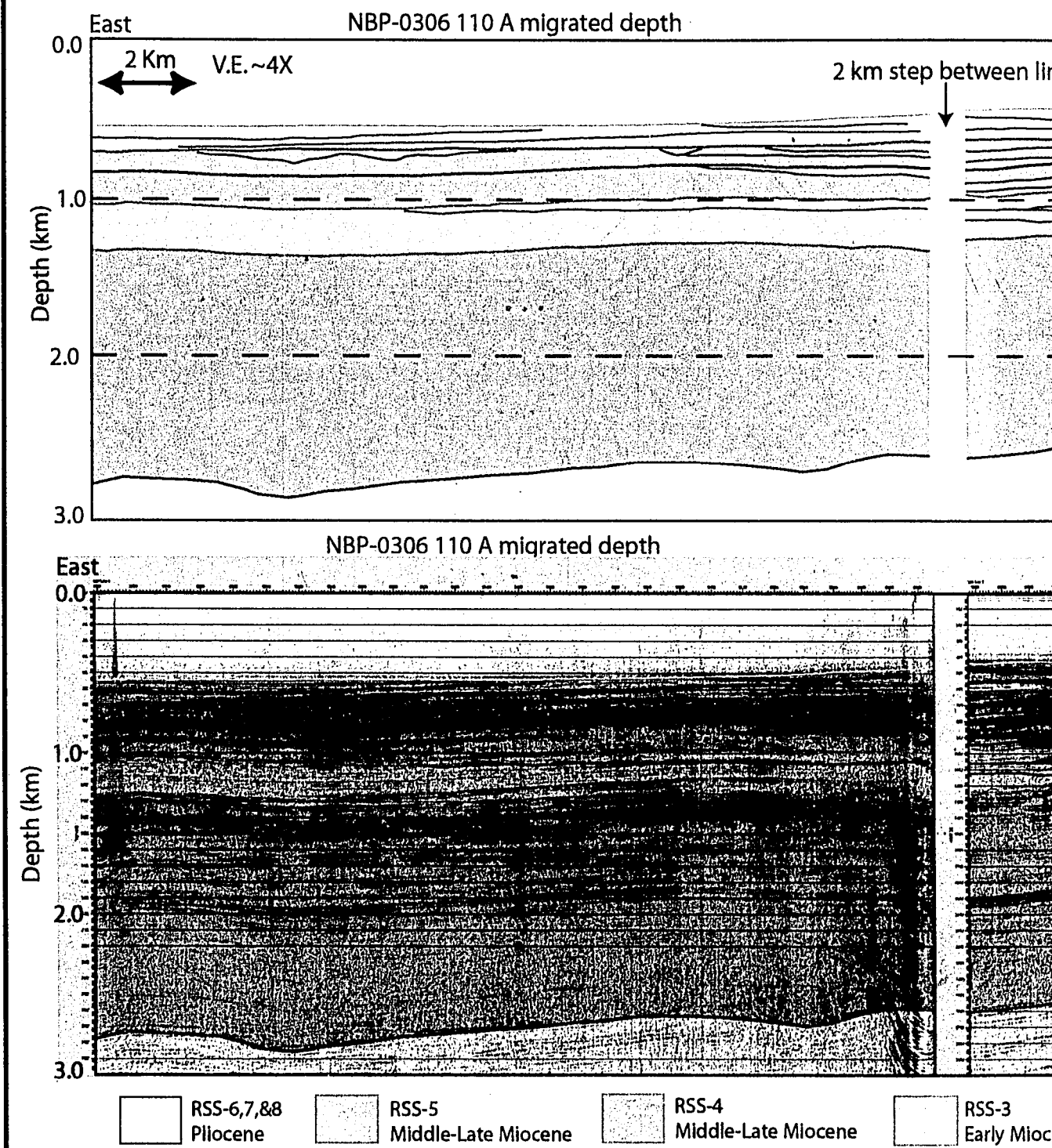
Other studies included further multibeam mapping of the MacKay Sea Valley in the western Ross Sea. These data added to mapping done on NBP-9601 and to a seismic survey that L. Bartek and S. Henrys conducted over the site in 1994. The new edge of the Ross Ice Shelf was also mapped during the surveys and east-west transits using radar bearings.

2) NBP-0306: The object of this cruise was to complete the survey of the B-15 iceberg calving site along the Ross Ice Shelf front that was attempted on NBP-0301. While transiting to the B-15 site, Russian seismic profile SM 87004-2 was tied to the C-19 site. More geophysical profiles were completed across the Central Trough and Central High as well.

Once at the B-15 site, a grid over a low-relief north-south topographic ridge near 172° W was completed. This ridge is comprised of several Plio-Pleistocene seismic stratigraphic units that are potential targets for drilling (Appendix A Fig. 1; see Chapter 2, figure 2-1c for location). Seismic data were tied to PD-90-22 and IFP-202 to the north. The SIS 1000 deep-tow side scan and chirp sub-bottom sonar system were deployed here and two Kasten cores were recovered with about 0.8-0.9 meters of sediment each. These cores were collected in a region once located under the ice shelf, prior to the B-15 calving event. Farther east, near 167° W, another grid was completed, including a tie north to NBP-9601 geophysical lines. This location is also a possible target for drilling into older strata in the Eastern Basin. The B-15 survey was completed with a grid in the Bay of Whales including a tie to NBP-0301 data in the region.

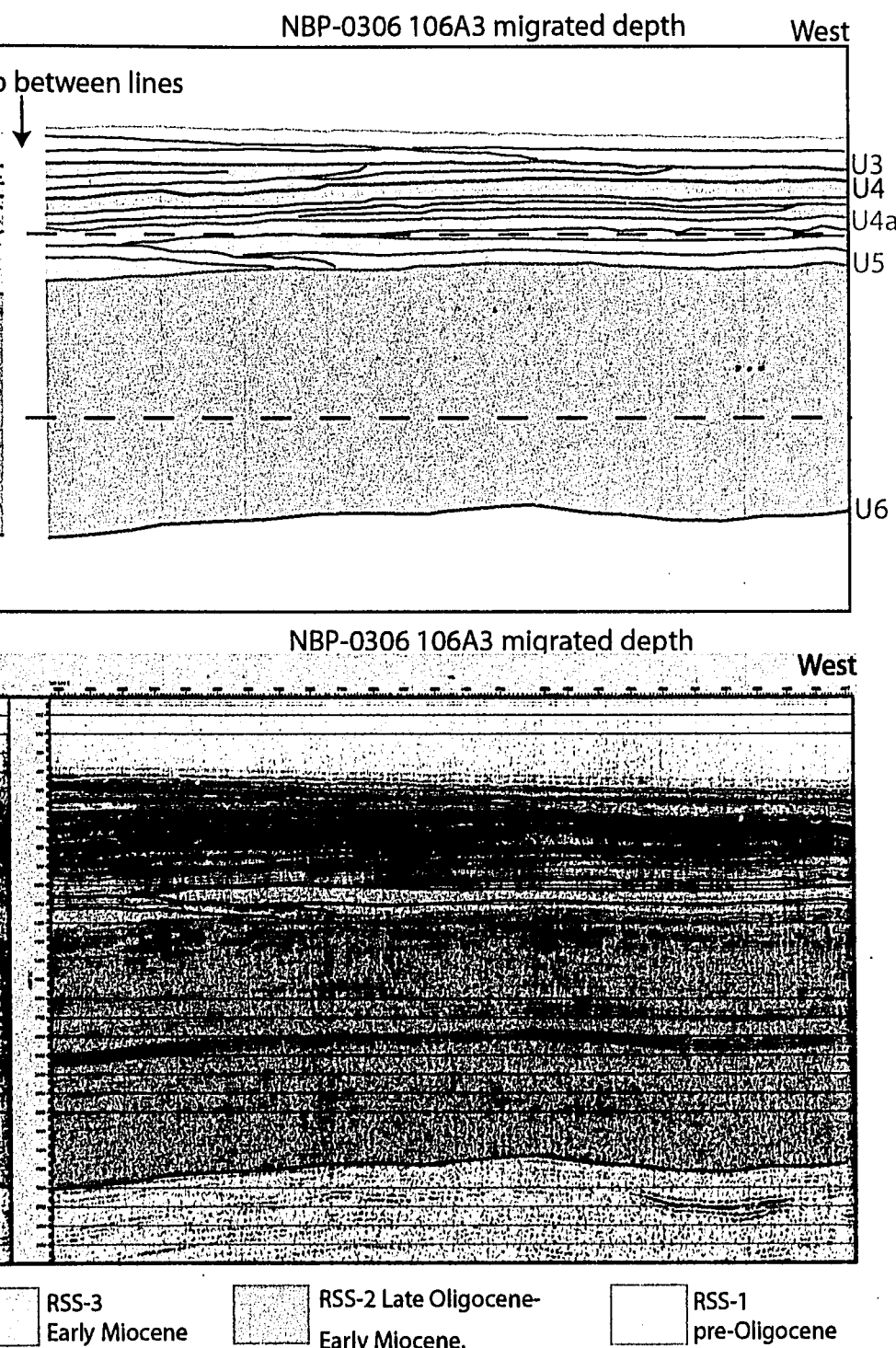
NBP-0306 Core #	Latitude	Longitude	Date Recovered
1	78° 13.578' S	171° 53.081' W	1/13/04
2	78° 08.658' S	171° 53.406' W	1/13/04

172 W Survey Site; Ross Ice Shelf Front, East

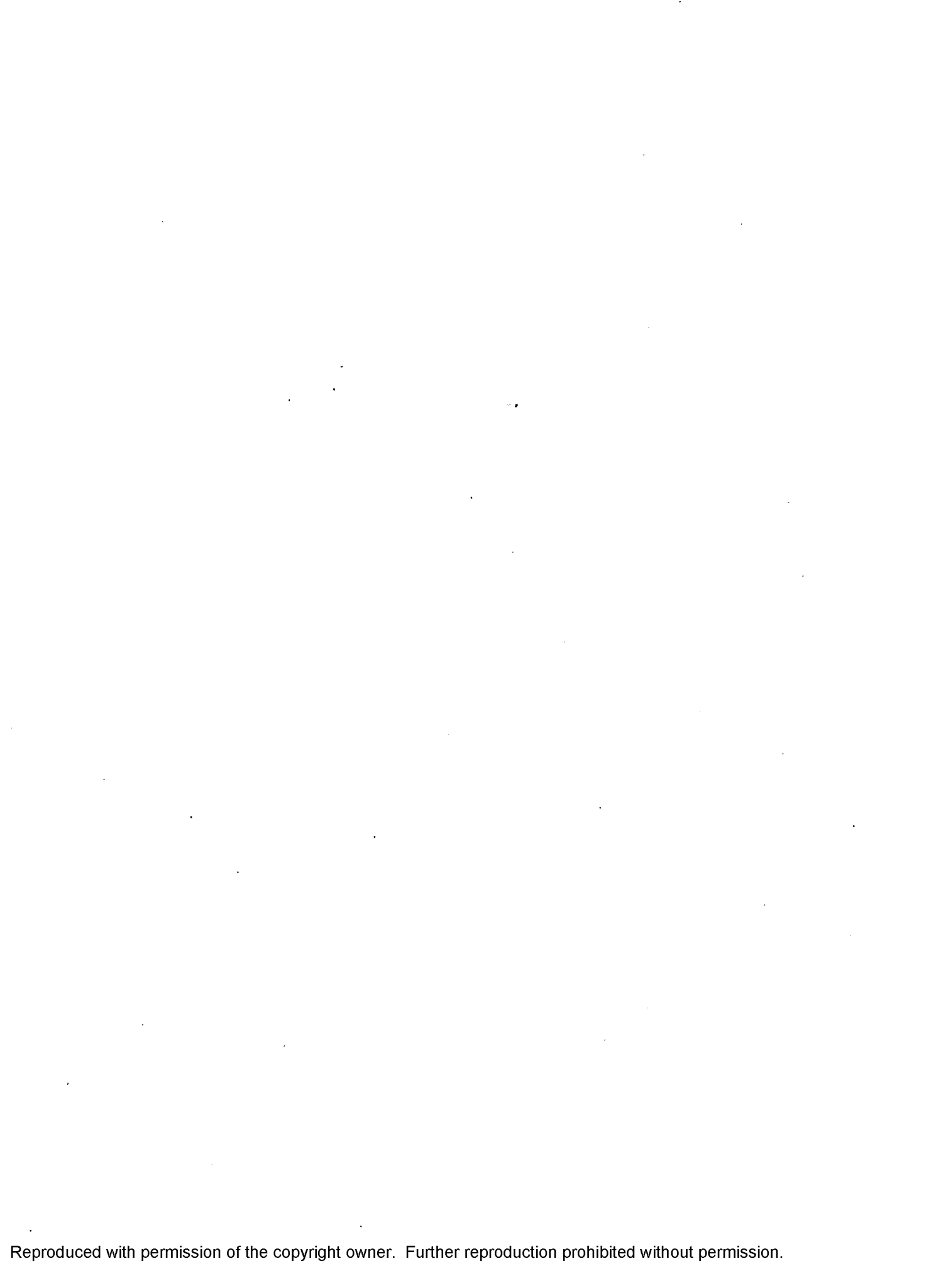




Front, Eastern Ross Sea



Appendix A Figure 1: Seismic stratigraphy at the 172 W site, eastern Ross Sea. Potential drill sites here would recover Plio-Pleistocene units RSS-6, 7 & 8, as well as Miocene RSS-5, RSS-4 and RSS-3. Sampling units here would study the glacial history of West Antarctica.



Reproduced with permission of the copyright owner. Further reproduction prohibited without permission.

Appendix B

Seismic Processing

MCS data was processed using Parallel Geoscience's Seismic Processing Workshop (SPW). SPW is PC-based software, using graphical user interfaces for processing of 2-D and 3-D seismic data. The two main components of SPW are the Flow Chart and Seisviewer. The flow chart is a graphical interface that allows each processing step to be designed, implemented and compiled. Seisviewer is used for viewing shot gathers, velocity models and seismic sections. Although slightly different processing techniques were applied to each line due to differences in noise, six basic steps have been applied to the data set and are outlined below. These steps are pre-processing and geometry definitions, velocity analysis, normal move out, multiple attenuation, stacking, and migration. Examples of flow charts used for processing NBP-0301 and NBP-0306 data can be found at the end of this section (Figs. 1&2).

A) Pre-processing and geometry definitions: Raw seismic data was recorded in SEG-D format and saved to data disks in SEG-Y format. Prior to any processing steps, raw seismic data must be converted from SEG-Y format to SPW format. This is done using the I/O Utility function of SPW. The first step of processing seismic data is defining the geometry of the survey, or relative spatial relationship between the ship, sound sources, and receivers for identification of common mid point locations. Files defining the source, receiver, and streamer are defined at this point.

Raw shot gathers are inspected to edit noisy or problematic traces. For example, the polarity of channel 13 had to be reversed throughout the data set due to a mistake in the wiring of the streamer. Other editing steps include killing of noisy and dead traces, or channels, as needed throughout the data. Also, NBP-0306 data and some of NBP-0301 data have been grouped into a uniform set of rectangular bins. Data are included in a particular bin if the midpoint falls within that bin. The traces in the bins are subsequently stacked. Traces are grouped in 25 m bins, with 12.5 m overlap between adjacent gathers to produce “super” gathers with twice the fold. This is done without reducing the number of stacked traces. In some cases where the shot spacing is less than 25 meters, the fold can be more than doubled.

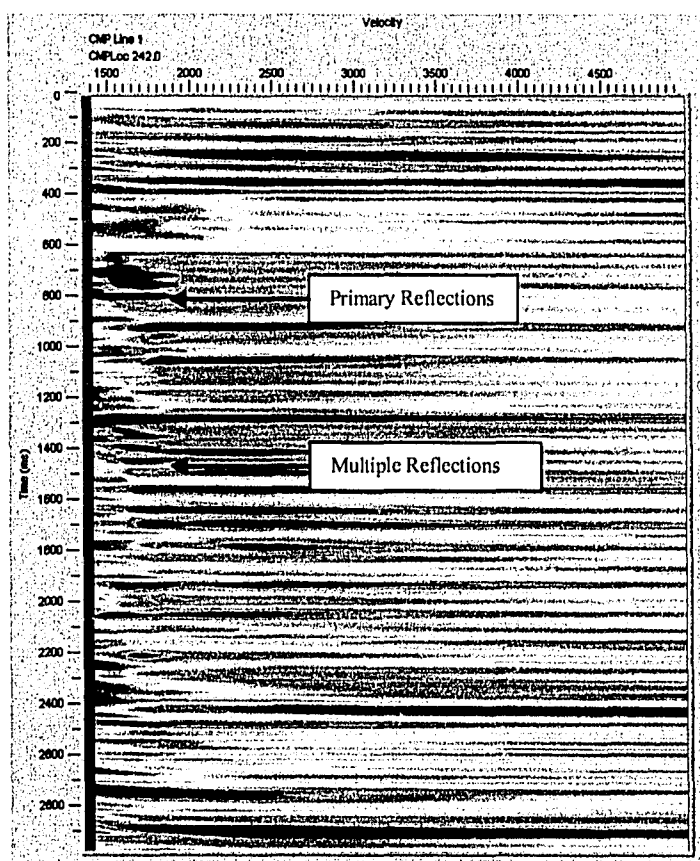
A spherical divergence correction is applied to correct for the attenuation of energy as the wave fronts spread away from the seismic source. SPW calculates the rate of energy loss and compensates for it by applying a gain function to the data to restore signal amplitudes with increasing two-way-travel-times. A time variant Butterworth filter is applied to filter out high (>110 Hz) and low frequency (<12 Hz) noise without removing real data. Depending on the amount of noise in each line, the frequency filtered is altered to optimize results. Each line processed has a frequency filter. However it may be applied at different points to maximize the effects of the filter.

B) Velocity analysis: Velocity analysis is a critical part of the processing procedure. Incorrect velocities can lead to inaccurate geology or artifacts in the data. Because two different methods of multiple attenuation (see Multiple Removal) were

used while processing the data, two different types of velocities were used. Regardless of the multiple attenuation method used, velocity analysis was completed by creating a velocity semblance model (the interactive velocity analysis tool of SPW). Velocity semblance is a statistical scaled velocity spectrum (Appendix B Fig. 1). A range of RMS velocities are applied over a function of two-way-travel-time and a measure of the degree of fit of a theoretically derived hyperbolic curve is made to hyperbolas found on the gathers. The measure of coherence is plotted as a function of time in a color contoured format and is used to pick the best RMS velocities that will correctly move out hyperbolas so that subsurface geology may be imaged after stacking.

Most NBP-0301 data went through two rounds of velocity analysis. This was done in conjunction with the F-K filter method of multiple attenuation. A first set of velocities were picked on shot gathers at 2 km intervals and were used to produce velocity semblance. Velocities were chosen intermediate to primary and multiple reflections, ensuring slower velocities were picked for primary reflections and faster velocities were picked for multiples. These velocities are called F-K velocities and were used for moving out the gathers prior to F-K filtering. F-K filtered gathers were grouped into common depth points (CDP) to form CDP gathers prior to the second round of velocity analysis. Semblance plots were created at 1 km intervals from the CDP gathers along the seismic line and stacking velocities were picked. Stacking velocities were chosen by selecting the best fit velocity for primary reflections only.

For NBP-0306 and some NBP-0301 data, the parabolic Radon Transform multiple removal method was applied in favor of the F-K filter method (see Multiple Removal). When using this processing method, only a single round of velocity analysis was necessary to select stacking velocities. Shot gathers were grouped into CDP gathers and semblance plots were created at 1 km intervals along the seismic line. Stacking velocities were chosen by selecting the best fit velocity for primary reflections. The stacking velocities were used to move out the data prior to multiple removal and stacking.



Appendix B, Figure 1: Semblance plot showing primary and multiple reflections.

C) Normal Move Out (NMO): NMO corrections were applied to gathers prior to multiple attenuation. The NMO correction applies a velocity function (picked from semblance plots) to the data set correcting for the move out of reflections as offset increases along the streamer. For NBP-0301 data, the NMO correction was first applied to gathers using the F-K velocity to over correct primary reflections and under correct multiple reflections. This was done to separate multiples from primary reflectors. For NBP-0306 and some NBP-0301 data, a NMO correction using stacking velocities was applied to CDP gathers. In this case, multiples reflections should remain under corrected, separating them from primary reflectors.

D) Multiple Attenuation: A majority of subsurface structure in the Ross Sea lies below water bottom and peg leg multiples. Therefore, a primary goal in processing was the removal of multiple energy to enhance images of real subsurface geology. Two different methods of multiple attenuation were applied to the data. This was done because a new and better de-multiple method was learned during data processing. Most of NBP-0301 data had a frequency-wave number (F-K) filter applied to remove multiples. The F-K filter transforms the overcorrected primary reflections and the undercorrected multiple reflections from the shot gather into F-K space. The primaries and multiples plot in different quadrants of F-K space. A surgical mute was applied to the transformed data, designed to cut out the multiple energy, leaving only primary reflections. Although this method produced good results, there is a possibility that primary reflections could be removed along with multiple energy. The F-K filter works well for multiple removal on far traces.

However it does not work as well on near traces because multiples here are harder to differentiate from primary reflections. As a result, most multiples on near traces are not fully filtered out and will stack in with the data, resulting in faint multiple reflections.

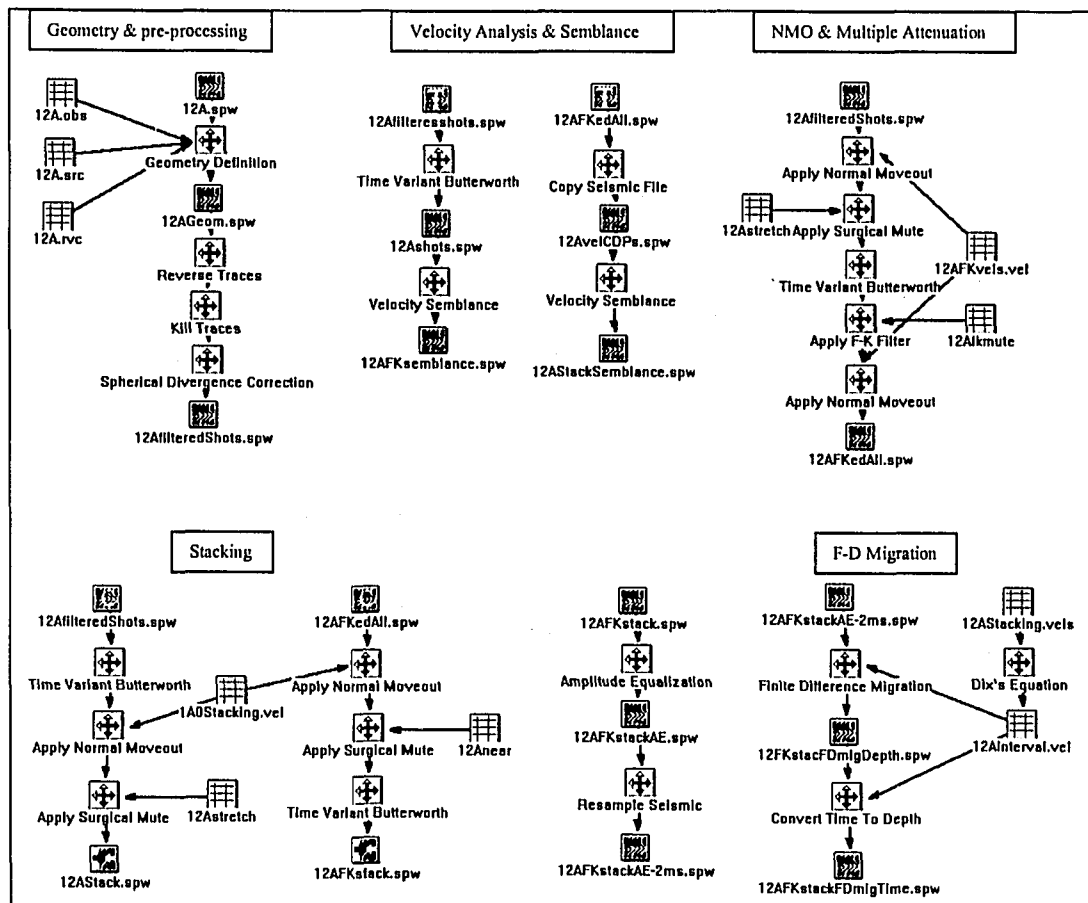
Since processing first began, a better method of multiple attenuation replaced the F-K filter technique. This method is the parabolic Radon Transform [Hampson, 1991] and was applied to NBP-0306 data and some NBP-0301 data. Prior to the Radon Transform, the data was binned in terms of even and odd CDPs. The odd CDPs are compacted into the file containing the even CDPs and run through the transform. This is done to minimize computing time. The parabolic Radon Transform changes the data from the x-y domain into τ -p domain (slowness). Parabolic Radon Transforms use offset curvature rather than just the apparent velocity used by F-K filtering, which results in multiple attenuation even on near traces. An early mute was applied to the transformed data designed to mute out primary reflections, leaving only multiples. This produces the multiple model. The multiple model was subtracted from the original CDP gathers resulting in the attenuation of multiple reflections. At this point the data was unpacked, meaning the compressed odd CDPs are relocated to their correct locations.

E) Stacking: Two stacks were compiled for each line processed: a regular stack without any multiple attenuation and a multiple attenuated stack. The regular stack uses geometry-corrected shot gathers and groups them into CDP gathers before applying a NMO correction using stacking velocities. An early mute is applied to the

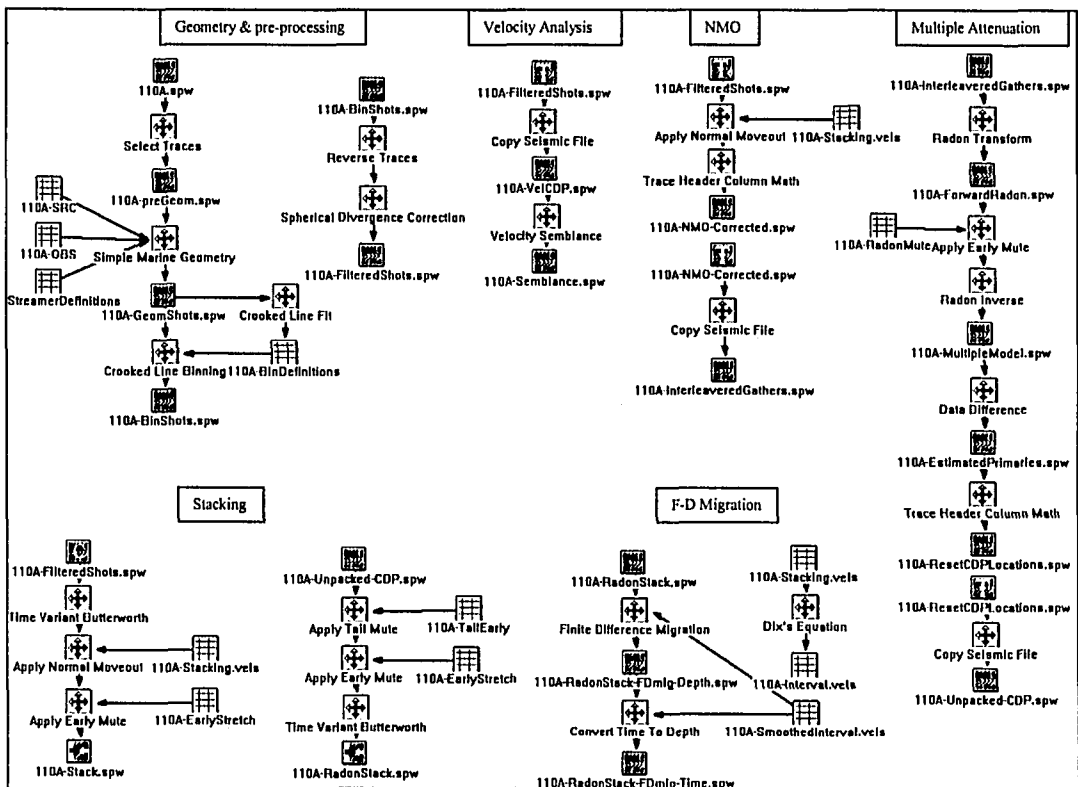
data to remove near traces starting at the multiple. The data is then stacked. The multiple attenuated stack uses CDP gathers that have been either processed via the F-K filter method or Radon Transform method and applies both an early and tail mute. The early mute is the same as in the regular stack. The tail mute removes far traces that may not have been moved out fully in the NMO correction. The data is then stacked.

F) Migration: After stacking is completed a 2-D post stack finite difference (F-D) migration is applied [*Claerbout*, 1985]. This migration is capable of locating reflectors in their correct positions even with steeply dipping reflections. It outputs a migrated section in both time and depth. In order for the F-D migration to work, a velocity model must be used. Stacking velocities were converted to interval velocities and displayed as a color velocity model. These velocities were smoothed to produce an interval velocity model used for the migration. Most of the NBP-0301 lines have been migrated as well as some of the NBP-0306 lines. Due to the time necessary to migrate the data, lines critical to understanding the subsurface geology were given priority for migration.

Appendix B, Figure 2: Typical FK-Filter Flow Chart



Appendix B, Figure 3: Typical Radon Transform Flow Chart



Appendix C

Seismic Processing Lists

Below are processing lists for NBP-0301 and NBP-0306 data. These tables describe the processing method that was applied to the lines. *Stack* refers to non-multiple attenuated seismic sections. *F-K Stack* refers to record sections with multiple attenuation using the F-K filter method. *Radon* refers to record sections with multiple attenuation using the parabolic Radon Transfer technique. *F-D Migrated* refers to whether or not the line has been migrated. A total of 6 people have worked on processing MCS data. Four were undergraduate students. A table is included showing who processed the lines.

NBP-0301 Processing List

Line #	Stack	FK Stack	Radon Stack	FD Migrated	Notes/Comments
1A	X		X		
1A0	X	X		X	
2A	X	X		X	
2B	X	X	X	X	
3A	X	X		X	
3B	X	X		X	
3B1	X	X		X	
3B2	X	X		X	
3B3	X	X		X	
3B4	X	X		X	
3B5	X	X		X	
4A	X		X	X	
4A1	X	X			
4A2	X	X		X	
4A3	X		X	X	
4B	X	X		X	4B, B1, C: processed as single line
4B1	X	X		X	4B, B1, C: processed as single line
4C	X	X		X	4B, B1, C: processed as single line
4D	X	X		X	4D, D1, D2: processed as single line
4D1	X	X		X	4D, D1, D2: processed as single line
4D2	X	X		X	4D, D1, D2: processed as single line
4D3					Several shots??
4D4	X	X		X	
4D5	X	X		X	5A, A1: processed as single line
5A1	X	X		X	5A, A1: processed as single line
5A2	X	X		X	
6A	X	X		X	
6A1	X	X		X	
6A2	X	X		X	
7A	X	X		X	

NBP	0301	Continued			
8A	X	X		X	
9A	X	X		X	
10A	X	X		X	
11A	X	X		X	
11A1	X	X		X	
12A	X	X		X	
12A1	X	X		X	
13A					Hundred shots or less
13A1	X	X			
13A2	X	X		X	
13A3	X	X		X	
13B	X	X		X	
13C	X	X		X	
14A	X		X	X	14A-A1 Processed together
14A1	X		X	X	
14A2	X		X	X	14A2-B Processed together
14B	X		X	X	
14C	X	X		X	
14D	X	X		X	
16A	X	X		X	16A-17A: processed as one line
17A	X	X		X	17A-B: processed as one line
17B	X	X		X	17A-B: processed as one line
18A	X	X		X	
18A1	X	X		X	
18B	X	X		X	18B: Part of loop not processed
18C	X	X		X	
22A	X		X	X	22A-23A processed together
23A	X		X	X	
27B	X	X		X	
28A	X	X			nothing to migrate
29A	X	X			nothing to migrate
29B	X	X			nothing to migrate
30A	X	X			
33A	X	X			
33A1	X	X		X	
34A	X		X	X	
34A1	X		X	X	
34B	X		X	X	
34C	X		X		
35A	X		X		
36A	X		X		
37A	X		X		37A, A1, A2 processed as single line
3A1	X		X		37A, A1, A2 processed as single line
37A2	X		X		37A, A1, A2 processed as single line
38A	X	X			
38A1	X	X			

NBP-0306 Processing List

Line #	Stack	Radon Stack	FD Migration
101A	X	X	
101B			
101C	X	X	
101D	X	X	
102A			
103A			
104A			
105A			
106A	X	X	X
107A	X	X	X
108A	X	X	X
109A	X	X	X
110A	X	X	X
110B	X	X	
110C			
111A			
112A			
113A			
114A			
115A			
116A			
117A			
118A			
119A	X	X	
120A	X	X	
121A	X	X	X
122A-B	X	X	
123A			
124A			
125A			
126A			
127A			
128A/A1			
128B			
128C/C1			
128D			
129A			
130A/A1			
131A	X	X	X
132A			
133A			
134A			
135A			
135B			
136A/A1			
136B			
137A			

People who processed MCS data

Processor	Lines Processed; NBP-0301	Lines Processed; NBP-0306
Robert Decesari	1A, 1A0, 4A3-12A1, 13A1, 34B-38A1	101A-D, 106A-110B, 119A-122B
Christopher Sorlien	2A-4A, 13A2-30A	
Sarah Hopkins	6A, 6A1, 33A, 33A1, 34A	
Michael Faulkner	4A1, 4A2	
Adam Morley	4A1, 4A2	
Adam Lazaro		107, 108A, 109A, 131A Started; not completed

Appendix D

Interpretation and Archiving

A) Interpretation: Processed seismic data were converted from SPW format back to SEGY format, and then imported into the Kingdom Suite interpretation software. There are two Kingdom projects, one in the eastern Ross Sea and one in the western Ross Sea. The western Ross Sea project encompasses the C-19 survey site. The C-19 project includes migrated and non-migrated seismic sections. For this reason, seismic sections are in terms of two-way-travel-time. However, several depth sections are in the project. All lines in the C-19 project have been interpreted and tied to existing Ross Sea seismic lines. The C-19 project also includes isopach maps of RSS-1-upper and RSS-2. These maps were made using a grid of interval velocities, imported as fake wells. Horizon contour maps have been made for unconformities RSU7, RSU6, RSU5a and RSU5. Free Air and Bouguer gravity grid as well as magnetic and bathymetry grids are also loaded into the project. Mapped horizons in the project can easily be exported as ascii files. SEGY seismic data can also be exported.

B) Archiving: Unprocessed seismic data from NBP-0301 and NBP-0306 are archived on DVD disks and DLT tapes. The University of North Carolina (Lou Bartek) and Lamont Doherty Earth Observatory (John Diebold) have copies of these data in addition to UCSB (Bruce Luyendyk). DVD's of the raw shot gathers are stored in Webb 2042 (Luyendyk lab) and the DLT tapes are stored at the Institute for Crustal Studies (ICS) at UCSB. The raw shot gathers are in SEGY-D form. Processed

seismic sections have been archived on CD and DVD and are also saved on external hard drives. Each disk contains folders labeled with each individual line processed. The folders contain files that are key to recreating the processing steps of the line. These files include: the flow chart (ex: 1A0.flo), regular stack (ex: 1A0-Stack), multiple attenuated stack (ex: 1A0-FKStack or 110A-RadonStack), stacking velocities, FK velocities, bin definitions, geometry card files, and mute files. Should the data need to be reprocessed, these files are key to understanding the processing steps already taken. The external hard drives and a copy of the back up CD's and DVD's are located in Webb 2042 (Luyendyk lab). A duplicate set of DVD's are stored at ICS as well.

Appendix E

DSDP Site 270, 271 & 272 Core Data

Below are tables of core data taken from the Initial Reports of the Deep Sea Drilling Project, Leg 28 [Hayes and Frakes, 1975]. Included are the core segments (Core #), the thickness of the section in meters (Core Int m), the percentage clay, silt, sand and diatoms in each core segment, and the sequence number. These values were used in the decompaction process to determine the porosity of the units.

DSDP 270

Core #	Core Int m	Clay %	Silt %	Sand %	Diatoms %	Sequence
1	0-6	52	22	12	14	RSS-2
2	6-15.5	67	25	5	3	RSS-2
3	15.5-25	50	25	10	15	RSS-2
4	25-25.5	60	25	15	0	RSS-2
5	25.5-35	63	25	12	0	RSS-2
6	35-44.5	50	40	10	0	RSS-2
7	43-55.5	?	?	?	?	RSS-2
8	53-63	?	?	?	?	RSS-2
9	63-72.5	75	20	5	0	RSS-2
10	72.5-82	80	15	5	0	RSS-2
11	82-91.5	?	?	?	?	RSS-2
12	91.5-101	?	?	?	?	RSS-2
13	101-110.5	60	30	10	0	RSS-2
14	110.5-120	60	25	15	0	RSS-2
15	120-129.5	75	20	5	0	RSS-2
16	129.5-139	65	25	10	0	RSS-2
17	139-148.5	60	35	5	0	RSS-2
18	148.5-158	61	29	10	0	RSS-2
19	158-167.5	68	24	8	0	RSS-2
20	167-177	51	20	29	0	RSS-2
21	177-186.5	53	28	19	0	RSS-2
22	186.5-196	72	26	2	0	RSS-2
23	196-205.5	49	34	17	0	RSS-2
24	205.5-215	68	30	2	0	RSS-2
25	215-224.5	54	39	7	0	RSS-2
26	224.5-234	44	41	15	0	RSS-2
27	234-243.5	30	52	18	0	RSS-2
28	243.5-253	35	47	18	0	RSS-2
29	253-242.5	45	43	13	0	RSS-2
30	262.5-272	40	47	13	0	RSS-2

DSDP	270	Continued				
31	272-281.5	55	38	7	0	RSS-2
32	281.5-291	50	42	8	0	RSS-2
33	291-300.5	32	48	20	0	RSS-2
34	300.5-310	35	52	13	0	RSS-2
35	310-319.5	36	46	18	0	RSS-2
36	319.5-329	42	43	15	0	RSS-2
37	329-338.5	62	36	2	0	RSS-2
38	338.5-348	32	60	8	0	RSS-2
39	348-357.5	33	45	22	0	RSS-2
40	357.5-367	28	44	28	0	RSS-2
41	367-370	32	55	13	0	RSS-2
42	370-376.5	30	50	20	0	RSS-2
43	376.5-386	49	31	20	0	RSS-2
44	386-395.5	45	25	35	0	RSS-2
45	395.5-405	?	?	?	0	RSS-1I?
46	405-409.5	?	?	?	0	RSS-1I?

DSDP 271

Core #	Core Int m	Clay %	Silt %	Sand %	Diatoms %	Sequence
1	21-30.5	35	55	10	0	RSS-8
2	40-49.5	40	28	30	2	RSS-7
3	49.5-59	35	31	32	2	RSS-7
4	59-68.5	40	20	40	0	RSS-7
5	68.5-78	51	30	19	0	RSS-7
6	78-87.5	50	23	25	2	RSS-7
7	?	?	?	?	?	RSS-7
8	97-106.5	5	45	50	0	RSS-7
9	106.5-116	70	17	10	3	RSS-7
10	?	?	?	?	?	RSS-7
11	?	?	?	?	?	RSS-7
12	135-144.5	60	15	25	0	RSS-7
13	144.5-154	60	20	20	0	RSS-7
14	154-163.5	70	5	15	10	RSS-7
15	165.5-175	?	?	?	?	RSS-7
16	175-184.5	45	0	55	0	RSS-6
17	?	?	?	?	?	RSS-6
18	?	?	?	?	?	RSS-6
19	?	?	?	?	?	RSS-6
20	213-222.5	40	10	40	10	RSS-6
21	222.5-232	45	20	15	20	RSS-6
22	232-241.5	44	15	16	25	RSS-6
23	241.5-251	35	25	40	0	RSS-6
24	255.5-265	32	15	23	30	RSS-6

DSDP 272

Core Int m	Clay %	Silt %	Sand %	Diatoms %	Other %	Sequence
4-13.5	65	25	5	5		RSS-8
13.5-23	60	28	9	3		RSS-8
23-32.5	49	31	5	15		RSS-8
32.5-42	58	32	7	3		RSS-5
42-51.5	48	35	12	5		RSS-5
51.5-61	50	28	8	14		RSS-5
61-70.5	67	23	5	5		RSS-5
70.5-80	53	35	7	5		RSS-5
80-89.5	60	29	7	4		RSS-5
89.5-99	51	30	11	8		RSS-5
99-108.5	47	33	9	11		RSS-5
108.5-118	43	43	9	5		RSS-5
118-127.5	?	?	?	?		RSS-5
127.5-137	13	11	1	75		RSS-5
137-146.5	40	32	8	20		RSS-5
146.5-156	31	27	9	33		RSS-4
156-165.5	31	26	8	35		RSS-4
165.5-175	15	15	0	70		RSS-4
175-184.5	20	12	1	67		RSS-4
184.5-194	30	15	5	50		RSS-4
194-203.5	19	16	2	63		RSS-4
203.5-213	30	20	4	46		RSS-4
213-222.5	28	12	5	55		RSS-4
222.5-232	25	20	5	50		RSS-4
232-241.5	25	20	5	50		RSS-4
241.5-251	20	20	0	60		RSS-4
251-260.5	30	16	7	47		RSS-4
260.5-270	25	10	0	50	15	RSS-4
270-279.5	33	24	5	38		RSS-4
279.5-289	16	20	4	60		RSS-3
289-298.5	24	6	0	70		RSS-3
298.5-308	36	18	6	40		RSS-3
308-317.5	14	24	2	60		RSS-3
317.5-327	30	27	3	40		RSS-3
327-336.5	33	18	9	40		RSS-3
336.5-356	?	?	?	?		RSS-3
346-355.5	35	18	5	42		RSS-3
355.5-365	42	25	3	30		RSS-3
356-374.5	65	30	6	0		RSS-3
374.5-385	65	25	10	0		RSS-3
385-393.5	65	30	5	0		RSS-3
393.5-403	70	28	2	0		RSS-3
403-412.5	55	35	10	0		RSS-3
412.5-422	70	25	5	0		RSS-3
422-431.5	70	25	5	0		RSS-3
431.5-441	?	?	?	?		RSS-3

Appendix F

Backstripping Technique and Code

Backstripping was performed using a Matlab iteration script taken from www.erdw.ethz.ch/Allen and modified for the Ross Sea. The code was written to decompact and backstrip the deepest sections of the Central Trough and Eastern Basin using thickness and lithology parameters outlined the text (dissertation Chapter 3-Tables 3-1, 3-2, & 3-3). All sediments above unconformity RSU6 are interpreted as post-rift. The decompaction and backstripping calculation follows the method outlined in box 9.1 and 9.2 of Allen and Allen [2005] (see Chapter 3 for reference). The process follows the equations listed in the text (Chapter 3). However, two intermediate steps not listed in the text, between the decompaction calculation and the calculation of tectonic subsidence, include determining sediment porosity with depth and the bulk density of the sediment at its decompacted depth. The new porosity is obtained by

$$\Phi = (\Phi_0/c) - (exp(-cy'_1) - exp(-cy'_2)) / (y'_2 - y'_1)$$

where Φ_0 is the observed porosity, c is a decay constant, and y'_1 and y'_2 are the decompacted depths. The bulk density, or mean sediment density, is obtained by

$$\rho_s = \sum_i \{(\Phi_i \rho_w + (1 - \Phi_i) \rho_{sgi}) / S\} y'_i$$

where Φ_i is the mean porosity of the i th layer, ρ_w is the density of water, ρ_{sgi} is the sediment grain density, y'_i is the thickness of the i th layer, and S is the total thickness of the column corrected for compaction. Eustatic and paleobathymetry corrections

were applied, using the equations outlined in dissertation chapter 3, to the sediment load corrected subsidence in an Excel script.

Predicted subsidence curves were computed from a finite difference heat flow calculation performed in Excel. Initial post-rift thermal conditions are given by

$$T_i = (T_m / (Y_m / \beta)) * d_i$$

Where T_i is the temperature at the i^{th} depth, T_m is the temperature of the mantle, β is the crustal stretching factor, and d_i is the i^{th} depth. Depth increments of 1,000 meters and time increments of 10,000 years were used and the calculation was computed for 95 Ma. Initial temperature vs. depth conditions were calculated assuming a 125 km thick lithosphere and a mantel temperature of 1330 ° C. Surface temperature was set to 0 ° C. Two calculations were done: a single rifting event and a two stage rifting event. Thermal subsidence for various stretching factors were calculated by

$$S_t = (\rho_m * \alpha_e (T_2 - T_1) (Y_c)) / \rho_m - \rho_w$$

where α_e is the thermal expansion coefficient (3.28×10^{-5} °C), T_2 is the average temperature at time step 2, T_1 is the average temperature at time step 1, and Y_c is the thickness of the crust. The predicted subsidence was plotted against the observed subsidence in Excel.

Matlab backstripping script used for this study:

```
clear
% Initial Parameters
%Unit Thickness
z_RSS1 = 4.705; % actual thickness of the RSS1 , in km;
z_RSS2 = 1.550; % actual thickness of RSS2 , in km;
z_RSS3 = 0.230; % actual thickness of RSS3, in km;
```

```
z_RSS4 =0.370; % actual thickness of RSS4, in km;  
z_RSS5 =0.400; % actual thickness of the RSS5 shale, in km;  
z_RSS7 =0.285; % actual thickness of the RSS7, in km; Includes RSS7&8;
```

%Surface Porosity

```
fi_RSS10 = 0.56; % surface porosity of the RSS1;  
fi_RSS20 = 0.589;% surface porosity of the RSS2;  
fi_RSS30 =0.643;% surface porosity of the RSS3;  
fi_RSS40 = 0.683;% surface porosity of the RSS4;  
fi_RSS50 =0.618; % surface porosity of the RSS5;  
fi_RSS70 =0.596; % surface porosity of the RSS7&8;
```

%Depth Coefficient

```
c1 = 0.39;% fi-depth coefficient in km-1 for RSS1;  
c2 = 0.44;% fi-depth coefficient in km-1 for RSS2;  
c3 = 0.42;% fi-depth coefficient in km-1 for RSS3;  
c4 = 0.37;% fi-depth coefficient in km-1 for RSS4;  
c5 = 0.43;% fi-depth coefficient in km-1 for RSS5;  
c7 = 0.43; % fi-depth coefficient in km-1 for RSS7&8 combined;
```

% Depth From Seafloor to Unconformities

```
y7 = 0;% actual top of the RSS7&8, Seafloor  
y6 = 0.285;% actual top of the RSS5, bottom of RSS7&8 (RSU3), in Km  
y5 = 0.685; % actual top of the RSS4 and bottom of the RSS5 (RSU4), in Km  
y4 = 1.055; % actual top of the RSS3 and bottom of the RSS4 (RSU4a), in Km  
y3 = 1.285; % actual top of the RSS2 and bottom of the RSS3 (RSU5), in Km  
y2 = 2.835 ; % actual top of the RSS1 and bottom of the RSS2 (RSU6), in Km  
y1 = 7.540; % actual bottom of sediment (basement/RSU7)  
y = 0; % surface conditions
```

%Densities

```
rho_w = 1030; % density of the sea water;  
rho_RSS1 = 2710 ; % density of RSS1  
rho_RSS2 = 2710 ; % density of RSS2  
rho_RSS3 = 2580 ; % density for the RSS3, in kg/m3;  
rho_RSS4= 2450 ; % density for the RSS4;  
rho_RSS5= 2640; % density of the RSS5;  
rho_RSS7= 2680; % density of the RSS7&8;  
rho_m = 3300; % density of the mantle
```

```

%Decompression Routine
% decompaction of the RSS1, 210-140MA (T1); x1_1 is the thickness of the RSS1 at time T1
eps = 0.0001 ;
error = 2*eps ;
x1_1 =1;
while error > eps
    xRSS11= z_RSS1-fi_RSS10/c1*(exp(-c1*y2)-exp(-c1*y1))+ fi_RSS10/c1*(exp(-c1*y)-exp(-c1* x1_1));
    error = abs(xRSS11-x1_1 )/ x1_1
    x1_1 = xRSS11
end

% decompaction of the RSS2, 140-100 MA (T2); x2_2 is the thickness of the RSS2 at time T2
eps = 0.0001 ;
error = 2*eps ;
x2_2=1;
while error > eps
    xRSS22= z_RSS2-fi_RSS20/c2*(exp(-c2*y3)-exp(-c2*y2))+ fi_RSS20/c2*(exp(-c2*y)-exp(-c2* x2_2));
    error = abs(xRSS22-x2_2)/x2_2
    x2_2 = xRSS22
end

% decompaction of the RSS1, 140-100MA (T2), x1_2 is the thickness of the RSS1 at time T2
eps = 0.0001 ;
error = 2*eps ;
x1_2 =1;
while error > eps
    xRSS12= (z_RSS1-fi_RSS10/c1*(exp(-c1*y2)-exp(-c1*y1))+ fi_RSS10/c1*(exp(-c1*xRSS22)-exp(-c1*x1_2)));
    error = abs(xRSS12-x1_2)/x1_2
    x1_2 = xRSS12
end

% decompaction of the RSS3, 100-65 MA (T3), x3_3 is the thickness of the RSS3 at time T3
eps = 0.0001 ;
error = 2*eps ;
x3_3 =1;
while error > eps
    xRSS33= (z_RSS3-fi_RSS30/c3*(exp(-c3*y4)-exp(-c3*y3))+ fi_RSS30/c3*(exp(-c3*y)-exp(-c3*x3_3)))
    error = abs(xRSS33-x3_3)/x3_3
    x3_3 = xRSS33

```

```

end

% decompaction of the RSS2 (Lower Cretaceous, 100-65MA (T3), x2_3 is the thickness of the RSS2 at time T3
cps = 0.0001 ;
error = 2*cps ;
x2_3= 1;
while error > cps
    xRSS23= z_RSS2-fi_RSS20/c2*(exp(-c2*y3)-exp(-c2*y2))+ fi_RSS20/c2*(exp(-c2*xRSS33)-exp(-c2*x2_3))
+ xRSS33 ;
    error = abs(xRSS23-x2_3)/x2_3
    x2_3= xRSS23
end

% decompaction of the RSS1, 100-65MA (T3), x1_3 is the thickness of the RSS1 at time T3
cps = 0.0001 ;
error = 2*cps ;
x1_3 =1;
while error > cps
    xRSS13= (z_RSS1-fi_RSS10/c1*(exp(-c1*y2)-exp(-c1*y1))+ fi_RSS10/c1*(exp(-c1*xRSS23)-exp(-c1*x1_3))) + xRSS23;
    error = abs(xRSS13-x1_3)/x1_3
    x1_3 = xRSS13
end

% decompaction of the RSS4, 65-55 MA(T4), x4_4 is the thickness of the RSS4 at time T4
cps = 0.0001 ;
error = 2*cps ;
x4_4 =1;
while error > cps
    xRSS44 = z_RSS4-fi_RSS40/c4*(exp(-c4*y5)-exp(-c4*y4))+ fi_RSS40/c4*(exp(-c4*y)-exp(-c4*x4_4));
    error = abs( xRSS44 -x4_4 )/x4_4
    x4_4 = xRSS44
end

% decompaction of the RSS3, 65-55 MA (T4), x3_4 is the thickness of the RSS3 at time T4
cps = 0.0001 ;
error = 2*cps ;
x3_4 =1;
while error > cps
    xRSS34= (z_RSS3-fi_RSS30/c3*(exp(-c3*y4)-exp(-c3*y3))+ fi_RSS30/c3*(exp(-c3*xRSS44 )-exp(-c3*x3_4))) + xRSS44 ;

```

```

error = abs(xRSS34-x3_4)/x3_4
x3_4 = xRSS34
end

% decompaction of the RSS2 (Lower Cretaceous, 65-55MA (T4), x2_4 is the thickness of the RSS2 at time T4
eps = 0.0001 ;
error = 2*eps ;
x2_4= 1;
while error > eps
    xRSS24= z_RSS2-fi_RSS20/c2*(exp(-c2*y3)-exp(-c2*y2))+ fi_RSS20/c2*(exp(-c2*xRSS34)-exp(-c2*x2_4))
+ xRSS34 ;
    error = abs(xRSS24-x2_4)/x2_4
    x2_4= xRSS24
end

% decompaction of the RSS1, 65-55MA (T4), x1_4 is the thickness of the RSS1 at time T4
eps = 0.0001 ;
error = 2*eps ;
x1_4=1;
while error > eps
    xRSS14= (z_RSS1-fi_RSS10/c1*(exp(-c1*y2)-exp(-c1*y1)))+ fi_RSS10/c1*(exp(-c1*xRSS24)-exp(-c1*x1_4)) + xRSS24;
    error = abs(xRSS14-x1_4)/x1_4
    x1_4 = xRSS14
end

% decompaction of the RSS5 , 55-0 Ma (T5), x5_5 is the thickness of the RSS5 at time T5
eps = 0.0001 ;
error = 2*eps ;
x5_5 =1;
while error > eps
    xRSS55= z_RSS55- fi_RSS50/c5*(exp(-c5*y6)-exp(-c5*y5))+ fi_RSS50/c5*(exp(-c5*y)-exp(-c5*x5_5));
    error = abs(xRSS55-x5_5)/x5_5
    x5_5 = xRSS55
end

% decompaction of the RSS4, 55-0MA(T4), x4_4 is the thickness of the RSS4 at time T5
eps = 0.0001 ;
error = 2*eps ;
x4_5=1;

```

```

while error > eps
    xRSS45 = ( z_RSS4-f1_RSS40/c4*(exp(-c4*y5)-exp(-c4*y4))+ f1_RSS40/c4*(exp(-c4*xRSS55)-exp(-c4*x4_5)) ) + xRSS55;
    error = abs( xRSS45 -x4_5 )/x4_5
    x4_5 = xRSS45
end

% decompaction of the RSS3,55-0 MA (T5), x3_5 is the thickness of the RSS3 at time T5
eps = 0.0001 ;
error = 2*eps ;
x3_5 =1;
while error > eps
    xRSS35= (z_RSS3-f1_RSS30/c3*(exp(-c3*y4)-exp(-c3*y3))+ f1_RSS30/c3*(exp(-c3*xRSS45)-exp(-c3*x3_5)) ) + xRSS45 ;
    error = abs(xRSS35-x3_5)/x3_5
    x3_5 = xRSS35
end

% decompaction of the RSS2 (Lower Cretaceous, 55-0MA (T5), x2_5 is the thickness of the RSS2 at time T5
eps = 0.0001 ;
error = 2*eps ;
x2_5= 1;
while error > eps
    xRSS25= z_RSS2-f1_RSS20/c2*(exp(-c2*y3)-exp(-c2*y2))+ f1_RSS20/c2*(exp(-c2*xRSS35)-exp(-c2*x2_5)) + xRSS35 ;
    error = abs(xRSS25-x2_5)/x2_5
    x2_5= xRSS25
end

% decompaction of the RSS1, 55-0MA (T5), x1_5 is the thickness of the RSS1 at time T5
eps = 0.0001 ;
error = 2*eps ;
x1_5 =1;
while error > eps
    xRSS15= (z_RSS1-f1_RSS10/c1*(exp(-c1*y2)-exp(-c1*y1))+ f1_RSS10/c1*(exp(-c1*xRSS25)-exp(-c1*x1_5)) ) + xRSS25;
    error = abs(xRSS15-x1_5)/x1_5
    x1_5= xRSS15
end

% decompaction of the RSS7&8 , 55-0 Ma (T7), x7_7 is the thickness of the

```

```

% RSS7 at time T7
eps = 0.0001 ;
error = 2*eps ;
x7_7=1;
while error > eps
    xRSS77= z_RSS7-fi_RSS70/c7*(exp(-c7*y7)-exp(-c7*y7))+ fi_RSS70/c7*(exp(-c7*y)-exp(-c7*x7_7));
    error = abs(xRSS77-x7_7)/x7_7
    x7_7 = xRSS77
end

% decompaction of the RSS5 , 55-0 Ma (T7), x5_7 is the thickness of the
% RSS5 at time T7
eps = 0.0001 ;
error = 2*eps ;
x5_7=1;
while error > eps
    xRSS57 = ( z_RSS5-fi_RSS50/c5*(exp(-c5*y6)-exp(-c5*y5))+ fi_RSS50/c5*(exp(-c5*xRSS77)-exp(-c5*x5_7)) ) + xRSS77;
    error = abs( xRSS57 -x5_7 )/x5_7
    x5_7 = xRSS57
end

% decompaction of the RSS4, 55-0MA(T7), x4_7 is the thickness of the RSS4
% at time T7
eps = 0.0001 ;
error = 2*eps ;
x4_7=1;
while error > eps
    xRSS47 = ( z_RSS4-fi_RSS40/c4*(exp(-c4*y5)-exp(-c4*y4))+ fi_RSS40/c4*(exp(-c4*xRSS57)-exp(-c4*x4_7)) ) + xRSS57;
    error = abs( xRSS47 -x4_7 )/x4_7
    x4_7 = xRSS47
end

% decompaction of the RSS3,55-0 MA (T7), x3_7 is the thickness of the RSS3
% at time T7
eps = 0.0001 ;
error = 2*eps ;
x3_7=1;
while error > eps

```

```

xRSS37= (z_RSS3-f1_RSS30/c3*(exp(-c3*y4)-exp(-c3*y3))+ f1_RSS30/c3*(exp(-c3*xRSS47 )-exp(-c3*x3_7)))+ xRSS47 ;
error = abs(xRSS37-x3_7)/x3_7
x3_7 = xRSS37
end

% decompaction of the RSS2 (Lower Cretaceous, 55-0MA (T7), x2_7 is the
% thickness of the RSS2 at time T7
eps = 0.0001 ;
error = 2*eps ;
x2_7= 1;
while error > eps
    xRSS27= z_RSS2-f1_RSS20/c2*(exp(-c2*y3)-exp(-c2*y2))+ f1_RSS20/c2*(exp(-c2*xRSS37)-exp(-c2*x2_7))
+ xRSS37 ;
    error = abs(xRSS27-x2_7)/x2_7
    x2_7= xRSS27
end

% decompaction of the RSS1, 55-0MA (T7), x1_7 is the thickness of the RSS1
% at time T7
eps = 0.0001 ;
error = 2*eps ;
x1_7=1;
while error > eps
    xRSS17= (z_RSS1-f1_RSS10/c1*(exp(-c1*y2)-exp(-c1*y1))+ f1_RSS10/c1*(exp(-c1*xRSS27)-exp(-c1*x1_7)))+ xRSS27;
    error = abs(xRSS17-x1_7)/x1_7
    x1_7= xRSS17
end

% Backstripped Porosity
f1_RSS11= f1_RSS10/c1 *(((exp(-c1*y)) - exp(-c1*x1_1))/(x1_1-y)) % porosity of the RSS1 at T1,
f1_RSS22= f1_RSS20/c2 *(((exp(-c2*y)) - exp(-c2*x2_2))/(x2_2-y)) % porosity of the RSS2 at T2,
f1_RSS12= f1_RSS10/c1 *(((exp(-c1*x2_2)) - exp(-c1*x1_2))/(x1_2-x2_2)) % porosity of the RSS1 at T2,
f1_RSS33= f1_RSS30/c3 *(((exp(-c3*y)) - exp(-c3*x3_3))/(x3_3-y)) % porosity of the RSS3 at T3,
f1_RSS23= f1_RSS20/c2 *(((exp(-c2*x3_3)) - exp(-c2*x2_3))/(x2_3-x3_3)) % porosity of the RSS2 at T3,
f1_RSS13= f1_RSS10/c1 *(((exp(-c1*x2_3)) - exp(-c1*x1_3))/(x1_3-x2_3)) % porosity of the RSS1 at T3,
f1_RSS44= f1_RSS40/c4 *(((exp(-c4*y)) - exp(-c4*x4_4))/(x4_4-y)) % porosity of the RSS4 at T4,
f1_RSS34= f1_RSS30/c3 *(((exp(-c3*x4_4)) - exp(-c3*x3_4))/(x3_4-x4_4)) % porosity of the RSS3 at T4,
f1_RSS24= f1_RSS20/c2 *(((exp(-c2*x3_4)) - exp(-c2*x2_4))/(x2_4-x3_4)) % porosity of the RSS2 at T4,
f1_RSS14= f1_RSS10/c1 *(((exp(-c1*x2_4)) - exp(-c1*x1_4))/(x1_4-x2_4)) % porosity of the RSS1 at T4,

```

```

fi_RSS55 = fi_RSS50/c5 *(((exp(-c5*y)) - exp(-c5*x5_5))/(x5_5-y)) % porosity of the RSS5 at T5,
fi_RSS45= fi_RSS40/c4 *(((exp(-c4*x5_5)) - exp(-c4*x4_5))/(x4_5-x5_5)) % porosity of the RSS4 at T5,
fi_RSS35= fi_RSS30/c3 *(((exp(-c3*x4_5)) - exp(-c3*x3_5))/(x3_5-x4_5)) % porosity of the RSS3 at T5,
fi_RSS25 = fi_RSS20/c2 *(((exp(-c2*x3_5)) - exp(-c2*x2_5))/(x2_5-x3_5)) % porosity of the RSS2 at T5,
fi_RSS15 = fi_RSS10/c1 *(((exp(-c1*x2_5)) - exp(-c1*x1_5))/(x1_5-x2_5)) % porosity of the RSS1 at T5,
fi_RSS77 = fi_RSS70/c7 *(((exp(-c7*y)) - exp(-c7*x7_7))/(x7_7-y)) % porosity of the RSS7 at T7,
fi_RSS57 = fi_RSS50/c5 *(((exp(-c5*x7_7)) - exp(-c5*x5_7))/(x5_7-x7_7)) % porosity of the RSS5 at T7,
fi_RSS47= fi_RSS40/c4 *(((exp(-c4*x5_7)) - exp(-c4*x4_7))/(x4_7-x5_7)) % porosity of the RSS4 at T7,
fi_RSS37= fi_RSS30/c3 *(((exp(-c3*x4_7)) - exp(-c3*x3_7))/(x3_7-x4_7)) % porosity of the RSS3 at T7,
fi_RSS27 = fi_RSS20/c2 *(((exp(-c2*x3_7)) - exp(-c2*x2_7))/(x2_7-x3_7)) % porosity of the RSS2 at T7,
fi_RSS17 = fi_RSS10/c1 *(((exp(-c1*x2_7)) - exp(-c1*x1_7))/(x1_7-x2_7)) % porosity of the RSS1 at T7,

% Increment of the Bulk Density from 100Ma to 0 Ma

rho_t1=((fi_RSS11*rho_w + (1-fi_RSS11)*rho_RSS1)/x1_1)* x1_1% increment due to the 1st layer;
rho_t2 = (fi_RSS12*rho_w + (1-fi_RSS12)*rho_RSS1)*((x1_2 - x2_2)/x1_2) + (fi_RSS22*rho_w + (1-fi_RSS22)*rho_RSS2)*(x2_2/x1_2)
rho_t3 = (fi_RSS13*rho_w + (1-fi_RSS13)*rho_RSS1)*((x1_3 - x2_3)/x1_3) + (fi_RSS23*rho_w + (1-fi_RSS23)*rho_RSS2)*(x2_3 - x3_3)/x1_3)+(fi_RSS33*rho_w + (1-fi_RSS33)*rho_RSS3)*(x3_3/x1_3)
rho_t4 = (fi_RSS14*rho_w + (1-fi_RSS14)*rho_RSS1)*((x1_4 - x2_4)/x1_4) + (fi_RSS24*rho_w + (1-fi_RSS24)*rho_RSS2)*(x2_4 - x3_4)/x1_4) + (fi_RSS34*rho_w + (1-fi_RSS34)*rho_RSS3)*(x3_4 - x4_4)/x1_4) + (fi_RSS44*rho_w + (1-fi_RSS44)*rho_RSS4)*(x4_4/x1_4)
rho_t5 = (fi_RSS15*rho_w + (1-fi_RSS15)*rho_RSS1)*((x1_5 - x2_5)/x1_5) + (fi_RSS25*rho_w + (1-fi_RSS25)*rho_RSS2)*(x2_5 - x3_5)/x1_5) + (fi_RSS35*rho_w + (1-fi_RSS35)*rho_RSS3)*(x3_5 - x4_5)/x1_5) + (fi_RSS45*rho_w + (1-fi_RSS45)*rho_RSS4)*(x4_5 - x5_5)/x1_5) + (fi_RSS55*rho_w + (1-fi_RSS55)*rho_RSS5)*(x5_5/x1_5)
rho_t7 = (fi_RSS17*rho_w + (1-fi_RSS17)*rho_RSS1)*((x1_7 - x2_7)/x1_7) + (fi_RSS27*rho_w + (1-fi_RSS27)*rho_RSS2)*(x2_7 - x3_7)/x1_7) + (fi_RSS37*rho_w + (1-fi_RSS37)*rho_RSS3)*(x3_7 - x4_7)/x1_7) + (fi_RSS47*rho_w + (1-fi_RSS47)*rho_RSS4)*(x4_7 - x5_7)/x1_7) + (fi_RSS57*rho_w + (1-fi_RSS57)*rho_RSS5)*(x5_7 - x7_7)/x1_7) + (fi_RSS77*rho_w + (1-fi_RSS77)*rho_RSS7)*(x7_7/x1_7)


```

% Backstripped Tectonic Subsidence using Airy model

```

Y0 = 0; % the subsidence started in the time 100 MA, so the thickness at that time is zero
Y1 = x1_1 * ((rho_m - rho_t1)/(rho_m-rho_w))
Y2 = x1_2 * ((rho_m - rho_t2)/(rho_m-rho_w))
Y3 = x1_3 * ((rho_m - rho_t3)/(rho_m-rho_w))
Y4 = x1_4 * ((rho_m - rho_t4)/(rho_m-rho_w))
Y5 = x1_5 * ((rho_m - rho_t5)/(rho_m-rho_w))
Y7 = x1_7 * ((rho_m - rho_t7)/(rho_m-rho_w))

```

References Cited

Allen, P. A., and J. R. Allen (2005), *Basin Analysis: Principles and Applications*, Blackwell Scientific.

Claerbout, J. F. (1985), *Imaging the earth's interior*, 398 pp., Blackwell Scientific, Boston.

Hampson, D. (1991), Inverse velocity stacking for multiple elimination, *J. Canadian Soc. Explor. Geophys.*, 22, 44-55.

Hayes, D. E., and L. A. Frakes (1975), General synthesis: Deep Sea Drilling Project 28, in *Initial Reports of the Deep Sea Drilling Project, Leg 28*, edited by D. E. Hayes and L. A. Frakes, pp. 919-942, U.S. Government Printing Office, Washington, D.C.